QUANTIFYING THE ELECTRICITY SAVINGS FROM THE USE OF HOME AUTOMATION DEVICES IN A RESIDENCE

A Dissertation

by

SUKJOON OH

Submitted to the Office of Graduate and Professional Studies of
Texas A&M University
in partial fulfillment of the requirements for the degree of

DOCTOR OF PHILOSOPHY

Chair of Committee,	Jeff S. Haberl
Co-Chair of Committee,	Juan Carlos Baltazar
Committee Members,	Charles H. Culp
	Bryan P. Rasmussen
Head of Department,	Robert Warden

December 2017

Major Subject: Architecture

ABSTRACT

This study quantifies the electricity savings to homeowners when they install and use Home Automation Devices (HADs), which are also called Internet of Things (IoT), in a residence. To accomplish this study, new analysis methods were developed that have built on and enhanced the features of existing energy analysis methods. A new inverse approach and a new two-way, calibrated simulation approach were combined to analyze the electricity savings from the installation and use of HADs. This study found that few of the previous studies about HADs that were reviewed developed methods for specifically quantifying the weather-normalized, hourly electricity savings to homeowners from the use of HADs. The review of the literature did find that homeowners using HADs wanted to use them automatically, without changing their lifestyle or experiencing discomfort, when turning on or turning off devices. Therefore, this study developed new, non-intrusive methods to help quantify the electricity savings to homeowners from the use of HADs using a combination of Smart Meter (SM) data and the corresponding weather data to analyze the weather-normalized savings from residences equipped with HADs.

First, a non-intrusive method was developed to automatically detect and quantify potential electricity savings of HADs using hourly electricity use data recorded by an SM (i.e., Level 0 Analysis) before the retrofit. To accomplish this, both an event detection process and an energy quantification process were developed. Second, a calibrated building energy simulation model (i.e., Level I Analysis) was developed for the case-

study residence to analyze selected HAD usage scenarios to better quantify the potential electricity savings to the homeowner from the use of the HADs. The calibrated simulation model was used to simulate different scenarios of thermostatically-controlled and non-thermostatically-controlled HADs. Third, an HAD was installed in the case-study house to quantify the before/after actual electricity savings from the use of the HADs (i.e., Level II Analysis). Specifically, in the case-study house, a wireless HAD thermostat with occupancy sensors was installed.

The results showed that the annual electricity savings resulting from Level 0 Analysis, Level I Analysis, and Level II Analysis were 987.8 kWh (8.3 %), 2,961.7 kWh (25.2 %), and 5,208.4 kWh (43.6 %), respectively. Differences in the savings among the three methods can be attributed to the assumptions made for each analysis as well as the limitations in the three methods. Using the Level II Analysis savings, when the costs of the new thermostat ($249) with the seven motion sensors ($237), including the installation fee ($100), were considered, the simple payback period was 1.0 year. Thermal comfort was also analyzed. The analysis showed no significant degradation of thermal comfort from the electricity savings during occupied hours. Finally, this study provides recommendations to help improve future quantification methods and reduce the uncertainty of predicting the electricity savings for residences equipped with HADs using hourly or sub-hourly electricity use data recorded by an SM.

DEDICATION

To

My Loving God, Wife and Family

ACKNOWLEDGEMENTS

First of all, I would like to sincerely thank my loving God for the meaningful guidance throughout the course of my life, including this research.

A doctoral journey cannot be traveled alone, and I have many to thank and appreciation for supporting my journey. First and foremost, I would like to thank my dissertation chair Dr. Jeff S. Haberl, who is my academic mentor. He provided incredible insight, knowledge, editing, and expert advice to motivate me to finish my doctoral journey. I also greatly appreciate my co-chair Dr. Juan-Carlos Baltazar, who provided his analysis and expertise with crucial feedback and guidance. Thank you also to, Dr. Charles H. Culp and Dr. Bryan P. Rasmussen for providing meaningful feedback and support as committee members. I also want to thank Dr. David E. Claridge, who has given me valuable feedback and advice despite his time constraints.

I would like to recognize my friends and colleagues at the Energy Systems Laboratory, especially the graduate assistant researchers of the Texas Emissions Reduction Plan (TERP) modeling group. Thank you for making this study rigorous.

Last but not least, thanks to my loving father, Sungwoo Oh, my loving mother, Jungnam Kim, my loving sister, Eunyoung Oh, and my sister's husband, Prof. Hee Chun Roh, and my wife's family for their best, endless love and encouragement. Most importantly, I really thank my wife, Soo Jeoung Han, for her beautiful support, patience and love. I am so thankful that I met my son, Michael Hanbyn Oh, during the last year of my doctoral journey. He gives us happiness.

CONTRIBUTORS AND FUNDING SOURCES

Contributors

This work was supervised by a dissertation committee consisting of Professors Jeff S. Haberl, Juan-Carlos Baltazar, and Charles H. Culp of the Department of Architecture and Professor Bryan P. Rasmussen of the Department of Mechanical Engineering. All work for the dissertation was completed independently by the student.

Funding Sources

Work on this dissertation and graduate study was partially supported by the ASHRAE Graduate Student Grant-In-Aid for the 2016-2017 academic year.

NOMENCLATURE

AMI	Advanced Metering Infrastructure
ANN	Artificial Neural Networks
ARMA	Autoregressive Moving Average
ASTM	American Society for Testing and Materials
BAS	Building Automation System
BWM	Box, Whisker, and Mean
CBE	Center for the Built Environment
CPP	Critical Peak Pricing
CS	Cooling Slope
CVR	Conservation Voltage Reduction
CV-RMSE	Coefficient of Variation of the Root-Mean-Square Error
DA	Distributed Automation
DCS	Distributed Control System
DER	Distributed Energy Resource
DG	Distributed Generation
DHW	Domestic Hot Water
DIY	Do It Yourself
DLC	Direct Load Control
EIA	Energy Information Administration
EIR	Energy Input Ratio

EMCS	Energy Management & Control System
EMS/SCADA	Energy Management Systems and Supervisory Control and Data Acquisition
ES	Energy Storage
E_{tot}	Building Electricity Use
EV	Electric Vehicle
$E_{w.i.}$	Weather-Independent Electricity Use
FDD	Fault Detection & Diagnostics
HAD	Home Automation Device
HAN	Home Area Network
HEMS	Home Energy Management Systems
HS	Heating Slope
HSPF	Heating Seasonal Performance Factor
HVAC	Heating, Ventilating, and Air Conditioning
IAT	Indoor Air Temperature
IHD	In-Home Display
IMT	Inverse Modeling Toolkit
IoT	Internet of Things
IQR	InterQuartile Range
JJH	James J. Hirsch & Associates
LAN	Local Area Network
LBNL	Lawrence Berkeley National Laboratory

MBE	Mean Bias Error
M&V	Measurement & Verification
NMBE	Normalized Mean Bias Error
NOAA	National Oceanic and Atmospheric Administration
OAT	Outside Air Temperature
ORNL	Oak Ridge National Laboratory
PCT	Programmable Communicating Thermostat
PHEV	Plug-in Hybrid EV
PNNL	Pacific Northwest National Laboratory
PRISM	PRInceton Scorekeeping Method
PSTAR	Primary and Secondary Term Analysis and Renormalization
PTAC	Package Terminal Air Conditioner
PV	Photovoltaic
P2P	Peer-to-Peer
RH	Relative Humidity
ROM	Reduced-Order Model
RTP	Real-Time Pricing
SEER	Seasonal Energy Efficiency Ratio
SG	Smart Grid
SM	Smart Meter
STEM	Short-Term Energy Monitoring
$T_{c.b.}$	Cooling Balance-Point Temperature

$T_{h.b.}$	Heating Balance-Point Temperature
T_{OA}	Outside Air Temperature
TOU	Time-Of-Use
TRY	Test Reference Year
VPP	Variable Peak Pricing

TABLE OF CONTENTS

Page

LIST OF FIGURES

Page

LIST OF TABLES

Page

CHAPTER I

INTRODUCTION

1.1. Background

Today, utility companies are installing Smart Meters (SMs) that record the hourly or sub-hourly (i.e., 15-minute interval) electricity consumption of their residential customers using wireless communication that sends the consumption data back to the utility through the utility grid (US EIA, 2015). In Houston, more than 2.4 million SMs have been installed (CenterPoint Energy, 2017; SMT, 2014). SMs can provide cost benefits for utilities because of potential electric demand reductions, faster outage detection, and faster restoration of service (CPUC, 2010). In order to help utilities reduce their electric demand, several studies have developed new approaches using data from SMs. For example, Mohsenian-Rad et al. (2010) and Ramchurn et al. (2011) developed demand management algorithms to reduce electric demand using the utility's communication network with the SMs. Their algorithms helped utility companies avoid high electric loads during peak hours by reducing the electric loads at participating customers' residences. In addition, Mathieu et al. (2011) developed a regression model using the 15-minute interval data from the SMs. This regression model can be used to evaluate electric demand response programs for utility companies, so they can better target the most effective measure for demand reduction. Darby (2010) also described how smart thermostats and smart appliances can be used to better manage their peak electric demand by wirelessly communicating with the grid. In her study, she explained

that utility companies can wirelessly control smart thermostats and turn on and off smart appliances to help reduce the electric demand on the grid during peak periods.

While utility companies are poised to benefit from SMs, homeowners can also benefit by reacting to timely information, which may improve the management of their electricity use through their SMs (CPUC, 2010; BES, 2013). For example, Darby reviewed the electricity saving benefits by interpreting the real-time data (i.e., SM data) using in-home, real-time displays. She showed that the proper interpretation of the real-time data can allow homeowners to check unusual electricity consumption and evaluate whether or not their energy reduction strategies are actually saving electricity. In addition, the use of home displays with real-time electricity use data helped homeowners turn their electric appliances on or off, use them less, or replace them with alternative ones, thereby saving electricity (Darby, 2010). Her study showed expected electricity saving opportunities of 15 % from the use of home displays with SM data.

More recently, the continued development of the wireless technologies and the proliferation of smart phones has accelerated the development and application of Home Automation Devices (HADs) that are capable of communicating with smart phones and SMs, which have the potential to benefit both utility companies and homeowners. This technology has recently become possible due to improvements in wireless remote controls and display technologies, as well as reduced device costs (Fitts, 2014). Protocols such as ZigBee (ZigBee Alliance, 2014), Z-Wave (Sigma Designs, 2014), Wi-Fi (Wi-Fi Alliance, 2014), INSTEON (INSTEON, 2014), and X10 (X10.com, 2013) have been developed and are now used to wirelessly connect the HADs using low power,

radio-frequency wireless networks (Frizell, 2014). Large companies such as Google and Apple have also been developing internet-connected HADs because the companies are interested in developing a digital framework to combine and manage HADs for homeowners to provide more convenience and increased functionality (Miller, 2014).

In summary, several utility companies and research institutes have shown interest in using SMs and HADs to help reduce peak electric demand for utility companies and reduce total electricity use for homeowners. However, almost all of the previous studies have focused on the peak electric demand reduction benefits for utility companies rather than the electricity usage reductions for homeowners (Mathieu et al., 2011; Price et al., 2013; Bouhou, 2014). In other words, it appears that utility companies and research institutes have mostly studied the methods for reducing the peak electric demand for the benefit of utility companies rather than studying methods for reducing the electricity consumption for homeowners. Few of the previous studies have focused on how much electricity use can be saved by homeowners when HADs are successfully combined with the electricity use data recorded by SMs and what the reasons would be for the savings. In addition, the previous studies have not developed analysis methods for better predicting the savings to homeowners from the use of HADs. Therefore, the purpose of this study is to develop new method(s) that can help homeowners better quantify and predict how they can reduce their electricity consumption when HADs are used with SMs. These proposed new method(s) will build on and enhance the features of existing analysis methods so they can be applied to the hourly and sub-hourly time scale of HADs.

1.2. Purpose and Objectives

The purpose of this study is to quantify and predict the electricity savings of homes equipped with Home Automation Devices (HADs) using the electricity use data recorded by Smart Meters (SMs) at the homeowner's electric service connection to the utility. This study will develop new method(s) that can help quantify and predict home energy savings from HADs using the interval electricity data recorded by SMs. The effectiveness of the methods will be verified using before-after measured data from a case-study house with a SM that is retrofitted with HADs.

This research has the following objectives:

1. Determine a baseline using hourly electricity consumption data from a case-study house equipped with a SM.
2. Select and develop new statistical models to better analyze hourly electricity savings from the case-study house equipped with HADs.
3. Develop a two-way calibrated building energy simulation model using the SM data and environmental data to better quantify and predict electricity savings from the use of HADs.
4. Quantify actual electricity savings from the use of HADs at the case-study house using the electricity use data recorded by the SM.

1.3. Organization of the Dissertation

This dissertation has six chapters, including: 1) Introduction, 2) Literature Review, 3) Significance and Limitations, 4) Methodology, 5) Results, and 6) Summary and Future Work, as well as supporting materials provided in appendices.

CHAPTER II

LITERATURE REVIEW

This literature review covers: (a) definitions and a review of smart home technologies including Smart Grid (SG), Smart Meters (SMs), Home Automation Devices (HADs), and Home Energy Management Systems (HEMs) (i.e., Section 2.1) and (b) a review of existing methods to analyze and predict energy use savings and peak electric demand reductions in buildings (i.e., Sections 2.2 and 2.3).

2.1. Defining Smart Home Technologies

Many utility companies have installed Smart Meters (SMs), also called Advanced Metering Infrastructure (AMI), for residential homes and commercial buildings in the U.S., which are the part of the Smart Grid (SG) that integrates an electricity grid with communication networks using software and hardware devices (Faruqui et al., 2011; Carvallo and Cooper, 2011). In 2013, approximately 52 million electric SMs were installed in the U.S. for residential, commercial, and industrial sector customers, including 46 million SMs for residential buildings (US EIA, 2013a). In addition, it has been estimated that approximately 65 million SMs will be installed for residential buildings by 2015 (Faruqui et al., 2011). Along with the growing interest in SMs, the development of the internet and internet-connected smart phones has also accelerated the applications of Home Automation Devices (HADs) that can also

communicate with SMs and smart phones (Faruqui et al., 2011; Fitts, 2014). The following subsections will cover the review of the SG, SMs, and HADs.

2.1.1. A Review of the Smart Grid (SG)

The Smart Grid (SG) is an electric utility grid that integrates the electricity grid with communication networks to monitor, control, and manage electric utility systems. The elements of the SG include: computerized and automated high-speed, two-way communication technology and digital devices (EPRI, 2008; Carvallo and Cooper, 2011; US DOE, 2015). The SG consists of the following sub-systems: Distributed Control Systems (DCSs), Energy Management Systems and Supervisory Control and Data Acquisition (EMS/SCADA), Distributed Automation (DA), Advanced Metering Infrastructure (AMI) (i.e., SMs), and Distributed Energy Resources (DERs). The DCSs connect central power plants with utility control centers (i.e., transmission and distribution grids), which are generally hard-wired, using high-speed connectivity. EMS/SCADA and DA are used to monitor and control electricity in transmission and distribution grids. AMI is used mostly to collect electricity use data to bill consumers for their electricity consumption using wireless communication networks. AMI can also be used to better manage electricity outage information and control peak electric demand. DERs, including Distributed Generation (DG), Electric Vehicle (EV), and Energy Storage (ES), are systems that manage electricity use at the end-use level of the SG (Carvallo and Cooper, 2011; EPRI, 2014). The first generation of the SG (i.e., Version 1.0) had EMS/SCADA, DA, and AMI. The second generation of the SG (i.e., Version

2.0) has additional DERs including DG, EV, and ES. The future SG (Version 3.0) will have additional energy roaming and Peer-to-Peer (P2P) energy trading functions, as well as other capabilities (Carvallo and Cooper, 2011).

According to Pratt et al.'s study, the SG can contribute to electricity savings and CO_2 emissions reduction. The study's results show that the SG can save electricity use and reduce CO_2 emissions in the U.S. using nine mechanisms: i) consumer information and feedback systems, ii) joint marketing of energy efficiency and demand response programs, iii) performance diagnostics in residential and small/medium commercial buildings, iv) Measurement & Verification (M&V) for energy efficiency programs, v) shifting load to more efficient generation, vi) support for additional EVs and plug-in hybrid EVs, vii) conservation voltage reduction and advanced voltage control, viii) solar generation support, and ix) renewable wind generation integration (Pratt et al., 2010).

Additionally, Pratt et al. reported that the potential total direct reduction using all the nine SG technologies was estimated to be approximately 12% for both electricity and CO_2 in 2030. The total indirect reduction was approximately 6% for both electricity and CO_2, where the direct reductions represent direct electricity and CO_2 emissions reductions through the applications of the SG technologies, and the indirect reductions indicate cost savings from the reinvestment of additional purchases for cost-effective energy efficiency measures or renewable energy (Pratt et al., 2010).

In the SG, consumer information and feedback systems (i.e., the first mechanism) were an approach to engage homeowners and provide effective feedback according to Pratt et al.'s study. Previous studies showed that a feedback system can change

consumers' consumption behavior. For example, Fischer, Faruqui et al., and Ehrhardt-Martinez et al.'s studies concluded that feedback systems can achieve 4% to 20% electricity savings (Fischer, 2008; Faruqui et al., 2010; Ehrhardt-Martinez et al., 2010). Feedback systems can effectively provide consumers information by compiling actual electricity use data based on a recent period (i.e., daily or weekly). Such systems may even suggest actions and show historical or normative electricity use as comparisons (Pratt et al., 2010). Using the direct calculation method, the study expected that the consumer information and feedback systems could save electricity use of 3% and reduce CO_2 emissions of 3% in the U.S. in 2030 (Pratt et al., 2010).

Pratt et al.'s study also investigated a joint marketing of energy efficiency and demand response programs (i.e., the second mechanism) to estimate the synergistic effect of energy efficiency and demand response programs (Pratt et al., 2010). Energy efficiency programs include one-time measures such as installing high-efficiency air conditioning systems or lighting equipment, which are different from demand response programs that involve customer curtailment behaviors such as lowering or raising thermostat setpoints in the summer or winter and turning off lighting equipment (Gardner and Stern, 2008). Utility companies often administer energy efficiency and demand response programs separately. Thus, Pratt et al.'s study expected that a joint program can offer reduced administration costs and increased savings from the energy efficiency and demand response programs if the two programs are combined. No savings and reductions were expected through the joint marketing of energy efficiency and demand response programs when the direct estimation was applied, but electricity

savings of 0.05% and CO_2 emissions reduction of 0.04% were expected in the U.S. in 2030 if the administration costs and the increased savings were reinvested for energy efficiency programs (i.e., the indirect estimation) (Pratt et al., 2010).

Performance diagnostics in residential and small/medium commercial buildings (i.e., the third mechanism) was also evaluated in Pratt et al.'s study. A performance diagnostics survey was conducted by profiling the data from Heating, Ventilating, and Air Conditioning (HVAC) systems in buildings to detect malfunctions of the systems using the SG's real-time sensing and two-way communication technology. In addition, the study reported that the SG can provide whole-building electricity use, duty cycles of HVAC systems, and present and future electricity prices to optimize electricity use, cost and system efficiency (Pratt et al., 2010). The study expected that the direct electricity savings of 3% and CO_2 emissions reduction of 3% were possible. No indirect savings and reductions were expected in the U.S. in 2030 through the performance diagnostics (Pratt et al., 2010).

Measurement and Verification (M&V) for energy efficiency programs in the SG (i.e., the fourth mechanism) can provide utilities with a method to measure and verify their energy efficiency programs. In addition, the M&V approach can provide other benefits such as system performance monitoring, operation and maintenance enhancement, and system fault detection using the real-time data sensing and two-way communication technology of the SG. The study expected direct electricity savings of 1%, CO_2 emissions reduction of 1%, indirect electricity savings of 0.5%, and CO_2

emissions reduction of 0.5% in the U.S. in 2030 through the M&V programs (Pratt et al., 2010).

Shifting load to more efficient generation (i.e., the fifth mechanism) was a strategy reviewed in Pratt et al.'s study to move electricity loads from a peak load time to an off peak load time. A demand response program and a distributed storage system can be used to shift loads, which are typically from an inefficient power plant to a more efficient power plant (i.e., generation resource). The study estimated that shifting load to a more efficient generation period could achieve direct electricity savings of 0.04% and CO_2 emissions reductions of 0.03% in the U.S. in 2030 (Pratt et al., 2010).

The support for additional Electric Vehicles (EVs) and Plug-in Hybrid EVs (PHEVs) (i.e., the sixth mechanism) was also one of the methods in the SG for electricity and CO_2 emissions reductions according to Pratt et al.'s study. EVs and PHEVs with on-board batteries that can be charged with electricity from a power plant can save electricity use and reduce CO_2 emissions compared to gasoline-fueled vehicles (Kintner-Meyer et al., 2007). The study mentioned that an additional benefit of the SG was that it can change the charging times of EVs and PHEVs to avoid inefficient peak electric load times on the grid. The study estimated that the support for additional EVs and PHEVs could achieve direct electricity savings of 3% and CO_2 emissions reductions of 3% in the U.S. in 2030 (Pratt et al., 2010).

Conservation voltage reduction and advanced voltage control (i.e., the seventh mechanism) were strategies that were also reviewed in Pratt et al.'s study to decrease and control the voltage in the electricity distribution system. The Conservation Voltage

Reduction (CVR) method can save electricity consumption at end-use device loads by lowering the voltage in the distribution system because the lower voltage lowers the electricity use (i.e., Watts = Amps x Volts). Unfortunately, the lower voltage used by CVR causes the utility's electric losses to increase since the voltage decrease can cause an increase in the electric current in the distribution system, which increases losses. Therefore, the SG's voltage management technology must optimize the voltage level within acceptable loss limits. The study estimated direct electricity savings of 2% and direct CO_2 emissions reductions of 2% in the U.S. in 2030 using the CVR and advanced voltage control. No indirect reductions were expected (Pratt et al., 2010).

Effective solar generation support in the SG (i.e., the eighth mechanism) was an approach to actively use solar photovoltaic (PV) systems in the SG, which was also reviewed in Pratt et al.'s study. PV systems that directly convert solar energy into electricity are becoming a viable strategy for distributed power production as PV system prices drop (Kroposki et al., 2008). Unfortunately, when a PV system generates more electricity than the electricity required by the residential or commercial building where the array is installed, the PV system generates reverse power flow from the building to the distribution system in the SG. This reverse power flow can be a serious problem because today's electricity grids (i.e., non-SG) do not control the voltage at each PV system and therefore must have short-circuit protection to block any unwanted reverse power flow into the distribution systems. Therefore, future SGs will need to be designed to operate with controlled reverse power flows (i.e., from the customer to the grid). Therefore, the study did not estimate direct and indirect electricity use and CO_2

emissions reductions using such types of PV system power generation supported by the SG. However, the study recommended the development of an estimation method for analyzing PV generation benefits in the SG (Pratt et al., 2010).

Renewable wind energy generation integration (i.e., the ninth mechanism) was a strategy to integrate wind energy generation into the SG, according to Pratt et al.'s study. The power generated from wind turbines has been increasing due to the improved economic competitiveness with federal tax credits. However, assimilating the wind power integration with the grid is a challenge because wind generation is unpredictable and has large ups and downs in the production of electric power as the wind speed varies. Thus, the SG using two-way communication and control technologies would be needed to increase the usability of the electric wind power generation as well as the integration in the use of demand response programs and distributed generation and storage systems (Todd et al., 2009). The study estimated that the renewable wind energy generation integration could achieve direct electricity savings of 0.02% and CO_2 emissions reductions of 0.02% in the U.S. in 2030. In addition, indirect electricity savings of 5% and CO_2 emissions reductions of 5% were expected from wind power generation in the U.S. in 2030 (Pratt et al., 2010).

In summary, the previous studies estimated that the SG can better control and manage electricity use on the electric grid. Furthermore, Pratt et al.'s 2010 study showed that there is a good potential for electricity savings and CO_2 emissions reduction from the use of nine specific SG technologies. However, the previous studies did not specifically analyze how much the use of Home Automation Devices (HADs) can

contribute to the electricity savings for homeowners in the SG. Therefore, this study will investigate how much electricity homeowners can save using before-after measurements of a case-study residence with HADs installed as well as simulation to quantify the electricity savings from the use of HADs. Specifically, this proposed study seeks to quantify homeowners' electricity savings in homes equipped with HADs and SMs through the use of statistical models and calibrated simulation models applied to measured data from a case-study house.

2.1.2. A Review of Smart Meters (SMs)

Smart Meters (SMs), also called Advanced Metering Infrastructure (AMI), are connected to the SG to provide benefits for utility companies and homeowners. Utility companies currently claim the following benefits from SMs: first, they can connect and disconnect their electric meters for customers remotely, which saves the costs associated with sending one or more utility personnel to a site; second, they can read the meters remotely through wireless technology, which also saves the costs of sending utility personnel; third, the use of SMs can provide electric demand reduction programs using time-based information (i.e., interval data) from buildings with SMs and wireless on/off load-shedding of selected loads (i.e., Direct Load Control (DLC)); fourth, utility companies can detect and pinpoint outages faster and restore service sooner because consumption can be monitored remotely; fifth, SMs can collect and store interval data meter readings for several days to provide data continuity during periods of power interruptions; sixth, SMs can be used to integrate data management systems into building

energy management systems; and seventh, some utility companies have proposed extending the SG and the AMI to appliances (i.e., Home Automation Devices (HADs)) using SMs, etc. (CPUC, 2010; Pratt et al., 2010; Sensus, 2015; BTU, 2015).

The key functionality of SMs is to communicate both ways between utility companies and customers using wireless radio frequency communications. With such a system, utility companies can receive meter readings from their customers and control electric loads using secured wireless channels, which can provide the benefits mentioned above for utility companies and homeowners. In addition, specially equipped SMs may have an additional wireless communication radio, which is called a Home Area Network (HAN). This HAN is a wireless network that has its own lower frequency, which is different from the radio frequency used between the utility companies and the SMs (SGCC, 2011; SDGE, 2015a). The HAN that connects the SMs and the Home Automation Devices (HADs) can provide new opportunities for saving energy for homeowners and reducing peak electric demand for utility companies.

Another key functionality of SMs is that they can record daily, hourly, 15-min interval, or shorter interval electricity consumption based on the type of SMs, while conventional electric utility meters only provide monthly electricity consumption and demand (US EIA, 2015). Such higher frequency consumption data can provide beneficial opportunities for utility companies and homeowners. For example, for utility companies, demand reduction programs using temporal or time-based information that relies on the interval electricity consumption data can reduce the need to build a new power plant by avoiding higher peak electric demand using a load-shedding program

with participating customers. For homeowners, in exchange for the inconvenience of load-shedding, the utility demand reduction programs can provide lower retail electricity rates because utility companies can share the savings from the avoided costs of building and operating new peak plants with their customers (CPUC, 2010).

Furthermore, using the interval electricity consumption data, time-based dynamic pricing programs and incentive-based programs can be used by utility companies, and information and control technologies can be used by specific devices in a house to save energy for homeowners (US DOE, 2012). Time-based dynamic pricing programs for the utility company benefits have various forms such as Time-Of-Use (TOU) rates, Real-Time Pricing (RTP), Variable Peak Pricing (VPP), and Critical Peak Pricing (CPP). The time-based dynamic pricing programs typically charge less for electricity use during non-peak load periods, and more during peak load periods using time information based on the hour-of-the-day and the day-of-the-week in order to shed electric loads or reduce peak electric demand. In addition, incentive-based programs for the utility company benefits can use Direct Load Control (DLC) systems equipped with wireless radio-controlled on/off switches. With the homeowners' agreement, utility companies can install DLC systems for end-use devices (e.g., air conditioning and water heating systems) and turn off the devices during a predetermined peak time. Utility companies may also provide homeowners financial incentives for their participation.

Finally, information and control technologies for homeowners can include the following: In-Home Displays (IHDs), mobile devices, web portals, Programmable Communicating Thermostats (PCTs), and other system management tools. IHDs, mobile

devices, and web portals, which are classified as information technologies, provide homeowners with improved feedback about their electricity use and cost information to better control their electricity use. PCTs and other management tools, which are classified as control technologies, provide homeowners more efficient control opportunities to manage their building systems such as air conditioning and water heating systems. Home Energy Management Systems (HEMS) with the Home Area Network (HAN) may also be used to automatically control the systems. For the utility company benefits, utility companies can also use the control technologies to control the systems using the incentive-based programs (e.g., DLC) (US DOE, 2012).

However, even though several studies have shown the potential benefits from SMs, most of the previous studies have focused on the benefits of the electric demand reduction for utility companies (Mohsenian-Rad et al. 2010; Ramchurn et al., 2011; Mathieu et al., 2011; Darby, 2010; US DOE, 2012; Harris et al., 2012). Few studies have reported the benefits of energy savings for homeowners. Therefore, this study will develop procedures to quantify and predict the electricity savings from SMs to homeowners, which are connected to Home Automation Devices (HADs), which is of interest to most homeowners who want to use SMs to save money on their own utility bills (Accenture, 2011).

2.1.3. A Review of Home Automation Devices (HADs) and Home Energy Management Systems (HEMS)

The development and wide-spread use of the internet and smart phones has recently accelerated the applications of Home Automation Devices (HADs) that can wirelessly communicate with the SMs. Many companies have shown interest in HADs using an

internet-connected technology, also called the Internet of Things (IoT) (Jasper, 2015; Moorhead, 2013). There are several HADs from vendors that feature wireless control of thermostats, power outlets, lighting devices (i.e., energy management), smoke and CO detection, water leak detection (i.e., convenience), security cameras (i.e., security), etc. Furthermore, the HADs that are wirelessly connected have potential energy saving opportunities by optimizing the performance of the homeowner's appliances (Faruqui et al., 2011; Fitts, 2014; Walsh, 2014; SDGE, 2015b; Nest, 2015). For instance, when a homeowner leaves from home, a wirelessly-connected thermostat (i.e., PCT) can be controlled by his or her smart phone to raise the setpoint temperature of an air conditioning system in the summer or lower the setpoint of a heating system in the winter, which can save energy and reduce costs for the homeowners (Nest, 2015). The U.S. Energy Information Administration's (US EIA) survey shows that the residential energy consumption of lighting, appliance, and electronic devices increased from 24% in 1993 to 35% in 2009, so the potential saving opportunities through the HADs have also been increasing (US EIA, 2013b). In addition, many HADs can now be controlled by the wireless network between the HADs using a Home Energy Management System (HEMS), which further increases their effectiveness (Bojanczyk, 2013a, 2013b).

For controlling different HADs, several Home Area Networks (HAN) have been developed using protocols such as: ZigBee (ZigBee Alliance, 2014); Z-Wave (Sigma Designs, 2014); Wi-Fi (Wi-Fi Alliance, 2014), INSTEON (INSTEON, 2014); and X10 (X10.com, 2013). HANs use lower frequency radio waves than the frequency of the devices used between the utility companies and their customers' SMs (SGCC, 2011;

SDGE, 2015a). For most practical purposes, HANs are considered a residential Local Area Network (LAN) for close communication between digital devices (i.e., HADs or IoT) in a house (King, 2010; Home Network, n.d.).

Using the HAN, the HEMS could analyze the data from HADs to better control and optimize the use of lights and appliances (i.e., HADs) connected to the HAN to provide homeowners with improved home automation (i.e., convenience), energy management, and security services (Bojanczyk, 2013a). The most advanced HEMS provides a web portal (i.e., web page), a stand-alone computer program, a mobile application device, or a dedicated In-Home Display (IHD) to help homeowners make informed decisions to better manage the lights and appliances in their residences (US DOE, 2012; Nest, 2015; Opower, 2015). In addition, some HEMS have a Programmable Communicating Thermostat (PCT) that can be used by both utility companies and homeowners to wirelessly control heating and cooling systems of a house (US DOE, 2012; Nest, 2015; Honeywell, 2015). Some HEMS may also provide Direct Load Control (DLC) using wireless control switches that can be activated under an agreement with the homeowner's utility company to turn lights and appliances on and off as well as cooling and heating systems to reduce electricity use during peak demand periods for the utility (US DOE). Finally, Do It Yourself (DIY) methods for HEMS are also being used to allow homeowners to create and use their own controller for HADs (Raspberry Pi, 2015; Arduino, 2015).

However, surveys show that the greatest interest of homeowners who want to use HADs and HEMS is to better control their lights and appliances and to do so without

committing their time and/or additional money to achieve home energy savings in a non-intrusive way (Accenture, 2011; Wesoff, 2011; Alford, 2015). Unfortunately, only a few studies have quantified the potential energy savings from the improved control of lights and appliances (i.e., HADs) by HEMS even though many companies claim that the HADs controlled by the HEMS can provide potential energy savings for homeowners (Nest, 2015; Opower, 2015).

Therefore, it is important to study and document the electricity savings from HADs separately or in combination with HEMS. Such a system should also be capable of improved predictions of energy savings for different scenarios to help reduce the uncertainty of the saving estimates. Verifying the potential savings from case study homes with measured data from HADs would also be an important milestone.

2.2. A Review of Previous Methods for Building Energy Analysis

Methods to analyze building energy use have been developed to more accurately estimate or predict energy use in buildings. Annual, monthly, daily, and hourly energy estimating methods have been developed to analyze and predict cooling and heating energy in a building. Such estimating methods can also be used to calculate energy savings, improve energy efficient designs, develop automated diagnostics, and provide improved cooling/heating load and operational controls using predictive models (Rabl, 1988; ASHRAE, 2013a).

According to the 2013 ASHRAE Handbooks of Fundamentals (ASHRAE, 2013a), building energy estimating methods can be categorized into three categories:

forward, inverse (or data-driven), and calibrated simulation methods. Forward methods use known descriptions or parameters of physical building characteristics such as a building size, HVAC system type, and operating schedules as inputs to a complex mathematical model of the dynamic heat transfer between a building and its environment. Such a model then calculates or predicts the energy use of the building for specific ambient climate conditions and occupancy schedules. Inverse methods deduce the building performance parameters from measured (i.e., actual) building performance data such as electricity, cooling, and heating use. Finally, calibrated simulations use the features of both the forward and the inverse methods to develop models of actual buildings that are tuned to measured data from the buildings.

Furthermore, forward and inverse methods are divided into two subcategories: steady-state methods and dynamic methods. Steady-state methods use a limited number of parameters to simplify the calculation of building energy consumption using daily or monthly energy use data rather than hourly or sub-hourly data. Dynamic methods account more accurately for changing conditions for cooling and heating loads in a building and the complexities of HVAC systems. Typically, Dynamic methods were developed for use in computer simulation programs with hourly or sub-hourly data (ASHRAE, 1981). In the next section, energy estimating methods will be reviewed including: forward, inverse, and calibrated simulation methods.

2.2.1. Building Energy Estimating Methods – Forward Methods

Forward methods use known descriptions or parameters of physical building characteristics, such as building size, HVAC system type, and operating schedule, as inputs to a complex mathematical model of the dynamic heat transfer between a building and its environment. Thus, forward methods can be used to predict energy consumption using the information that describes the building design characteristics before a building is physically built. Forward methods are further classified as steady-state methods or dynamic methods.

Forward steady-state methods tend to be simplified methods (i.e., fewer calculations) that are used to calculate energy consumption (ASHRAE, 2013a). Forward steady-state methods include the following: the degree-day method (ASHRAE, 1962), the variable-base degree-day method (Fels, 1986; Reddy et al., 1997; Sonderegger, 1998), the forward bin method (ASHRAE, 1976), and the modified bin method (ASHRAE, 1981; Knebel, 1983).

The degree-day method uses the temperature difference between a balance-point temperature and an outside air temperature. The balance-point temperature indicates a temperature at which heat gains inside a building counterbalance heat losses to the outside. The degree-day method calculates the temperature difference between the balance-point temperature and the outside air temperature over a specific time period (i.e., daily or hourly) to characterize a climate's heating or cooling demands. The calculation results are defined as degree-days or degree-hours (ASHRAE, 1962, 2013). The modified degree-day method was developed to account for system efficiency and

performance using correction factors (ASHRAE, 1976). In addition, the variable-base degree-day method was developed to improve the modified degree-day method. The variable-base degree-day method uses the degree days, which are a function of the building's actual balance-point temperature, to consider the differences in the thermostat setpoint schedules in a building (ASHRAE, 1985, 2013). This method was also applied in the PRInceton Scorekeeping Method (PRISM) for analyzing residential energy use (Fels, 1986).

The bin method is an update to the previous degree-day method. The bin method calculates building energy consumption within temperature bins (usually 5 F° intervals) and multiplies the energy used in each consumption bin by the hours that fall within the temperature bins over a given period. This approach improves the previous degree-day methods because it can consider various system efficiencies and the heat gain from occupants or other internal loads using separated temperature intervals (i.e., bins) (ASHRAE, 1976, 2013). In addition, the modified bin method improves the bin method by accounting for occupied and unoccupied periods and diversified loads rather than peak loads. In addition, the modified bin method (Knebel, 1983) separately calculates conduction, infiltration, internal, and solar loads and adds the loads to estimate the total energy consumption. The modified bin method also provides an improved analysis for HVAC systems in a building versus the bin method because the modified bin method uses more realistic equipment efficiencies at the part load conditions of HVAC systems (ASHRAE, 1981, 2013; Knebel, 1983).

Forward dynamic methods are more detailed than steady-state methods (i.e., more calculations) because they consider short time interval effects such as thermal mass. Forward dynamic methods generally use hourly or sub-hourly energy consumption data, which allow them to analyze dynamic building loads, operational controls and diagnostics. Forward dynamic methods can also be used to calculate energy savings and to evaluate different designs. Forward dynamic methods include the following: the response factor method (Mitalas and Stephenson, 1967; Stephenson and Mitalas, 1967) and the whole-building energy simulation method (Winkelmann et al., 1993; LBNL and JJH, 1998; Crawley et al., 2001).

Forward dynamic methods more accurately account for the detailed building energy use compared to the steady-state methods (ASHRAE, 2013a). For example, the whole-building energy simulations calculate hourly or sub-hourly building energy consumption using multiple layers of calculations, including: space cooling and space heating loads, secondary HVAC system loads, and primary equipment loads (i.e., plant). Currently, the whole-building energy simulation method is a widely-used approach that uses the forward dynamic method. Such simulation models have become readily available as advanced, high-speed computers with large amounts of memory have become available that allow users to consider a multitude of input parameters. EnergyPlus, DOE-2.1E, eQUEST, and TRNSYS are the most widely used whole-building energy simulation programs in the U.S. To calculate the energy use in a building, EnergyPlus (Crawley et al., 2001) uses the Heat Balance Method (Pedersen et al., 1997). Whereas, DOE-2.1E (Winkelmann et al., 1993) and eQUEST (LBNL and

JJH, 1998) use the Weighting Factor Method (Mitalas and Stephenson, 1967; Stephenson and Mitalas, 1967), and TRNSYS (Klein et al., 1976) uses the Thermal Network Method (Paschkis, 1942; Buchberg, 1958) and the Heat Balance Method to calculate the dynamic space heating and cooling loads. The detailed equations used in the computer simulation programs require thousands of calculations to account for the thermal mass effect in a building (ASHRAE, 2013a). The origins of the dynamic space cooling and heating load calculation methods can be found in Oh and Haberl's 2016 study (Oh and Haberl, 2016; Oh, 2013).

In summary, forward methods use known descriptions or parameters of physical building characteristics. Forward methods require detailed parameter information to accurately calculate building energy use. If only a few parameters are available, then the result of a forward method may be inaccurate. Therefore, for this study, detailed parameters of the case-study residence and the use of Home Automation Devices (HADs) will be used to calculate the building energy use with a two-way, calibrated whole-building energy simulation.

2.2.2. Building Energy Estimating Methods – Inverse Methods

Inverse methods deduce building's performance parameters from measured (i.e., actual) building performance data, such as electricity, chilled water, and hot water use. Thus, inverse methods can have fewer parameters than forward methods. This is because measured building energy data is typically limited to fewer parameters due to the difficulty and cost of installing and maintaining various sensors and collecting and

processing the data from the sensors. However, in certain cases, inverse methods can have higher accuracy than un-calibrated forward methods because inverse methods are based on actual performance data (ASHRAE, 2013a).

Inverse methods have also been classified as steady-state or dynamic methods in the same fashion as forward methods. In general, steady-state inverse methods are simplified methods (i.e., fewer calculations) that do not consider the short-term effects such as thermal mass, system on/off, or occupancy parameters. Inverse steady-state methods generally use monthly, weekly, or daily energy consumption data rather than hourly or sub-hourly consumption data. In spite of this, inverse steady-state methods can be used to develop accurate baseline models if sufficient measured data are available (ASHRAE, 2013a). Steady-state, inverse methods include the following: simple linear regression models (Ruch and Claridge, 1991; Kissock et al., 1998), multiple linear regression models (Haberl, 1986; Dhar, 1995; Dhar et al., 1998, 1999a, 1999b; Sonderegger, 1998; Katipamula et al., 1998; Ali et al., 2011), improved multiple linear regression models (Abushakra et al., 2012; Paulus, 2012), an inverse bin method (Thamilseran and Haberl, 1994), change-point models (Ruch and Claridge, 1991; Kissock et al., 1998), improved change-point models (Sever et al., 2011; Kissock, 2015; Abushakra et al., 2012), piecewise-linear models (Mathieu et al., 2011), and Reduced-Order Models (ROMs) (Cole et al., 2014).

Widely-used, inverse steady-state methods for analyzing building energy performance include change-point linear models, simple linear regression models, and multiple linear regression models (Curtiss et al., 2001; Haberl and Culp, 2013). The

change-point linear and simple linear regression models usually use the outdoor dry-bulb temperature as the independent variable because it is the most crucial independent variable for calculating building energy use. The two parameter (2P) linear regression model has two parameters where one is the y-axis intercept, which sometimes represents the base energy consumption, and the other is the slope of energy use as a function of the outside temperature, which can be used to analyze a building that always uses either cooling or heating energy (Curtiss et al., 2001; ASHRAE, 2013a). The three parameter (3P) change-point linear regression model has one more parameter that describes the change point to differentiate between weather-independent energy use and weather dependent (i.e., the outside temperature) energy use. The 3P change-point linear model is widely used for monthly utility bill analyses of residential buildings (Curtiss et al., 2001; ASHRAE, 2013a; Baltazar et al., 2014).

The four parameter (4P) change-point linear model has an additional parameter that represents the lower or upper slope below or above the change point. The 4P model is useful in analyzing energy consumption in commercial buildings because it provides an improved model of cooling or heating energy use in commercial buildings (Ruch and Claridge, 1991; Curtiss et al., 2001; ASHRAE, 2013a). Finally, the five parameter (5P) change-point linear model has one additional parameter that represents a second change point. The 5P model provides an improved model in buildings that have both electric cooling and electric heating systems (Kissock et al., 1998; Curtiss et al., 2001; ASHRAE, 2013a).

In addition, multiple linear regression models can also be used to analyze energy consumption that accounts for multiple independent variables such as the day-of-the week, outside air temperature, humidity, solar, and wind data. The users of these models can calculate the impact of multiple influencing parameters when it is needed. However, the users should carefully choose the independent variables because the independent variables can be correlated (i.e., they can be related to one or more of the other independent variables), which can over-state or under-state the importance of a single variable (Haberl, 1986; Kissock et al., 2001; Curtiss et al., 2001; ASHRAE, 2013a).

Inverse dynamic methods are more detailed than inverse steady-state methods (i.e., more parameters and calculations) and can consider short-term effects such as thermal mass. In some cases, such models can even use differential equations to describe a building's energy use (Curtiss et al., 2001; Haberl and Culp, 2013). Inverse dynamic methods generally use hourly or sub-hourly energy consumption data, so they can be used to analyze heating and cooling loads and certain operational controls and diagnostics as well as to measure energy savings from building retrofits. Inverse dynamic methods include the following: Artificial Neural Networks (ANN) methods (Kreider and Wang, 1991; Kreider and Haberl, 1994), Autoregressive Moving Average (ARMA) models (Seem and Hancock, 1985; Rabl, 1988; Reddy, 1989; Armstrong et al., 2006), differential equation methods (Rabl, 1988), thermal network methods (Sonderegger, 1978; Rabl, 1988; Reddy, 1989), modal analysis methods (Bacot et al., 1984; Rabl, 1988), and equation-based methods (Wetter et al., 2011).

One widely used example of an inverse dynamic method is the Artificial Neural Network (ANN) method. The ANN method has several layers (i.e., neurons) to connect input parameters and outputs (i.e., regression coefficients) using input, hidden, and output layers. These connections transport unique information from the input parameters (i.e., sending neurons) to the model outputs (i.e., receiving neurons). In the ANN, the outputs "learn" from the inputs to minimize model errors until the user's accuracy goal has been achieved. After the learning process (i.e., training the ANN to the training dataset), an activation function is determined and used so the ANN can accurately predict a new output when presented with new inputs. Although ANNs can provide high accuracy, it is completely dependent on the training data that is used to train the model. Furthermore, its neurons or parameters may not have physical meanings like the forward methods nor can it accurately predict conditions outside the range of the training data (Curtiss et al., 2001; ASHRAE, 2013a).

In summary, inverse methods use actual building performance data and coincident weather data to determine regression coefficients, while forward methods use assumed input data, engineering equations, and representative or actual weather data to calculate the building energy use. For this study, the inverse approach will be used to quantify and predict the building energy use for a case-study residence with HADs. In addition, since the parameters of inverse models may not have physical meaning, and inverse models may not accurately predict conditions outside of the range of the measured data that were used to determine the regression coefficients, forward dynamic

methods (i.e., calibrated, whole-building energy simulation) will be used to quantify and predict the energy use from the new, occupancy-driven schedules of HADs.

2.2.3. Building Energy Estimating Methods – Calibrated Simulation Methods

The whole-building computer simulation mentioned in the previous section (i.e., forward method) can be calibrated using measured energy use data, indoor environmental conditions obtained from an existing building, and coincident weather data. Such a calibrated simulation can be considered a hybrid, inverse method because the inputs of the computer simulation are adjusted to better fit the simulation data to measured energy use data in much the same way a simple linear regression model is fit to measured energy use data. Such an approach has been called a calibrated simulation method. Calibrated simulation methods can provide more accurate predictions than statistical methods, especially when specific parameters can be varied to determine their influence on the overall energy use (ASHRAE, 2013a).

Reddy reviewed the existing methods for calibrating computer simulation models (Reddy, 2006), including: calibration based on manual, iterative, and pragmatic intervention (Diamond and Hunn, 1981; TRC, 1984; Hsieh, 1988; Kaplan et al., 1990a, 1990b; Hunn et al., 1992; Norford et al., 1994; Lunneberg, 1999; Pedrini et al., 2002; Yoon et al., 2003), calibration based on a suite of informative graphical comparative displays (Bronson et al., 1992; Haberl et al., 1993a, 1993b, 1993c; Bou-Saada and Haberl, 1995a, 1995b; Haberl et al, 1996; Haberl and Abbas, 1998a, 1998b; Haberl and Bou-Saada, 1998), and calibration based on special tests and analytical procedures

including: intrusive blink-tests (Soebarto, 1997; Shonder et al., 1998), Short-Term Energy Monitoring (STEM) tests (Subbarao, 1988; Manke et al., 1996), macro parameter estimation methods (Reddy et al., 1999), and signature analysis methods (Knebel, 1983; Katipamula and Claridge, 1993; Liu and Claridge, 1998; Wei et al., 1998; Haves et al., 2001; Liu et al., 2003, 2004). In addition, calibration methods using analytical/mathematical methods were reviewed, such as sensitivity analysis, identifiability analysis, numerical optimization, and uncertainty analysis (Sun and Reddy, 2006). In this effort, Reddy covered additional literature to more comprehensively review the known calibration methods.

Coakley et al. also reviewed the existing methods for calibrating computer simulations (Coakley et al., 2014). In comparison to Reddy's 2006 review, Coakley et al. categorized the calibration methods as manual methods and automated methods. The manual methods included characterization techniques (i.e., building and site audits) (Thumann and Younger, 2008), short-term end-use monitoring (STEM) (TRC, 1984), high-resolution data (Clark et al., 1993), and intrusive testing (Soebarto, 1997)), advanced graphical approaches (i.e., 3-D comparative plots) (Bou-Saada and Haberl, 1995b; Haberl and Bou-Saada, 1998), graphical statistical indices (Bou-Saada and Haberl, 1995b), signature analysis (Katipamula and Claridge, 1993), parameter reduction (i.e., day-typing and zone-typing) (Kaplan et al., 1990b), data disaggregation (Akbari et al., 1988; Akbari, 1995), procedural extensions (i.e., evidence-based development) (Bou-Saada and Haberl, 1995b; Yoon et al., 2003), sensitivity analysis (Clark et al., 1993), and uncertainty quantification (Reddy et al., 2007a, 2007b).

The automated methods included optimization techniques (i.e., objective functions (Hitchcock et al., 1991; Baltazar, 2006), penalty functions (Carroll and Hitchcock, 1993; Sun and Reddy, 2006), Bayesian calibration (MacKay, 1994) and alternative modeling techniques (i.e., Artificial Neural Networks (ANN)) (Neto and Fiorelli, 2008), Primary and Secondary Term Analysis and Renormalization (PSTAR) (Subbarao, 1988), and meta-modeling (Eisenhower et al., 2012). In summary, the Coakley et al. study extended Reddy's 2006 review using a new categorization (i.e., manual methods and automated methods) and covered additional methods published since 2006. Coakley et al. also covered literature outside the HVAC and building energy industry to provide a more comprehensive review of the calibration methods.

In summary, researchers have developed many different calibrated simulation methods to better analyze building energy use than the use of forward and inverse methods alone. In most cases, calibrated simulation methods take a longer time to calculate building energy use than other inverse methods because of the tedious nature of the calibration. However, calibrated simulation methods can include more accuracy and complexity through the use of detailed independent variables or inputs, including various schedules, varying system and equipment performance efficiencies, etc. For analyzing HADs, calibrated simulation methods are useful to more accurately estimate each end-use signature and schedule of the HADs because calibrated simulation methods have detailed parameters that can account for various schedules, etc.

2.3. A Review of Previous Methods for Real-Time Measurement & Verification (M&V), Fault Detection & Diagnostics (FDD), Commissioning, and Building Automation System (BAS)/Energy Management & Control System (EMCS)

This section provides a summary of the previous studies about real-time M&V, FDD, Commissioning, and BAS/EMCS. The details of this review were described in the previous study (Oh et al., 2014). M&V is used to quantify and verify energy savings before/after building exterior envelope modification or retrofit system/equipment installation is made using measured data. FDD is used to analyze historical data collected from whole or individual system performance to find where a fault may be detected and the possible reason of a fault. Commissioning is used to ensure that all building systems and equipment are correctly installed and operated as intended by the designer (Blanc, 1999). Typically, FDD can be categorized by one of the three following methods, which can also be used for M&V and Commissioning: a) quantitative methods, b) qualitative methods, and c) historical data methods (Katipamula and Brambley, 2005).

Quantitative methods use explicit mathematical models of systems or equipment to check building performance. These methods are the most reliable, but are the most complex and intensive of all the methods. Qualitative methods use knowledge bases or previously demonstrated qualitative relationships. The qualitative approach is appropriate for most environments and non-critical processes. However, this approach may not be applicable for the special circumstances in buildings. Finally, the historical data method (e.g., inverse method) uses statistical relationships between historical measured data from systems or equipment. This method is useful when less accuracy is

required and when there may be inadequate explanations for performance. However, this method requires a large amount of data.

As computers, building systems, and equipment have improved, real-time data has become more available for M&V, FDD, and Commissioning. In addition, big datasets (or big data) from multiple real-time datasets provides new opportunities for M&V, FDD, and Commissioning using large datasets from BAS/EMCS (or HEMS). BAS/EMCS are systems to control building HVAC systems and equipment (or HADs). BAS/EMCS using real-time data can be connected to the Smart Grid (SG) using real-time data sensing and two-way communication technology (Pratt et al., 2010). Buildings connected to the SG can have improved opportunities to analyze building systems or equipment because real-time M&V, FDD, and Commissioning can be applied to the multiple datasets from a central location at a utility. In addition, occupancy behavior related to energy use in buildings is becoming a crucial factor to better understand building energy performance and comfort (Hong et al., 2017). For residences, whole-building electricity use (i.e., SM data) and end-use electricity use (i.e., HAD data) with occupancy detection data can be used to better analyze electricity and demand savings using real-time M&V, FDD, and Commissioning approaches. For this study, large amounts of SM and HAD data will be used to quantify and predict electricity consumption/savings for a case-study house using M&V and FDD approaches.

2.4. Summary of Literature Review

This literature review covered the definitions and previous works regarding smart home technologies including: Smart Grid (SG), Smart Meters (SMs), and Home Automation Devices (HADs) and Home Energy Management Systems (HEMs). In addition, this literature review included a review of the existing methods used to analyze and predict building energy savings and peak electric demand reductions.

The findings obtained from this literature review are summarized as follows:

- Previous studies estimated that the SG can better control and manage electricity use. These studies showed there is a good potential for electricity savings for utilities and CO_2 emissions reductions from the use of nine specific SG technologies. However, the previous studies did not specifically analyze how much HADs could contribute to the electricity savings for homeowners.
- Several studies showed the potential benefits from SMs, focusing on the benefits of the electric demand reductions for utilities. Few studies covered the benefits of energy savings for homeowners.
- Surveys showed that the greatest interest of homeowners who want to use HADs and HEMS is to better control their lights and appliances and to do so without committing their time and/or additional money to achieve home energy savings in a non-intrusive way. Unfortunately, few of the studies have quantified actual energy savings from HADs controlled by HEMS even though many companies claim that the HADs controlled by the HEMS can provide potential energy savings for homeowners.

- Forward methods calculate energy consumption using known physical descriptions or parameters that describe a building's characteristics and equations regarding the heat transfer processes. However, forward methods require detailed information to accurately calculate building energy use. If only a few parameters are used, the results of a forward method can be inaccurate.
- Inverse methods use actual building performance data to determine the regression coefficients or parameters. However, the parameters from inverse models may not have physical meaning. In addition, inverse models may not always accurately predict conditions outside of the range of the measured data that were used to determine the regression coefficients or may not be useful if conditions change in the building (i.e., change in thermostat setting).
- Many different calibrated simulation methods have been developed to better analyze building energy use. Calibrated simulation methods can include more accuracy and complexity than uncalibrated methods by using detailed independent variables or inputs, including various system on/off or temperature setpoint schedules.
- As computers, building systems, and HVAC equipment have developed and improved, real-time data has become more widely-available, which has allowed it to be an important issue for M&V, FDD, and Commissioning. Big data from large, real-time databases provides new opportunities for M&V, FDD, and Commissioning using BAS/EMCS (e.g., HEMS). Finally, SM and HAD data with occupancy detection can be used to better analyze energy and demand

savings using real-time M&V, FDD, and Commissioning approaches. However, very few of the previous studies specifically analyzed how the use of HADs can contribute to electricity savings for homeowners.

In summary, most of the previous studies have focused on analyzing building energy use from SM data to provide energy saving benefits for utility companies rather than homeowners. In addition, the previous studies focused only on interval or hourly data from SMs (i.e., whole-building electricity data) and did not include the impact of interval data from Home Automation Devices (HADs). In the previous studies, in general, although regression methods were used to characterize savings, very few forward, inverse, and calibrated simulation methods were used to specifically analyze potential energy savings from the HADs for homeowners. Furthermore, the previous studies of calibrated simulation methods did not always provide detailed procedures about how to process hourly SM data for use with a calibrated simulation. In addition, the previous studies showed that big data can provide new opportunities to analyze building energy use. Therefore, there is a need to develop new approaches to better quantify energy consumption and savings from HADs when SM data is available.

CHAPTER III

SIGNIFICANCE AND LIMITATIONS OF THE STUDY

This study develops new procedures to quantify and predict the electricity savings of residences equipped with Home Automation Devices (HADs) using hourly electricity consumption data recorded by Smart Meters (SMs). Such a study is significant because few studies have focused on how much electricity use can be saved for homeowners when HADs are applied in a residence using data recorded by a SM. In addition, this study provides improved suggestions that show how homeowners can use HADs to save electricity use in their homes.

This proposed study has the following limitations:

1. This study focuses on energy savings from HAD capabilities rather than energy conservation measures, renewable energy systems, electric vehicles, or energy storage systems.
2. This study focuses on residences located in hot and humid climate zones. Therefore, the savings reported in this study may not apply to similar houses in different climates.

CHAPTER IV

METHODOLOGY

This chapter provides three methods to quantify electricity savings using interval electricity use data recorded by a SM along with coincident weather data. Such methods can analyze the savings from residences equipped with HADs. In this study, a HAD is a device that includes: wireless, programmable thermostats (i.e., Programmable Communicating Thermostat (PCT)); lighting and daylighting controls (e.g., window shades); appliance controls (e.g., internet-connected refrigerators, clothes washers and dryers, dish washers, ranges and ovens, televisions, etc.); and Domestic Hot Water (DHW) control systems, which may work with occupancy sensors. To accomplish the stated purpose, three methods were developed: 1) a statistical method to automatically quantify potential electricity savings from HADs using only SM data, 2) a two-way, calibrated simulation method to quantify detailed-potential electricity savings with additional information for a house, and 3) an M&V method to quantify actual electricity savings from a house when before/after HAD and SM data are available.

The overall methodology of this study is shown in Figure 4-1. The detailed procedures in each method are described in the following sections: Section 4.1. Development of a statistical method (Level 0 Analysis) for automatically quantifying potential electricity savings from HADs; Section 4.2. Development of a calibrated simulation method (Level I Analysis) for quantifying detailed-potential electricity savings, and Section 4.3. Development of an M&V method (Level II Analysis) for quantifying actual electricity savings. Finally, Section 4.4 summarizes the three methods.

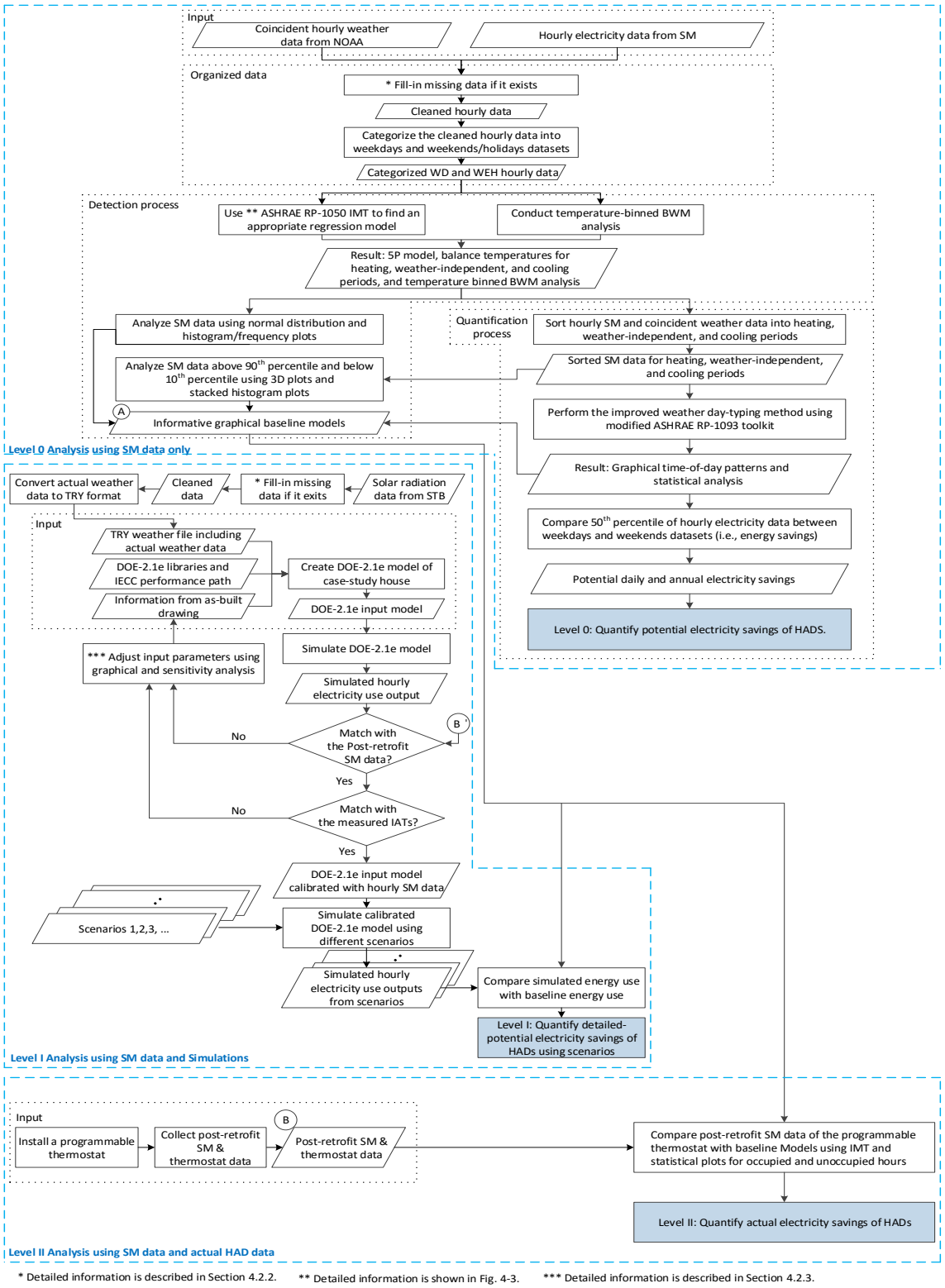

Figure 4-1. Overall methodology.

4.1. Development of a Statistical Method (Level 0 Analysis) for Automatically Quantifying Potential Electricity Savings from HADs

In this analysis, a non-intrusive method was developed to quantify the potential electricity savings from HADs using only SM data. This method (i.e., Level 0 Analysis) is intended to work without detailed physical information (e.g., drawings) about a house, relying instead on only the hourly electricity use data from a SM installed at the electric service entrance to a house and the corresponding hourly weather data (i.e., outside air temperature (OAT)) from a nearby National Oceanic and Atmospheric Administration (NOAA) (NOAA, 2016) site.

To accomplish the Level 0 analysis, the following new procedure was developed as shown in Figure 4-2. The first step in the procedure was to organize the data. To begin, the hourly SM and the coincident hourly OAT data for one year (i.e., baseline period from April 15th, 2015 to April 14th, 2016) were collected from the local utility of a case-study house and from the NOAA website, respectively. The collected data were then prepared for analysis by filling-in the missing data and merged into one file. The details for filling-in the missing data are described in Section 4.2.2. In addition, the cleaned data were categorized into two periods: weekdays and weekends/holidays. In this study, holidays include the following days: Memorial day, Independence day, Labor day, Thanksgiving days (two days), Christmas day to New Year's day (eight days), Martin Luther King, Jr. day, and Spring Break days (two days).

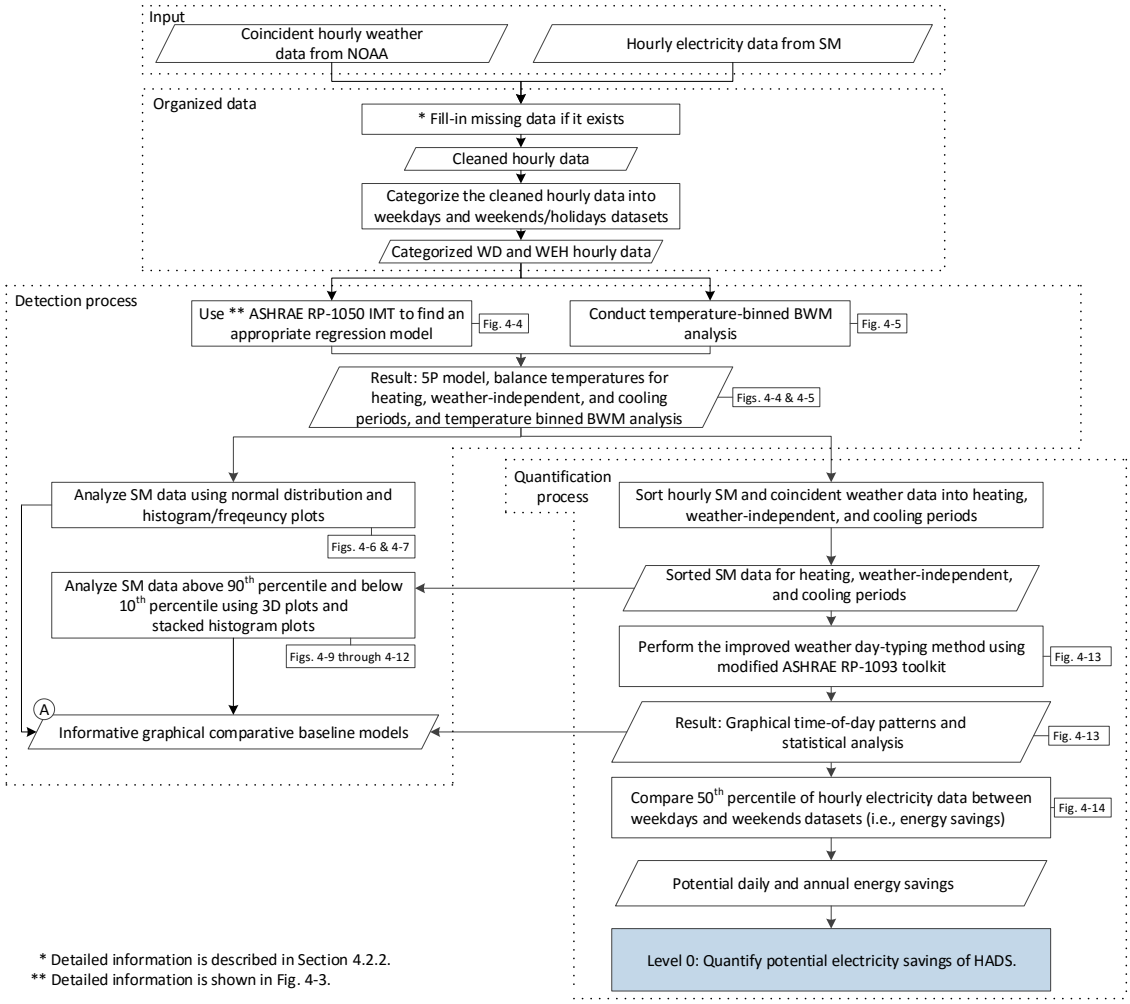

Figure 4-2. Diagram for quantifying potential electricity savings (Level 0 Analysis).

As the second step in the process (i.e., detective process), the ASHRAE RP-1050 Inverse Modeling Toolkit (IMT) (Kissock et al., 2001) was used with the SM data and the coincident OAT data to find an appropriate change-point linear regression model and the balance-point (i.e., change-point) temperatures to differentiate between heating, weather-independent (i.e., non-HVAC or non-heating and cooling period), and cooling periods. The IMT provides linear regression models, variable-base degree-day models, and change-point linear regression models for evaluating building energy use data. In

this study, the change-point linear regression models of the IMT were used to find the balance-point temperatures of the whole-building electricity use. Furthermore, two different change-point linear regression models were used, one for weekdays and one for weekends/holidays, respectively. Figure 4-3 shows an example of the linear and change-point linear regression models from the IMT for building energy use.

The change-point linear regression models typically use coincident outdoor dry-bulb temperature as an independent variable because it is usually the most important explanatory variable for determining building energy use. The IMT change-point linear regression models include: one parameter (1P), two parameter (2P), three parameter (3P), four parameter (4P), and five parameter (5P) models. The one parameter (1P) linear regression model has a single parameter (i.e., mean model) that determines a single value on the y-axis as average energy consumption. The two parameter (2P) linear regression model has two parameters where one is the y-axis intercept at x equal to zero, which may represent the baseline energy consumption at temperatures equal zero. The other parameter is the slope of energy use as a function of outside temperature, which can be used to analyze a building that always uses either cooling or heating energy (Curtiss et al., 2001; ASHRAE, 2013a). Although the 1P and 2P linear regression models provide parameters that characterize the average energy use of dataset, they do not provide change-point temperatures, which are important to this study. In the case that the 1P and 2P models are useful, two models would be used, one for weekdays and one for weekends/holidays, as shown in Figure 4-3.

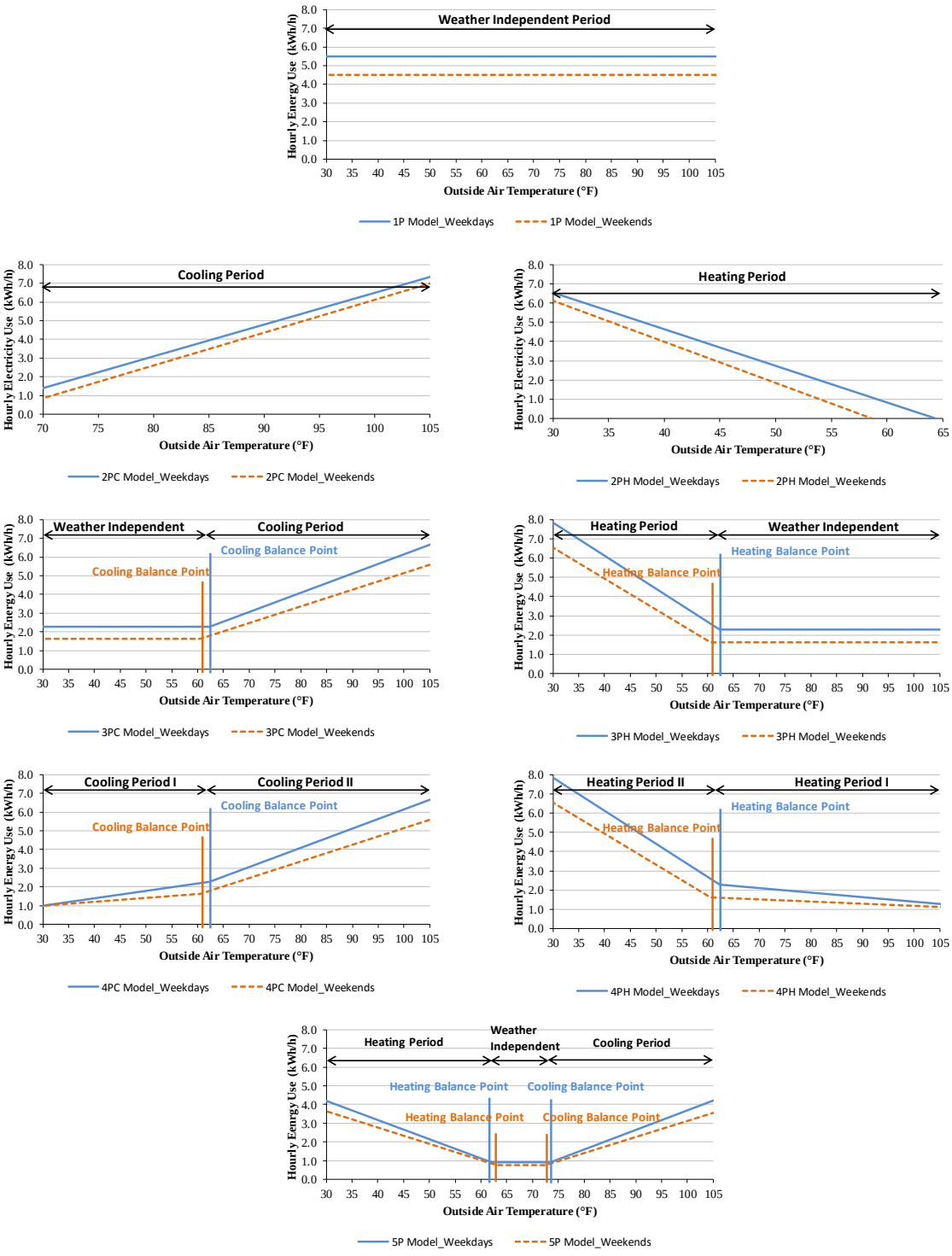

Figure 4-3. Examples of linear and change-point linear regression models from the IMT (Kissock et al., 2001).

The three parameter (3P) change-point linear regression model has an additional parameter that determines a change point to differentiate between weather-independent energy use and weather-dependent energy use. The 3P model has been widely used for monthly utility bill analysis of residential buildings (Curtiss et al., 2001; ASHRAE, 2013a; Baltazar et al., 2014). The four parameter (4P) change-point linear regression model has an additional parameter (i.e., the fourth parameter) that represents the lower or upper slope below or above the change point. The 4P model is useful in analyzing energy consumption in commercial buildings because it provides an improved model of cooling or heating energy use for commercial buildings that have year-around cooling and heating requirements (Ruch and Claridge, 1991; Curtiss et al., 2001; ASHRAE, 2013a).

Finally, the five parameter (5P) change-point linear regression model has an additional parameter (i.e., the fifth parameter) that represents a second change point. The 5P model has two change points to differentiate between heating, weather-independent, and cooling energy use. The 5P change-point model provides an improved model in buildings that have both electric heating and electric cooling systems where there is a distinct separation between heating and cooling change-point temperatures (Kissock et al., 1998; Curtiss et al., 2001; ASHRAE, 2013a). In this study, the 5P change-point linear regression model was used because the only energy source of the case-study house for heating and cooling was electricity, and the monthly average daily electricity use exhibited heating, weather-independent, and cooling signatures. Eq. (1) shows a functional form of the 5P change-point linear regression model (Kissock et al., 2003).

$$Y = \beta_1 + \beta_2(X_1 - \beta_3)^- + \beta_4(X_1 - \beta_5)^+ \quad (1)$$

Where Y is the building electricity use, X_1 is the outside air temperature, β_1 is the constant term (i.e., the y-axis intercept), β_2 is the left slope, β_3 is the left change point, β_4 is the right slope, β_5 is the right change point, and $(\ )^-$ and $(\ )^+$ are the notations that the values of the parentheses shall be zero when they are positive and negative, respectively (Kissock et al., 2003). The left change point β_3 (i.e., heating balance-point temperature) and the right change point β_5 (i.e., cooling balance-point temperature) divides the periods of hourly electricity use data into the three periods: heating period, non-heating and non-cooling period (i.e., non-HVAC or weather-independent period), and cooling period. To identify the change points, the IMT used the algorithms from a two-stage grid search. The IMT also provides a standard error calculation for each coefficients for the model (Kissock et al., 2001). Eq. (2) shows a functional form of the Standard Error (SE).

$$\beta_{true} = \beta_{estimated} \pm t(1 - \frac{\alpha}{2}, n - p)\sqrt{\frac{\sum_{i=1}^{n}(\hat{Y}_i - Y_i)^2}{n}} \quad (2)$$

Where t is the t distribution, α is the probability, n is the number of data points, p is the number of the parameters, $\hat{Y}_i$ is the predicted value from the model, and Y_i is the measured value. Figure 4-4 shows an example of the IMT's 5P model with change

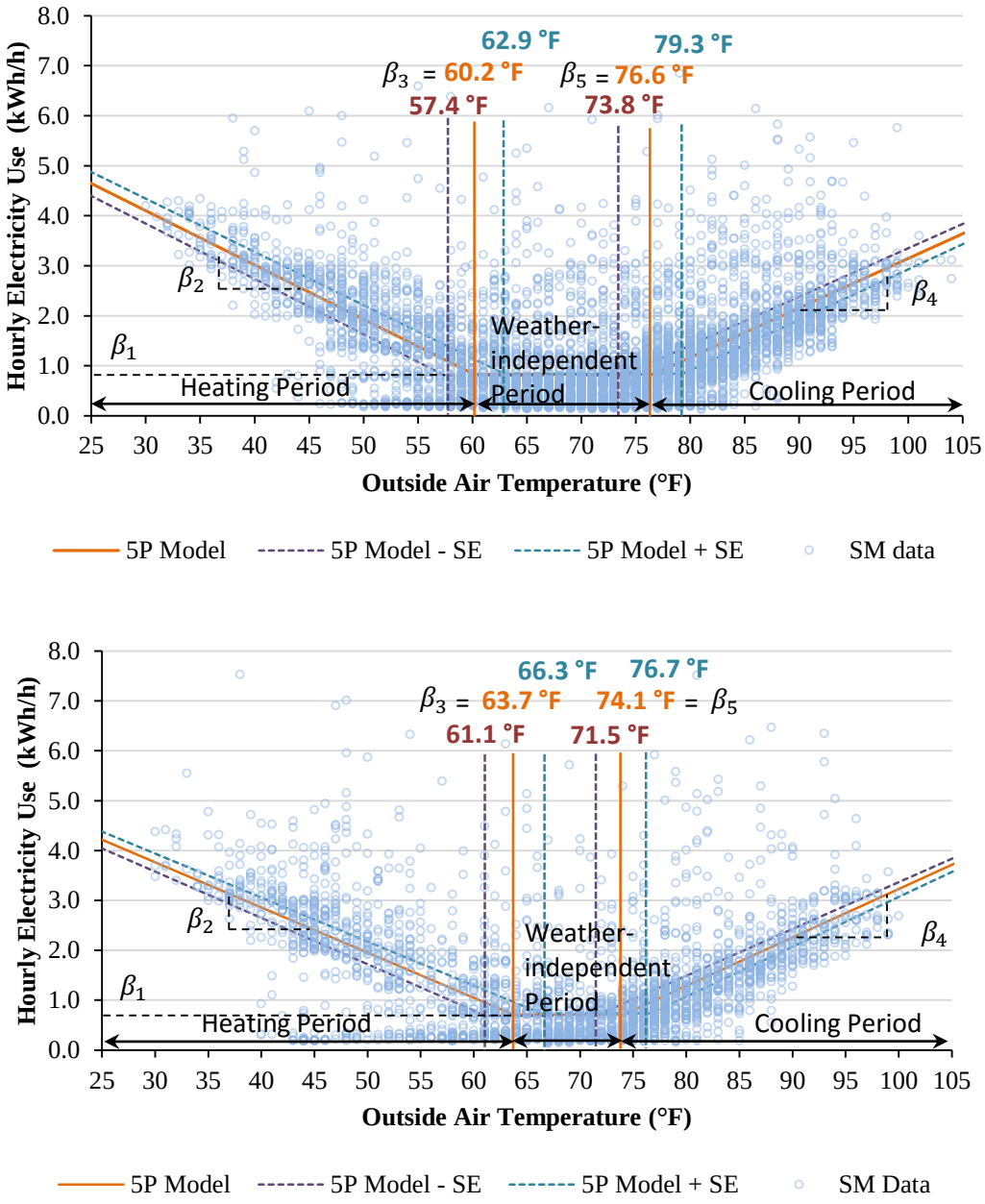

Figure 4-4. Example of the 5P model with change points and uncertainty for the weekdays (upper) and the weekends/holidays (lower) for the SM baseline period from April 15th, 2015 to April 14th, 2016.

points (i.e., balance-point temperatures) and uncertainty (i.e., SE) along with the electricity use from the case-study house during the weekdays and the weekends/holidays, respectively.

For the weekdays, the heating balance-point temperature of 60.2 °F and the cooling balance-point temperature of 76.6 °F separated the hourly electricity use that was recorded by the SM (i.e., SM data) into the three periods of heating, weather-independent, and cooling periods. For the weekends/holidays, the heating balance-point temperature of 63.7 °F and the cooling balance-point temperature of 74.1 °F separated the hourly SM data into the three periods. Table 4-1 summarizes the results of the 5P model.

Table 4-1. 5P change-point linear regression model results.

	Heating balance-point temperature (°F) (Left change point)	Cooling balance-point temperature (°F) (Right change point)	Left slope (kWh/°F)	Right slope (kWh/°F)	Y-axis intercept (kWh)
Weekdays	60.15	76.59	-0.109	0.099	0.827
Standard Error	2.74	2.74	0.002	0.002	0.012
Weekends/holidays	63.70	74.08	-0.091	0.097	0.711
Standard Error	2.59	2.59	0.002	0.003	0.024

In addition, a temperature bin analysis was performed and displayed as binned Box, Whisker, and Mean (BWM) plots (Bou-Saada, 1994). This analysis used a quartile analysis (Ott and Longnecker, 2010) to statistically check the signature of SM data against the OAT data. The binned BWM plot shows the 10^{th}, 25^{th}, 50^{th} (median), 75^{th}, and 90^{th} percentile as well as minimum, mean, and maximum values over temperature bins. In this study, 5 °F temperature bins were used. In addition, the accuracy of the 5P change-point linear regression models was checked using the interquartile ranges (IQR) of the BWM plots. Figure 4-5 shows an example of the temperature bin analysis using

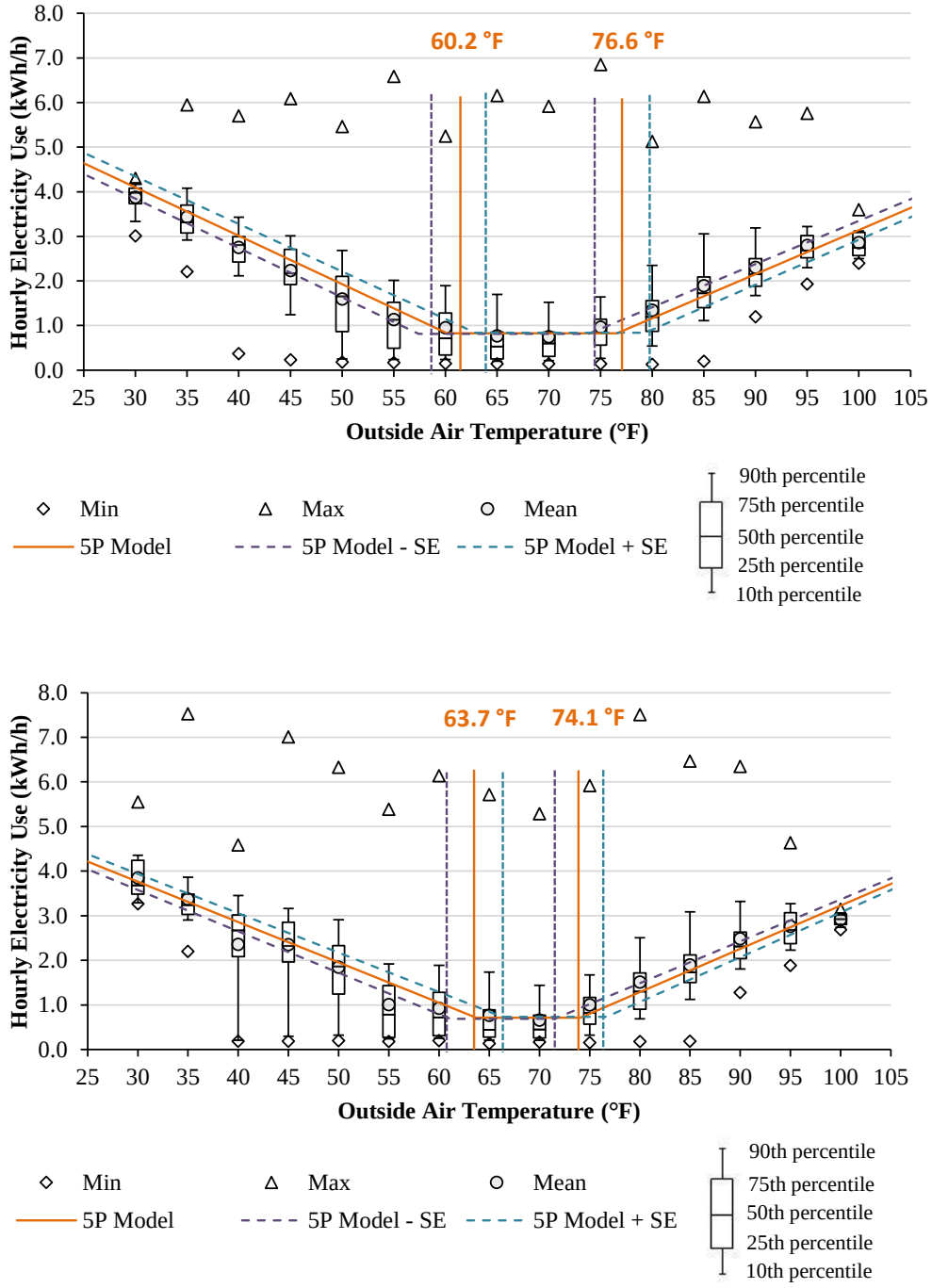

Figure 4-5. Example of the temperature bin analysis using the binned BWM plots with the 5P model during the weekdays (upper) and the weekends/holidays (lower) for the SM baseline period from April 15th, 2015 to April 14th, 2016.

the binned, quartile approach superimposed onto the 5P change-point linear models for the weekdays (upper) and the weekends/holidays (lower).

After the temperature bin analysis, histogram/frequency plots using 5 °F temperature bins were developed to check for outliers in the SM data. Figure 4-6 and Figure 4-7 show histogram/frequency plots using the 5 °F temperature bins. Using the histogram/frequency plots with superimposed normal distribution, abnormal energy use patterns can be detected. In addition, the histogram/frequency plots can be used as an informative graphical comparative analysis (Haberl and Abbas, 1998a, 1998b) to calibrate the baseline simulation model of the next calibrated simulation method (i.e., Level I Analysis).

In addition to the 5 °F temperature binned BWM plots and 5 °F temperature binned histogram/frequency plots, additional plots were developed to show the hourly electricity use above the 90^{th} percentile and below the 10^{th} percentile, which were analyzed to detect abnormal energy use and occupancy patterns, respectively. These plots were constructed in the following fashion: First, using the balance-point temperatures from the baseline period (Figure 4-4), binned BWM plots for the weekdays and the weekends/holidays were categorized into six regions, respectively. The six regions represent the three different heating, weather-independent, cooling periods above the 50^{th} percentile, as well as three different periods below the 50^{th} percentile. Fig 4-8 shows the binned BWM plots with the balance-point temperatures for the weekdays and the weekends/holidays along with the six regions. In addition, Table 4-2 summarizes the number of hours for each of the six regions.

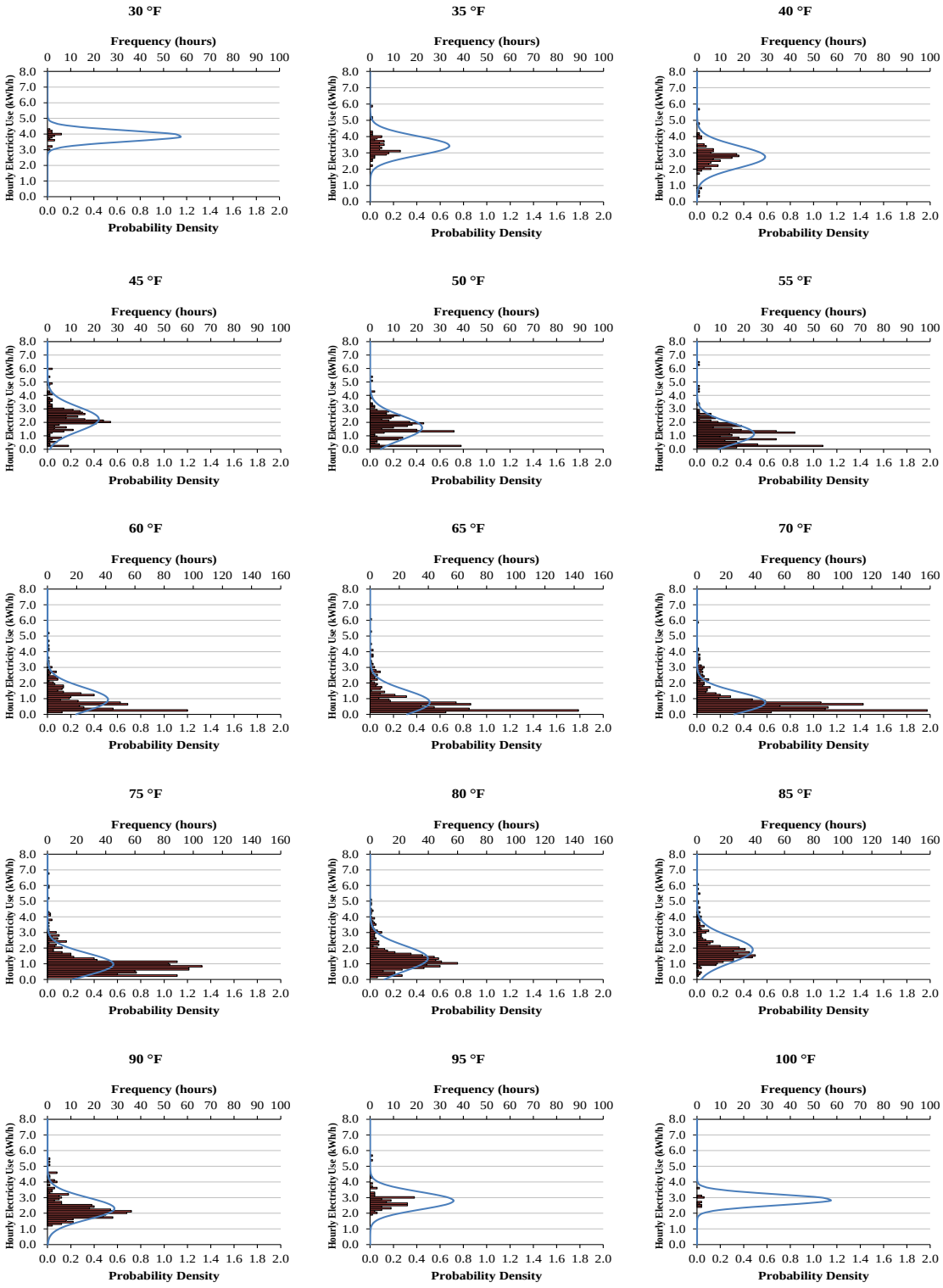

Figure 4-6. Histogram/frequency plots using 5 °F bins for the weekdays.

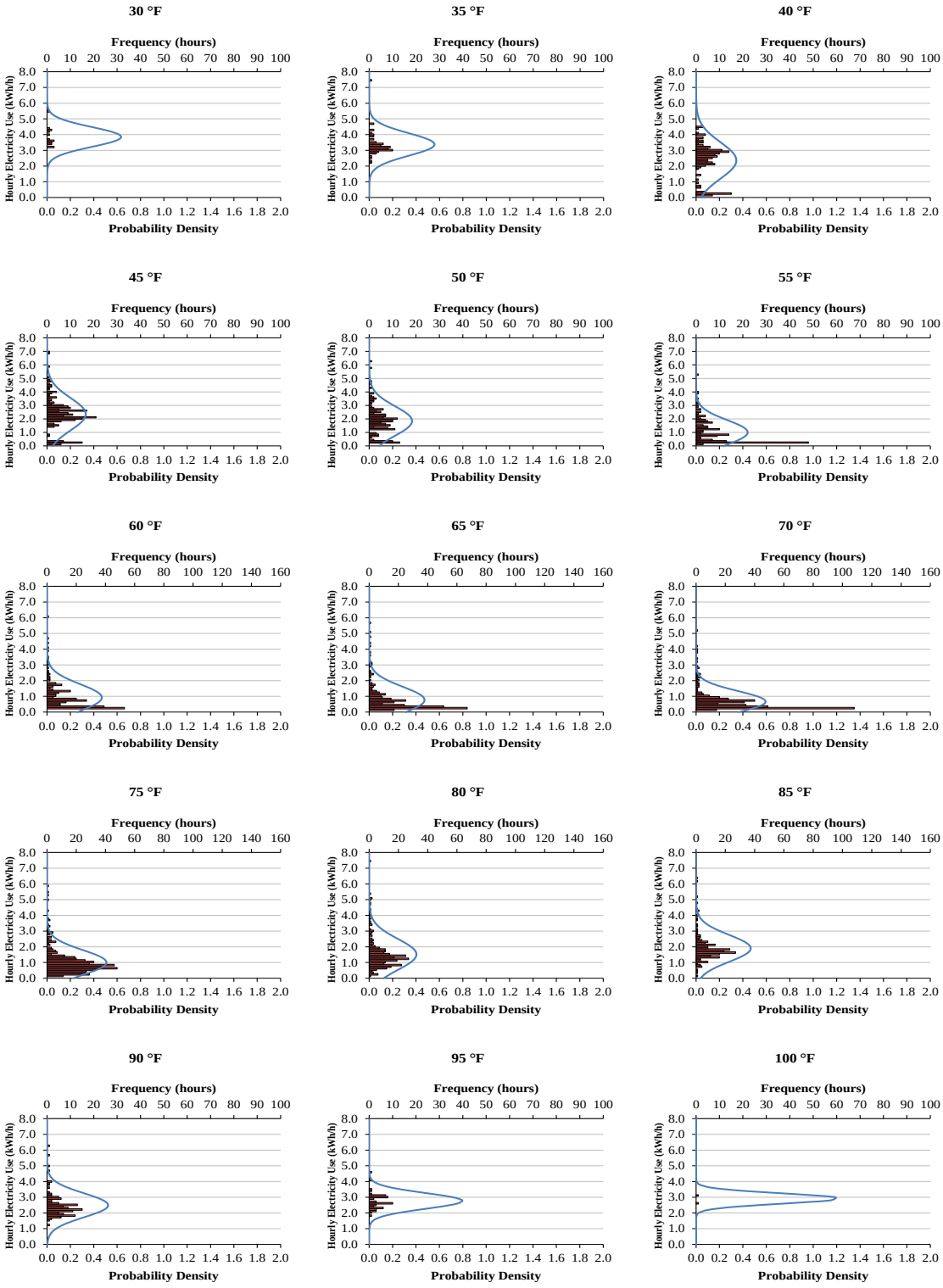

Figure 4-7. Histogram/frequency plots using 5 °F bins for the weekends/holidays.

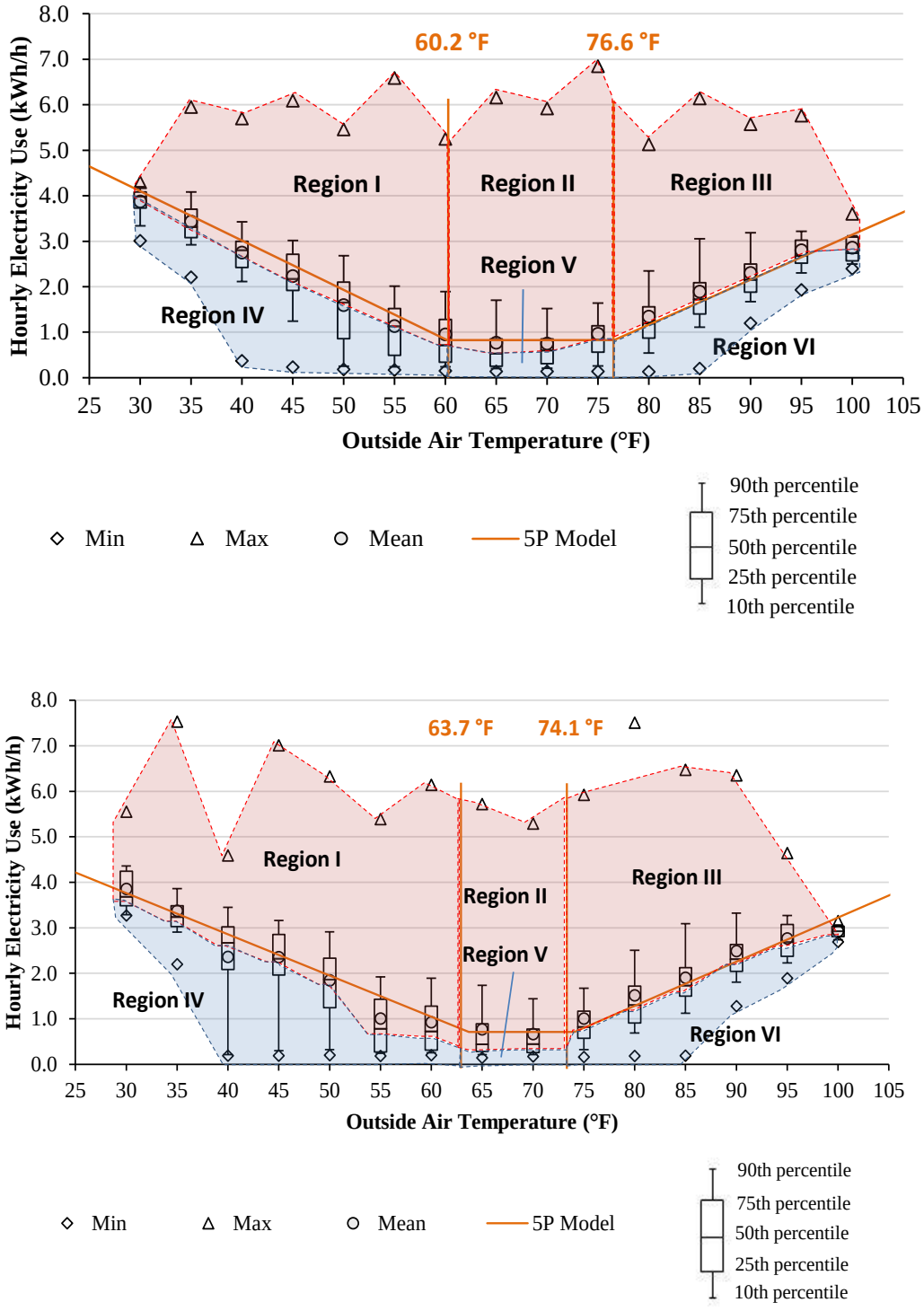

Figure 4-8. Binned BWM plots with the baseline balance-point temperatures for the weekdays (upper) and the weekends/holidays (lower) by six region.

Table 4-2. Number of energy hours above and below the 50th percentile.

Number of frequency hours above 50th	Region I (for heating period)	Region II (for weather-independent period)	Region III (for cooling period)	Total
Weekdays	700	1161	1134	2995
Weekends/holidays	506	360	561	1427
Total	1206	1521	1695	4422
Number of frequency hours below 50th	Region IV (for heating period)	Region V (for weather-independent period)	Region VI (for cooling period)	Total
Weekdays	684	1222	1027	2933
Weekends/holidays	490	364	551	1405
Total	1174	1586	1578	4338

Based on the six regions, three-dimensional (3D) energy plots were developed to help visually detect when the hourly electricity use above the 90th percentile (i.e., energy pattern) and hourly electricity use below the 10th percentile (i.e., occupancy patterns) occurred during both the hour-of-day and the day-of-year as well as knowing the amount of the hourly electricity use at the points (Christensen, 1984). Figure 4-9 shows an example of the 3D energy use plot, which represents data points above the 90th percentile during weekdays for the heating period (i.e., Region I), based on the heating balance temperature from the baseline 5P change-point linear regression model. In addition, hourly histograms were calculated to detect an overall hour-of-day pattern. This example plot shows that the hourly electricity use above the 90th percentile from the middle of October to the end of April most likely occurred during evening and morning hours for weekdays and weekends/holidays, respectively.

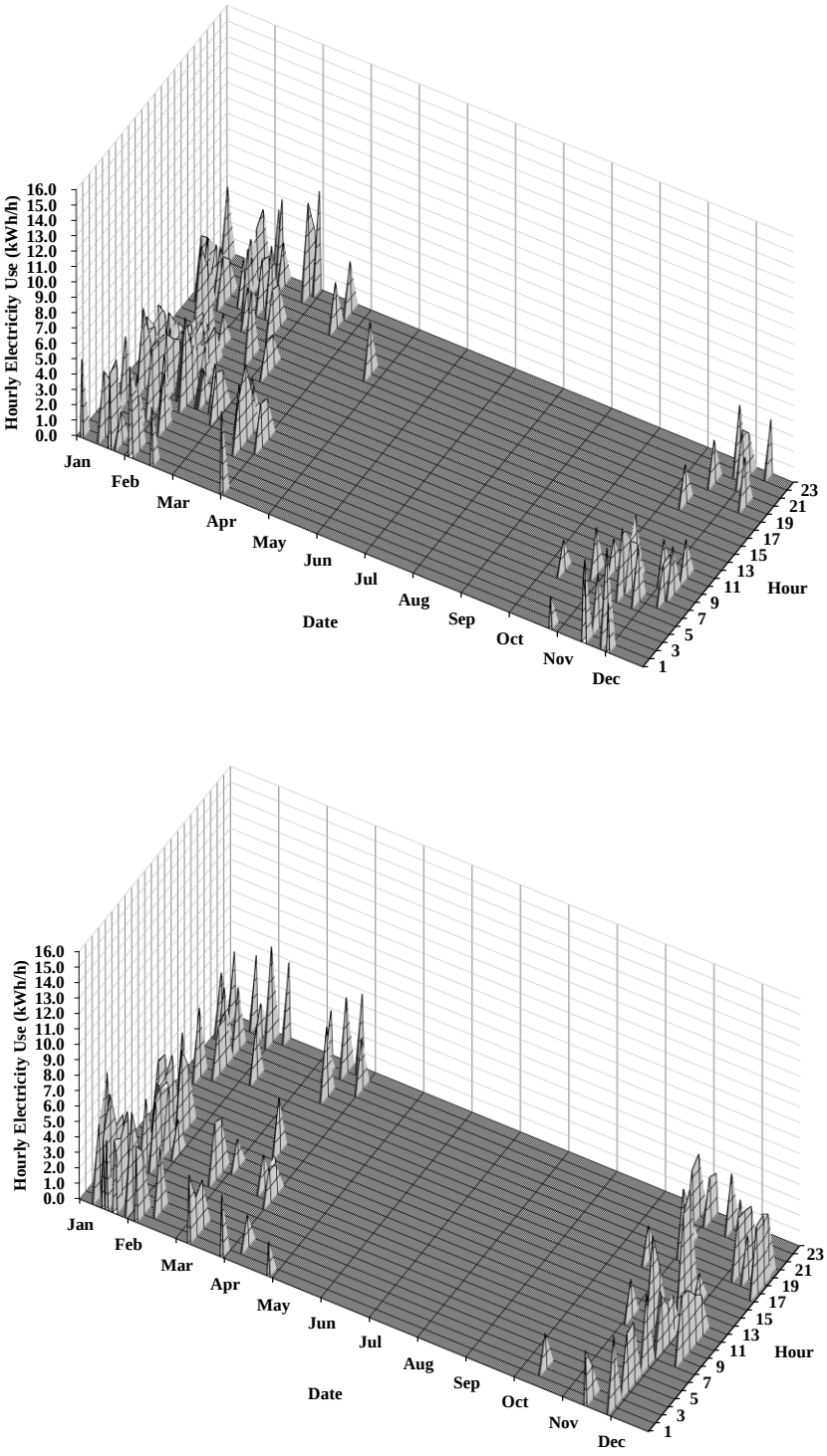

Figure 4-9. Example of a 3D energy use plot showing hourly electricity use above the 90th percentile during weekdays (upper) and weekends/holidays (lower) for the heating period.

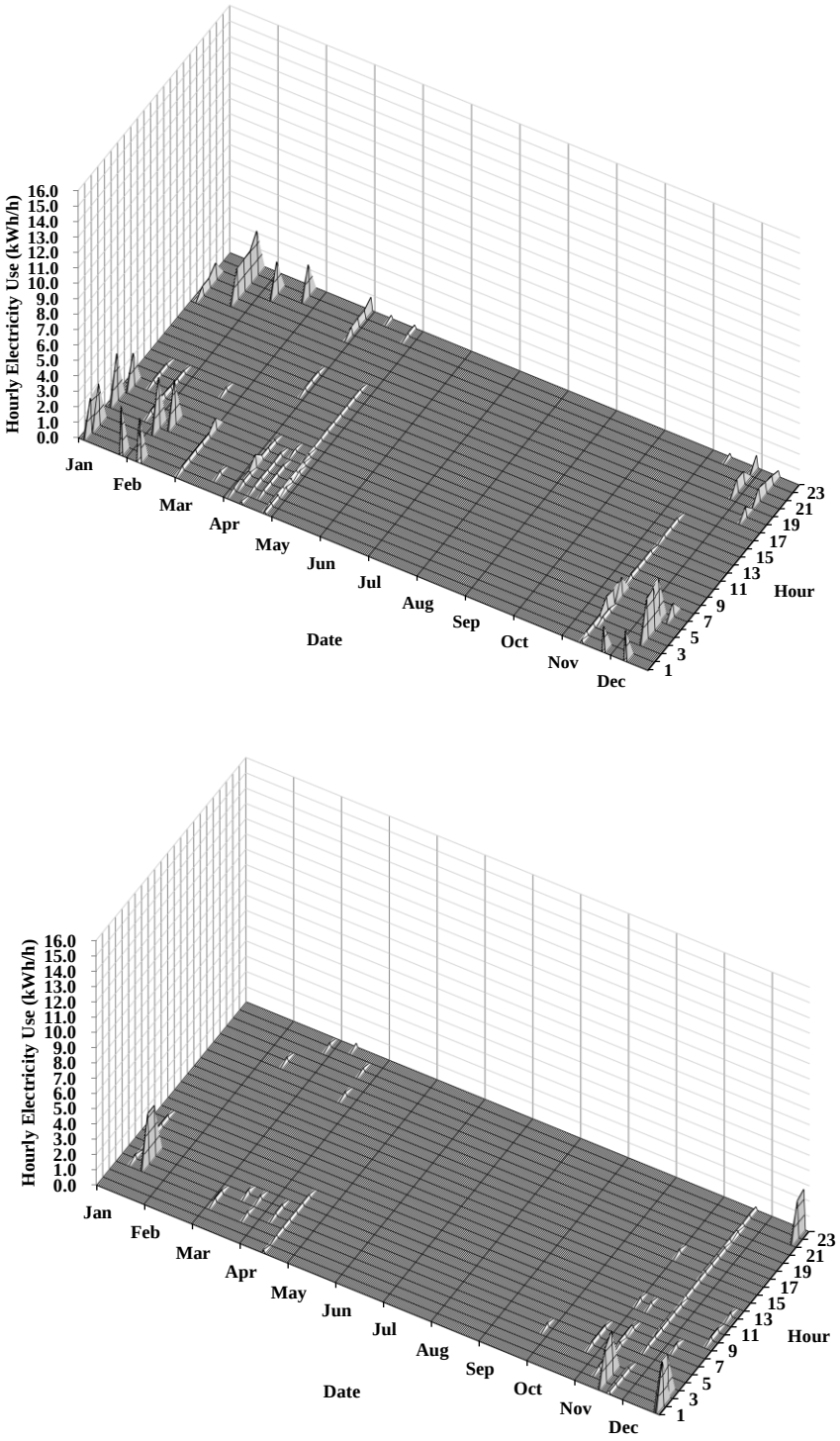

Figure 4-10. Example of a 3D energy use plot showing hourly electricity use below the 10th percentile during weekdays (upper) and weekends/holidays (lower) for the heating period.

Figure 4-10 shows the 3D energy use plots, which represent data points below the 10^{th} percentile (i.e., occupancy pattern) during weekdays (upper plot) and weekends/holidays (lower plot) for the heating period (i.e., Region IV). This example shows the electricity use below the 10^{th} percentile mainly happened from the middle of November to the end of April during evening and morning hours for weekdays and at the end of September to the middle of April during morning hours for weekends/holidays.

Furthermore, hour-of-day, day-of-week, stacked histogram plots were developed to determine the energy and occupancy patterns of the hourly electricity use. In this analysis, it was assumed that the hourly electricity use above the 90^{th} percentile represented energy patterns during the heating, weather-independent, and cooling periods when the electricity use was well above average. This was because the pattern of high energy use above the 90^{th} percentile of each period may be indicating the energy consumption of heating, weather-independent, and cooling related systems or appliances.

Figure 4-11 shows an example of the hour-of-the-day, day-of-the-week, stacked histogram plots representing energy use patterns for the heating period. In this example, there were ten or more hours above the 90^{th} percentile energy use during the weekday period (upper plot) at 9:00 am for the heating period. The reason for this observed condition seems to indicate that a large electric load, such as the Domestic Hot Water (DHW) system was operating, most frequently at 9:00 am on Monday through Thursday. In the same way, it was observed that a large electric load (i.e., the DHW system) operated most frequently during the weekend/holiday period (lower plot) at 9:00 am on Saturday and Sunday.

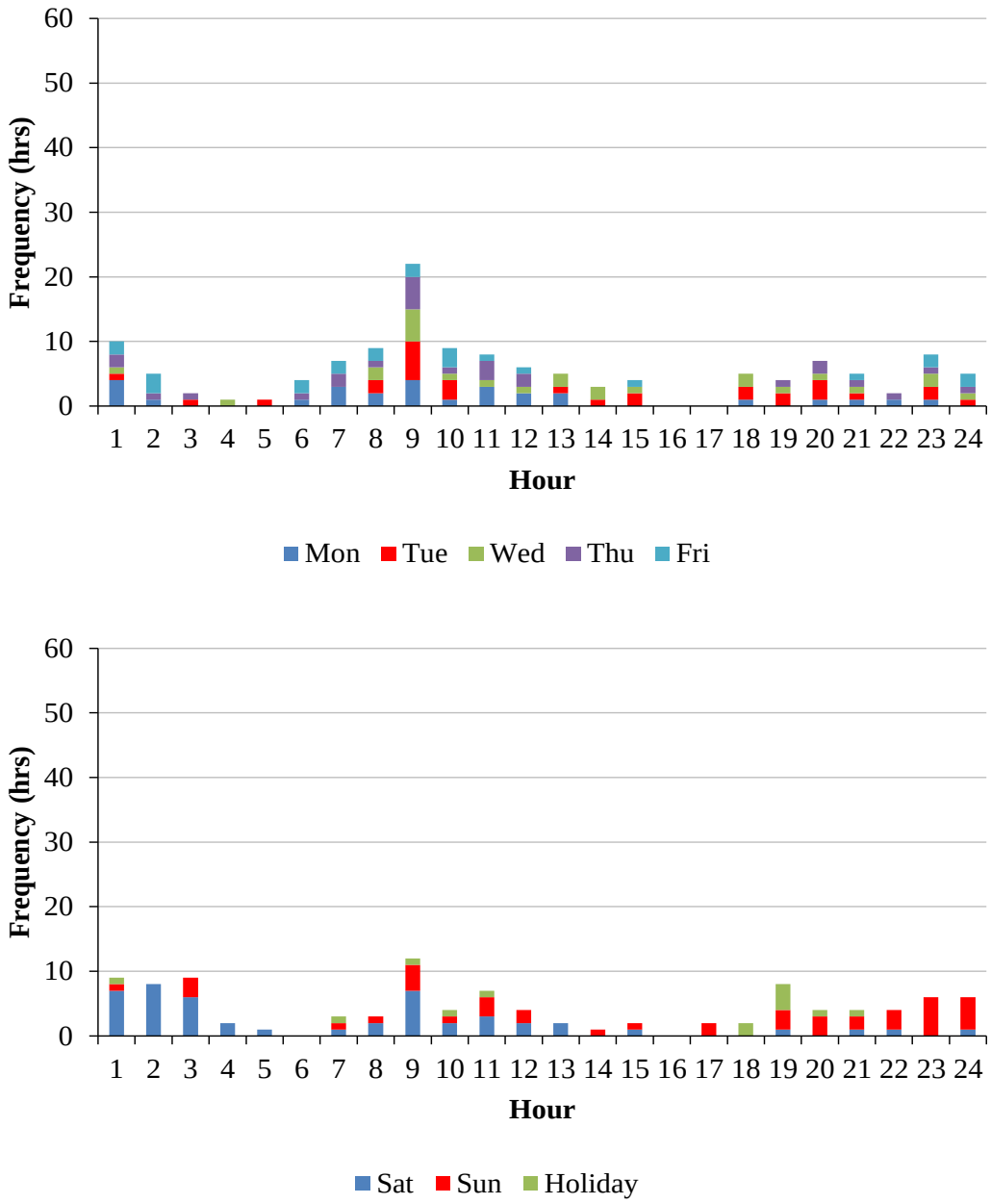

Figure 4-11. Example of the hour-of-the-day, the day-of-the-week, stacked histogram plots showing hours above the 90th percentile representing energy use patterns during weekdays (upper) and weekends/holidays (lower) for the heating period.

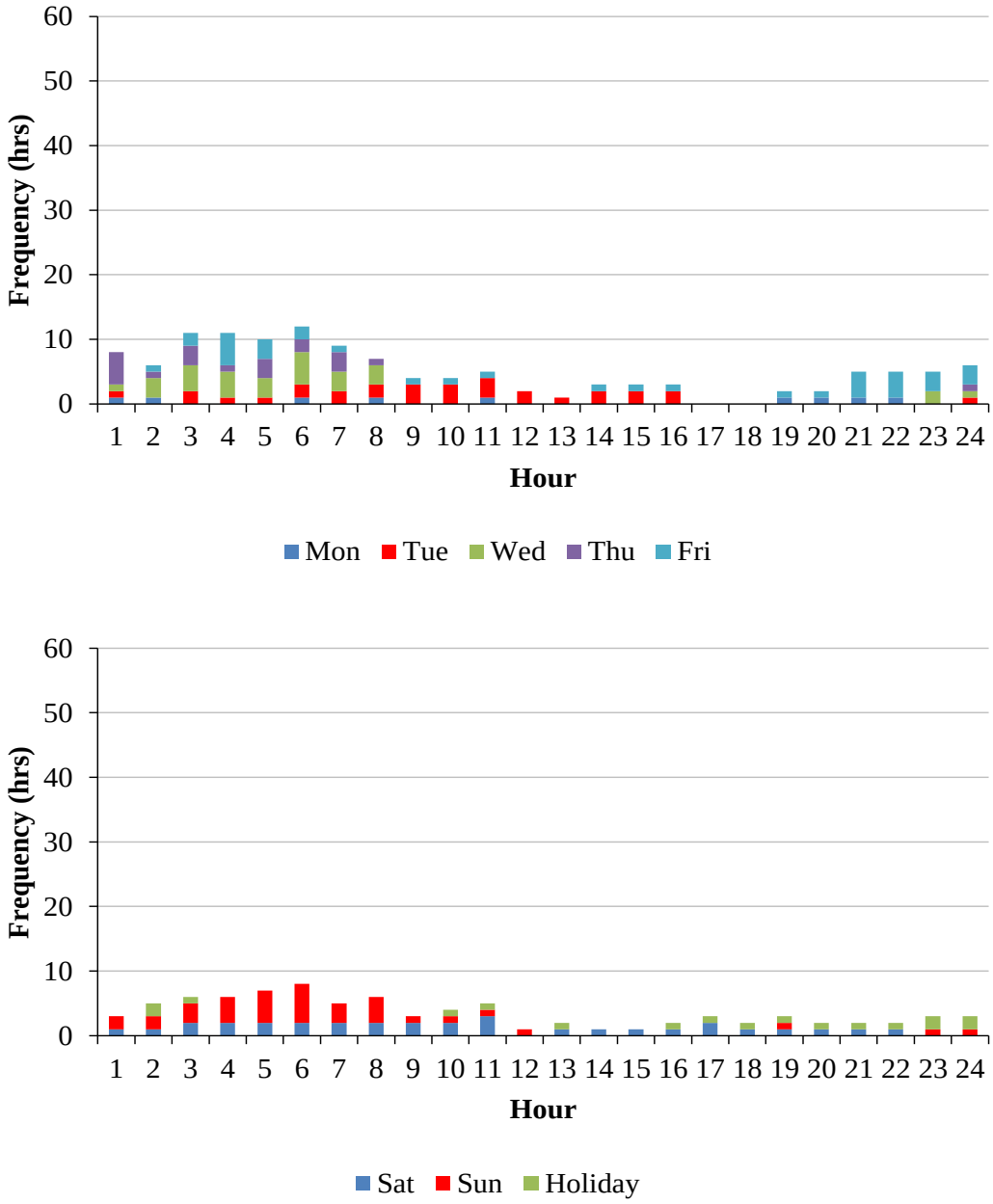

Figure 4-12. Example of the hour-of-the-day, the day-of-the-week, stacked histogram plots showing hours below the 10th percentile representing occupancy patterns during weekdays (upper) and weekends/holidays (lower) for the heating period.

It was also assumed that the hourly electricity use below the 10th percentile (i.e., when the electricity use was well below normal) represented occupancy pattern(s) when an occupant was inactive or outside the home during the heating, weather-independent, and cooling periods. This was because the patterns of low energy use below the 10th percentile of each period may indicate the low energy consumption patterns of occupants who were inactive (e.g., sleeping) or outside a house, which presents opportunities for turning-down or turning-off heating and cooling systems, appliances and lights.

Figure 4-12 shows an example of the hour-of-the-day, day-of-the-week, stacked histogram plots representing occupancy patterns for the heating period. In this example, there were more hours below 10th percentile energy use during weekdays (upper plot) from 1:00 am to 8:00 am, which seems to indicate the homeowner was inactive or outside the house during the hours.

Overall, the number of hours below the 10th percentile were less than the number of hours above the 90th percentile. Table 4-3 shows the frequency of the hours for the weekdays and the weekends/holidays for the six different regions.

Table 4-3. Number of energy hours above the 90th and below the 10th percentile.

Number of hours above 90th percentile	Region I (for heating period)	Region II (for weather-independent period)	Region III (for cooling period)	Total
Weekdays	132	236	225	593
Weekends/holidays	103	70	113	286
Total	235	306	338	879
Number of hours below 10th percentile	Region IV (for heating period)	Region V (for weather-independent period)	Region VI (for cooling period)	Total
Weekdays	124	205	206	535
Weekends/holidays	85	56	113	254
Total	209	261	319	789

In addition, the 3D energy use plots and the hour-of-the-day, day-of-the-week, stacked histogram plots can be used for informative graphical comparisons to help calibrate a baseline simulation model to be used in the next Level I analysis section (i.e., calibrated simulation method).

Third, a method for quantifying potential electricity savings was also developed. As a first step in this process, an improved weather day-typing method that includes the quartile approach (Bou-Saada and Haberl, 1995a) was developed using the balance-point temperatures from the baseline 5P change-point linear regression model. In this study, the ASHRAE RP-1093 toolkit (Abushakra et al., 2001) was modified to conduct the weather day-typing analysis. The ASHRAE RP-1093 toolkit was originally developed to examine measured, hour-of-day load profiles for lighting and receptacle loads for use by building energy simulation programs (Abushakra et al., 2001).

It should be noted that the weather day-typing method used in this study is an improved weather day-typing method because the three different day-type periods were chosen statistically by the balance-point (change-point) temperatures of the baseline 5P model generated by the IMT. In other words, the hourly electricity use data was first categorized by the heating, weather-independent, and cooling periods, which were determined statistically by the balance-point temperatures from the 5P model.

Next, the improved weather day-typing method was used to analyze the hourly electricity use data to find the characteristics of each period. To accomplish this the hour-of-day patterns for occupied and unoccupied hours as well as weekday and weekends/holiday periods were analyzed for the three different periods. In addition,

quartile and statistical analysis were applied to determine the statistical features of the hour-of-day patterns. Figure 4-13 shows an example of the new weather day-typing analysis including the quartile approach for the heating period (i.e., periods when the coincident OATs were lower than 60.2 °F (weekdays) and 63.7 °F (weekends/holidays)) as determined by the IMT's 5P change-point linear regression model.

In Figure 4-13, it can be observed that the interquartile range (IQR) of the weekend/holiday weather day-typing plot is wider than the IQR of the weekday plot, which implies that the homeowner's energy consumption during weekends/holidays was more unpredictable than weekdays. In other words, during the weekend/holiday periods, more frequently, the homeowner's electricity use during early morning hours varied versus the weekday periods. In addition, the weather day-typing plot**s** using the quartile approach can be used in the graphical analysis to better calibrate a baseline simulation model for the next Level I analysis (i.e., calibrated simulation method).

Finally, the 50^{th} percentile of the hourly electricity use for the weekdays and the weekends/holidays were compared to examine potential energy savings from the use of HADs for the representative hour-of-day energy use patterns for heating, weather-independent, and cooling periods. In this analysis, it was assumed that the 50^{th} percentile of the hourly electricity use was representative of the average hourly electricity use. Figure 4-14 shows an example of the 50^{th} percentile differences between the weekdays and the weekends/holidays for the heating period.

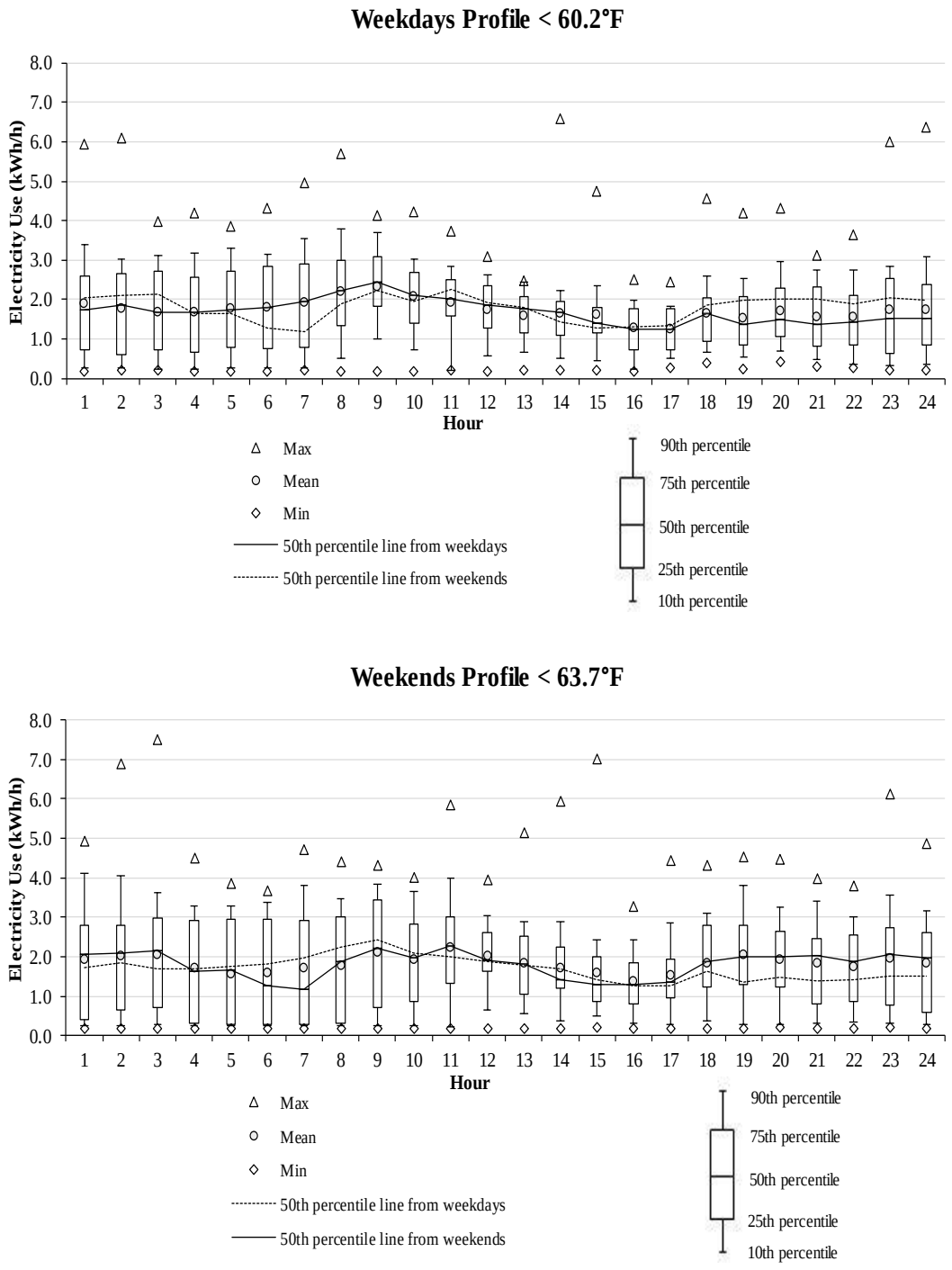

Figure 4-13. Example of the new weather day-typing plots using the quartile analysis during weekdays (upper) and weekends/holidays (lower) for the heating period.

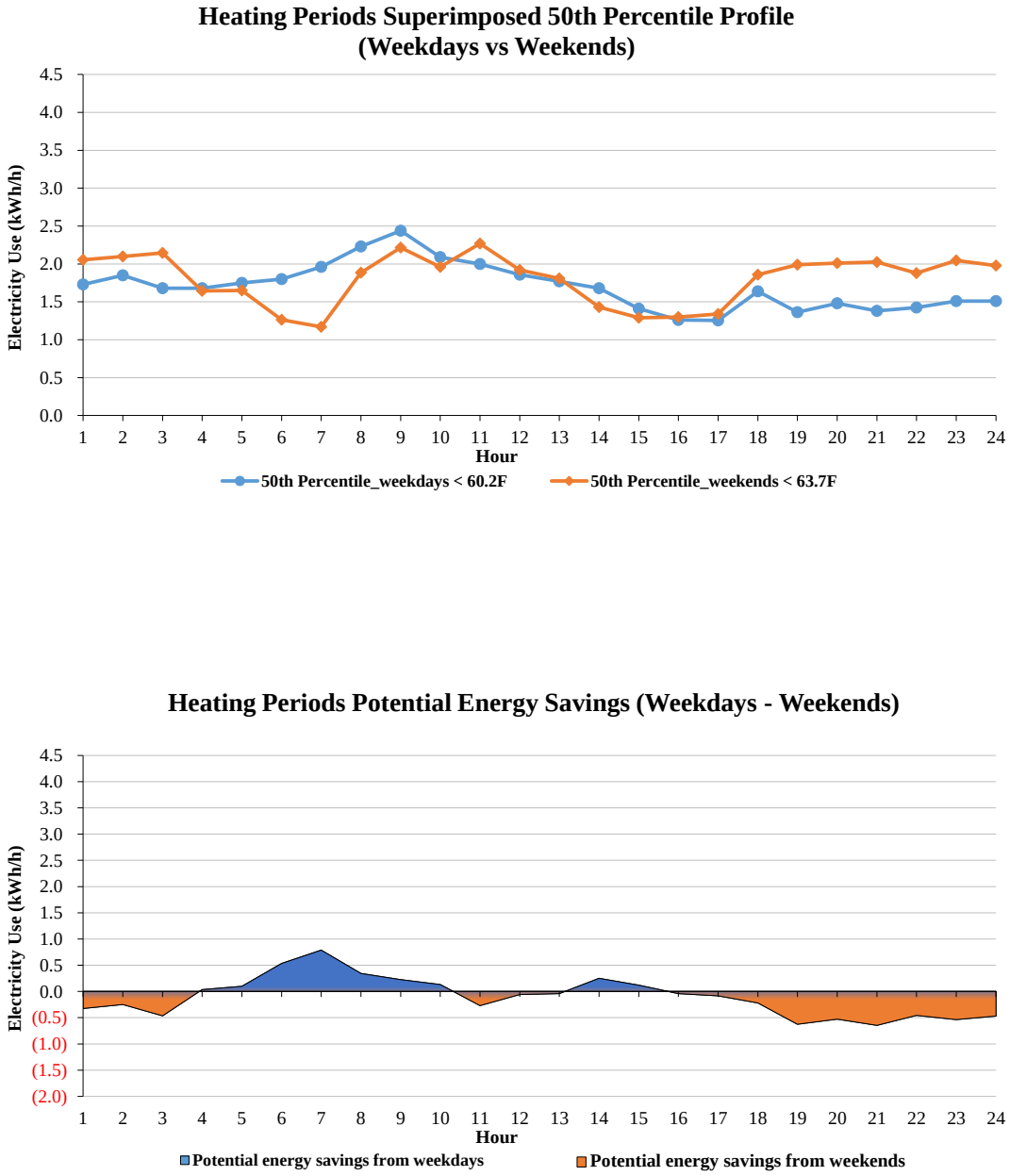

Figure 4-14. Example of potential energy savings for the heating period, which is a result of comparing the 50th percentile for the weekdays and the weekends/holidays.

In Figure 4-14, the differences (i.e., shaded area) of the plot represent potential energy savings of a representative day based on the differences in the hour-of-day energy pattern between weekdays and weekends/holidays. In other words, there is a possibility that a homeowner can save energy based on the differences in the hour-of-day energy patterns between weekdays and weekends. This saving estimation method used the homeowner's previously-recorded, hour-of-day energy patterns, so the method could be applied non-intrusively to hourly electricity use data from SMs to analyze an occupant's energy behavior patterns. For heating, weather-independent, and cooling periods, the potential savings (shaded area) may represent energy savings from differences in operation in heating, weather-independent, and cooling related systems or appliances, respectively. For example, in Figure 4-14, the potential energy savings of the representative day for the heating period is 6.9 kWh, based on this method, which includes the potential energy savings of 2.4 kWh for weekdays (the blue-filled area); and the potential energy savings of 4.5 kWh for weekends (the orange-filled area). Overall, the daily potential savings of 6.9 kWh may result from improved control of heating related systems or appliances.

The daily savings can also be quantified annually based on the days during the heating period when the OAT are below the heating balance-point temperature (i.e., Regions I and IV). In this example, the heating balance-point temperatures from the 5P model was 60.2 °F and 63.7 °F for the weekdays and the weekends/holidays, respectively. Thus, the days during the heating period below these balance-point temperatures would be 58 days and 42 days, respectively. For quantifying the annual

energy savings, the weekday's potential daily energy savings of 2.4 kWh is multiplied by 58 days, and the weekend/holiday's savings of 4.5 kWh is multiplied by 42 days. The result of this calculation is 328.4 kWh, and the expected saving cost is $38.0. In this study, the cost of the electricity was assumed to be $0.1156/kWh based on the US EIA's data for Texas 2015 (US EIA, 2016). Table 4-4 summarizes the results of the potential energy savings during the heating period.

Table 4-4. Potential energy savings for the heating period.

Daily potential energy savings (kWh)			
from Weekdays	from Weekends/holidays	Total savings (kWh)	
2.4	4.5	6.9	
Balance-point temperature (°F)			
from Weekdays	from Weekends/holidays		
60.2	63.7		
Number of heating days (Region I + IV)			
from Weekdays	from Weekends/holidays		
58	42		
Annual potential energy savings (kWh)			
from Weekdays	from Weekends/holidays	Total savings (kWh)	Total cost savings ($)
140.6	187.8	328.4	38.0

In summary, a non-intrusive statistical method (i.e., Level 0 Analysis) was developed to automatically detect and quantify potential energy savings from the use of HADs using hourly electricity use data recorded by a SM. In this method, the IMT was used with the hourly SM data and coincident hourly weather data to find an appropriate regression model and the balance-point temperatures to differentiate between the heating, weather-independent, and cooling periods. The hourly SM data was then categorized into the three periods for the weekdays and the weekends/holidays. In addition, the SM data was further categorized into the six regions shown using the binned quartile approach. Using these six regions, 3D energy use plots and the hour-of-

the-day, day-of-the-week, stacked histogram plots were used to help further determine the reasons for the energy use patterns and possible relationships to the occupancy patterns.

For quantifying the electricity energy savings, an improved weather day-typing method, which uses the quartile approach, was used to find the hour-of-the-day energy use patterns for the weekdays and the weekends/holidays for each period. Finally, potential energy savings were quantified using the different energy patterns for weekdays and weekends/holidays for each period.

For the next level of analysis (i.e., Level I Analysis), which uses calibrated simulation, the results from the histogram/frequency plots with superimposed normal distribution, the 3D energy use plots, and the hour-of-the-day, day-of-the-week, stacked histogram plots obtained from this Level 0 Analysis can be used to help inform the graphical comparative models to better match the simulated hourly energy use with the SM data to create a baseline to help quantify the electricity savings from the use of HADs.

4.2. Development of a Calibrated Simulation Method (Level I Analysis) for Quantifying Detailed-Potential Electricity Savings

This section describes the procedure used to calibrate the building energy simulation (i.e., Level I Analysis), which includes information gathered from the previous section (i.e., Level 0 Analysis). In the previous Level 0 Analysis, the non-intrusive statistical method was developed using only the SM data and the corresponding weather data. In this Level I Analysis, a calibrated simulation method was developed to help quantify the detailed-potential savings from the use of HADs using simulations based on the information of the case-study house as well as the SM electricity data and the corresponding weather data.

The calibrated simulation method is an M&V approach that uses a simulation model calibrated to actual measured data (ASHRAE, 2014). In this study, hourly measured electricity use data from the SM, as well as measured Indoor Air Temperature (IAT) data, was used for the calibration of a DOE-2.1E simulation model (Winkelmann et al., 1993). The following subsections include descriptions of the case-study house, the weather data used for simulation, and the calibrated simulation method developed for this Level I Analysis.

Figure 4-15 shows the overall method of this Level I Analysis. First, the input parameters for the DOE-2.1E simulation model were prepared using general information from drawings. In addition, the performance path (i.e., simulation) information of the 2000 or 2009 International Energy Conservation Code (IECC) (ICC, 2000, 2009) was used to create nominal values that the general information does not cover. Next, actual weather data of the post-retrofit period from February 10th, 2017 to March 31st, 2017 were collected and converted to the Test Reference Year (TRY) format for the DOE-2.1E simulation model. After simulating with the DOE-2.1E model with the parameters during the post-retrofit period, the model was calibrated using the measured SM and IAT data during one week of the post-retrofit period from February 20th, 2017 to February 26th, 2017. In other words, IATs from the case-study house were also matched with simulated IATs (i.e., two-way calibration). The informative graphical analysis, developed in the previous section (i.e., Level 0 Analysis), was used to guide the calibration process. In addition, a sensitivity analysis using the IMT model's coefficients was used for the annual calibration

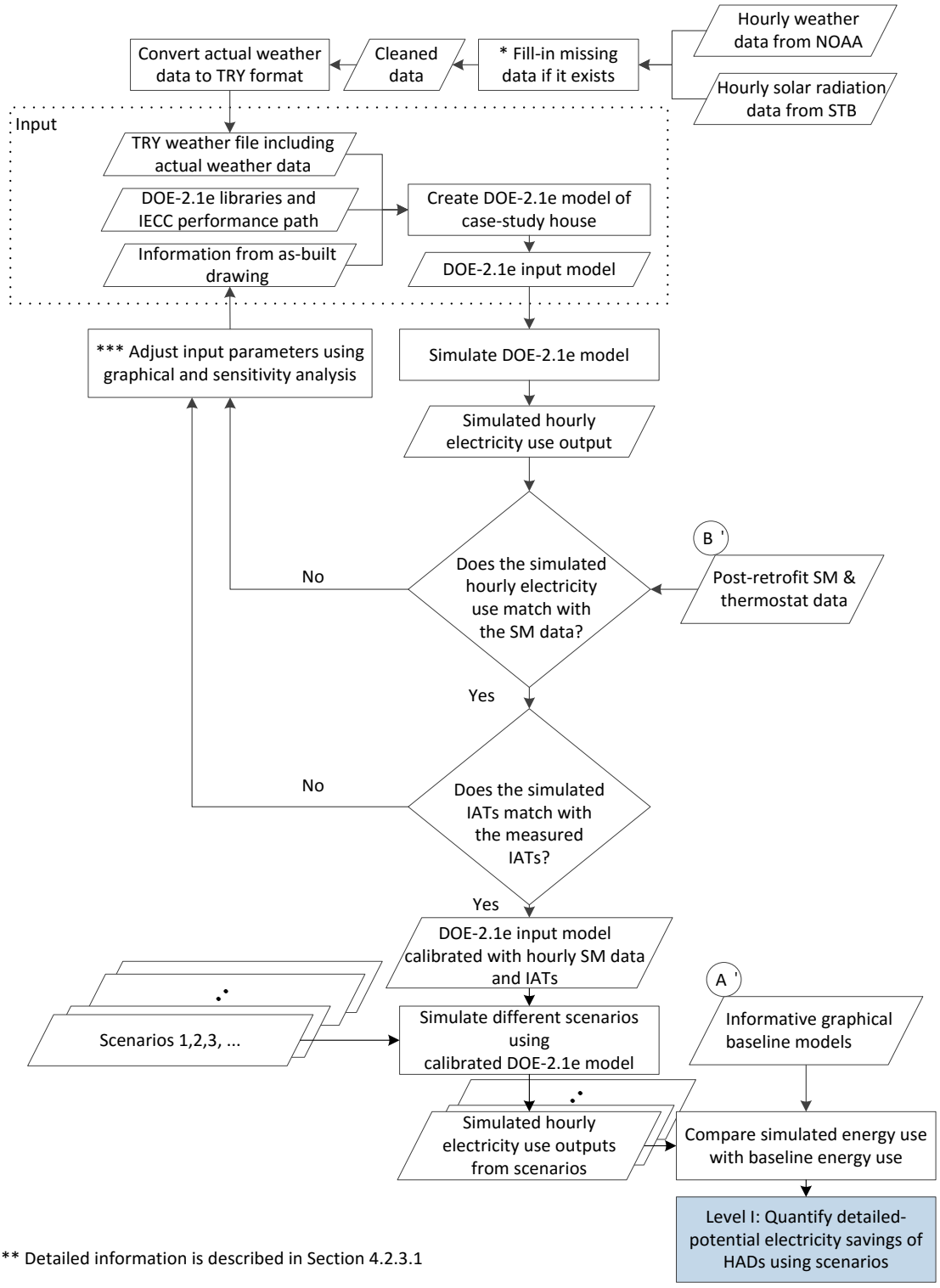

Figure 4-15. Diagram for quantifying detailed-potential electricity savings (Level I Analysis).

using the SM data and the weather data of the baseline period from April 15th, 2015 to April 14th, 2016.

Finally, to quantify detailed-potential electricity savings from the use of HADs, different scenarios were developed, using thermostatically controlled HADs and non-thermostatically controlled HADs.

4.2.1. Description of the Case-Study House

The case-study house is a one-story, fourplex townhouse, constructed in 1982, located in Bryan, Texas. The house is a single-family house with two bedrooms, and one and a half bathrooms with a total conditioned floor area of 1,199 ft^2. The front of the house faces west. Two other townhouses are attached on the north and south sides, respectively. Figure 4-16 shows the bird's eye view of the case-study house (Google, n.d.). Figure 4-17 and Figure 4-18 show the front view (west) and the back view (east), respectively. On the east side, there is a fixed shade above the parking lot that is located about 1foot away from the case-study house. Figure 4-19 shows a plan view of the case-study house. Additional information for the case-study house is shown in Table 4-5. Unknown parameters in the table indicate that the parameters were assumed using the performance path of the 2000 or 2009 International Energy Conservation Code (IECC) or the default values of DOE-2.1E libraries. The information was used to create a DOE-2.1E model. Appendix A includes a letter from the Texas A&M Institutional Review Board (IRB) regarding the approval of the use of the data from the case-study house.

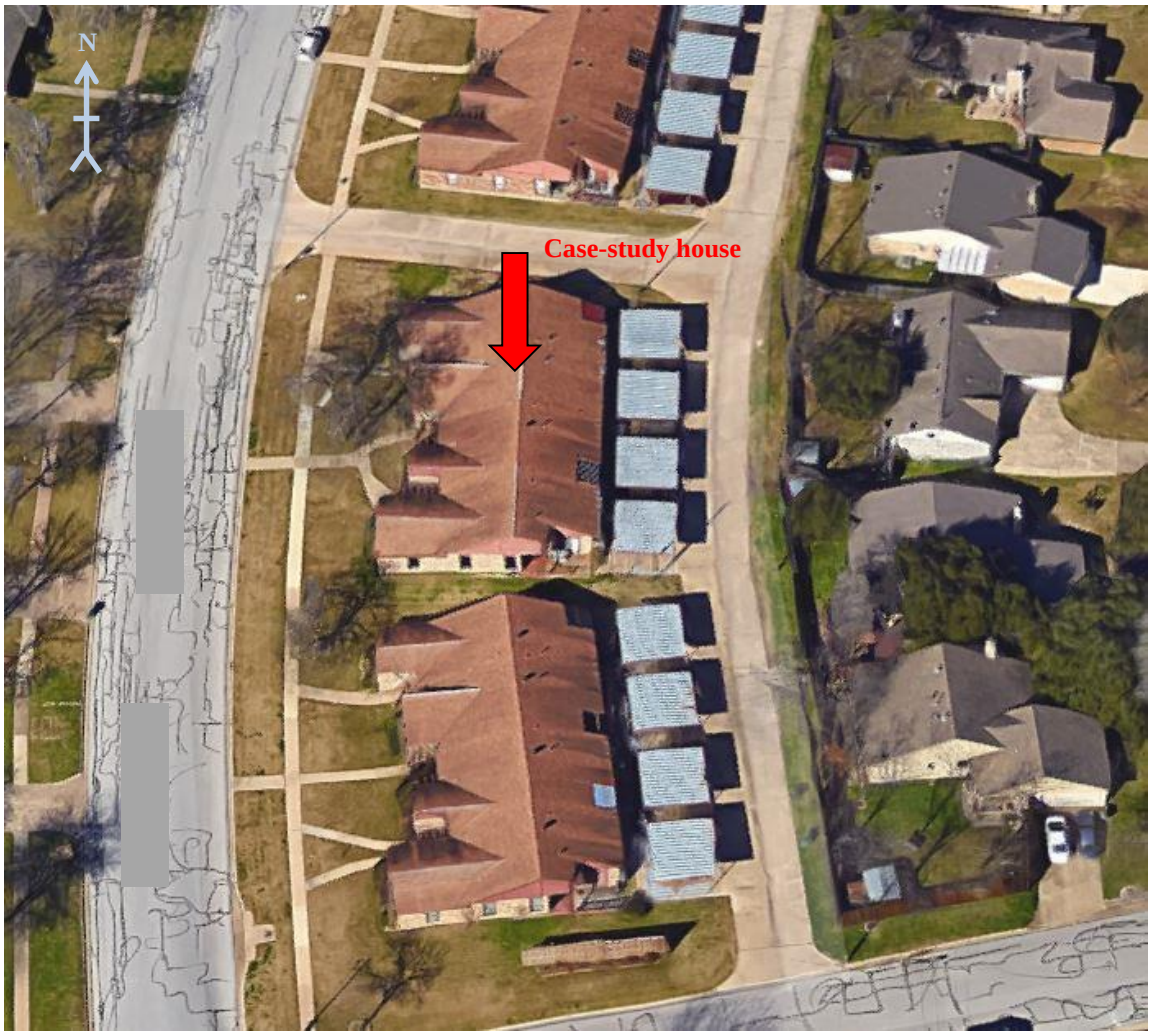

Figure 4-16. Satellite view of the case-study house (Google, n.d.).

Figure 4-17. Front view (west) of the case-study house (Author's photo).

Figure 4-18. Back view (east) of the case-study house (Author's photo).

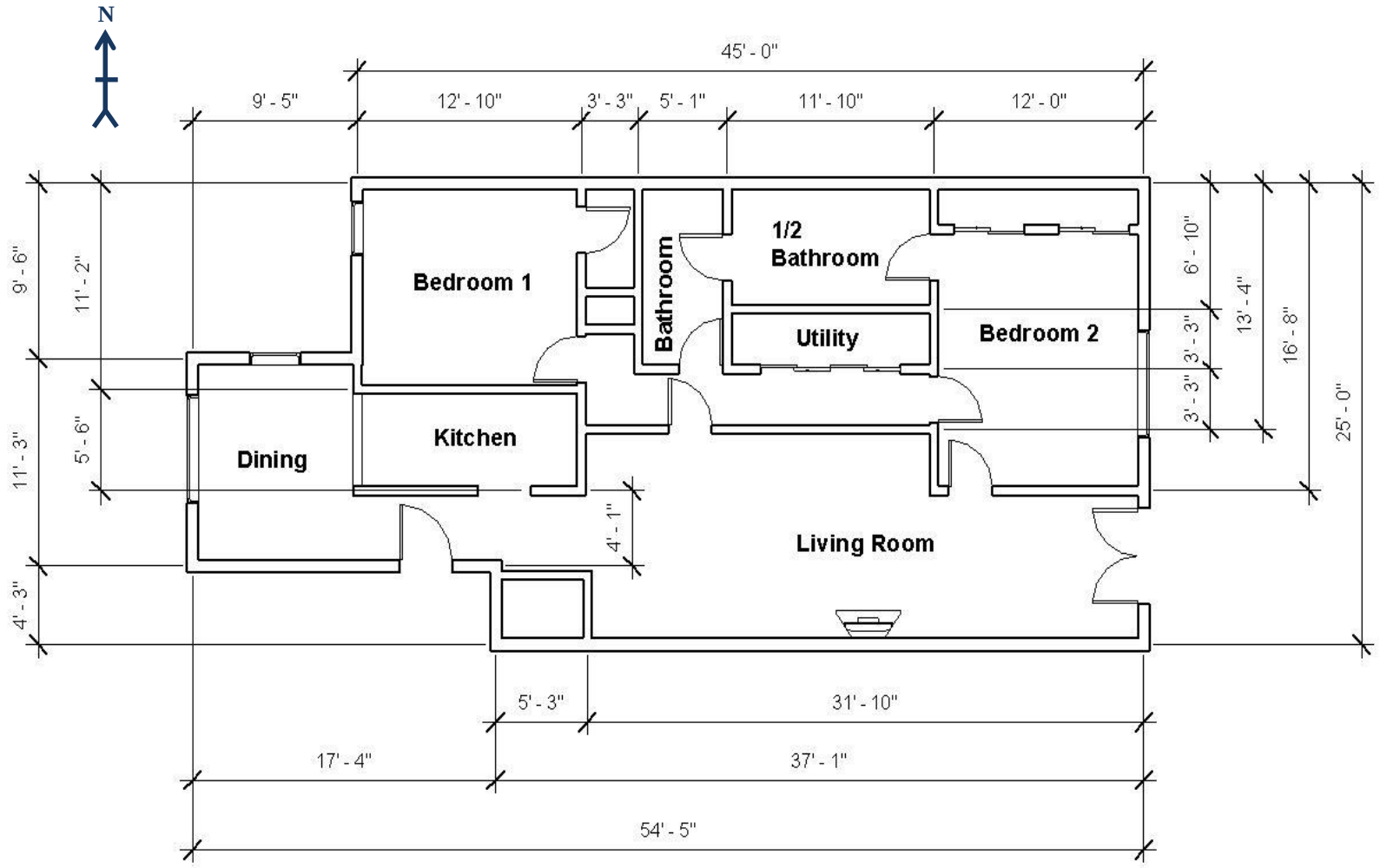

Figure 4-19. Plan view of the case-study house.

Table 4-5. Information for the case-study house.

Construction	Information for preliminary simulation
House type	Townhouse, attached house
Constructed year	1982
Orientation	West
Gross area	1,199 ft^2
Number of floors	1
Height	9 ft
Construction	Unkown (Wood assumed for simulation using 2009 IECC)
Floor	Slab-on-grade
Wall color	Dark
Wall area	1,429 ft^2
Wall R-value	Unkown (12.24 assumed for simulation using 2009 IECC)
Stud spacing	2x4
Window type	Single pane
Window area	103 ft^2
Frame type	Aluminum or steel
U-factor	Unkown (0.65 assumed for simulation using 2009 IECC)
SHGC	Unkown (0.30 assumed for simulation using 2009 IECC)
Roof configuration	Unconditioned, vented attic
Roof color	Medium
Roof R-value	Unkown (27.8 assumed for simulation using 2009 IECC)
Roof slope	45°
Space conditions	
Number of occupants	1
Setpoint	Heating 74°F / Cooling 75°F
Heating system	
Fuel	Electricity
System Type	Heat pump
Capacity	Unkown (24,000 Btu/hr assumed for simulation using 2009 IECC)
Efficiency	Unkown (HSPF 6.8 assumed for simulation using 2000 IECC)
Location	Attic
Manufacturer / year	Goodman CPKJ30-10 / approx. 2006

Table 4-5. Continued.

Cooling system	
Fuel	Electricity
System Type	Heat pump
Capacity	Unkown (2 tonnage assumed for simulation using 2009 IECC)
Efficiency	Unkown (SEER 10 assumed for simulation using 2000 IECC)
Location	Attic
Manufacturer / year	Goodman CPKJ30-10 / approx. 2006
DHW system	
Fuel	Electricity
Capacity	Unkown (40 gallon assumed for simulation using 2009 IECC)
Efficiency	Unkown (EIR 1 assumed for simulation using DOE-2.1E libraries)
Location	Conditioned zone
Manufacturer / year	Whirlpool EE2H4DRX9R5V / Unkown
Appliances	
Internal equipment	Refrigerator (x1), clothe washer (x1), clothe dryer (x1), dish washer (x1), range and oven (x1), television (x2), laptop (x1)
Lighting	Interior lighting: overhead light bulbs (x20) and lamp (x1) Exterior lighting (x1)

To create the calibrated baseline model, hourly electricity use data recorded by the SM for the baseline period[1] from April 15th, 2015 to April 14th, 2016 as well as the post-retrofit period from February 10th, 2017 to March 31st, 2017 was used. Table 4-6 shows the total monthly electricity use (kWh/month) and the monthly average daily electricity use (kWh/day) during the utility billing periods. In addition, a comparison of the measured electricity use data to the monthly utility bills is shown in Appendix B. During the analysis, it was observed that the hourly electricity use data recorded by the SM was slightly different from the monthly utility bills. One of the possible reasons could be a difference in the time when the electricity meter was read each month.

[1] The hourly electricity use data for February 29th, 2016, the leap day, was not used for this study.

Table 4-6. Hourly sum & monthly average daily electricity use of the case-study house.

	Billing period		Days in billing period	Hourly sum of monthly electricity use (kWh/Month)	Hourly sum - monthly avg. daily elec. use (kWh/Day)
	Start date	End date			
April	4/15/2015	5/13/2015	29	620.37	21.39
May	5/14/2015	6/15/2015	33	898.06	27.21
June	6/16/2015	7/15/2015	30	1015.19	33.84
July	7/16/2015	8/13/2015	29	1315.00	45.34
August	8/14/2015	9/14/2015	32	1277.68	39.93
September	9/15/2015	10/14/2015	30	841.49	28.05
October	10/15/2015	11/12/2015	29	595.76	20.54
November	11/13/2015	12/16/2015	34	1014.06	29.83
December	12/17/2015	1/13/2016	28	1269.18	45.33
January	1/14/2016	2/11/2016	29	1530.87	52.79
February	2/12/2016	3/15/2016	33	880.37	26.68
March	3/16/2016	4/13/2016	29	670.07	23.11
Total or Average			365	11,928.10	32.84

4.2.2. Weather Data Used for Building Energy Simulation

In order to create a calibrated building energy simulation model, actual weather data were converted to a format for use by the DOE-2.1E program. In this study, the Test Reference Year (TRY) format was used for the baseline simulation model. The TRY format includes the following weather information (Kim, 2014): dry-bulb temperature (°F), wet-bulb temperature (°F), dew-point temperature (°F), wind speed (knot), wind direction (degree), global solar radiation (Btu/hr-ft^2), direct normal solar radiation (Btu/hr-ft^2), and station pressure (inHg). The location of the case-study house was in Bryan, Texas, so the NOAA weather data from the nearby weather station at the College Station airport was used for the dry-bulb temperature, the wet-bulb temperature, the

dew-point temperature, the wind speed, the wind direction, the precipitation, and the station pressure (NOAA, 2016). The distance between the case-study house and the weather station was approximately 5.7 miles. In addition, global solar radiation and direct normal solar radiation data were obtained from a Solar Test Bench (STB) on the roof of the Langford building at Texas A&M University, which was located 3.3 miles away from the case-study house.

All weather data were collected using an hourly interval. However, sometimes the data had missing records, which were less than or equal to six hours. In such cases, missing periods were filled-in using linear interpolation using Eq. (3) (Long, 2006; Kim and Baltazar, 2010)

$$f(t_n) = f(t_1) + \left(\frac{f(t_2)-f(t_1)}{t_2-t_1}\right) \times \text{ n} \quad (3)$$

where $f(t_n)$ is the value of the missing period to be filled, $f(t_1)$ and $f(t_2)$ are the values close to the value of the missing period, and n is the length in hours of the missing period.

After the missing data were filled-in, all the weather data were formatted according to the required format of .TPE and .INP types (see Appendix C) for the DOE-2.1E model. Finally, the two files were combined and converted to the TRY format using the DOE-2 weather processor (Buhl, 1999). Figure 4-20 shows the overall procedure of this weather data conversion for simulation.

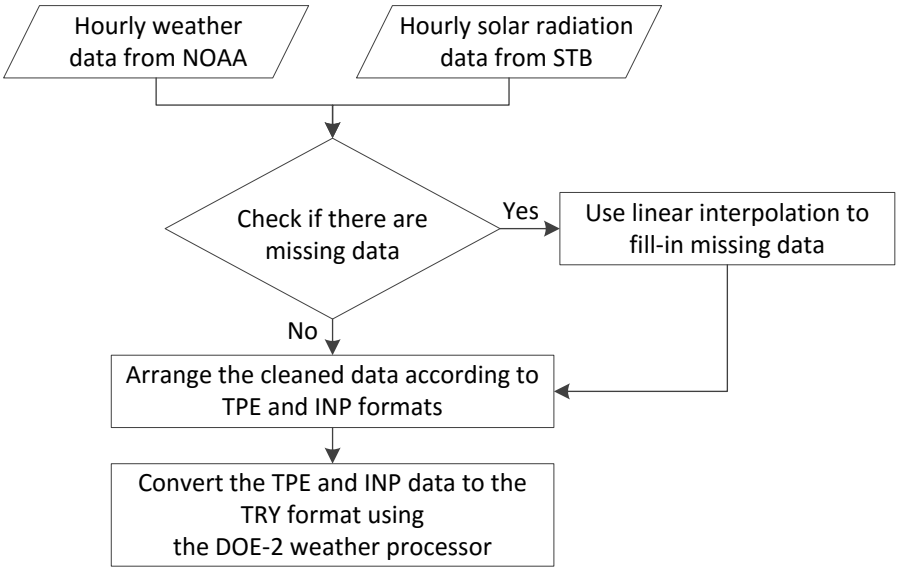

Figure 4-20. Overall procedure for processing weather data for simulation.

4.2.3. Calibrated Simulation Method (Level I Analysis)

In the next step, a calibrated simulation method (Level I Analysis) using several scenarios was developed and applied to quantify the detailed-potential energy savings from the use of HADs. After the hourly simulation model was calibrated to the hourly and the monthly average daily electricity use data for the baseline conditions, the calibrated simulation model was then used to simulate different usage and time-schedule scenarios using thermostatically controlled and non-thermostatically controlled HADs. Thermostatically controlled HADs are HADs that impact the air conditioning and heating systems, which are directly affected by inside and outside temperatures and are indirectly influenced by occupant behavior (Johnson et al. 2014). Non-thermostatically controlled HADs include lighting equipment and other appliances such as a refrigerator,

dish washer, clothes washer/dryer, etc., which are directly affected by occupant behavior.

This section has the following subsections: 1) a discussion of the calibration method for the hourly simulation model using the SM electricity and the IAT data, 2) scenarios for the calibrated simulation model, and 3) the use of the scenarios to quantify the detailed-potential electricity savings.

4.2.3.1. Calibrated Simulation Method (Level I Analysis)

Whole-building simulation models such as DOE-2.1E and EnergyPlus, mentioned in Section 2.2.1, can be calibrated using measured energy use and environmental data (e.g., indoor conditions and coincident weather data) obtained from an existing building. In other words, the inputs of a simulation model are adjusted to allow simulated energy use to better match measured energy use. Such an approach is called a calibrated simulation method (ASHRAE, 2013a). In this study, the DOE-2.1E simulation model was calibrated using the hourly electricity use data recorded by the SM, interior conditions, and coincident weather data. The Indoor Air Temperature (IAT) calibration (Bou-Saada, 1994), informative graphical comparative analysis (Bou-Saada and Haberl, 1995a, 1995b; Haberl et al, 1996; Haberl and Abbas, 1998a, 1998b; Haberl and Bou-Saada, 1998), and sensitivity analysis (Manke et al., 1996; Kim, 2014; Sever et al., 2011) were used in the calibration process.

First, the DOE-2.1E model was created using the house information contained in Table 4-5 and the appropriate information from the 2000 or 2009 IECC performance

path and the DOE-2.1E libraries (i.e., nominal values). In the next step for the calibration process for the hourly calibration, hourly electricity use, measured Indoor Air Temperatures (IATs), weather, occupancy, and thermostat data (i.e., heating and cooling setpoints and HVAC system schedule) were used in the calibration process. Detailed methods for collecting the data will be described in Section 4.3.

Figure 4-21 shows a flowchart of the hourly calibration method used in this study, which used one week of data from the post-retrofit period from February 20th, 2017 to February 26th, 2017. For this week, the measured IATs, weather, occupancy detection, and thermostat data (heating and cooling setpoints, HVAC system-on times) were used to calibrate the simulated hourly electricity use to the measured hourly electricity use recorded by the SM using the Normalized Mean Bias Error (NMBE) and the Coefficient of Variation of the Root-Mean-Square Error (CV-RMSE). After that, simulated IATs were compared with the measured IATs, also using the NMBE and the CV-RMSE. In this step, improvements were made over the previous study (Bou-Saada, 1994), which include the new statistical IAT indices. This two-way calibration process provided an improved hourly calibration for the simulation model by representing the electricity use and the IAT characteristics of the case-study house for the calibration period.

To enter the hourly occupancy diversity factors into the DOE-2.1E simulation, one-minute interval occupancy data from portable occupancy sensors placed in the case-study house were converted to hourly diversity factors using the average of the 60 minutes from the one minute occupancy data (see Figure 4-37). During the selected

week from February 20th, 2017 to February 26th, 2017, there were no holidays, so the diversity factors for holidays were assumed to be the same as the diversity factors used for Sunday. The selected week was then used as a representative week for the monthly average daily simulation using the baseline period from April 15th, 2015 to April 14th, 2016. Finally, the simulated, whole-building electricity use from the calibrated DOE-2.1E model was compared with the baseline SM electricity data, which was previously discussed in Section 4.1 (Level 0 Analysis).

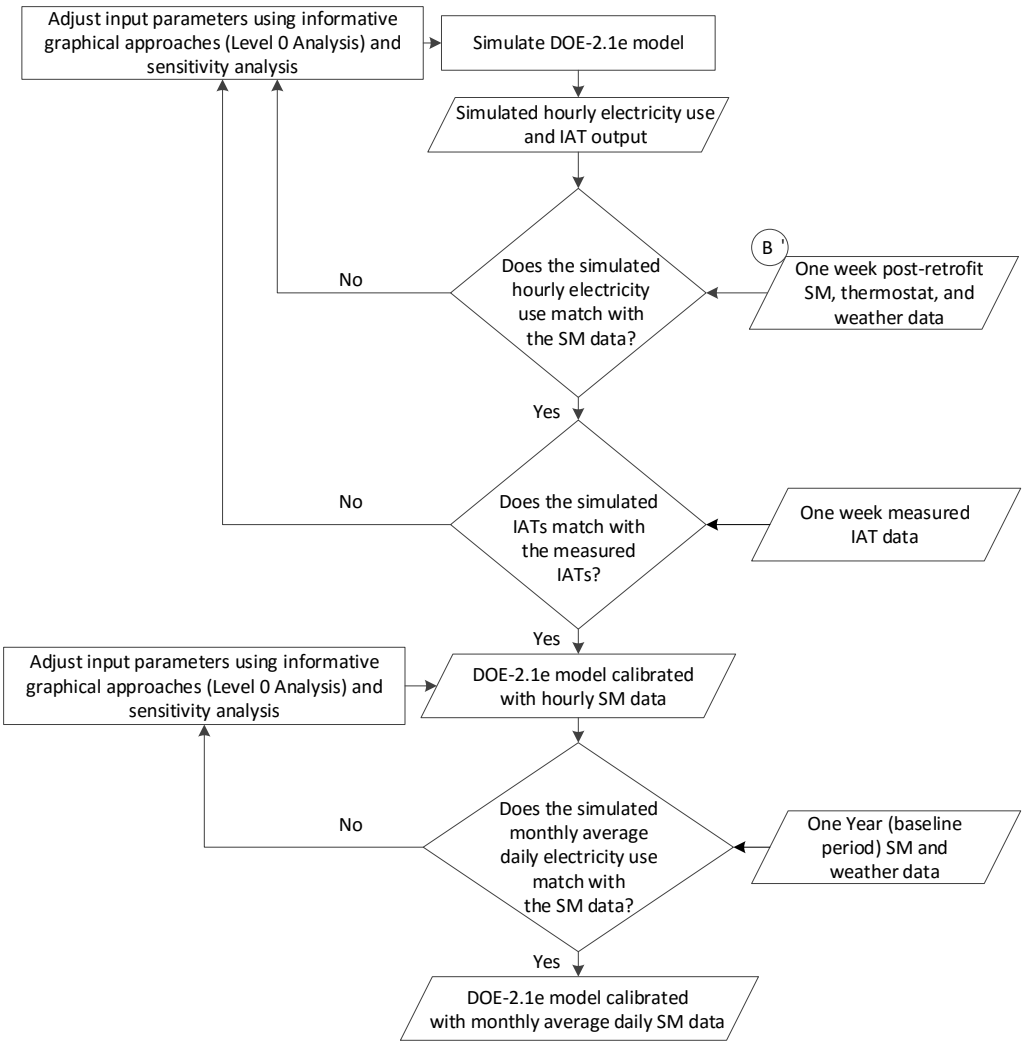

Figure 4-21. Procedure to calibrate the DOE-2.1E model.

For the next step in the calibration process, a sensitivity analysis was performed using the 5P change-point linear regression model along with monthly average daily electricity use and the corresponding OAT. To accomplish this, the hourly electricity use data and the simulated electricity use data were converted to the monthly average daily electricity along with monthly average daily OAT. Next, the 5P model was used, as previously discussed in Section 4.1.

Using Eq. (1) from the previous section, the total electricity use can be expressed as Eq. (4).

$$E_{tot} = E_{w.i.} + HS(T_{OA} - T_{h.b.})^{-} + CS(T_{OA} - T_{c.b.})^{+} \quad (4)$$

Where E_{tot} is the building electricity use, T_{OA} is the outside air temperature, $E_{w.i.}$ is the weather-independent electricity use, HS is the heating slope that represents heating energy use by the outside air temperature, $T_{h.b.}$ is the heating balance point (change point) temperature that begins heating space conditioning, CS is the cooling slope that represents cooling energy use by the outside air temperature, $T_{c.b.}$ is the cooling balance point (change point) temperature that begins cooling space conditioning, and $(\ )^{-}$ and $(\ )^{+}$ are the notations that the values of the parentheses shall be zero when they are positive and negative, respectively (Kissock et al., 2003; Sever et al., 2011). Figure 4-22 shows the coefficients of the 5P model.

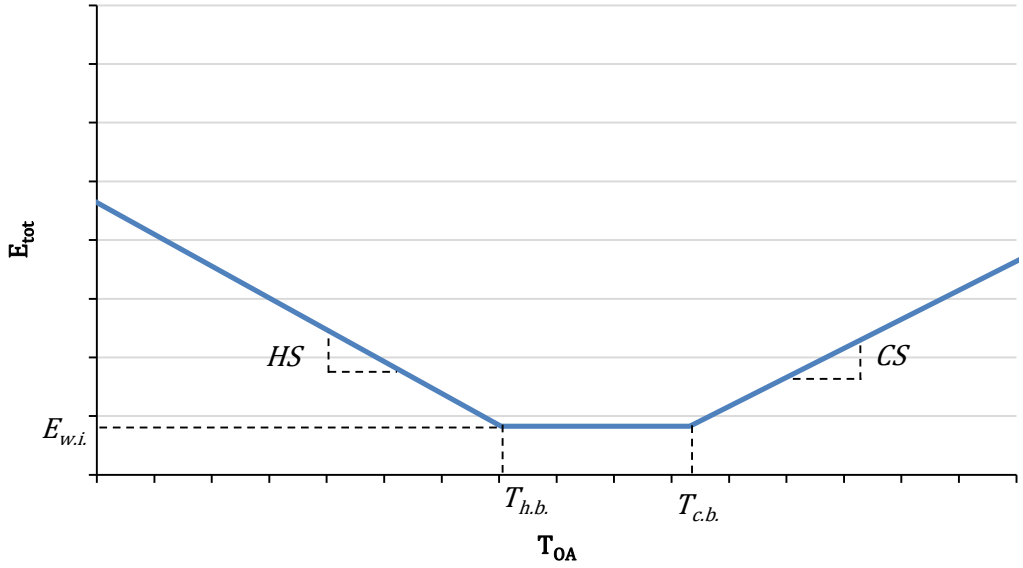

Figure 4-22. 5P change-point linear regression model showing the coefficients (Sever et al., 2011).

The 5P change-point linear model is particularly useful because the coefficients of the 5P model have been shown to have physical significance (i.e., physical characteristics), which can be used to evaluate certain energy conservation and operation measures in a building (Kim, 2014). For example, the $E_{w.i.}$ coefficient of the 5P model represents the weather-independent electricity use in a house. This weather-independent electricity use, often includes the electricity use of the lighting equipment and appliances (e.g., refrigerators, clothe washers and dryers, dish washers, ranges and ovens, televisions, etc.). The coefficients of HS and CS represent heating loads/heating system efficiency and cooling loads/cooling system efficiency, respectively. The coefficients of HS and CS are expressed using Eq. (5) and Eq. (6).

$$HS = \frac{HC}{\eta_h} \quad (5)$$

$$CS = \frac{CC}{\eta_c} \quad (6)$$

Where η_h and η_c are heating system efficiency and cooling system efficiency, respectively. In addition, HC is the heating coefficient, which represents the heat loss through the building envelope (e.g., walls, windows, doors, roof, and floor) and heat loss due to infiltration and ventilation. CC is the cooling coefficient which represents heat gain through the building envelope and heat gain from the building infiltration and ventilation. The coefficients of HC and CC can be expressed as Eq. (7) and Eq. (8), respectively.

$$HC = UA + V\rho C_p \quad (7)$$

$$CC = UA + V\rho C_p \quad (8)$$

Where U is the overall envelope conductance, A the overall envelope area, V is the overall infiltration and ventilation volume rate, ρ is the air density, and C_p is the air specific heat.

Finally, $T_{h.b.}$ is the heating balance-point (change-point) temperature that indicates the beginning of the space heating. $T_{c.b.}$ is the cooling balance-point (change-point) that indicates the beginning of the space cooling. The coefficients of $T_{h.b.}$ and $T_{c.b.}$ are expressed as Eq. (9) and Eq. (10), respectively.

$$T_{h.b.} = T_{h.set.} - \frac{Q_i}{HC} \quad (9)$$

$$T_{c.b.} = T_{c.set.} - \frac{Q_i}{CC} \quad (10)$$

Where $T_{h.set.}$is the heating setpoint temperature, $T_{c.set.}$is the cooling setpoint temperature, and Q_i is the internal heat gain (e.g., solar heat gain, lighting equipment, appliances, and occupants). Table 4-7 shows a summary of the relationships between each coefficient and physical meaning.

Table 4-7. Summary of the relationships between the change point linear model coefficients and physical meanings (Kim, 2014; Sever et al., 2011).

Coefficient	Expression	Physical meaning
$E_{w.i.}$	$E_{w.i.} = E_{w.i.}$	Weather-independent electricity use from wireless internet-connected lighting and daylighting control equipment, appliances (e.g., wireless internet-connected refrigerators, clothe washers and dryers, dish washers, ranges and ovens, televisions, etc.), and DHW systems.
HS	$HS = \frac{HC}{\eta_h}$	Heating energy use by the OAT. It varies by heating load and heating system efficiency.
CS	$CS = \frac{CC}{\eta_c}$	Cooling energy use by the OAT. It varies by cooling load and cooling system efficiency.
HC	$HC = UA + V\rho C_p$	Conductive heat loss through building envelope and convective heat loss through infiltration and ventilation.
CC	$CC = UA + V\rho C_p$	Conductive heat gain through building envelope and convective heat gain through infiltration and ventilation.
$T_{h.b.}$	$T_{h.b.} = T_{h.set.} - \frac{Q_i}{HC}$	Heating balance-point (change-point) temperature that begins heating space conditioning. It varies by wireless connected heating thermostat setpoint, internal heat gain, and heating load.
$T_{c.b.}$	$T_{c.b.} = T_{c.set.} - \frac{Q_i}{CC}$	Cooling balance-point (change-point) temperature that begins cooling space conditioning. It varies by wireless connected cooling thermostat setpoint, internal heat gain, and cooling load.

Using the relationship between the coefficients and the physical meanings, the 5P change-point linear regression model (i.e., the initial model) from the DOE-2.1E hourly simulation results was compared to the baseline hourly electricity use data after converting to monthly average daily values. Next, the coefficients of the initial 5P model were changed by observing the physical meanings that best matched the case-study house. For example, increasing the heating thermostat setpoint in the simulation causes the heating balance-point temperature $T_{h.b.}$ to be higher because the coefficient $T_{h.b.}$ indicates the beginning temperature of the onset of the space heating. Another example where the heating system efficiency was decreased caused the heating slope HS to have a steeper slope because a steeper slope HS means a higher heating energy use. Figure 4-23 shows graphical examples of the 5P model changes caused by varying each coefficient, which represents physical meaning. For example, if the weather-independent electricity use increased, $E_{w.i.}$ would be increased (i.e., upper plot). If cooling load is increased and/or cooling system efficiency is decreased, CS would be increased (i.e., middle plot). Finally, if heating thermostat setpoint is increased, the internal load is decreased, and/or heating load is increased, $T_{h.b.}$ would be increased (i.e., lower plot). Table 4-8 provides a summary of the impact of a coefficient change versus the physical meaning.

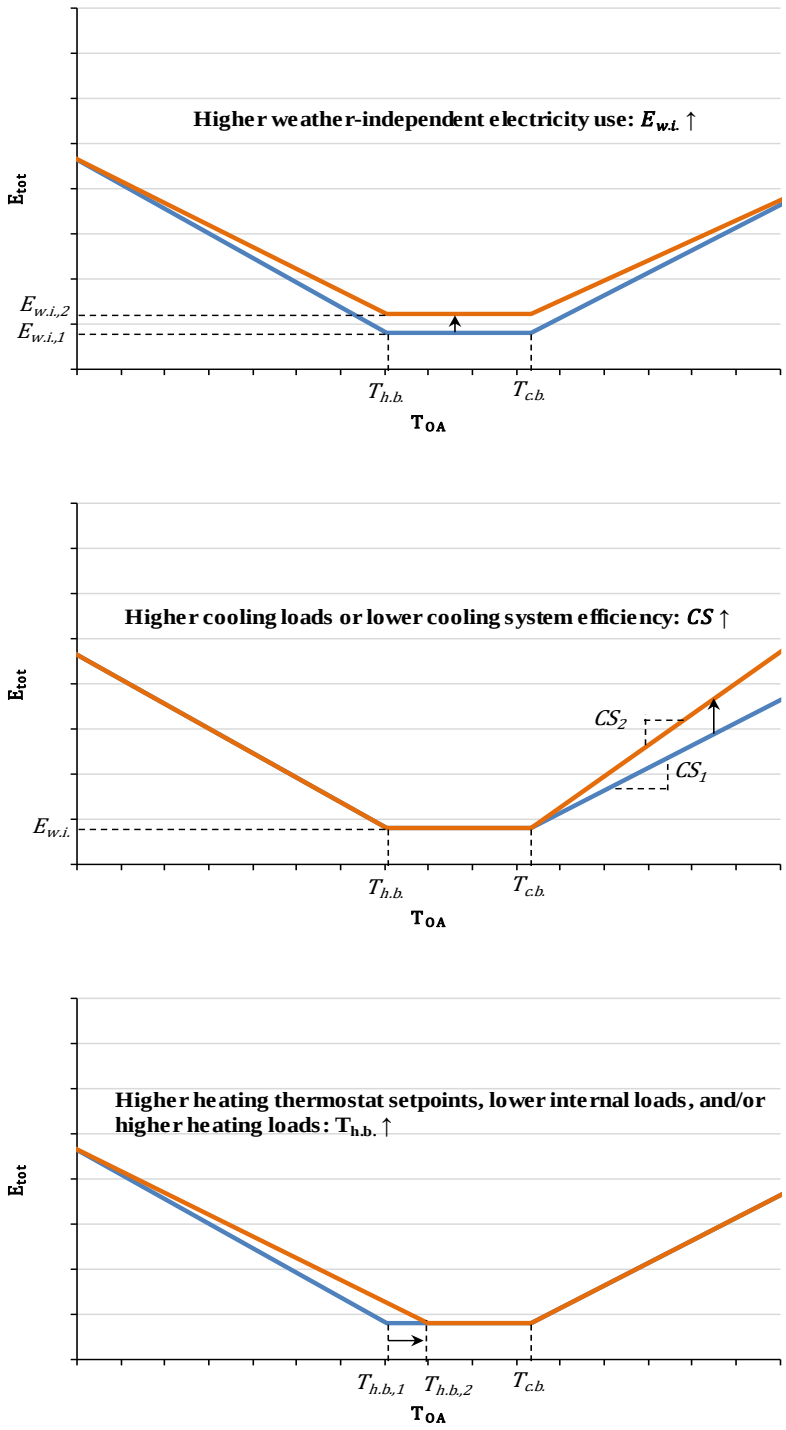

Figure 4-23. Changes of 5P linear regression model by varying the physical coefficients: increasing $\boldsymbol{E_{w.i.}}$ (upper), increasing $\boldsymbol{CS}$ (middle), and increasing $\boldsymbol{T_{h.b.}}$ (lower) (Kim, 2014; Sever et al., 2011).

Table 4-8. Summary of the coefficient change versus physical meaning (Kim, 2014; Sever et al., 2011).

Coefficient	Expression	Physical meaning	Coefficient change
$E_{w.i.}$	$E_{w.i.} = E_{w.i.}$	Higher weather-independent electricity use.	$E_{w.i.} \uparrow$
		Lower weather-independent electricity use.	$E_{w.i.} \downarrow$
HS	$HS = \frac{HC}{\eta_h}$	Higher heating loads (conduction and convective heat losses) and/or lower heating system efficiency.	$HS \uparrow$
		Lower heating loads (conduction and convective heat losses) and/or higher heating system efficiency.	$HS \downarrow$
CS	$CS = \frac{CC}{\eta_c}$	Higher cooling loads (conduction and convective heat gains) and/or lower cooling system efficiency.	$CS \uparrow$
		Lower cooling loads (conduction and convective heat gains) and/or higher cooling system efficiency.	$CS \downarrow$
$T_{h.b.}$	$T_{h.b.} = T_{h.set.} - \frac{Q_i}{HC}$	Higher heating thermostat setpoints, lower internal loads, and/or higher heating loads.	$T_{h.b.} \uparrow$
		Lower heating thermostat setpoints, higher internal loads, and/or lower heating loads.	$T_{h.b.} \downarrow$
$T_{c.b.}$	$T_{c.b.} = T_{c.set.} - \frac{Q_i}{CC}$	Higher cooling thermostat setpoints, lower internal loads, and/or higher cooling loads.	$T_{c.b.} \uparrow$
		Lower cooling thermostat setpoints, higher internal loads, and/or lower cooling loads.	$T_{c.b.} \downarrow$

To check the agreement between the 5P model from the measured electricity use and the 5P model from calibrated simulation results, the Normalized Mean Bias Error (NMBE) (%) and the Coefficient of Variation of the Root-Mean-Square Error (CV-RMSE) (%) were used as statistical indices (ASHRAE, 2014).

$$\mathrm{NMBE} = \frac{\frac{\sum_i (y_i - \widehat{y_i})}{(n-p)}}{\bar{y}} \times 100 \tag{10}$$

$$\mathrm{CV-RMSE} = \frac{\sqrt{\frac{\sum_i (y_i - \widehat{y_i})^2}{(n-p)}}}{\bar{y}} \times 100 \tag{11}$$

Where y_i is the SM electricity data, $\widehat{y_i}$ is the calibrated simulation data, $\bar{y}$ is the average of the SM data, n is the number of data points, and p is the number of parameters.

ASHRAE Guideline 14-2014 suggests the NMBE of 5 % and the CV-RMSE of 15 % for monthly calibration and the NMBE of 10 % and the CV-RMSE of 30 % for hourly calibration as maximum limits, respectively (ASHRAE, 2014).

4.2.3.2. Scenarios for the calibrated simulation model

To quantify detailed-potential electricity savings from the use of HADs, different scenarios were developed for the calibrated DOE-2.1E simulation model. For the scenarios, the case-study house was divided into seven zones in order to analyze each zone. In addition, the HADs were categorized into two groups: thermostatically controlled HADs and non-thermostatically controlled HADs. Thermostatically controlled

HADs include the wireless, programmable thermostat for the air-conditioning and heating systems and the DHW system, which can be directly affected by inside and outside temperatures and indirectly influenced by occupant behavior (Johnson et al., 2014). Non-thermostatically controlled HADs include lighting equipment with motion sensors and other appliances such as a dish washer and clothes washer/dryer, which can be directly affected by occupant behavior. To focus on the opportunities of the electricity savings rather than the electric demand savings, only the thermostat and lighting equipment were selected for this analysis. For future work, other appliances would need to be analyzed. For the thermostatically controlled HADs (i.e., wireless programmable thermostat with motion detection) and the non-thermostatically controlled HADs (i.e., lighting equipment with motion detection), one week of measured occupancy detection data from the portable occupancy data loggers was selected to determine the occupancy schedules for each zone. Using these thermostat and lighting schedules, the following scenarios were developed (Table 4-9).

Table 4-9. Summary of the scenarios.

Component	Scenario 1	Scenario 2	Scenario 3	Scenario 4	Scenario 5
Thermostat setback schedule for a whole day	1 to 5 ℉ setback	-	-	-	-
Thermostat nighttime setback schedule	-	1 to 5 ℉ setback	-	-	-
Thermostat setback schedule using occupancy detection	-	-	1 to 5 ℉ setback	-	-
HVAC system multi-zone control using occupancy detection	-	-	-	1 to 5 ℉ setback for seven zones	-
Lighting schedule using occupancy detection	-	-	-	-	Occupancy detection for lighting

4.2.3.3. Use of scenarios to quantify detailed-potential electricity savings

The scenarios that were developed were used to quantify the detailed-potential electricity savings of the wireless, programmable thermostat and lighting controls with occupancy detection sensors. The simulated, baseline electricity use during the baseline period from April 15th, 2015 to April 14th, 2016 was compared with the simulated electricity use from the calibrated DOE-2.1E model with the different scenarios during the same period (i.e., weather normalization). To obtain the simulated electricity use, the coincident weather data of the baseline period was converted to the TRY format, which was previously discussed in Section 4.2.2. Finally, monthly average daily savings were calculated using the different scenarios.

4.3. Development of an M&V Method (Level II Analysis) for Quantifying Actual Electricity Savings

This section describes the new method that was developed to quantify the actual electricity savings from the use of HADs (i.e., Level II Analysis), including new methods to measure and characterize IATs and occupancy patterns of each zone. Figure 4-24 shows the procedures used in the Level II Analysis. In this analysis, a wireless, programmable thermostat with motion detection (i.e., one of the HADs) was installed in the case-study house. Hourly electricity consumption from the period after the wireless thermostat installation (i.e., post-retrofit period) was then collected. Then, the actual electricity savings for 50 days from February 10th, 2017 to March 31st, 2017 (i.e., the post-retrofit period) was calculated by comparing the measured hourly electricity use

data during the post-retrofit period with the electricity use predicted from the change-point linear model using coefficients from the baseline period. In addition, the weather-normalized, annual electricity savings were calculated using the coefficients from the change-point linear models from the post-retrofit period and the coefficients from the baseline period. For this analysis, the IMT and statistical analysis were used to quantify the performance for the two different periods (i.e., occupied hours and unoccupied hours). The two periods were categorized using the data obtained from seven occupancy data loggers.

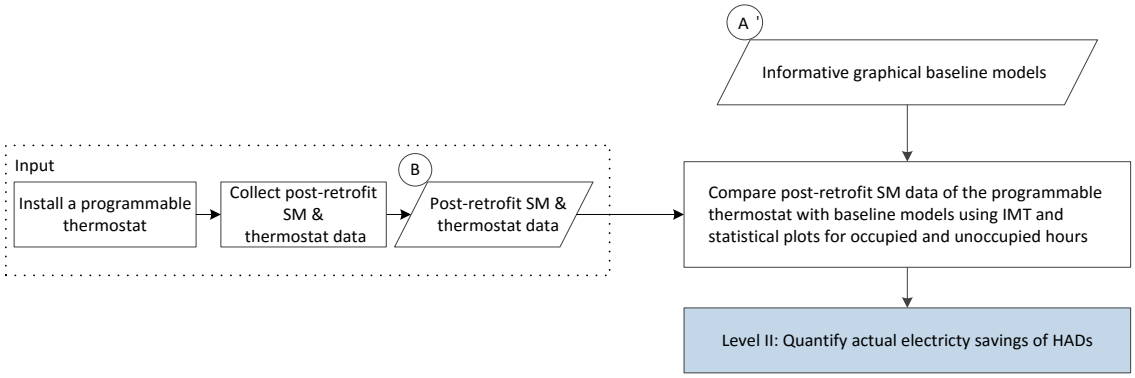

Figure 4-24. Diagram for quantifying actual electricity savings (Level II Analysis).

In addition, to check the thermal comfort during the post-retrofit period, average IATs and Relative Humidity (RH) (%) from occupied hours and unoccupied hours during the post-retrofit were examined using a 5 °F binned quartile analysis and ASHRAE Standard 55-2013 (ASHRAE, 2013b). Figure 4-25 shows the flowchart of the process used to check thermal comfort using the average IATs and RH based on the ASHRAE Standard 55-2013.

The IATs measured from the seven zones at the case-study house were collected during the post-retrofit period, and the average IATs were calculated. Next, the hourly occupancy diversity factors for each zone were calculated using the 1-minute interval data from each occupancy data loggers of the seven zones. The average, hourly occupancy diversity factors from the seven zones were then calculated. Using average, hourly occupancy diversity factors of zero and non-zero, the hours were categorized into the unoccupied hours and the occupied hours, respectively. Finally, the Relative Humidity (RH), recorded at the new thermostat (see Figure 4-26), was used to analyze if indoor environmental conditions were met for the comfort zones (i.e., graphic comfort zone method) of ASHRAE Standard 55-2013.

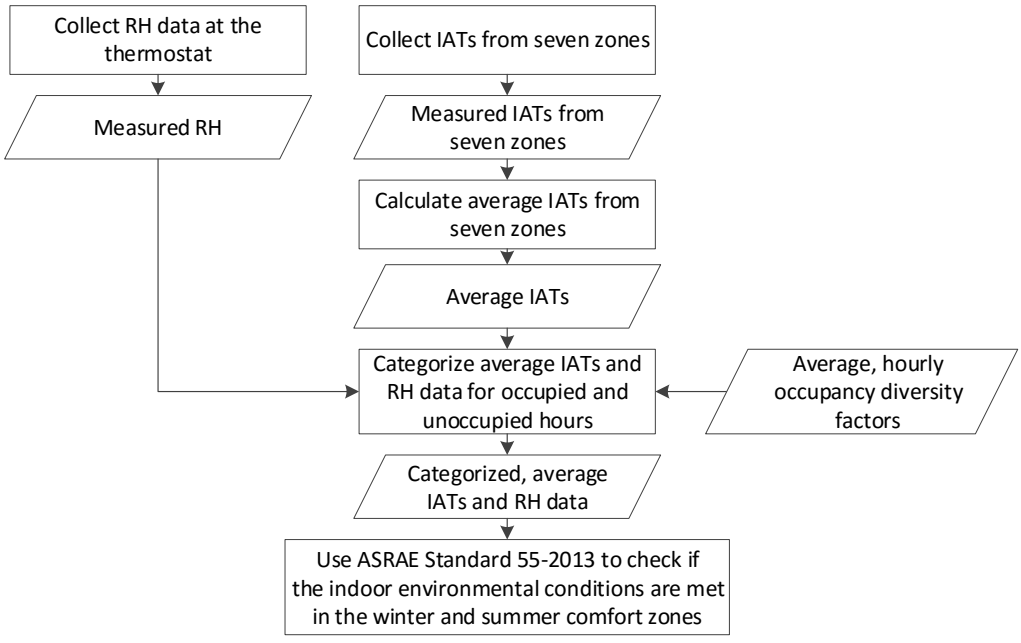

Figure 4-25. Flowchart to check thermal comfort using the average IATs and RH during the post-retrofit period.

To collect the IATs, eight portable temperature data loggers were installed to cover each zone in the case-study house as well as at the location of the thermostat. Figure 4-26 shows the locations of the eight temperature data loggers. Prior to taking the measurements, the temperature data loggers were calibrated using a three-point calibration process based on the American Society for Testing and Materials (ASTM) Standard E77-14 (ASTM, 2014). Appendix D shows the procedure of the three-point calibration and the resultant calibration.

Figure 4-27 provides the locations of the zones and diffusers. Seven zones were chosen based on the diffuser locations of the HVAC system. During the measurement period, it was observed that the hallway was used as the return air path for the HVAC system. In addition, it was observed that there were the clothes washers/dryers and the DHW system in the utility room, which warmed up the return air because the door of the utility room was normally opened. Therefore, for future studies of similar condition, it is recommended that IATs be measured at the utility room to more accurately calculate average IATs for the return air.

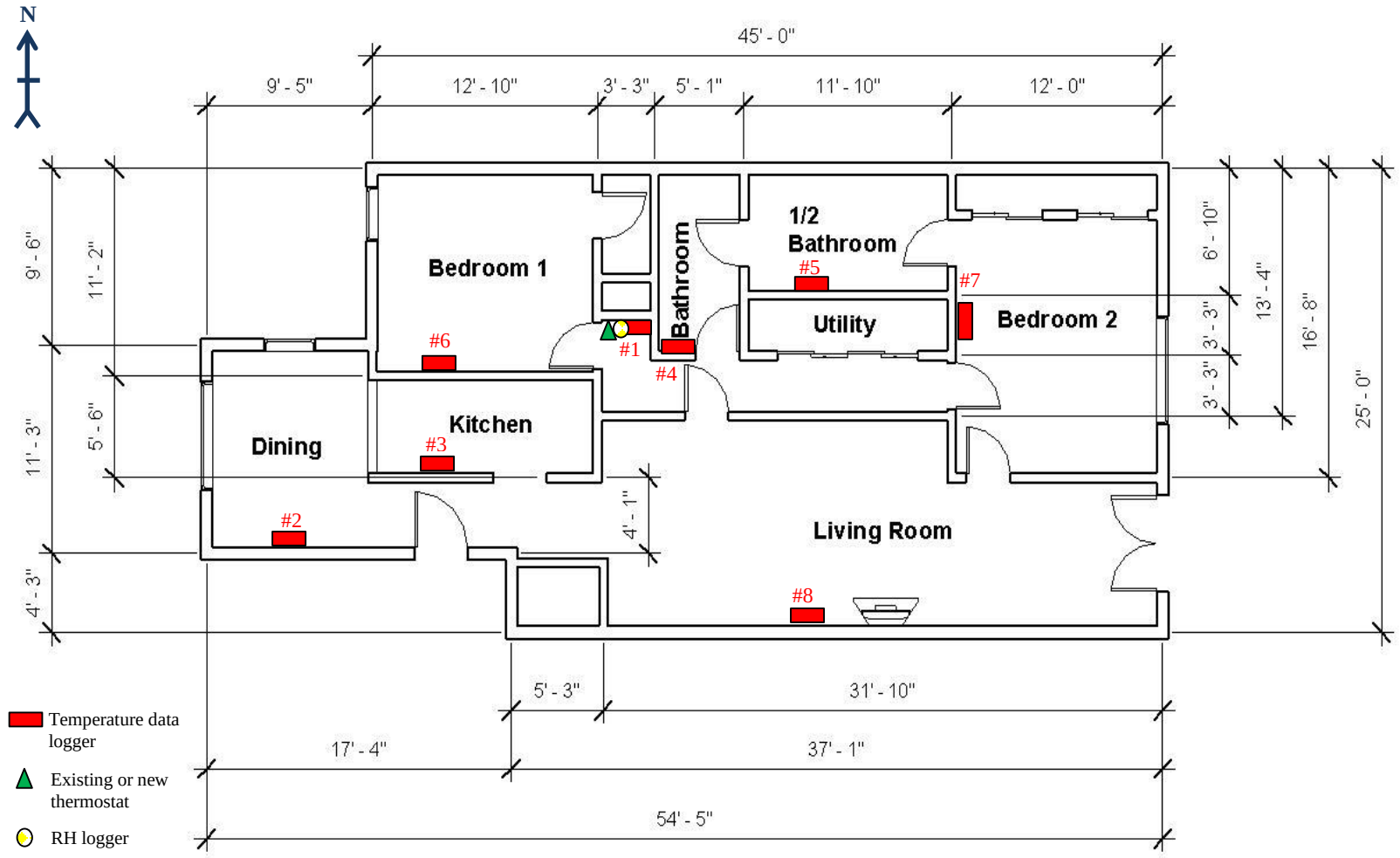

Figure 4-26. Plan view showing the thermostat and the eight temperature data loggers in the case-study house.

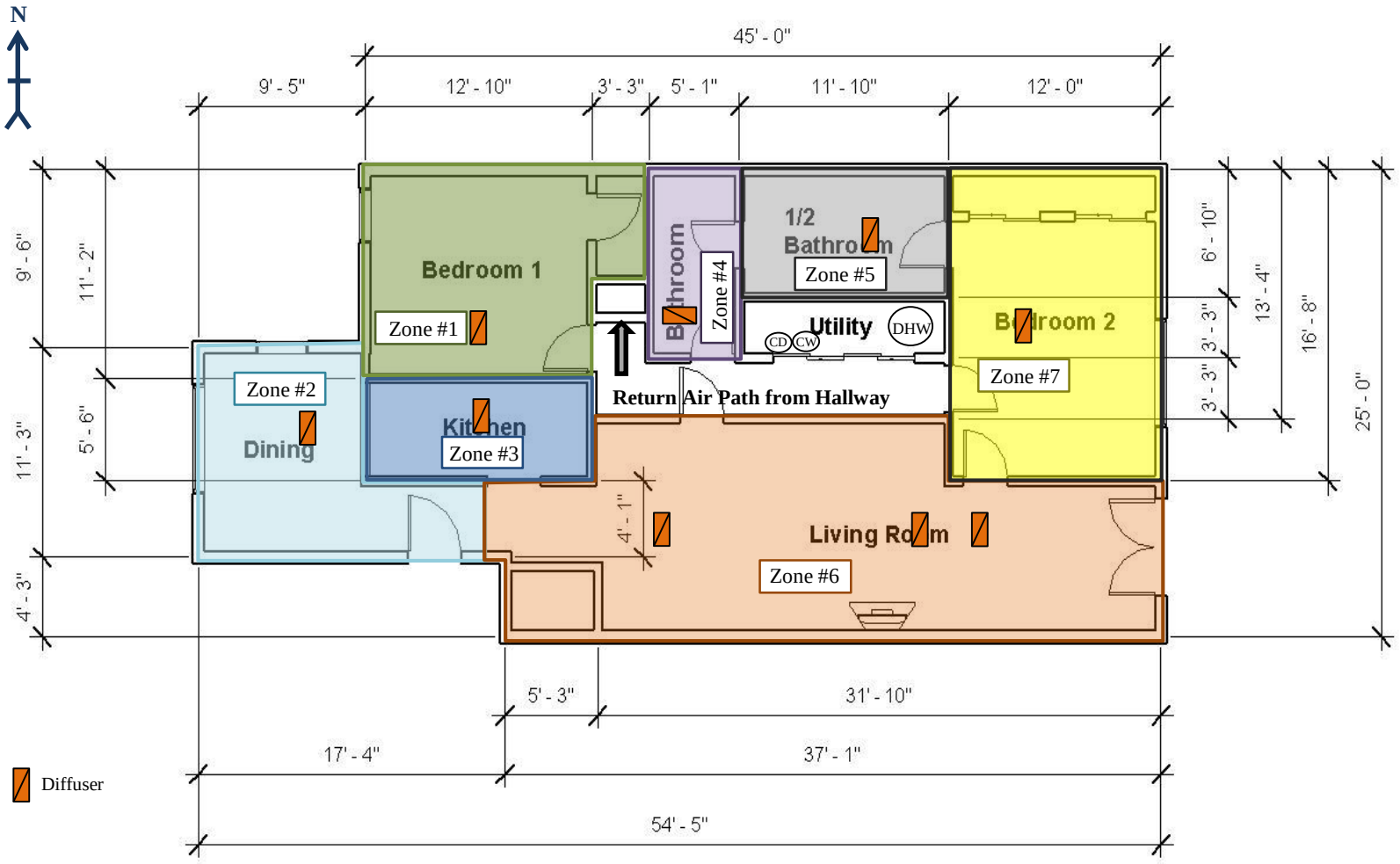

Figure 4-27. Plan view showing the seven zones and the diffuser locations.

The IATs measured from the eight data loggers during the nine months (from August 1st, 2016 to January 31st, 2017) were analyzed using time series and BWM plots. Figure 4-28 shows time series plots of the IATs, and Figures 4-29 and 4-30 show plots of the IATs versus the OATs during the same period using the statistical BWM plots. The time series plots (Figure 4-28) show that the IATs on September 12th and 13th, 2016, were exceptionally high, and the IATs from December 19th to December 21th, 2016, were exceptionally low. In addition, the data logger #7 had missing data from August 26th, 2016 at 7:00 am to September 29th at 5:00 pm.

After excluding the exceptional data and missing data from the analysis, the final BWM plots (Figures 4-29 and 4-30) were created to analyze the trends of the IATs versus the OATs. The calculated heating and cooling balance-point temperatures from the baseline period were also included in the figures to visually divide heating, non-heating and cooling, and cooling periods. The heating balance point of 60.2 °F and the cooling balance point of 76.6 °F were used for the weekdays. The balance points were obtained from the weekday 5P change-point linear model of the baseline period (from April 15th, 2015 to April 14th, 2016). In addition, the heating balance point of 63.7 °F and the cooling balance point of 74.1 °F were used for the weekends/holidays. These balance points were obtained from the weekend/holiday 5P model of the baseline period. During the pre-retrofit period, the heating setpoint of 74.0 °F and the cooling setpoint of 75.0 °F were used.

During the weekdays (Figure 4-29), Data Logger #1 showed relatively constant IATs because the data logger was installed near the location of the existing thermostat.

Data Logger #2 showed that the IATs in the dining area of the case-study house were significantly affected by the coincident OATs. This was because the dining room has large windows facing west. During the weekdays, the maximum (81.7 ℉) and the minimum (63.9 ℉) IATs for all the data loggers were recorded at the data logger #2 in the dining room (Zone #2). During the weekends/holidays (Figure 4-30), the maximum (82.5 ℉) IAT was recorded at Data Logger #3 in the kitchen (Zone #3) when the OAT was inside the 70-75 ℉ bin. The minimum (65.8 ℉) was recorded at Data Logger #2 when the OAT was inside the 20-25 ℉ bin.

It should be noted that the trends of the individual IATs from the seven zones were different from the trends of the IATs from the thermostat location. In other words, different zones had different IATs even though one thermostat controlled the whole house.

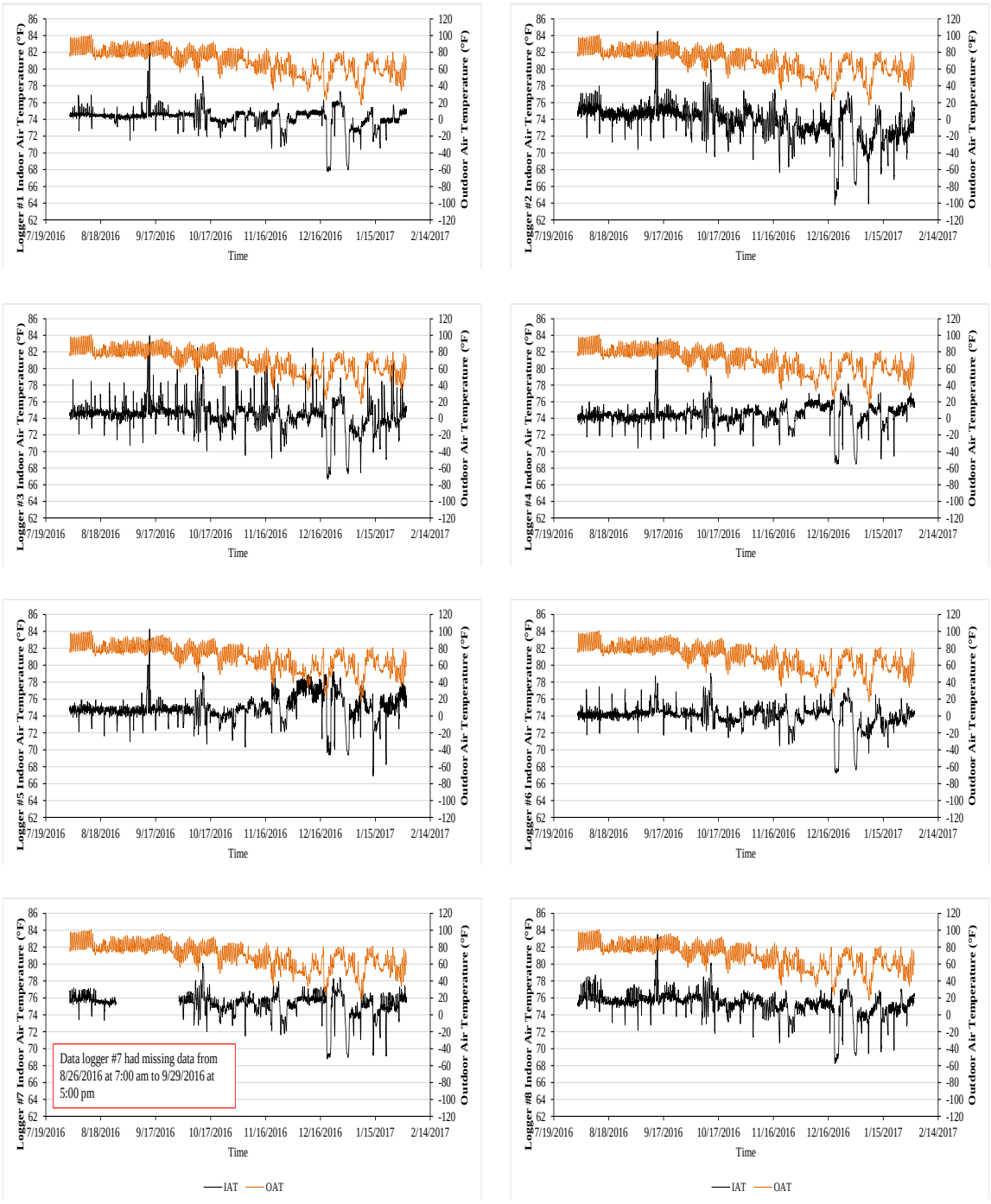

Figure 4-28. IATs from the eight data loggers during the pre-retrofit period (August 1st, 2016 to January 31st, 2017).

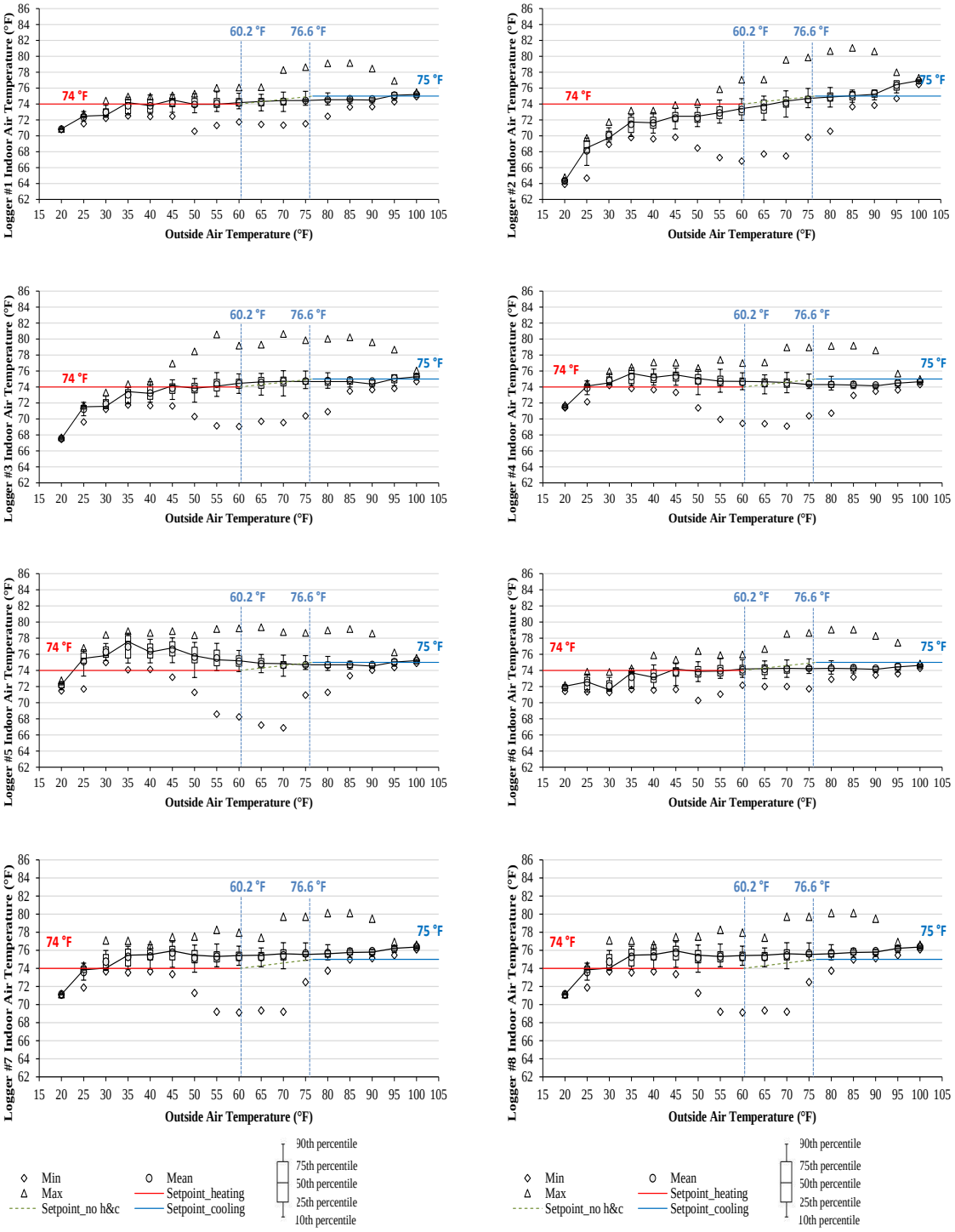

Figure 4-29. IATs versus OATs from the eight data loggers before the retrofit during weekdays (August 1st, 2016 to January 31st, 2017).

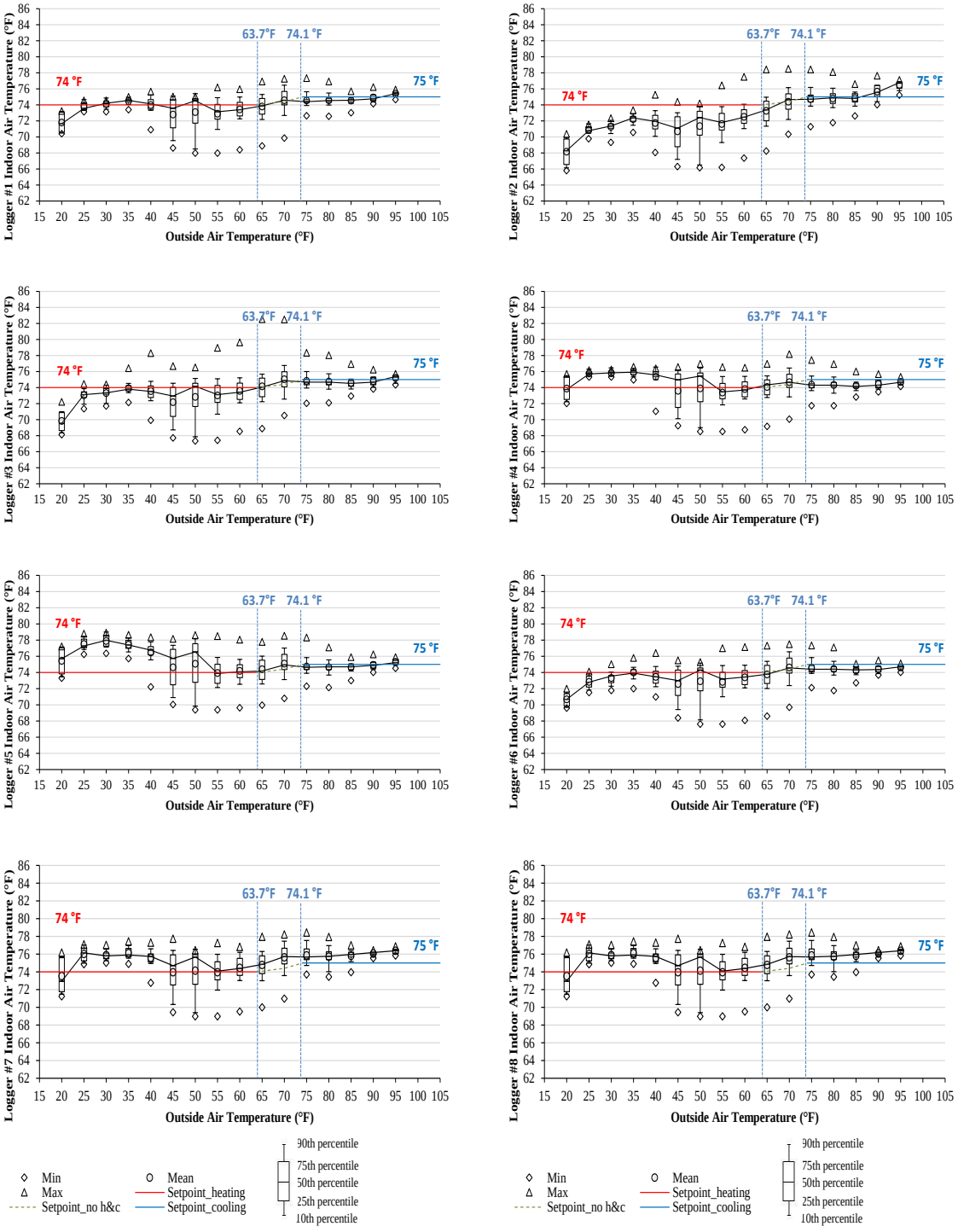

Figure 4-30. IATs versus OATs from the eight data loggers before the retrofit during weekends/holidays (August 1st, 2016 to January 31st, 2017).

Figure 4-31 for weekdays and Figure 4-32 for weekends/holidays show the IATs from the same eight data loggers after the new wireless, programmable thermostat with the motion detection was installed. In these plots, the blue dotted lines show the 50th percentile from the data collected from the same data loggers for the period before the thermostat retrofit. In the plots, it can be seen that the 50th percentile of the IATs after the retrofit was lower than the IATs before the retrofit (i.e., the blue dotted lines) during the heating period (when the OATs were lower than the heating balance-point temperatures of 60.2 °F for the weekdays and 63.7 °F for the weekends/holidays, respectively).

For the cooling period (when the OATs were higher than the cooling balance-point temperatures of 76.6 °F for the weekdays and 74.1 °F for the weekends/holidays, respectively), the 50th percentile after the retrofit was higher than the 50th percentile before the retrofit. Such trends begin to explain the reason for the significant electricity reductions to the homeowner for heating and cooling when the new wireless, programmable thermostat with the motion sensors was used because the lower effective heating setpoints resulted in lower heating electricity use during the heating period, and the higher cooling effective setpoints resulted in lower cooling electricity use during the cooling period.

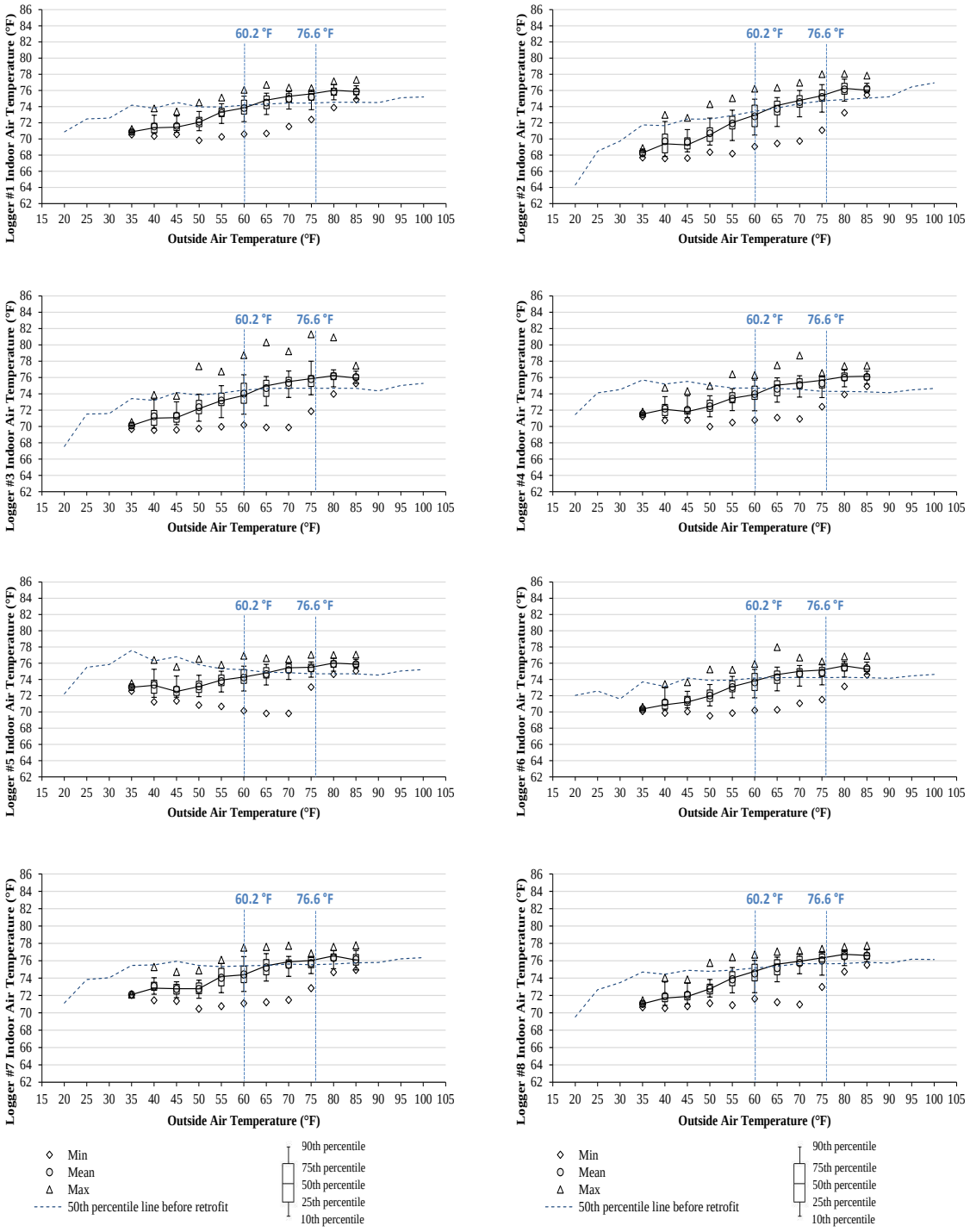

Figure 4-31. IATs versus OATs from the eight data loggers after the retrofit during weekdays (February 10th, 2017 to March 31th, 2017).

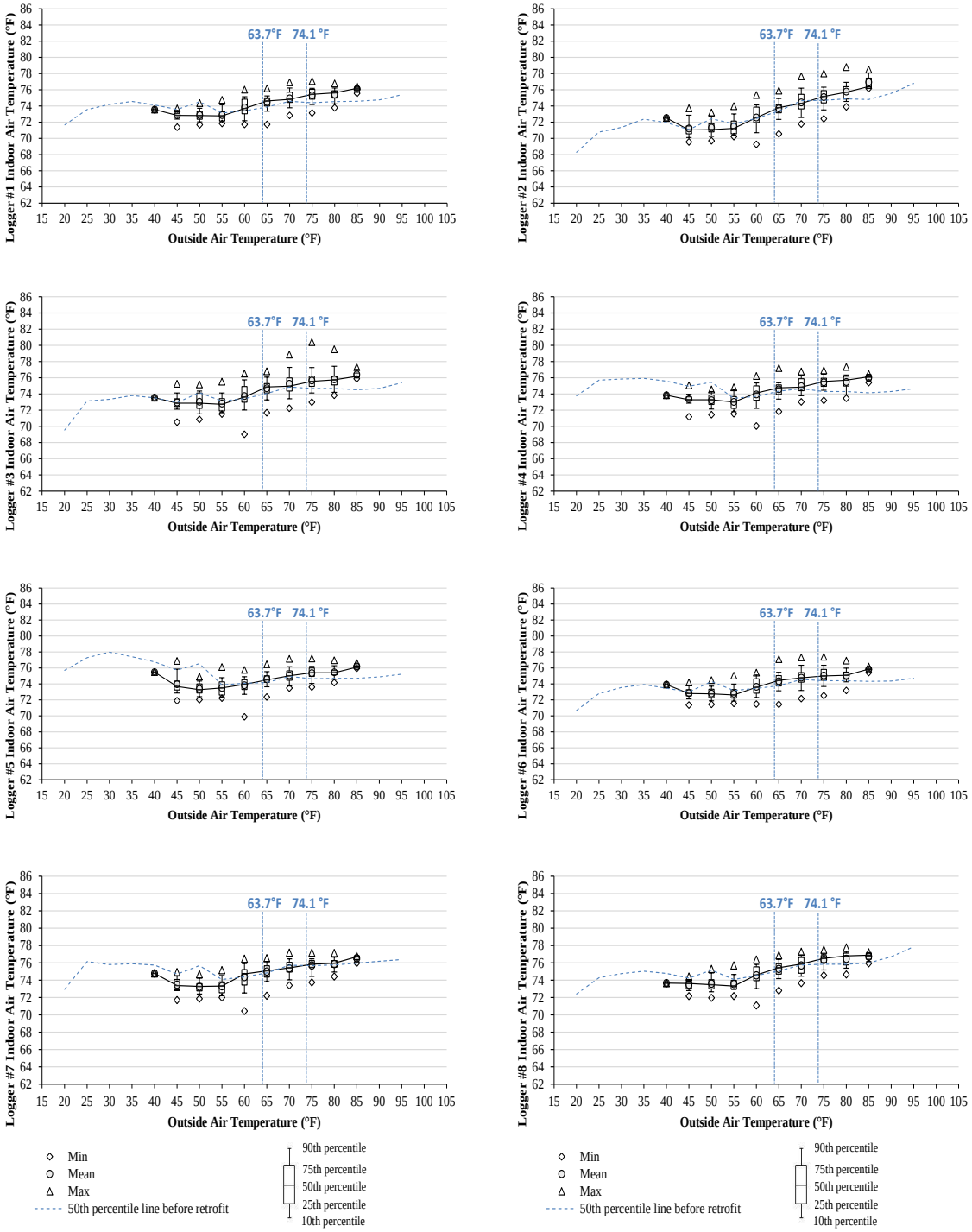

Figure 4-32. IATs versus OATs from the eight data loggers after the retrofit during weekends/holidays (February 10th, 2017 to March 31th, 2017).

In addition, the hourly whole-building electricity use from the case-study house was compared between the pre-retrofit and the post-retrofit periods. To begin with, time series plot were developed to inspect the data, then the IMT and the BWM plots were used to analyze the hourly electricity use data. Figure 4-33 shows the hourly electricity use and the average IATs from the eight data loggers as time series plots. In the analysis, it was observed that the hourly electricity use was significantly reduced during the post-retrofit period when compared to the pre-retrofit period. The primary reason for this appears to be the lower effective heating setpoint and higher cooling setpoint of the new wireless, programmable thermostat with the motion sensors compared to the previous thermostat setting. In addition, the occupancy detection function appears to reduce the electricity use because the new thermostat resets the heating and cooling setpoints to less consumptive mode (i.e., setpoint setback schedule) when the thermostat detects unoccupied hours, which indicates an occupant was not in the house. Also shown in Figure 4-33, more frequently, the average IATs during the post-retrofit period had larger variations compared to the pre-retrofit period because the heating and the cooling setpoints were lower and higher, respectively.

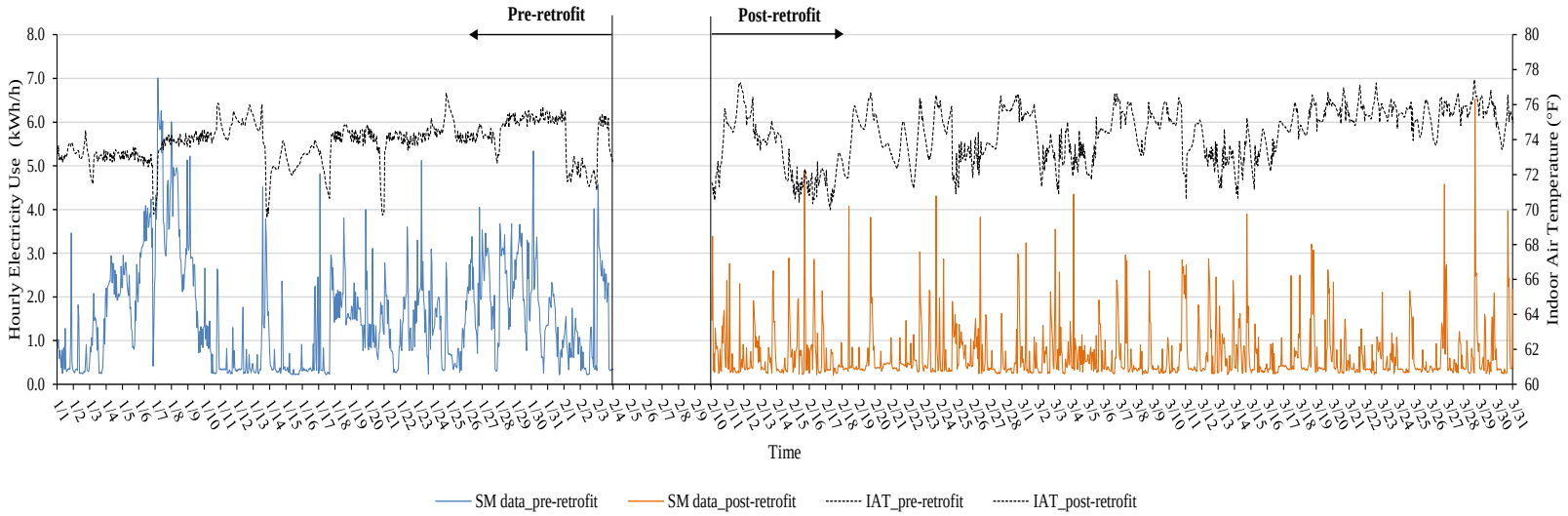

Figure 4-33. Time series plots for hourly electricity use and average IATs for the pre-retrofit period (January 1st, 2017 to February 10th, 2017) and the post-retrofit (February 10th, 2017 to March 31st, 2017).

Using the IMT, 5P change-point linear regression models were developed for the post-retrofit period. Figures 4-34 and 4-35 show the hourly electricity use data and the whole-building 5P models during the weekdays and the weekends/holidays for the post-retrofit period, respectively. Each 5P model for the post-retrofit period shows significantly lower heating balance-point temperatures[2] (see Figure 4-34 and 4-35). The BWM plots were also created to compare the trends between the pre-retrofit and the post-retrofit periods. The 50th percentile electricity use data for the post-retrofit period shows much lower electricity use compared to the pre-retrofit period over the OATs.

As previously mentioned, to analyze the occupancy patterns in each zone of the case-study house, occupancy detection data loggers were installed in each zone as shown in Figure 4-36. To accomplish this, the occupancy detection loggers were set to record 1-minute interval data which was sufficient to detect the occupant's presence in each zone. These 1-minute data were then averaged to hourly data prior to the analysis. Appendix E shows the specification of the occupancy data loggers, which were installed.

[2] It is expected that the 5P models for the post-retrofit period will have higher cooling balance-point temperatures if more SM data is collected for the cooling period (e.g., over 80 °F of the OATs) due to higher cooling setpoints.

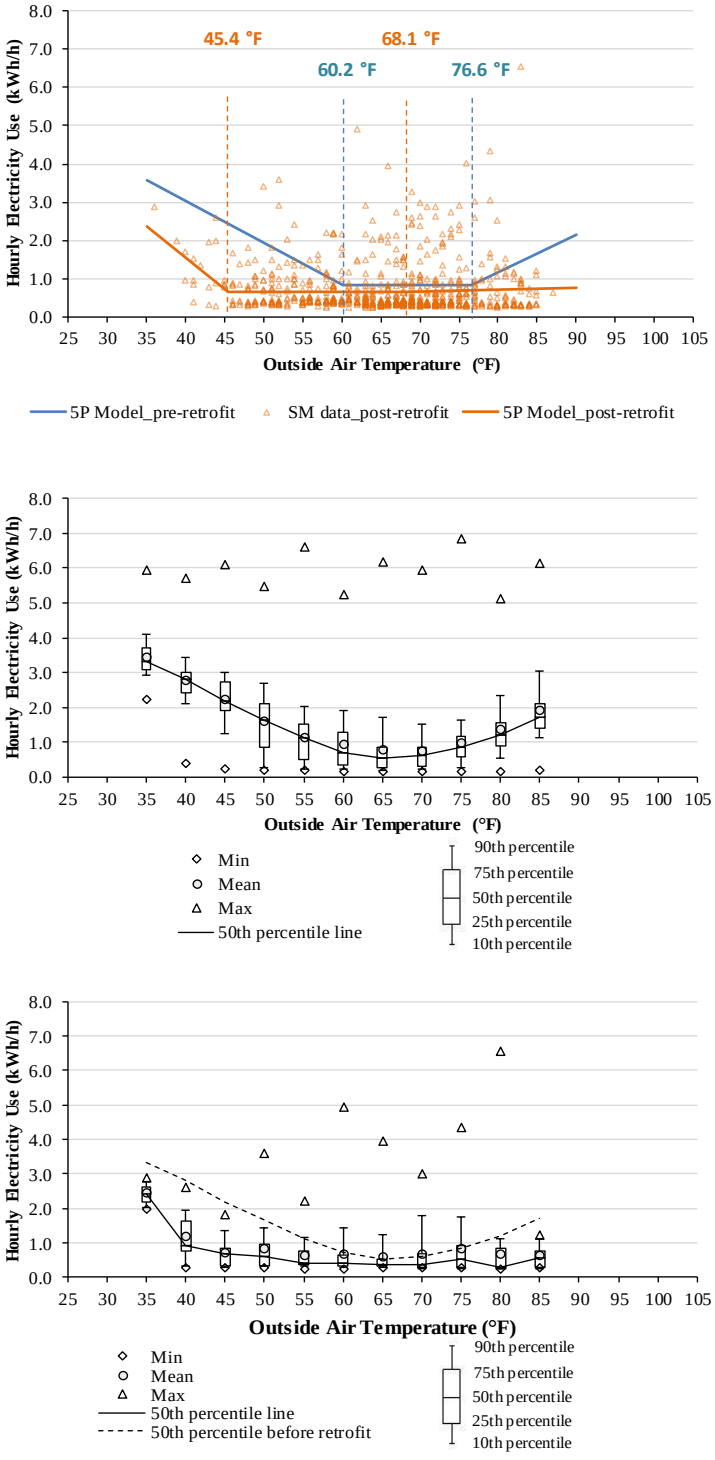

Figure 4-34. Comparison of the electricity use data for the baseline period and the post-retrofit during weekdays (upper), the BWM plot for the baseline period (middle), and the BWM plot for the post-retrofit period (lower).

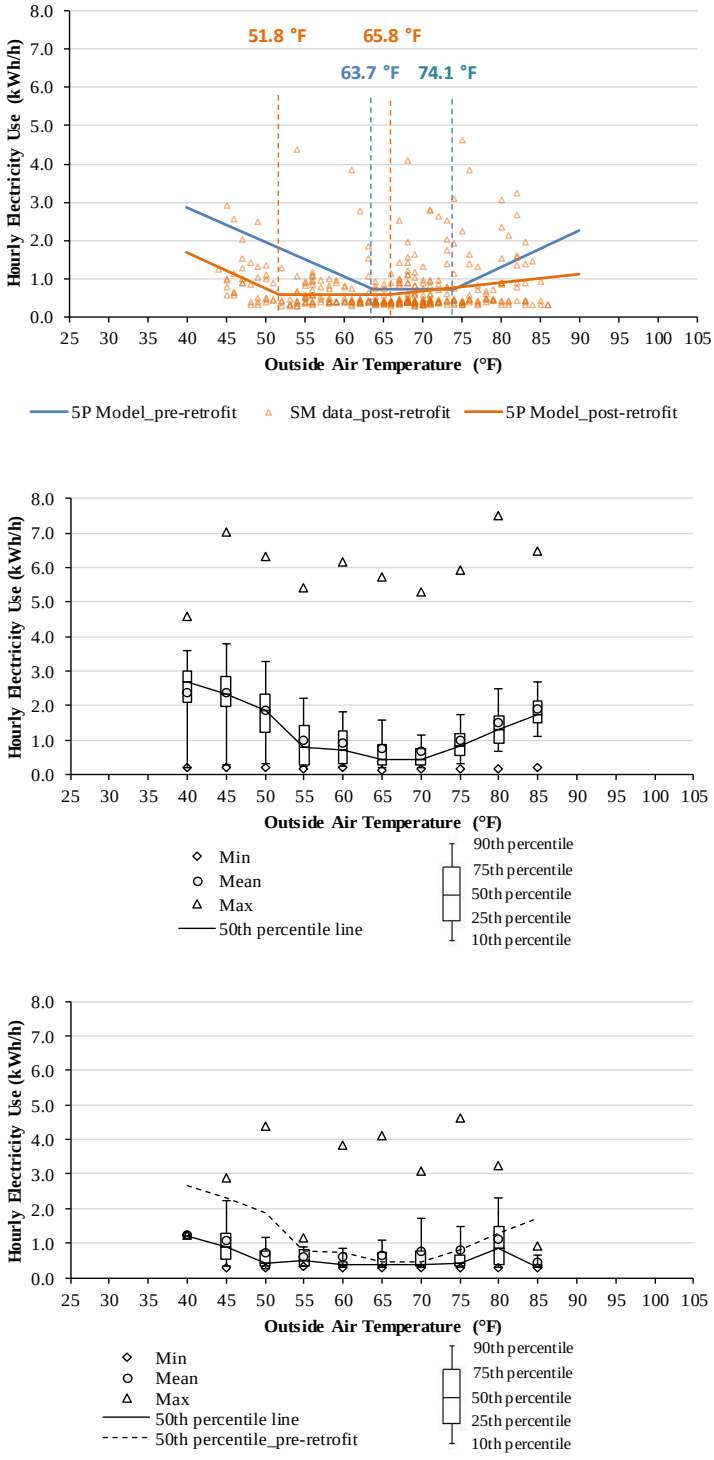

Figure 4-35. Comparison of the electricity use data for the baseline period and the post-retrofit during weekends/holidays (upper), the BWM plot for the baseline period (middle), and the BWM plot for the post-retrofit period (lower).

The occupancy data collected for the week from Monday, February 20th, 2017 to Sunday, February 26th, 2017 were used to determine the diversity factors of the DOE-2.1E simulation for the calibration, which was previously mentioned in Section 4.2.3.1. In addition, the occupancy data that were collected for the post-retrofit period from February 10th, 2017 to March 31st, 2017 were also used for the diversity factors to analyze actual electricity savings of the new wireless, programmable thermostat with the motion detection.

Figure 4-37 shows the diversity factors for each zone during one week, which shows an example of the occupancy pattern. During this period, the occupant of the case-study house stayed mostly in the living room (Zone #6). In addition, the occupant stayed primarily the bedroom #1 (Zone #1) on Friday evening and the bedroom #2 (Zone #7) for sleeping. The dining room (Zone #2) and the kitchen (Zone #3) were used for lunch and dinner times. The bathrooms (Zones #4 and #5) were normally used during both before/after work times and morning and evening times.

It should be noted that the occupancy detection logger in the bedroom #2 showed inaccurate detection when the occupant was sleeping (i.e., less than 0.3). Therefore, in the future, it is recommended that the occupancy detection logger be tested with a person in bed to observe if the logger correctly detects the person. This inaccuracy could affect the performance of HADs when occupancy detection is not activated in the nighttime even though an occupant is at home.

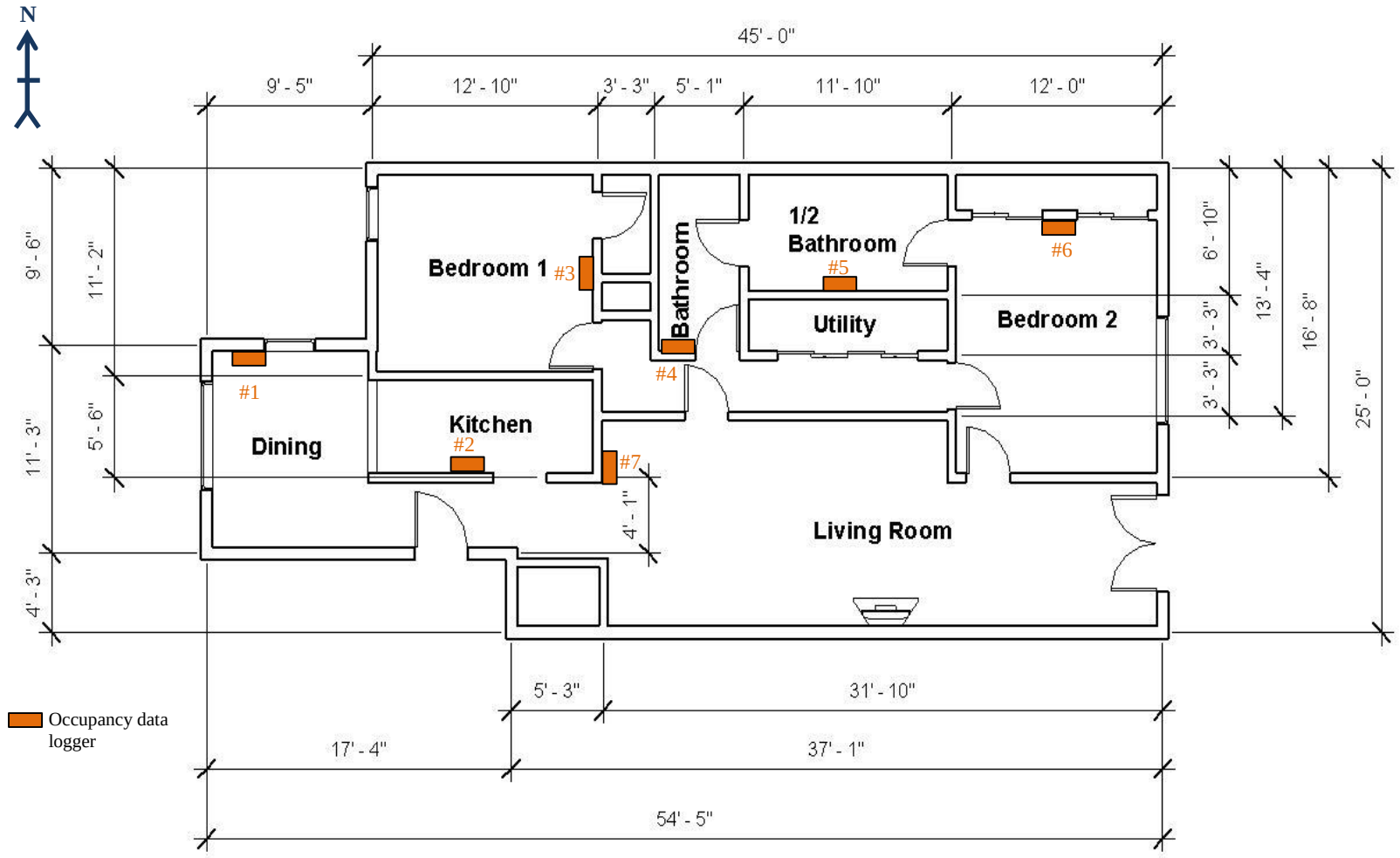

Figure 4-36. Plan view showing the seven occupancy data loggers in the case-study house.

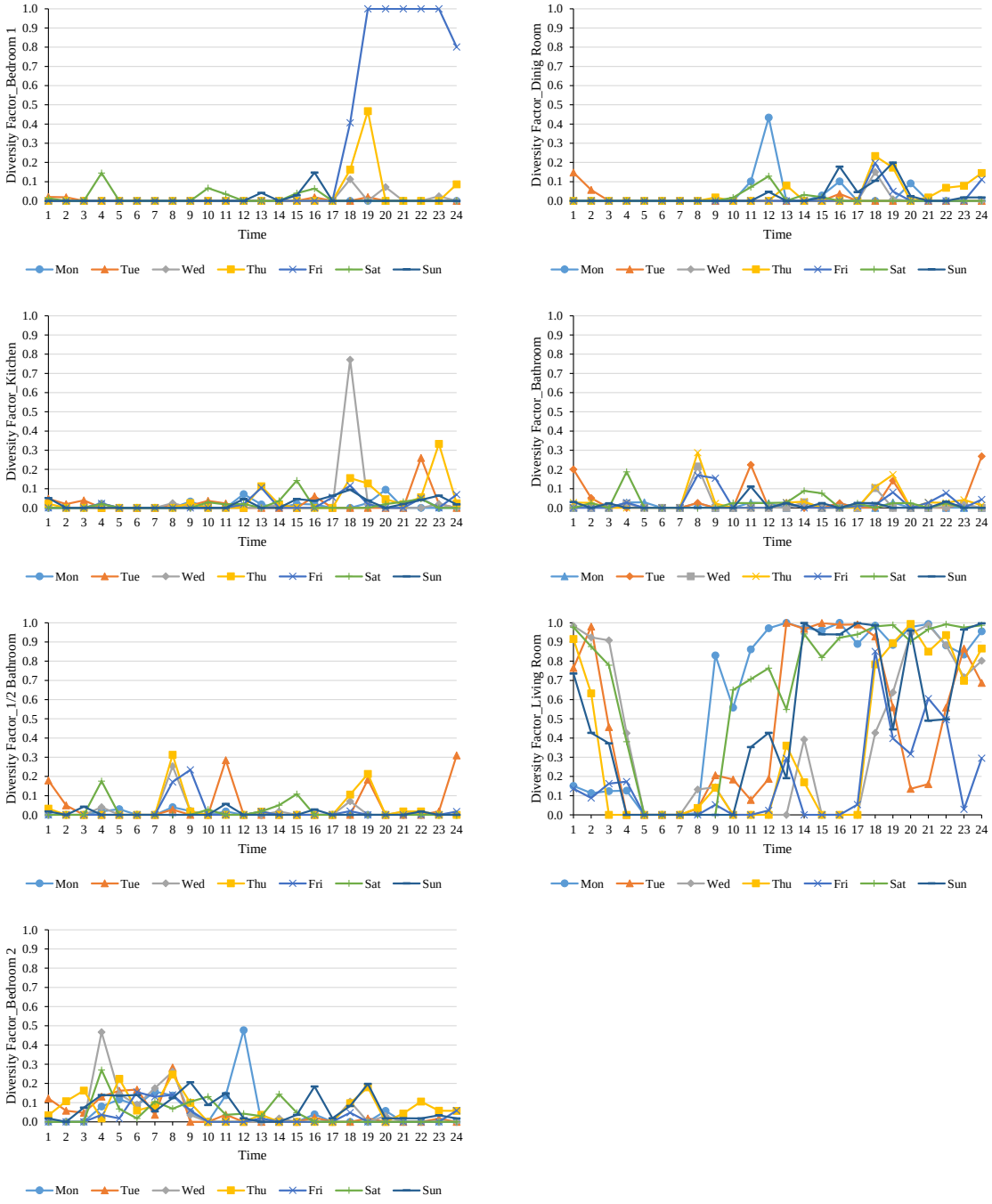

Figure 4-37. Diversity factors for each zone showing occupancy patterns from February 20th, 2017 to February 26th, 2017.

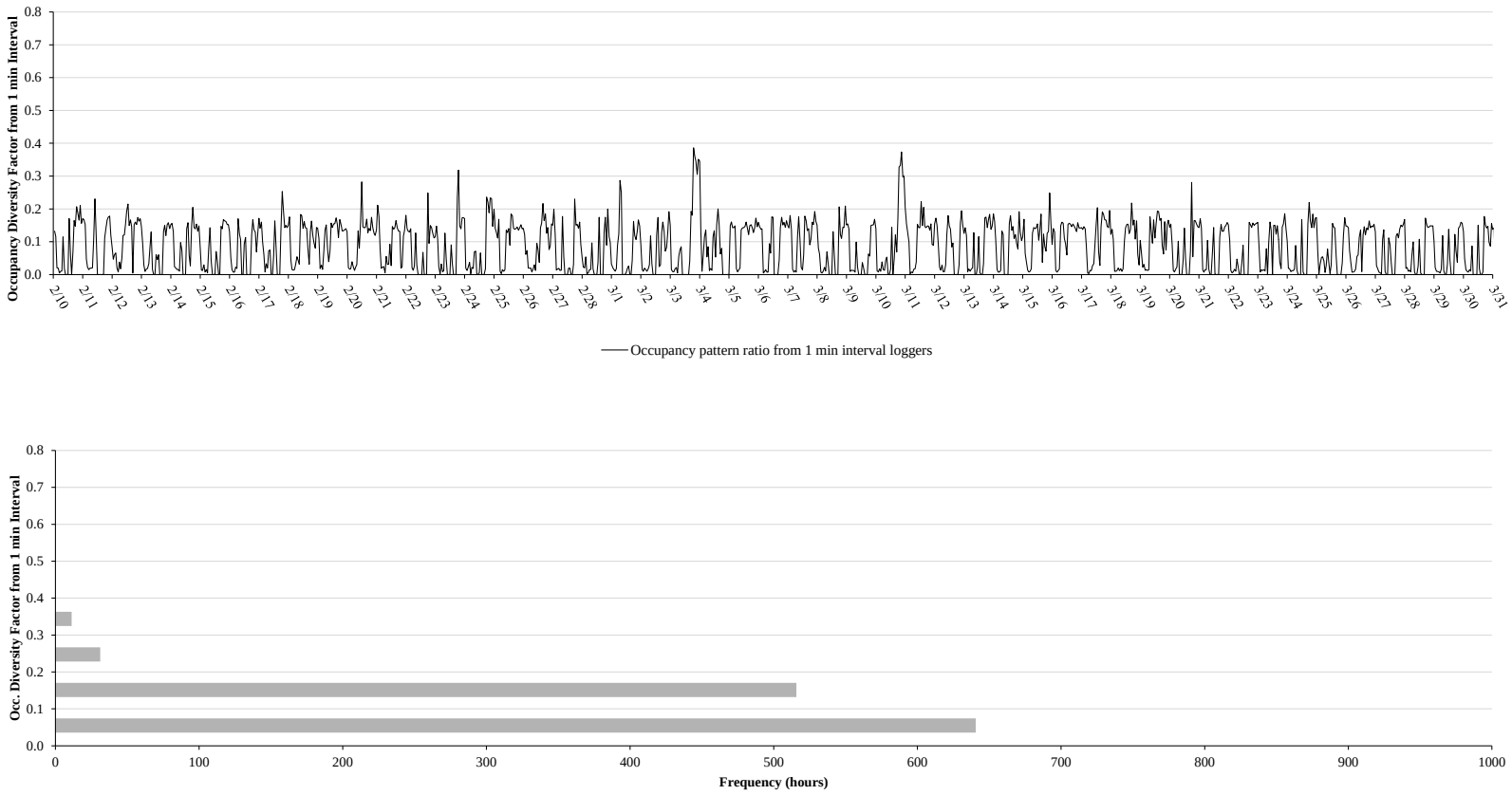

Figure 4-38. Average occupancy diversity factors from the seven zones in the time series plot (upper) and the histogram (lower) for the post-retrofit period (February 10th, 2017 to March 31st, 2017).

In addition, Figure 4-38 shows a time-series plot (upper plot) and a histogram of the average diversity factors (lower plot) from the seven zones during the post-retrofit period (February 10th, 2017 to March 31st, 2017). In the figure, the histogram shows that the most frequent diversity factor was in the range of 0.0 and 0.1, which indicates that most of the zones in the house were unoccupied.

The average diversity factors from each zone were also used to analyze the electricity use during occupied and unoccupied hours for the post-retrofit period. When the average diversity factors were not zero, the hours were categorized as occupied hours. In the same way, when the average diversity factor indicated zero, the hours were categorized as unoccupied hours. Using the occupied and unoccupied categorization, the hourly electricity data that was collected during the post-retrofit period was analyzed using a change-point linear model (i.e., the IMT model) and compared with the IMT model of the baseline period. In this analysis, the statistical BWM plots were also created to compare the trends between the pre-retrofit and the post-retrofit periods for the occupied and the unoccupied hours, respectively. From the BWM analysis, the 50th percentile of the electricity use for the post-retrofit period was compared with the 50th percentile for the pre-retrofit period.

Figure 4-39 and Figure 4-40 show the 5P change-point linear models and the BWM plots for the occupied hours during weekdays and weekends/holidays, respectively. Figure 4-41 and Figure 4-42 show the 5P change-point linear models and the BWM plots for the unoccupied hours during weekdays and weekends/holidays,

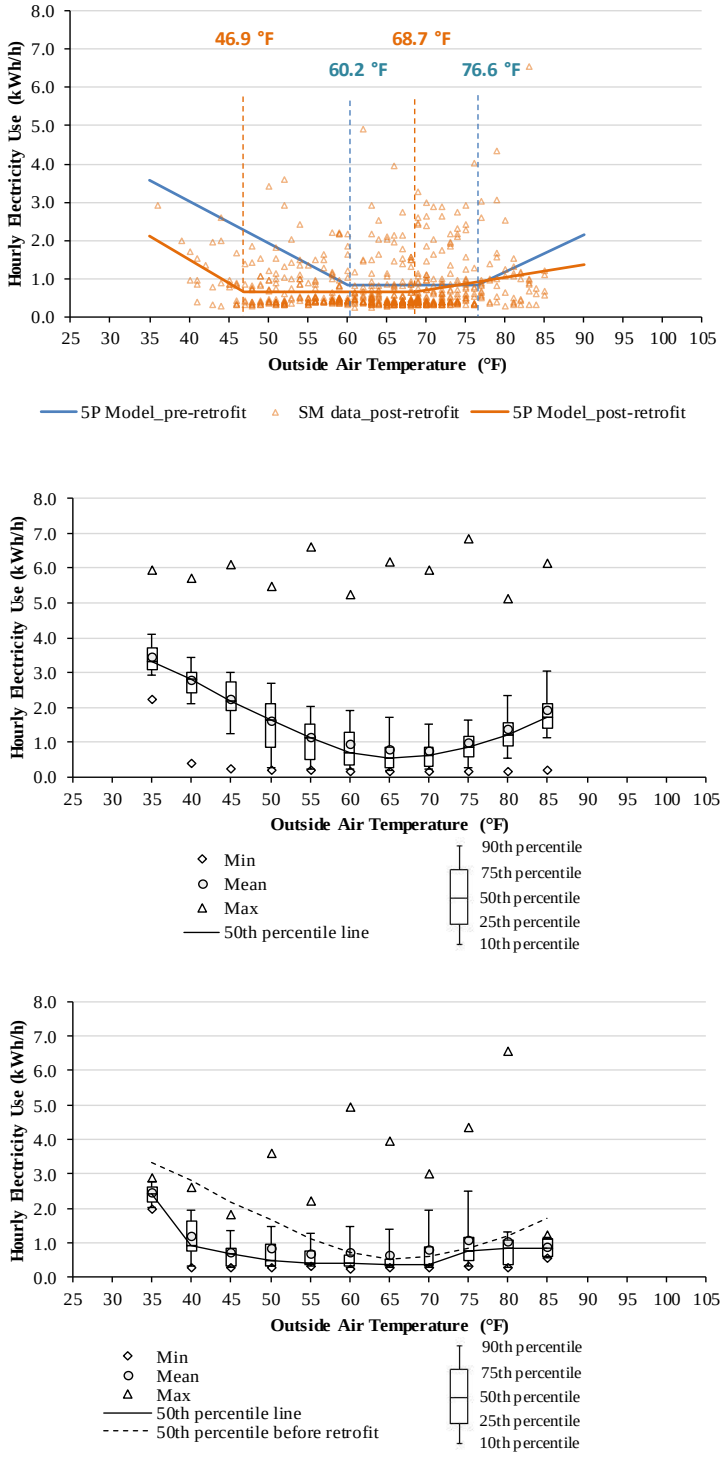

Figure 4-39. Comparison of 5P models for the baseline period and the post-retrofit period during the weekdays for the occupied hours (upper), the BWM plot for the baseline period (middle), and the BWM plot for the post-retrofit period (lower).

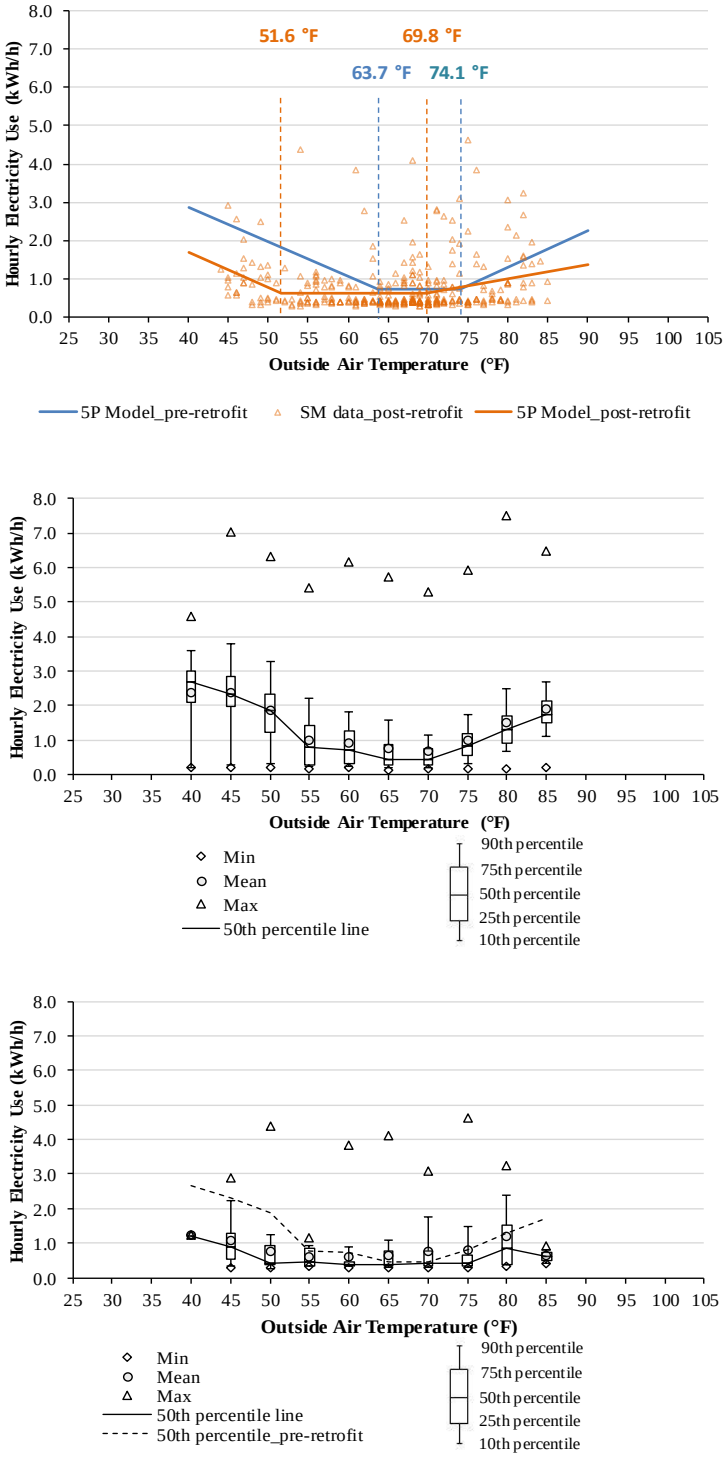

Figure 4-40. Comparison of 5P models for the baseline period and the post-retrofit period during the weekends/holidays for the occupied hours (upper), the BWM plot for the baseline period (middle), and the BWM plot for the post-retrofit period (lower).

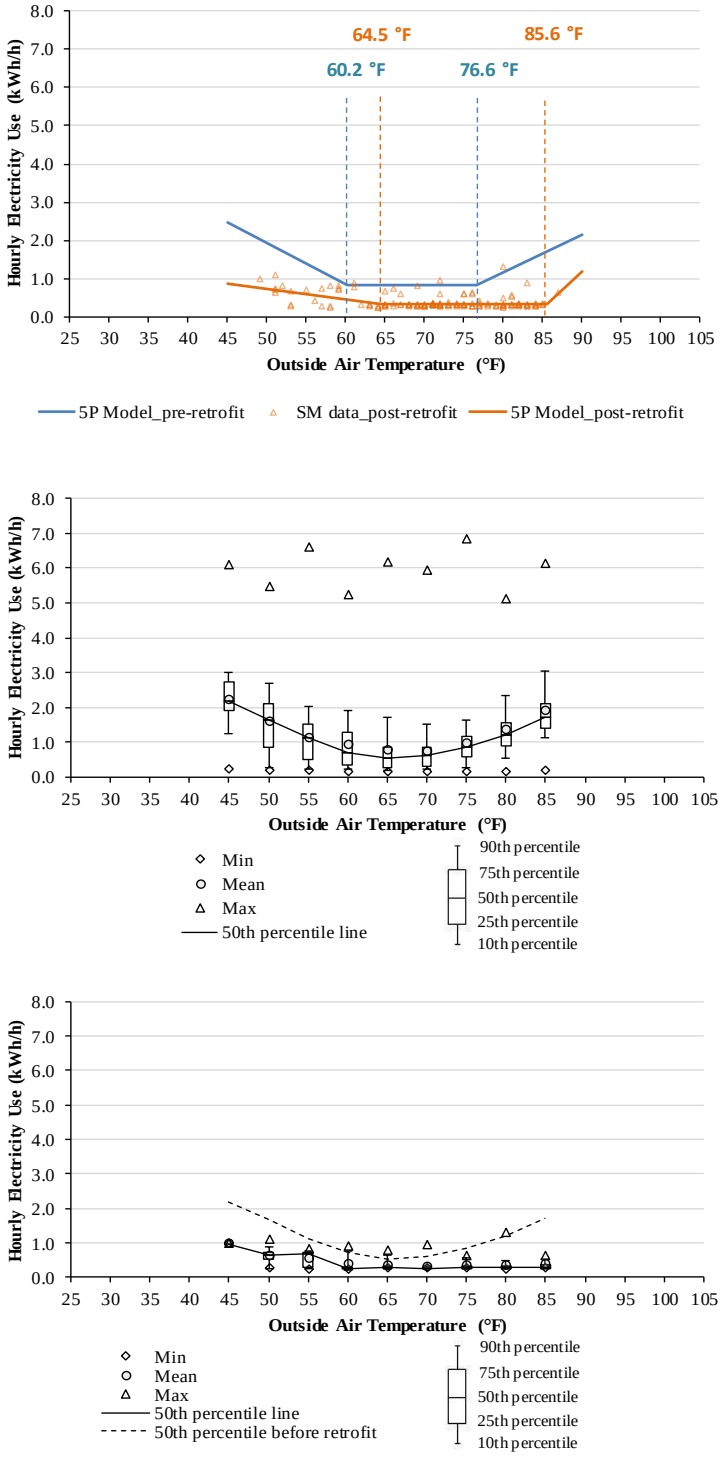

Figure 4-41. Comparison of 5P models for the baseline period and the post-retrofit period during the weekdays for the unoccupied hours (upper), the BWM plot for the baseline period (middle), and the BWM plot for the post-retrofit period (lower).

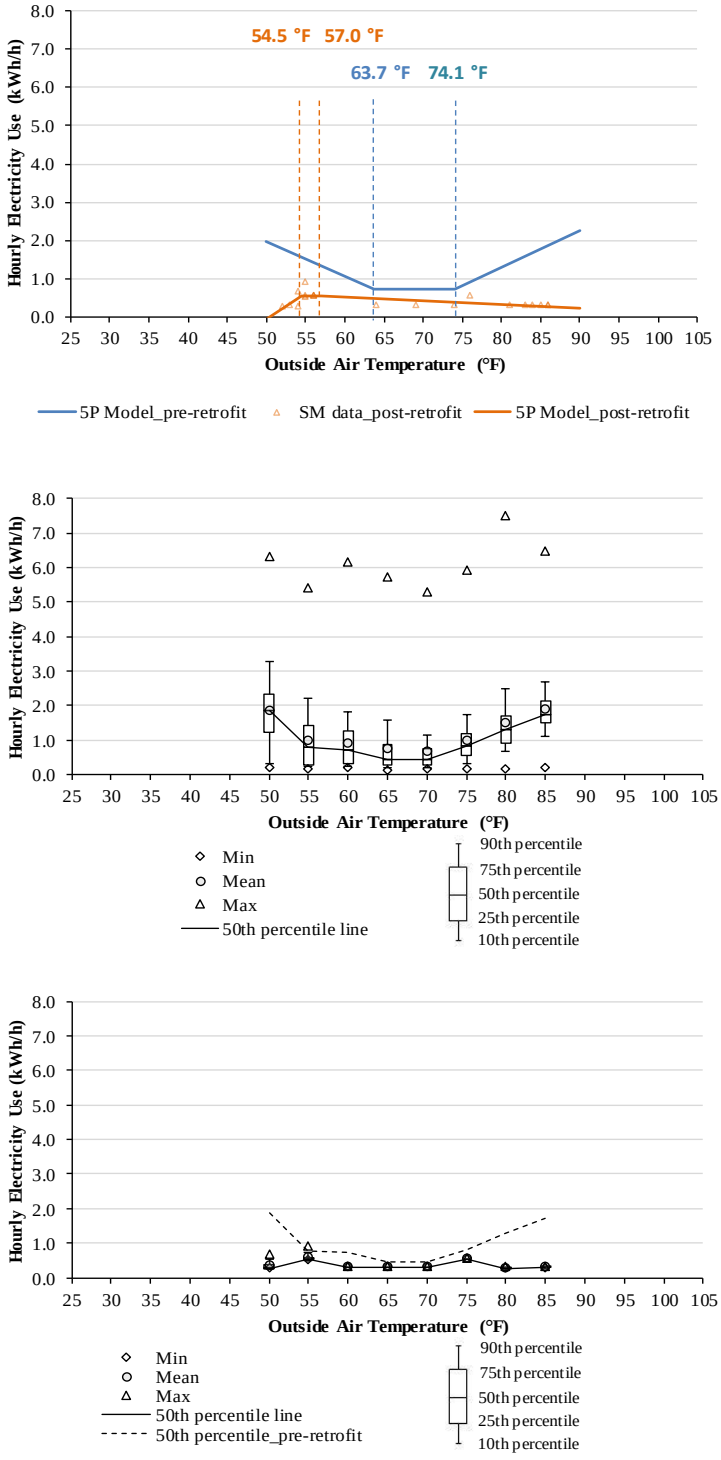

Figure 4-42. Comparison of 5P models for the baseline period and the post-retrofit period during the weekends/holidays for the unoccupied hours (upper), the BWM plot for the baseline period (middle), and the BWM plot for the post-retrofit period (lower).

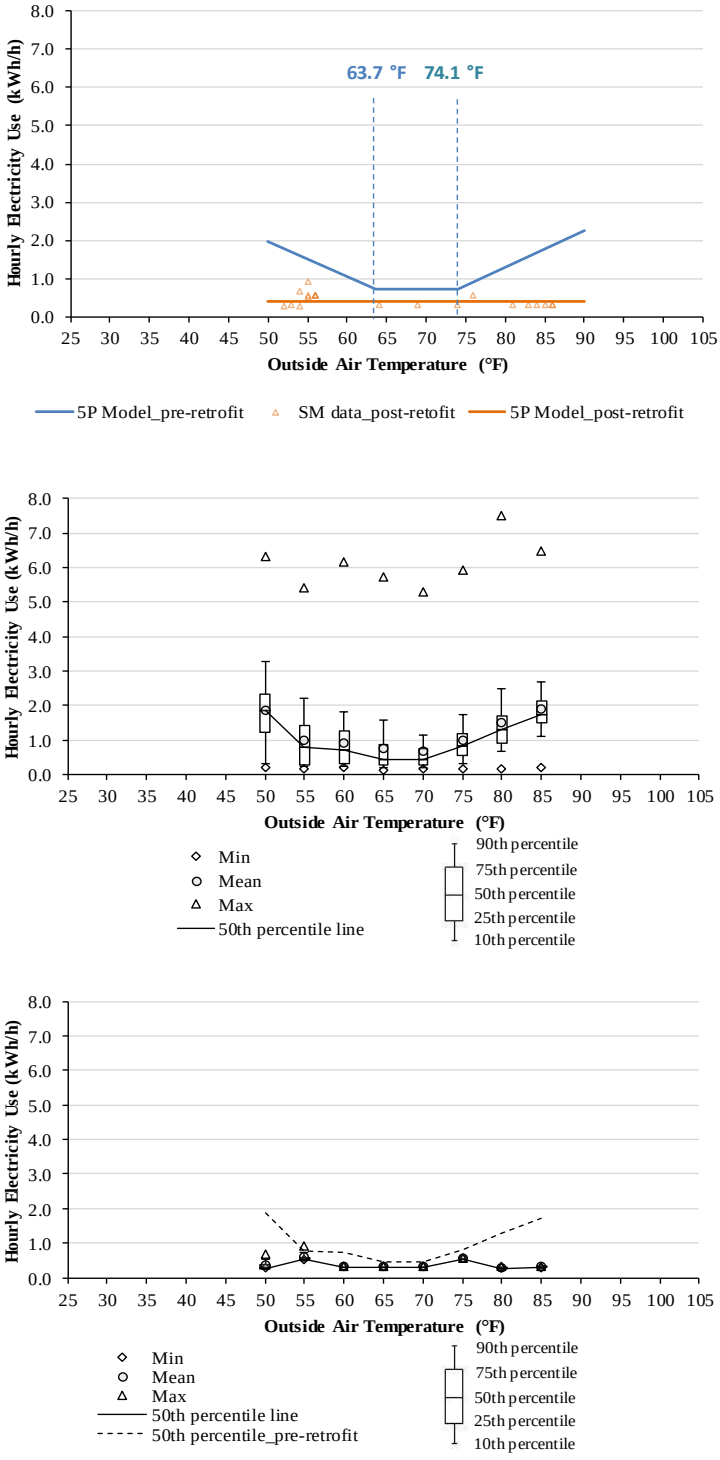

Figure 4-43. Comparison of 5P and corrected 1P model for baseline period and post-retrofit period during weekends/holidays for unoccupied hours (upper), the BWM plot for the baseline period (middle), and the BWM plot for the post-retrofit period (lower).

respectively. Even though the 5P model is generally used for all electric houses, for the unoccupied hours of the weekends/holidays during the post-retrofit period, the 5P model did not appropriately fit with the hourly electricity use data (i.e., the slopes of the heating and cooling periods were negative (physically unreasonable)). Thus, a 1P model was used to better fit with the SM data for the unoccupied hours, as shown in Figure 4.43.

The quartile analysis in the BWM plots showed that the electricity use for the unoccupied hours had lower interquartile ranges (IQRs) by 5 ºF bin than the electricity use for the occupied hours. It also appears that the electricity use for the unoccupied hours were more predictable.

In addition to the actual electricity saving analysis method using the average occupancy diversity factors, the thermal comfort also was examined for the occupied hours and the unoccupied hours during the post-retrofit period using the average IATs and the RH from the location of the thermostat. In the analysis, the average IATs and the RH were used to check the thermal comfort when the programmable thermostat setback (i.e., occupied hours) and the occupancy detection setback (i.e., unoccupied hours) achieved the electricity savings. In this analysis, it was assumed that indoor air speed was 20 ft/min, that the operative temperature was the same with the average IAT[3], and that the occupant's average metabolic rate was 1.1 met. The comfort zones for winter (i.e., 1.0 clo) and summer (i.e., 0.5 clo) from ASHRAE 55-2013 (ASHRAE, 2013b) and the humidity ratio (lb $_{H2O}$ / lb $_{DRY\ AIR}$) versus the average IAT plot were used to check thermal comfort during the post-retrofit period.

[3] For the future study, operative temperatures calculated from mean radiant temperatures and dry-bulb temperatures should be considered to examine thermal comfort.

4.4. Summary of Methodology

For this study, three methods were developed to quantify the electricity savings of HADs. First, a non-intrusive method (i.e., Level 0 Analysis) was developed to quantify the potential electricity savings from the use of HADs using only interval electricity use data recorded by a SM and coincident weather data (i.e., no detailed house information). Second, a calibrated simulation method (i.e., Level I Analysis) was developed to help quantify the detailed-potential savings from the use of HADs using simulations with the information from the case-study house as well as the hourly electricity use data and the corresponding weather data. Third, an M&V method (i.e., Level II Analysis) was developed to quantify the actual electricity savings from the use of HADs. The results of the three methods will be presented in the next section.

CHAPTER V

RESULTS

This section presents the results of this study, which are presented in the following sections: 1) estimated potential electricity savings from the use of HADs using interval electricity use data recorded by a SM (i.e., Level 0 Analysis), 2) detailed, potential electricity savings achieved by simulation scenarios (i.e., Level I Analysis), and 3) actual electricity savings measured from the case-study house (i.e., Level II Analysis).

5.1. Results of the Statistical Method (Level 0 Analysis)

As previously discussed, a non-intrusive statistical method was developed to detect and quantify potential electricity savings from HADs using electricity use data and corresponding OATs without physical information about the dwelling (e.g., drawings, wall R-values, window U-factors, etc.).

To test this method, the hourly electricity use data from the case-study house and the corresponding OAT data from April 15th, 2015 to April 14th, 2016 were used. For the analysis of the detection process (see Figure 4-2), the IMT was used to find an appropriate change-point regression model and the balance-point (i.e., change-point) temperatures to differentiate between heating, weather-independent, and cooling periods. Figure 5-1 shows the IMT's 5P change-point linear model with the balance-point temperatures and uncertainty indicators (i.e., SE) for the case-study house during the weekdays and the weekends/holidays, respectively. In the analysis, the heating (60.2 °F)

and cooling (76.6 °F) balance-point temperatures from the 5P change-point linear model for the weekdays divided the hourly SM data into the three periods of heating, weather-independent, and cooling periods. In the same way, the heating (63.7 °F) and cooling (74.1 °F) balance-point temperatures from the 5P model for the weekends/holidays divided the hourly SM data into the three periods.

In the analysis of the case-study house for the baseline period, it was observed that the balance-point temperature range between the heating and cooling points for the weekday model was larger than the range for the weekend/holiday model. This difference seems to indicate that the occupant of the case-study house appears to have a lower observed heating setpoint and a higher cooling setpoint during the weekdays. The reason for this would appear to be that the occupant spent more time outside the house during the weekdays than the weekends/holidays, which lowered the effective heating setpoint or turned off the heating system. In a similar fashion, it appears that the observed cooling sepoint was raised or turned off the cooling system during the weekdays more often than the weekends/holidays.

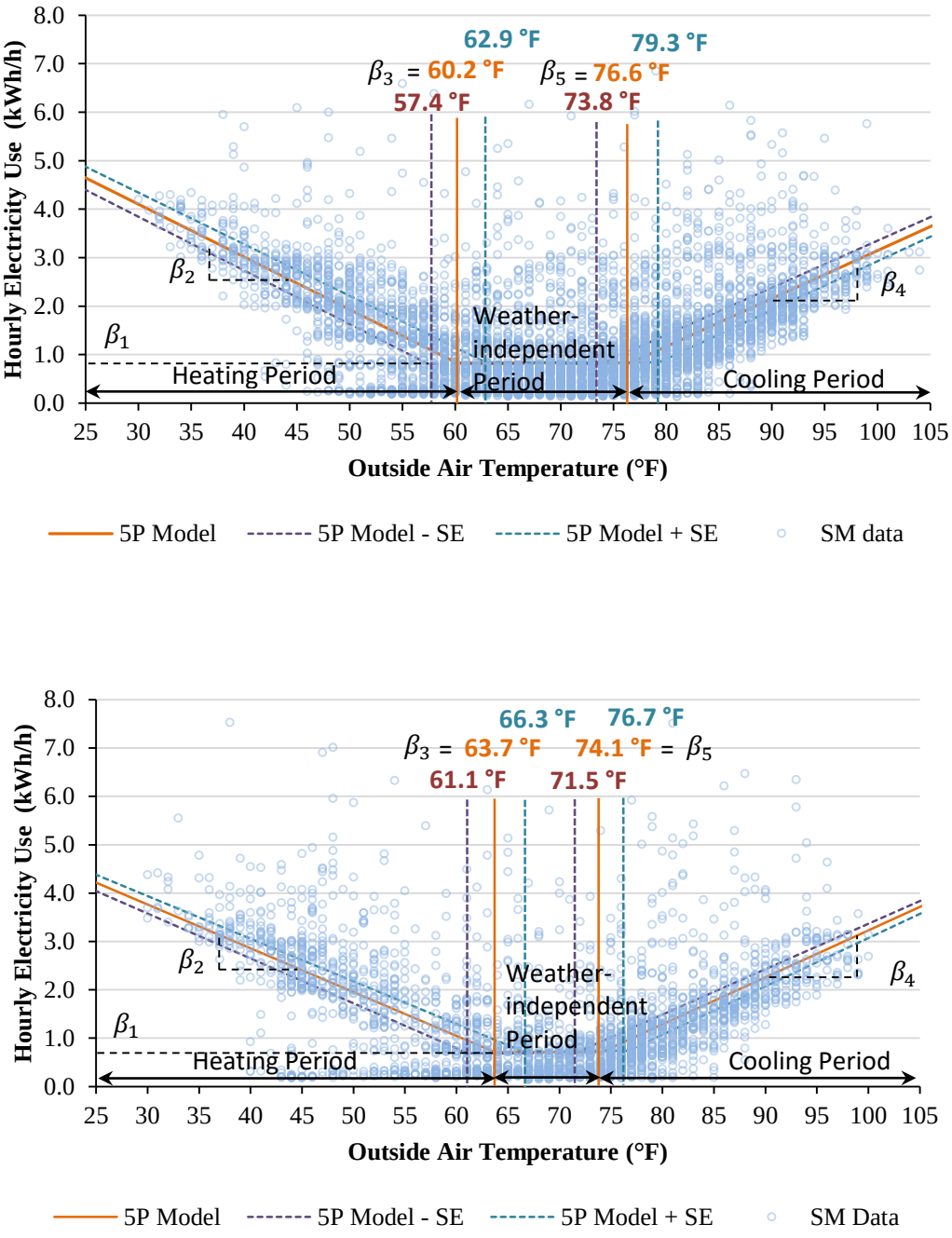

Figure 5-1. 5P model with change points and uncertainty for the weekdays (upper) and the weekends/holidays (lower) for the SM baseline period from April 15th, 2015 to April 14th, 2016.

For the weekdays, the calculated heating balance-point temperature of 60.2 °F and cooling balance-point temperature of 76.6 °F divided the hourly electricity use data into the three periods of heating, weather-independent, and cooling periods. For the weekends/holidays, the heating balance-point temperature of 63.7 °F and the cooling balance-point temperature of 74.1 °F divided the hourly electricity use data into the three periods. Table 5-1 summarizes the results of the 5P change-point linear regression model.

Table 5-1. 5P change-point linear regression model results.

	Heating balance-point temperature (℉) (Left change point)	Cooling balance-point temperature (℉) (Right change point)	Left slope (kWh/℉)	Right slope (kWh/℉)	Y-axis intercept (kWh)
Weekdays	60.15	76.59	-0.109	0.099	0.827
SE	2.74	2.74	0.002	0.002	0.012
Weekends/holidays	63.70	74.08	-0.091	0.097	0.711
SE	2.59	2.59	0.002	0.003	0.024

In addition, a 5 °F temperature bin analysis was performed using a binned, Box, Whisker, and Mean (BWM) approach to statistically check the characteristics of the electricity use data against the OAT (°F) data. The binned BWM plot shows the 10^{th}, 25^{th}, 50^{th} (median), 75^{th}, and 90^{th} percentile as well as minimum, mean, and maximum values over 5 °F temperature bins. Figure 5-2 shows the temperature bin analysis using the binned quartile approach. The results show the weekend/holiday model had lower 10^{th} percentile values for the 40 °F and 45 °F bins than those of the weekday model. This seems to indicate that comparatively lower electricity consumption occurred during the times of these bins. The figure also shows that the 5P models were mostly inside the IQRs, which indicates a good model shape.

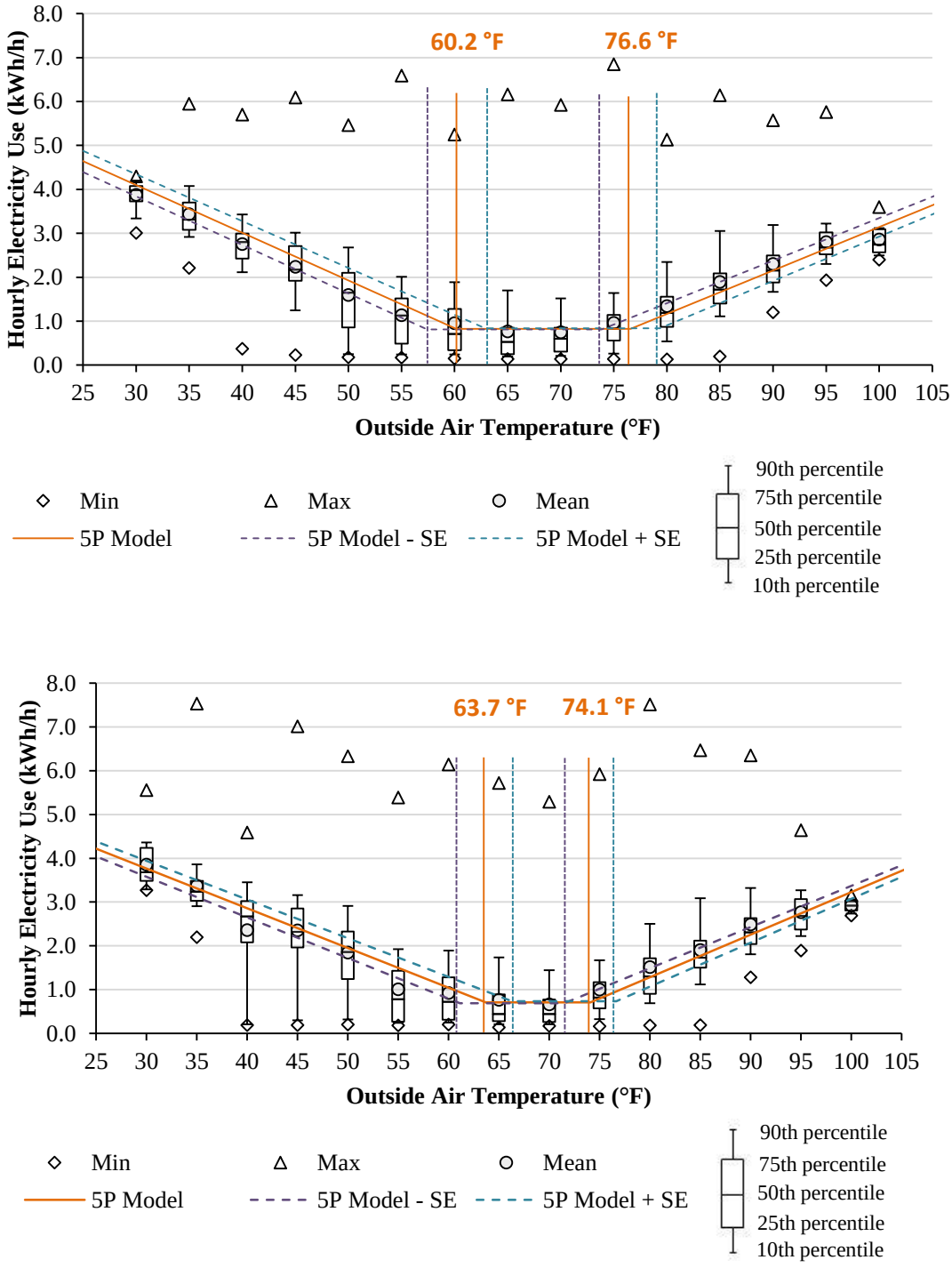

Figure 5-2. Temperature bin analysis using binned quartile approach with the 5P model superimposed during the weekdays (upper) and the weekends/holidays (lower).

After the temperature bin analysis, histogram/frequency plots using 5 °F bins were developed to check the outliers in the electricity use data. Figure 5-3 and Figure 5-4 show the frequency plots using 5 °F bins for the weekdays and the weekends/holidays, respectively. Using the 5 °F bin histogram/frequency plots with superimposed normal distribution, abnormal energy patterns can be detected. In Figure 5-3, the plots for the weekdays showed skewed histogram shapes in the 50 °F and 70 °F bin ranges. In a similar fashion, in Figure 5-4, the histogram/frequency plots for the weekends/holidays showed skewed shapes in the 40 °F and 70 °F bin ranges. The histogram/frequency plots for the weekends/holidays showed that lower energy consumption occurred in the 40 °F and 45 °F bin ranges compared to the weekdays. The skewed shapes of 40 °F and 45 °F bin ranges were expected from the previous temperature bin analysis plot for the weekends/holidays (see Figure 5-2) because the 10^{th} percentile values of the BWM plots were close to the minimum values.

From the analysis, it appears that the normal distribution and histogram/frequency plots are useful statistical plots that can be used as an informative graphical and comparative analysis tool to compare and calibrate a baseline simulation model of the next calibrated simulation method (i.e., Level I Analysis).

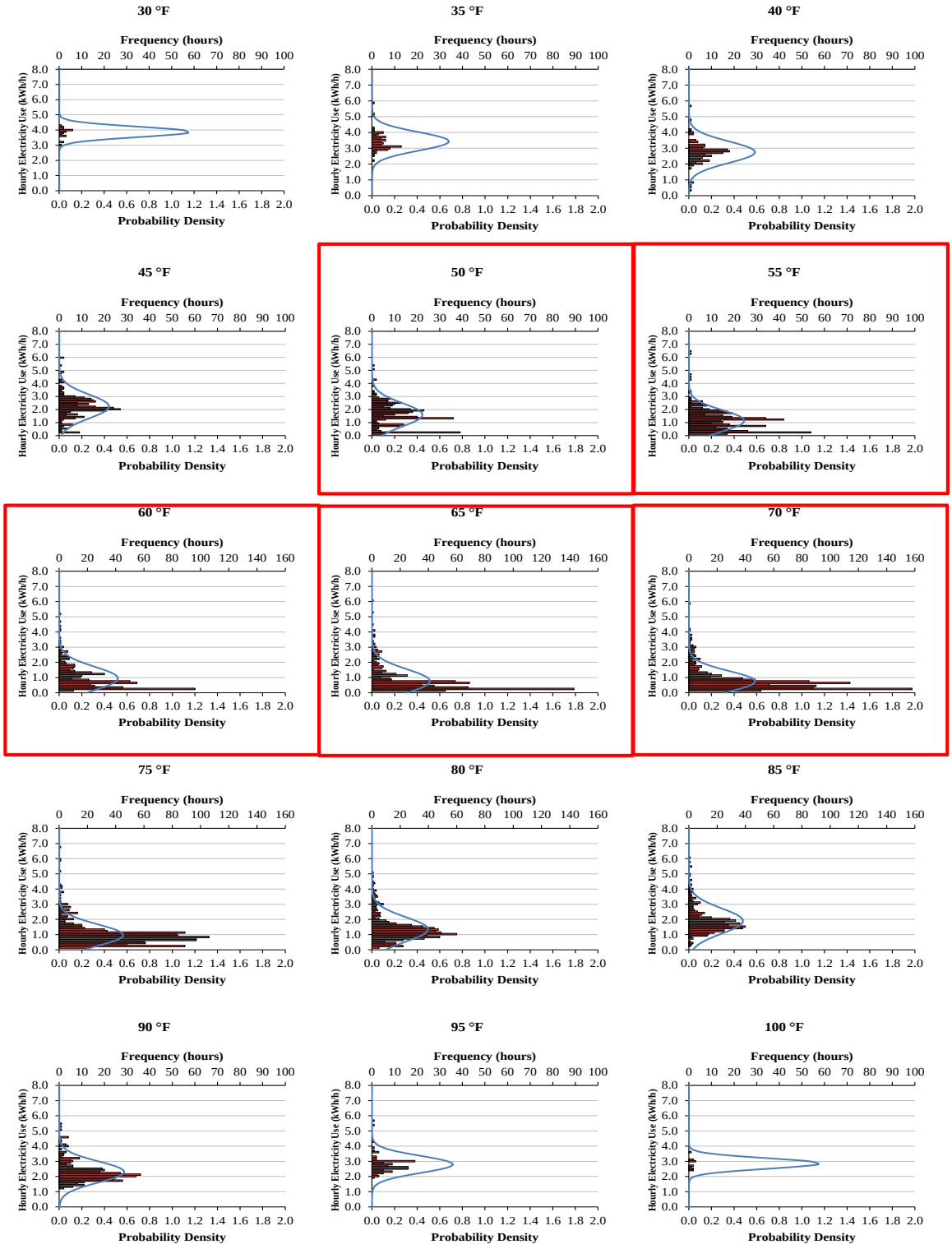

Figure 5-3. Histogram/frequency plots using 5 °F bins for the weekdays.

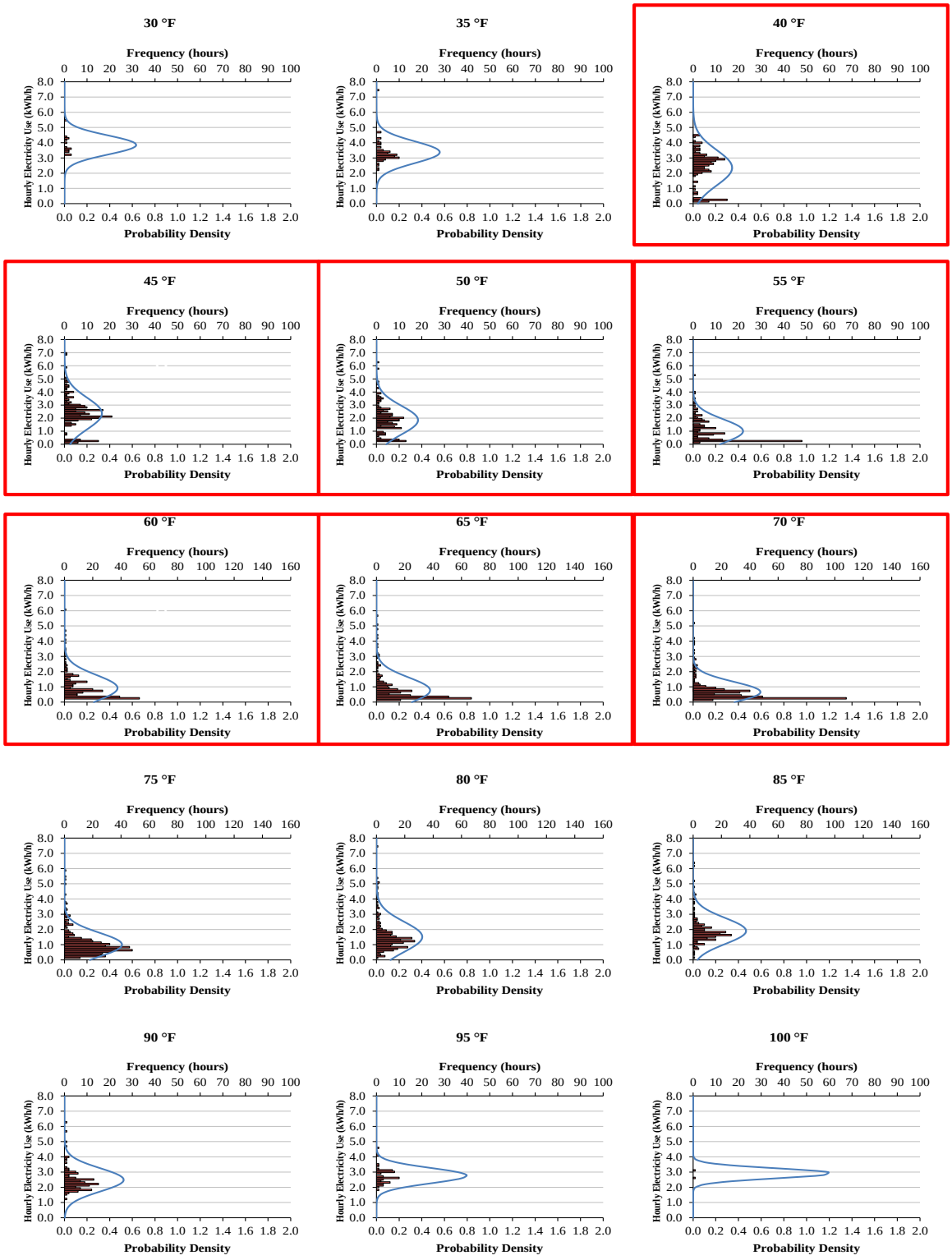

Figure 5-4. Histogram/frequency plots using 5 °F bins for the weekends/holidays.

In addition to the binned quartile analysis and 5 °F histogram/frequency plots, several additional plots were developed to help analyze the SM data above the 90th percentile and below the 10th percentile, which were used to further analyze energy and occupancy patterns, respectively. These plots were constructed in the following fashion: First, using the baseline balance-point temperatures, the binned BWM plots for the weekdays and the weekends/holidays categorized the data into six regions, respectively. These six regions represent three different heating, weather-independent, cooling periods above the 50th percentile, as well as three different periods below the 50th percentile. Figure 5-5 shows the resultant 5P change-point linear model and the binned BWM plots with the balance-point temperatures for the weekdays and the weekends/holidays arranged by the six regions.

Table 5-2 summarizes the number of hours for each of the six regions. The most frequent hours above the 50th percentile for the weekdays occurred in the weather-independent period (Region II). For the weekends/holidays, the most frequent hours occurred in the cooling period (Region III). In the same way, the most frequent hours below the 50th percentile for the weekdays occurred in the weather-independent period (Region V). For the weekends/holidays, the most frequent hours occurred in the cooling period (Region VI).

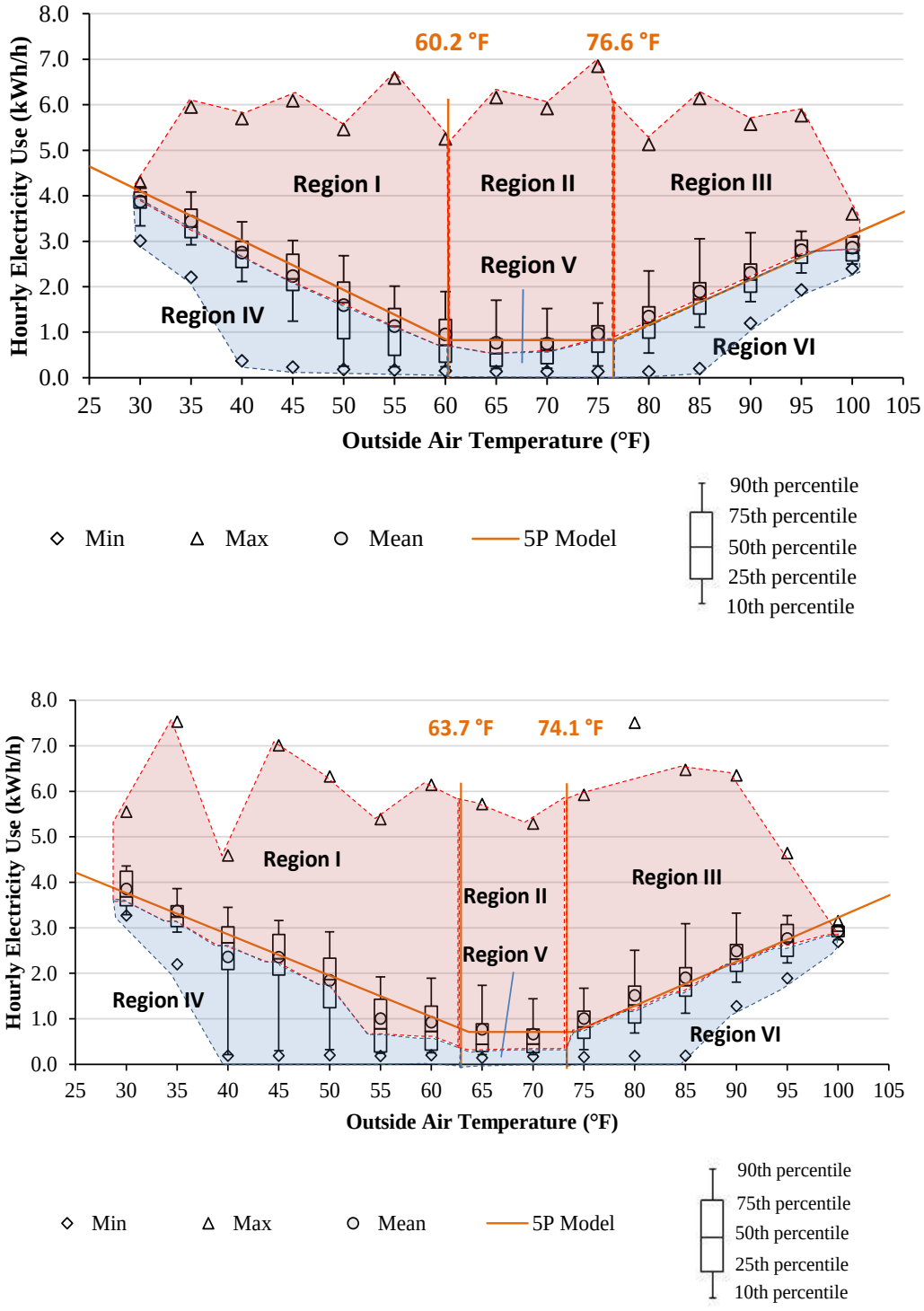

Figure 5-5. Binned BWM plots with the baseline balance-point temperatures for the weekdays (upper) and the weekends/holidays (lower) by the six regions.

Table 5-2. Number of energy hours above and below the 50th percentile.

Number of frequency hours above 50th	Region I (for heating period)	Region II (for weather-independent period)	Region III (for cooling period)	Total
Weekdays	700	1161	1134	2995
Weekends/holidays	506	360	561	1427
Total	1206	1521	1695	4422
Number of frequency hours below 50th	Region IV (for heating period)	Region V (for weather-independent period)	Region VI (for cooling period)	Total
Weekdays	684	1222	1027	2933
Weekends/holidays	490	364	551	1405
Total	1174	1586	1578	4338

Finally, based on the six regions (Figure 5-5), 3D energy use plots were developed to help visually inspect the hourly electricity use above the 90th percentile (i.e., energy use pattern) and hourly electricity use below the 10th percentile (i.e., occupancy patterns) during both hour-of-day and day-of-year periods to better determine when the hourly electricity use was occurring and the overall hour-of-day pattern. Figure 5-6 shows the 3D energy use plot for data points above the 90th percentile during the weekdays and the weekends/holidays for the heating period (i.e., Region I), based on the heating balance temperature from the 5P model. The figure shows that the hourly electricity use above the 90th percentile (i.e., heating related electricity use) occurred mostly from the middle of November to the end of February during evening and morning hours for weekdays and weekends/holidays, respectively. Figure 5-7 shows the 3D energy use plot for the weather-independent period (i.e., Region II). The figure shows that the hourly electricity use above the 90th percentile (i.e., weather-independent electricity use) occurred mostly from the middle of February to the middle of May and

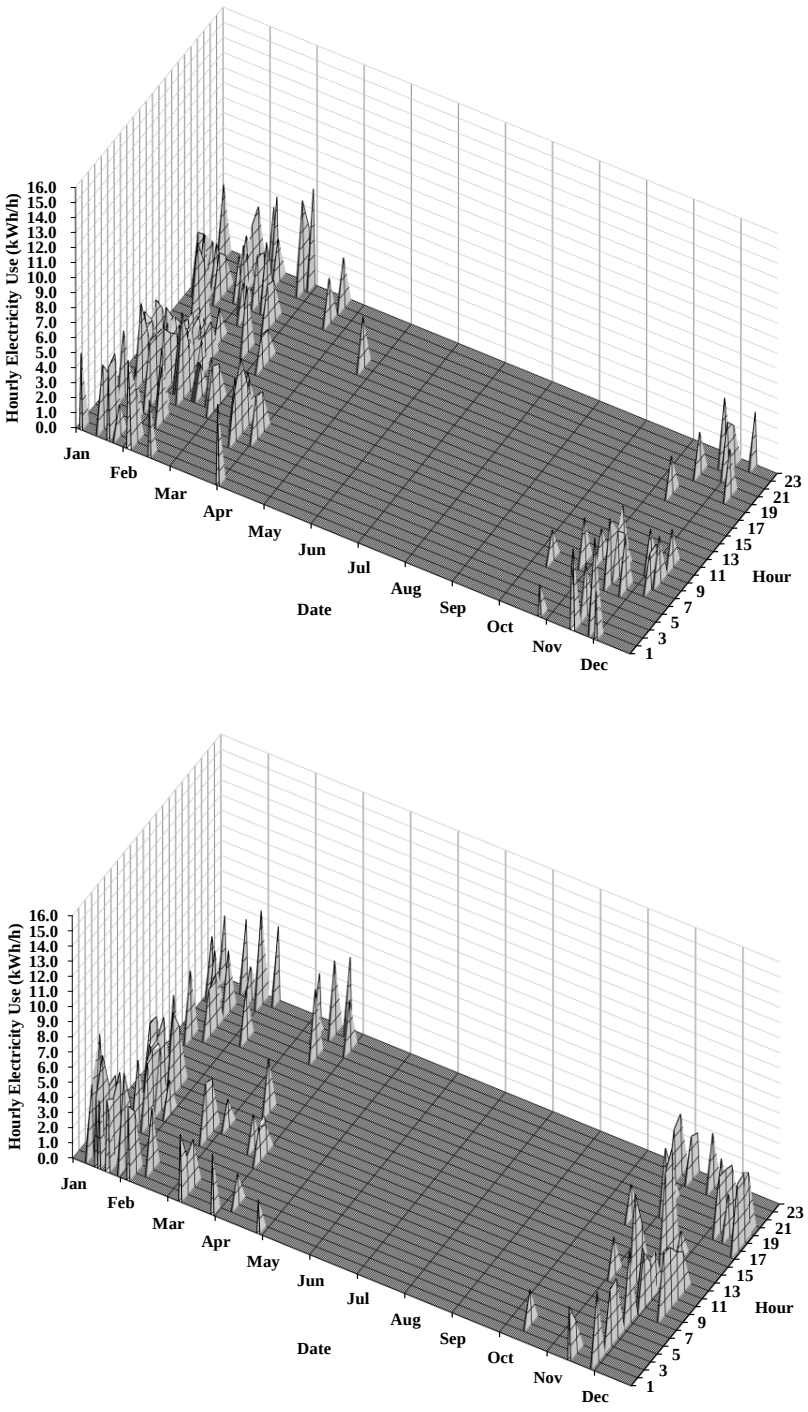

Figure 5-6. 3D energy use plot showing electricity use above the 90th percentile during weekdays (upper) and weekends/holidays (lower) for the heating period.

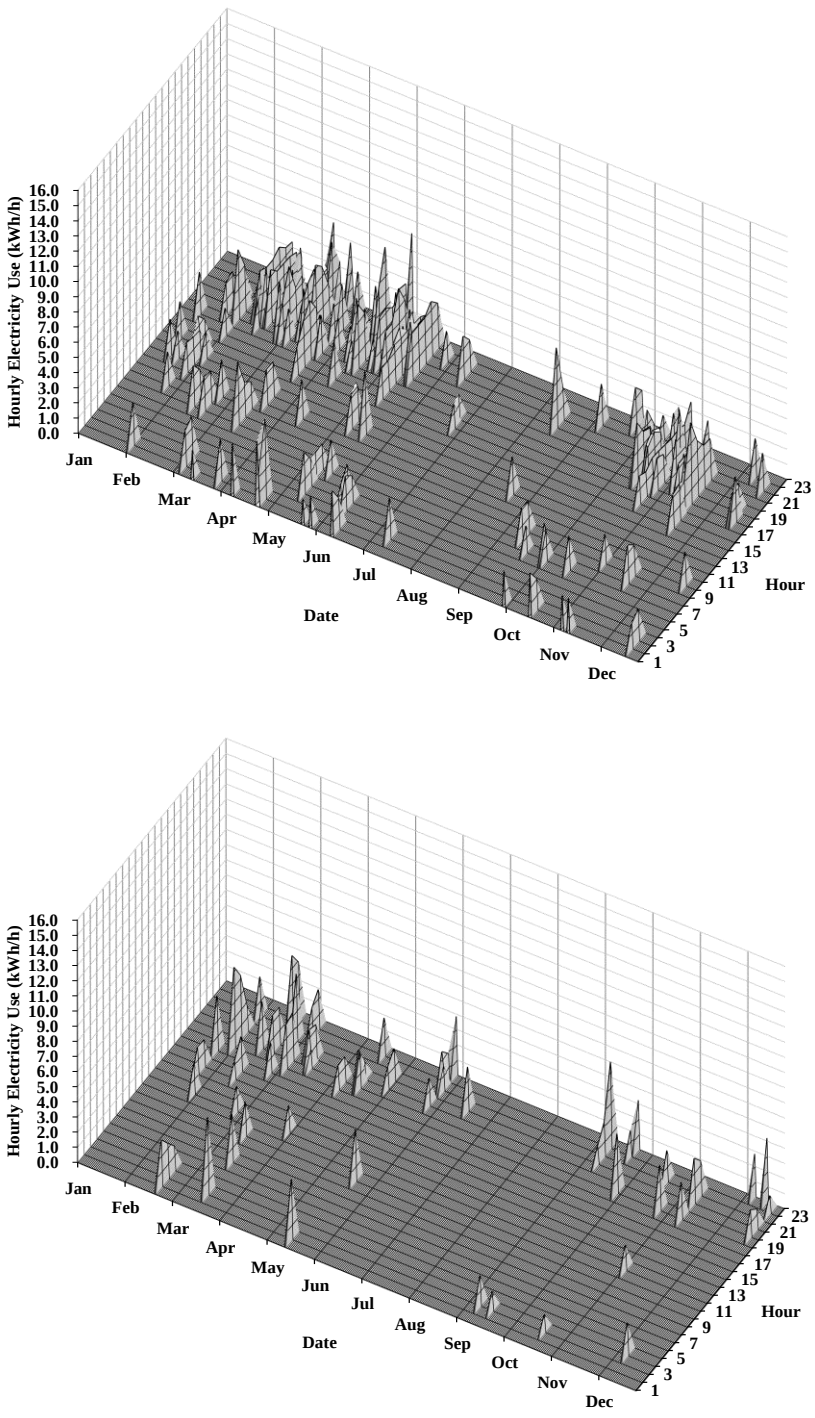

Figure 5-7. 3D energy use plot showing electricity use above the 90th percentile during weekdays (upper) and weekends/holidays (lower) for the weather-independent period.

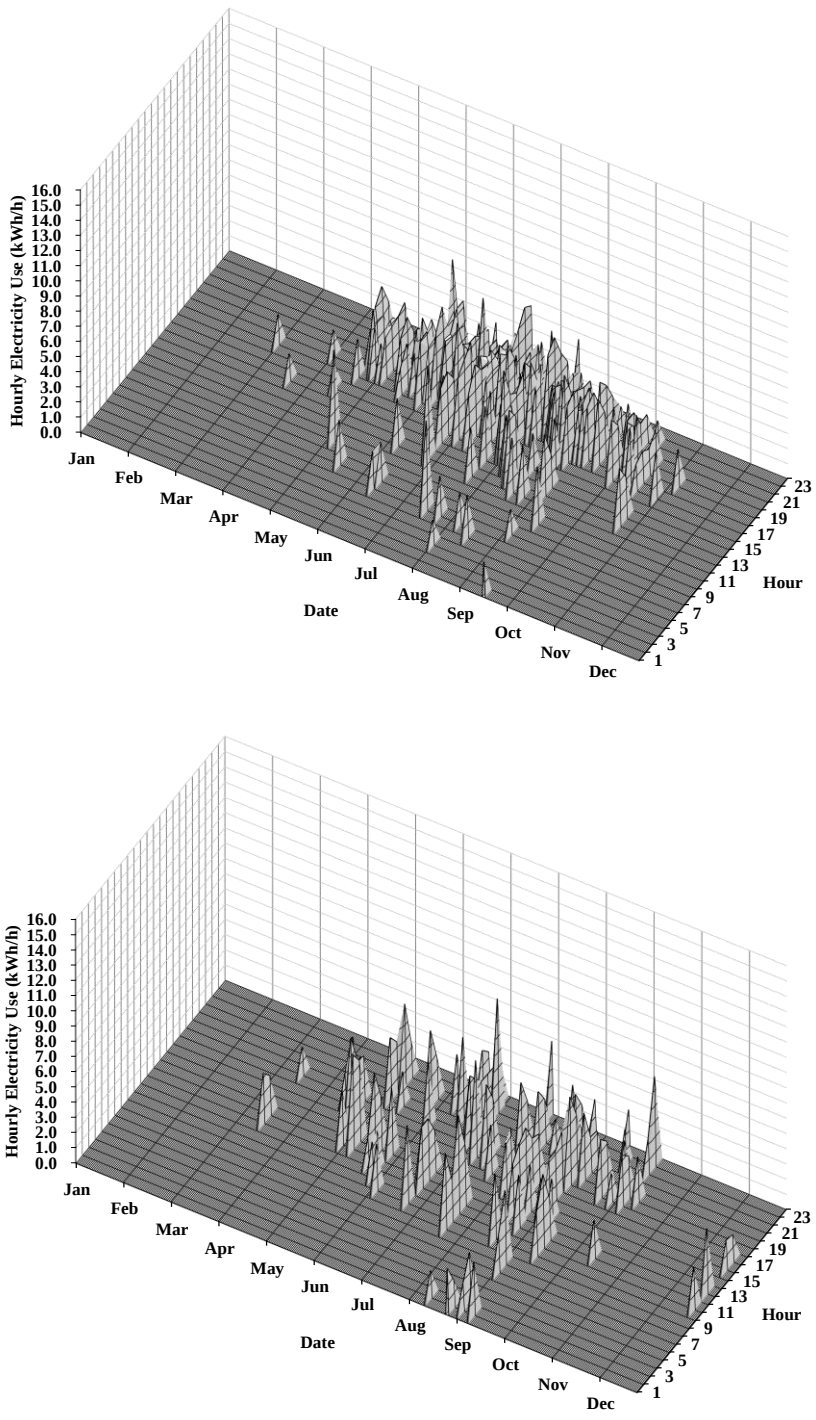

Figure 5-8. 3D energy use plot showing electricity use above the 90th percentile during weekdays (upper) and weekends/holidays (lower) for the cooling period.

from the beginning of October to the middle of November during nighttime hours for both the weekdays and weekends/holidays.

Figure 5-8 shows the 3D energy use plot for the cooling period (i.e., Region III). The figure shows that the hourly electricity use above the 90th percentile (i.e., cooling related electricity use) occurred mostly from the middle of May through the end of September during nighttime hours for both the weekdays and weekends/holidays.

In the analysis, it was assumed that the electricity use below the 10th percentile represented occupancy patterns when the occupant was not in the house or the occupant was inactive (e.g., sleeping). Figure 5-9 shows the 3D energy use plot below the 10th percentile during weekdays and weekends/holidays for the heating period (i.e., Region IV). The figure shows the electricity use below the 10th percentile occurred mainly from the middle of November to the end of April during nighttime and morning hours for the weekdays and from the beginning of November to the middle of April during nighttime and morning hours for weekends/holidays.

Figure 5-10 shows the 3D energy use plot below 10th percentile during weekdays and weekends/holidays for the weather-independent period (i.e., Region V). The figure shows the electricity use below the 10th percentile occurred primarily from the middle of January to the end of June and from the beginning of September to the end of December during working hours for the weekdays. For the weekends/holidays, the electricity use below the 10th percentile occurred mainly from the beginning of October to the end of December and from the middle of February to the beginning of June.

Figure 5-11 shows the 3D energy use plot below the 10th percentile during weekdays and weekends/holidays for the cooling period (i.e., Region VI). The electricity use below the 10th percentile occurred mainly from the beginning of February to the middle of December during working hours for the weekdays. For the weekends/holidays, the electricity use below the 10th percentile occurred mainly from the beginning of February to the end of December during working hours.

Table 5-3 summarizes the frequency of the hours above the 90th percentile and below the 10th percentile during the weekdays and the weekends/holidays using the six different regions. Overall, the most frequent pattern above the 90th percentile occurred during the cooling period, which indicates there could be more opportunities for electricity savings. The most frequent hours below the 10th percentile also occurred during the cooling period. These most likely were the hours when the occupant was inactive (e.g., sleeping) or outside the house and represent the hours of lower electricity use.

Table 5-3. Number of energy frequency hours above the 90th and below the 10th percentile.

Number of frequency hours above 90th	Region I (for heating period)	Region II (for weather-independent period)	Region III (for cooling period)	Total
Weekdays	132	236	225	593
Weekends/holidays	103	70	113	286
Total	235	306	338	879
Number of frequency hours below 10th	Region IV (for heating period)	Region V (for weather-independent period)	Region VI (for cooling period)	Total
Weekdays	124	205	206	535
Weekends/holidays	85	56	113	254
Total	209	261	319	789

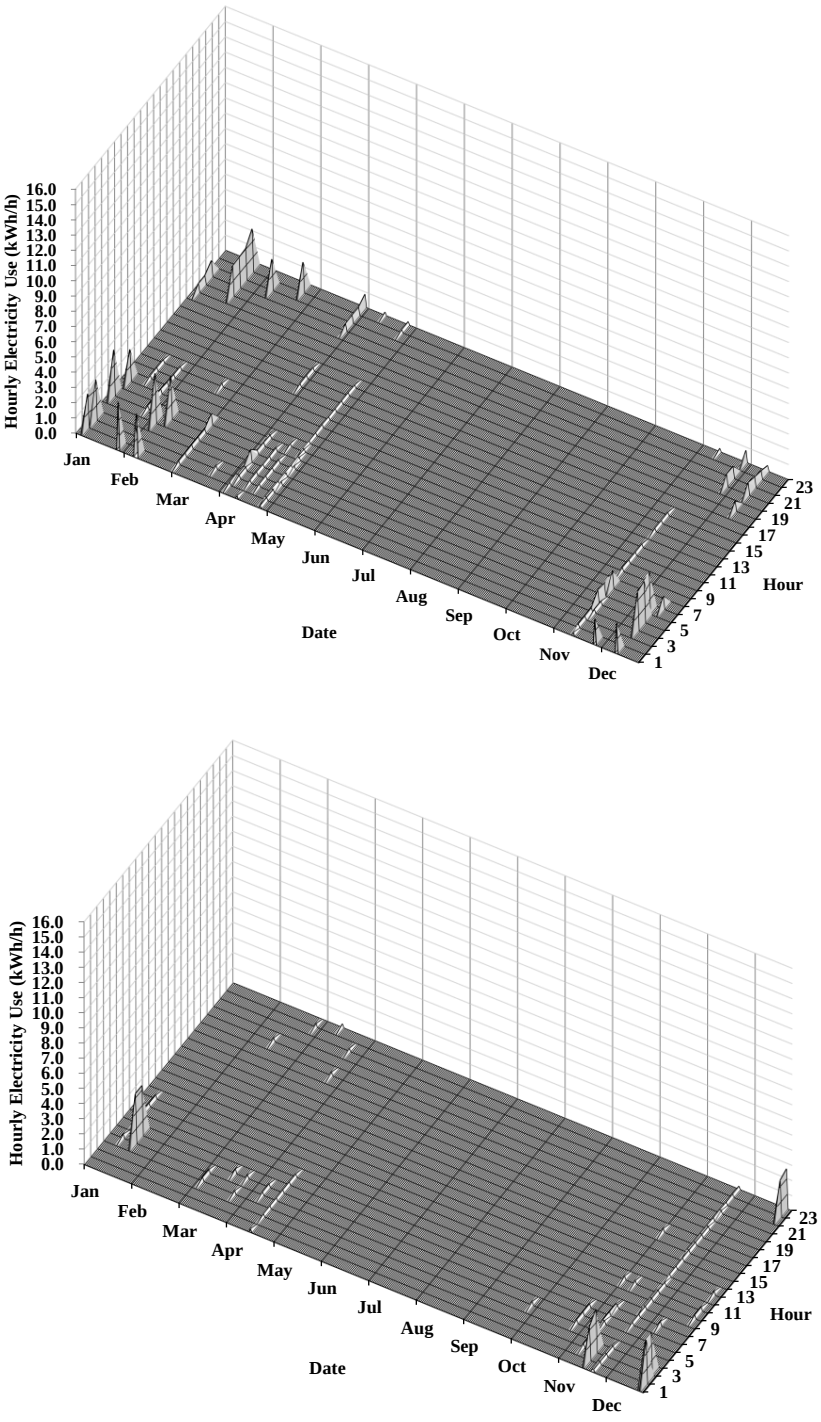

Figure 5-9. 3D energy use plot showing electricity use below the 10th percentile during weekdays (upper) and weekends/holidays (lower) for the heating period.

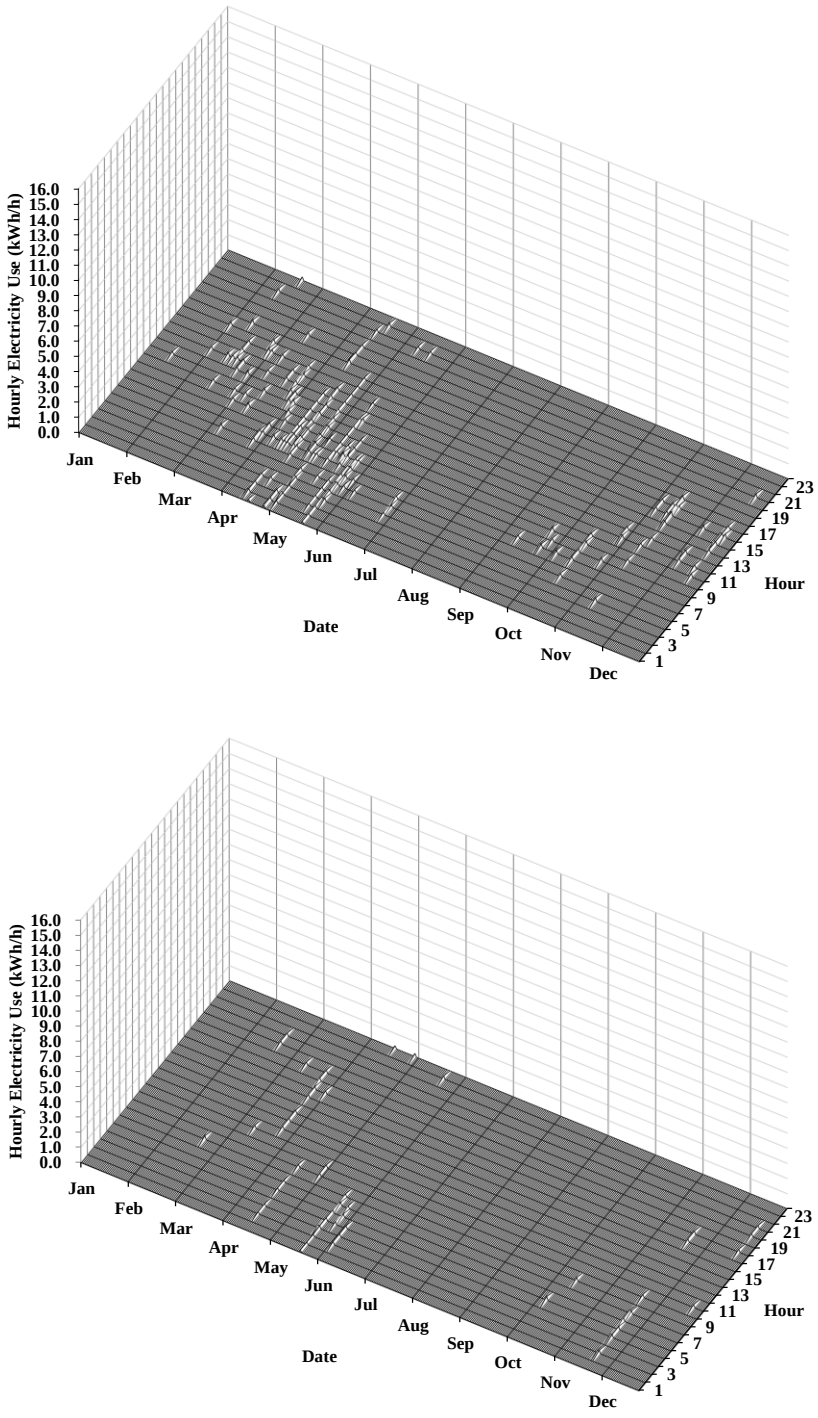

Figure 5-10. 3D energy use plot showing electricity use below the 10th percentile during weekdays (upper) and weekends/holidays (lower) for the weather-independent period.

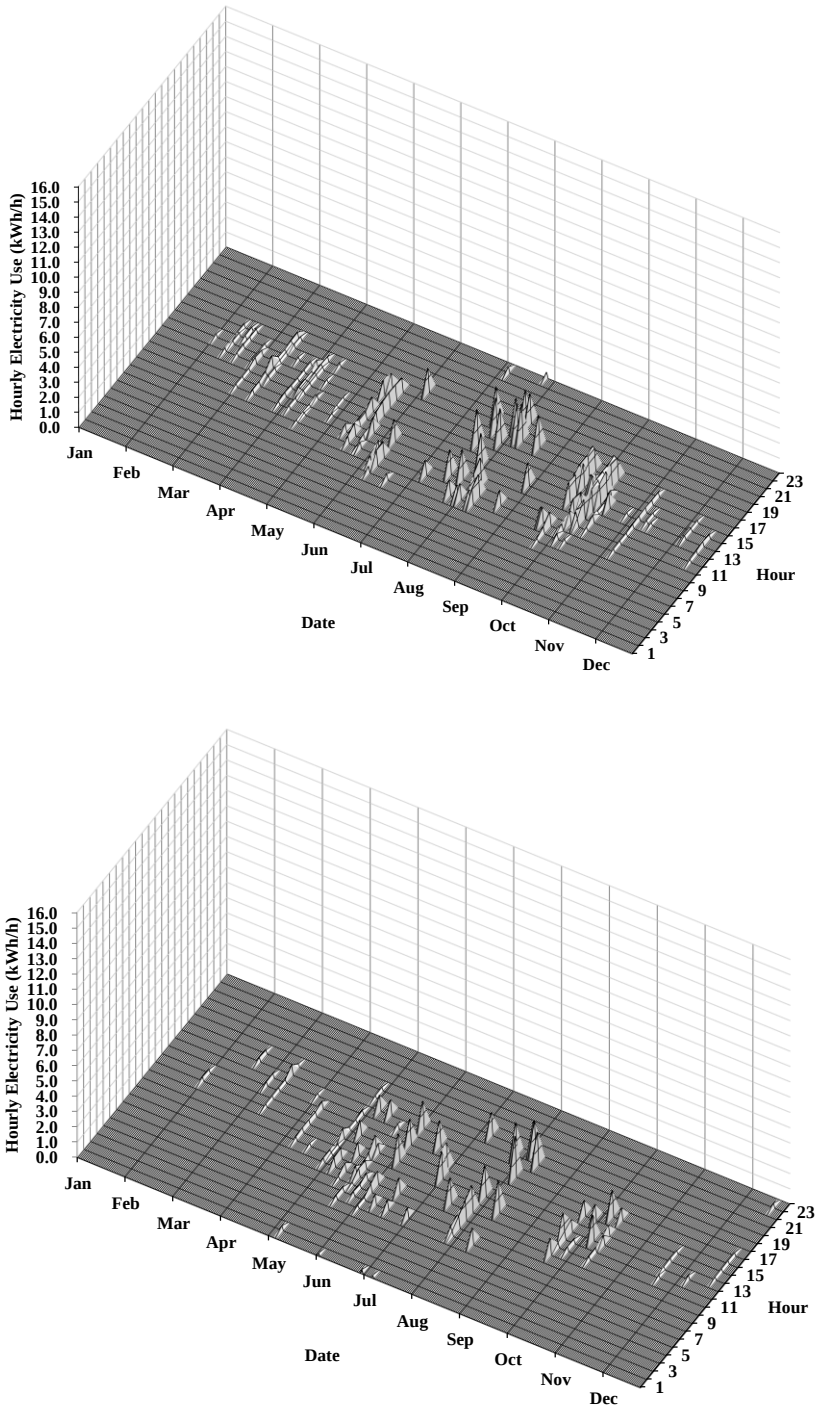

Figure 5-11. 3D energy use plot showing electricity use below the 10th percentile during weekdays (upper) and weekends/holidays (lower) for the cooling period.

Finally, the hour-of-the-day, day-of-the-week, stacked histogram plots were developed to help analyze the energy use and occupancy patterns of the hourly electricity use. Figure 5-12 shows hourly energy use patterns above the 90th percentile for the heating period. During this period, there were ten or more hours above the 90th percentile energy use during the weekdays and the weekends/holidays at 9:00 am. It was also observed that the large number of hours above the 90th percentile occurred at 9:00 am, which most likely represented the Domestic Hot Water (DHW) system use because the electricity used for the operation of the DHW system occurred in the morning after the occupant showered before leaving for work.

Figure 5-13 shows the hour-of-the-day, day-of-the-week, stacked histogram plots representing energy use patterns for the weather-independent period. During this period, there were ten or more hours above the 90th percentile energy use during the weekdays from 6:00 pm to 1:00 am. It was estimated that lighting and other appliances (e.g., cooking devices, televisions, etc.) were mainly operated during these hours, which was the reason for the high energy use. During the weekends/holidays, it can be observed that the devices not associated with heating or cooling were used starting at around 7:00 pm.

Figure 5-14 shows the hour-of-the-day, day-of-the-week, stacked histogram plots representing energy use patterns for the cooling period. During this period, there were ten or more hours above the 90th percentile during the weekdays from 5:00 pm to 10:00 pm. It was estimated that the cooling system was most likely operated during these hours. During the weekends/holidays, it can be seen that the cooling system was most likely used at 6:00 pm and 7:00 pm.

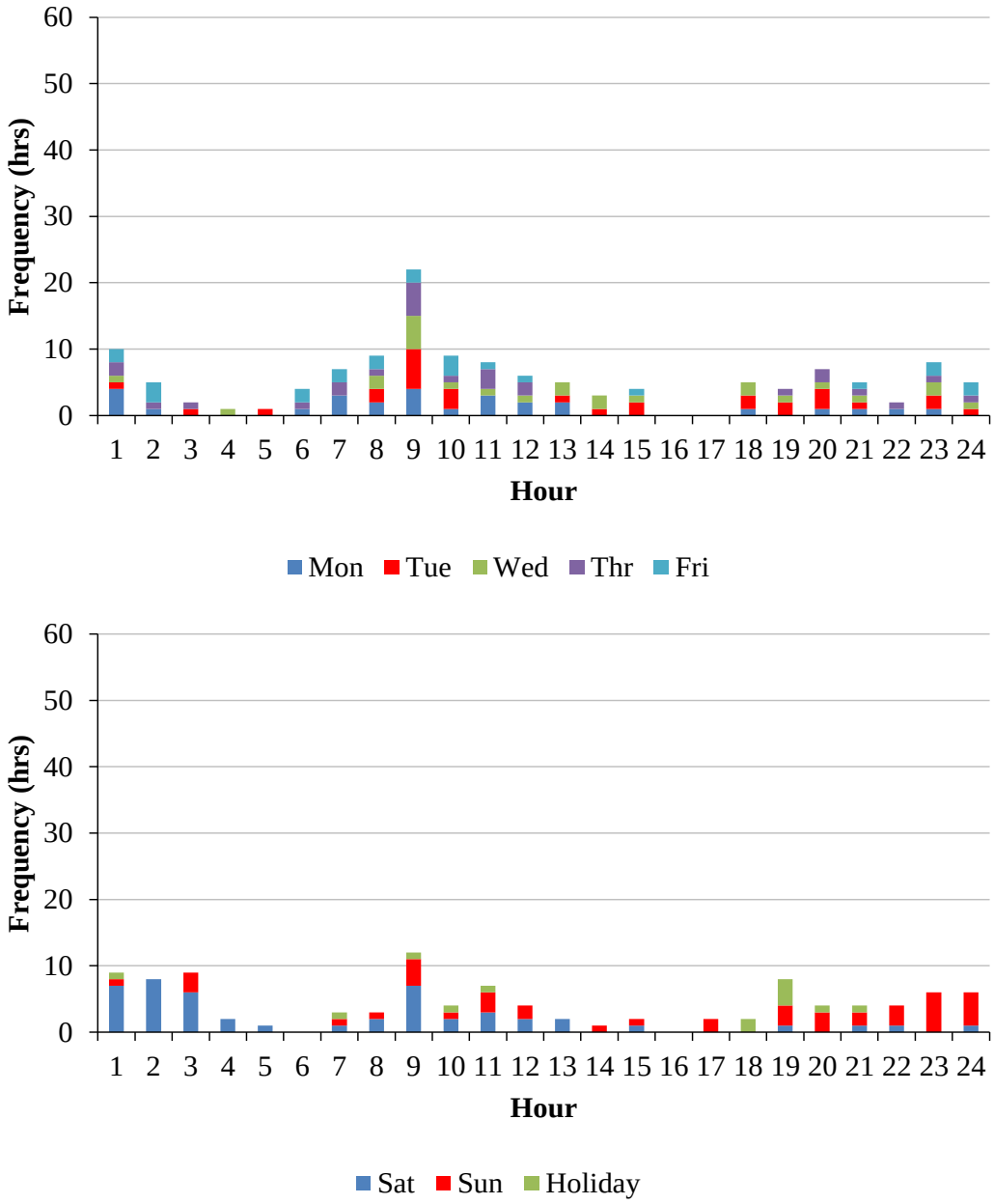

Figure 5-12. Hour-of-the-day, day-of-the-week, stacked histogram plots showing hours above the 90th percentile representing energy use patterns during weekdays (upper) and weekends/holidays (lower) for the heating period.

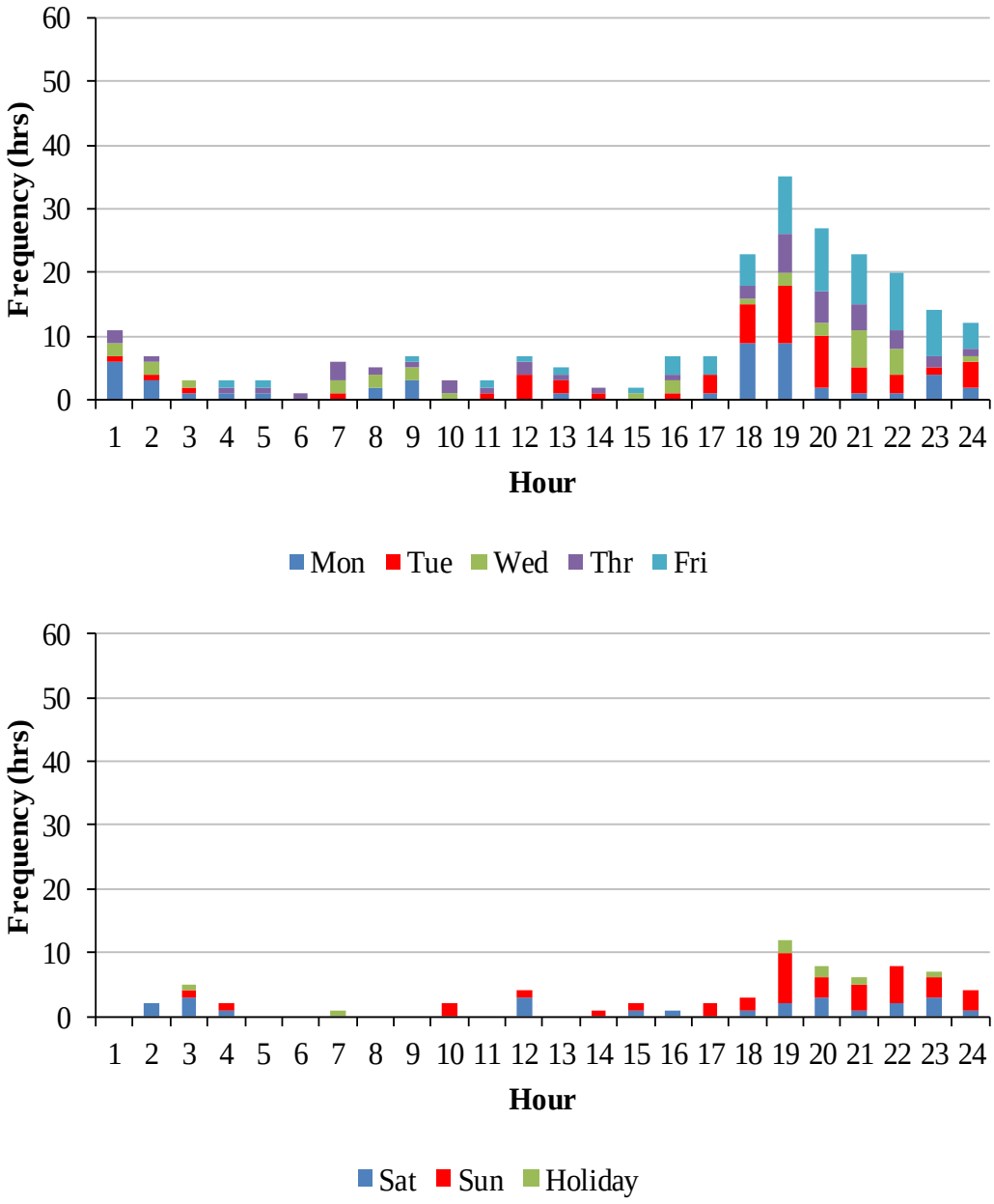

Figure 5-13. Hour-of-the-day, day-of-the-week, stacked histogram plots showing hours above the 90th percentile representing energy use patterns during weekdays (upper) and weekends/holidays (lower) for the weather-independent period.

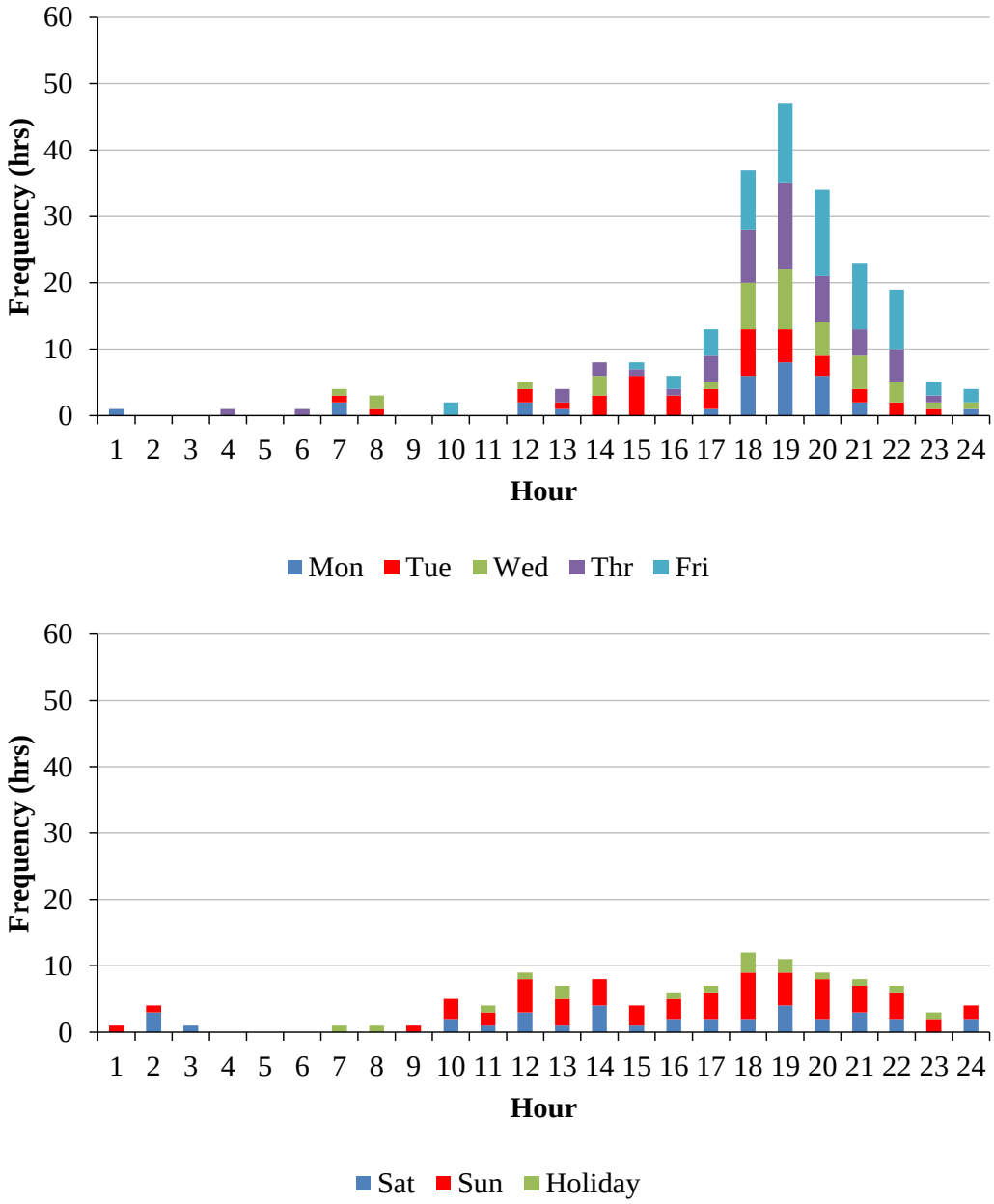

Figure 5-14. Hour-of-the-day, day-of-the-week, stacked histogram plots showing hours above the 90th percentile representing energy use patterns during weekdays (upper) and weekends/holidays (lower) for the cooling period.

The hourly electricity use below the 10th percentile may represent periods of minimum energy use and occupancy patterns during the heating, weather-independent, and cooling periods. This was because the patterns of low energy use below the 10th percentile of each period tend to indicate minimum energy consumption patterns when occupants were inactive (e.g., sleeping) or outside a house. Figure 5-15 shows the hour-of-the-day, day-of-the-week, stacked histogram plot representing occupancy patterns for the heating period. In this period, there were more hours of occurrence below the 10th percentile energy use during the weekdays from 1:00 am to 8:00 am, which implies the occupant was inactive or requiring less electricity use during these hours. A similar trend was also shown during the weekends/holidays.

Figure 5-16 shows the hour-of-the-day, day-of-the-week, stacked histogram plot representing occupancy patterns for the weather-independent period. In this plot, the electricity use data below the 10th percentile during the weekdays occurred frequently between 8:00 am through 4:00 pm on Monday through Friday, which implies the occupant was inactive or outside the house during the hours. The electricity use data below the 10th percentile for the weather-independent period during the weekends/holidays showed fewer hours.

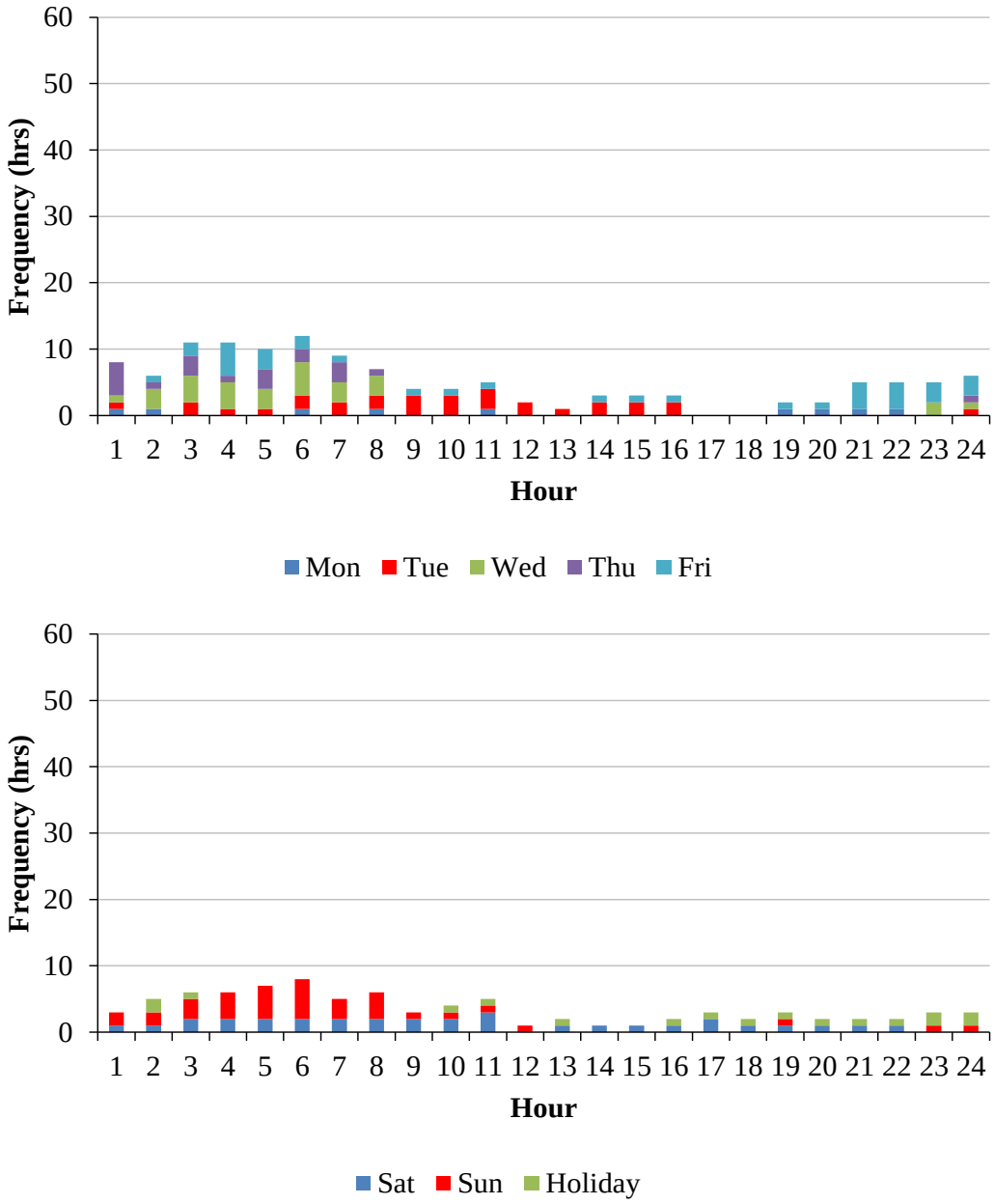

Figure 5-15. Hour-of-the-day, day-of-the-week, stacked histogram plots showing hours below the 10th percentile representing occupancy patterns during weekdays (upper) and weekends/holidays (lower) for the heating period.

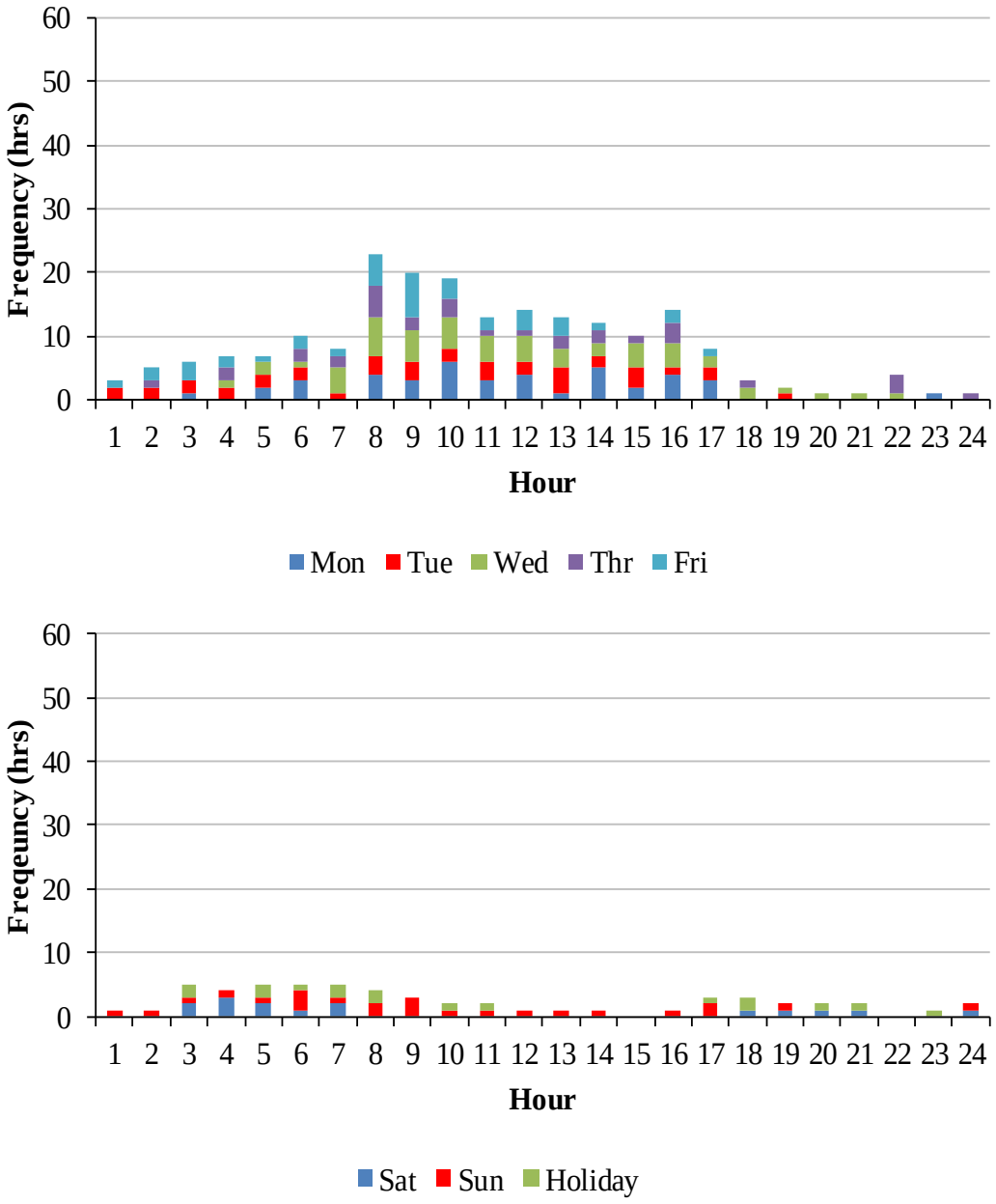

Figure 5-16. Hour-of-the-day, day-of-the-week, stacked histogram plot showing hours below the 10th percentile representing occupancy patterns during weekdays (upper) and weekends/holidays (lower) for the weather-independent period.

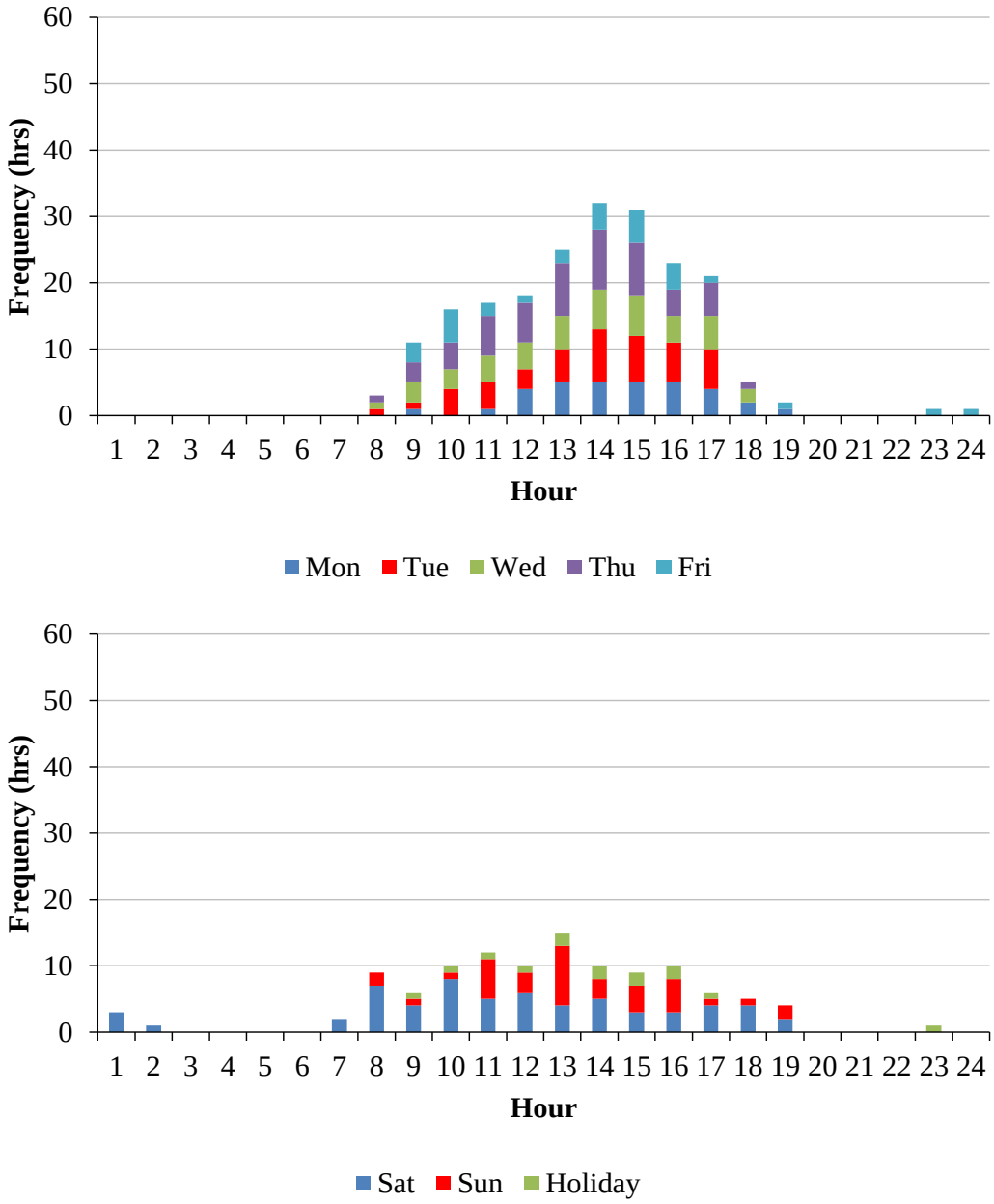

Figure 5-17. Hour-of-the-day, day-of-the-week, stacked histogram plot showing hours below the 10th percentile representing occupancy patterns during weekdays (upper) and weekends/holidays (lower) for the cooling period.

Figure 5-17 shows the new hour-of-the-day, day-of-the-week, stacked histogram plot representing occupancy patterns for the cooling period. In this plot, the hourly electricity use data below the 10th percentile for the cooling period occurred during the weekdays frequently between 9:00 am through 5:00 pm on Tuesday through Friday, as well as 12:00 pm through 5:00 pm on Friday. The low energy use implies inactivity or absence of the occupant. The electricity use below the 10th percentile for the cooling period during the weekends/holidays occurred many times from 8:00 am through 4:00 pm on Saturday and Sunday.

Next, for the quantification process (see Figure 4-2), a method for quantifying potential electricity savings was developed. Figure 5-18 shows the new weather day-typing plot that used an hourly quartile approach analysis during the heating period (i.e., lower than 60.2 °F (weekdays) and 63.7 °F (weekends/holidays)), which were determined by the 5P change-point linear model. In this analysis, the interquartile range (IQR) of the weekend/holiday weather day-typing plot was wider than the weekday plot, which indicates that the homeowner's energy consumption during weekends/holidays was more unpredictable. In other words, on average, the homeowner's electricity use during the weekends/holidays varied more than during the weekdays.

Figure 5-19 shows the new weather day-typing plot, which included the quartile approach for the weather-independent period (i.e., between 60.2 °F and 76.6 °F (weekdays) and between 63.7 °F and 74.1 °F (weekends/holidays)) with the change points determined by the 5P change-point linear model. The IQRs of both the weekends and the weekdays/holidays were narrower compared to other heating and cooling

periods. However, during the evening hours from 6:00 pm to 10:00 pm on the weekdays and 7:00 pm on the weekdays/holidays, the IQRs covered a wider range, which indicates the homeowner's energy consumption during these hours was more unpredictable.

Figure 5-20 shows the weather day-typing plot that used the quartile analysis for the cooling period (i.e., higher than 76.6 °F (weekdays) and 74.1 °F (weekends/holidays)) with the change points determined by the IMT's 5P model. In the figure, the IQRs of both the weekends and the weekdays/holidays were also wider from 10:00 am to 8:00 pm, which indicates the homeowner's energy consumption during these hours was more unpredictable.

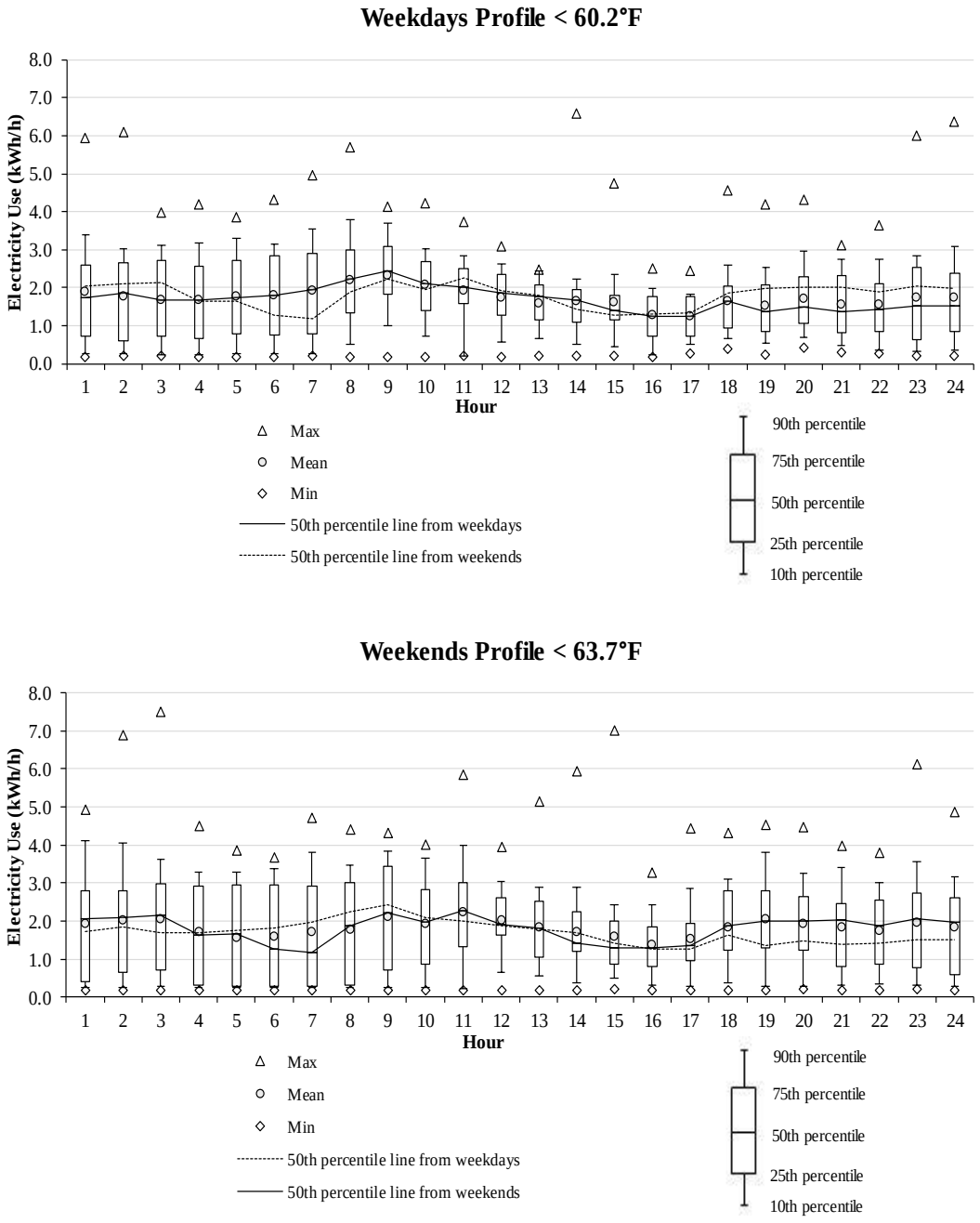

Figure 5-18. New weather day-typing plot using the quartile approach during weekdays (upper) and weekends/holidays (lower) for the heating period.

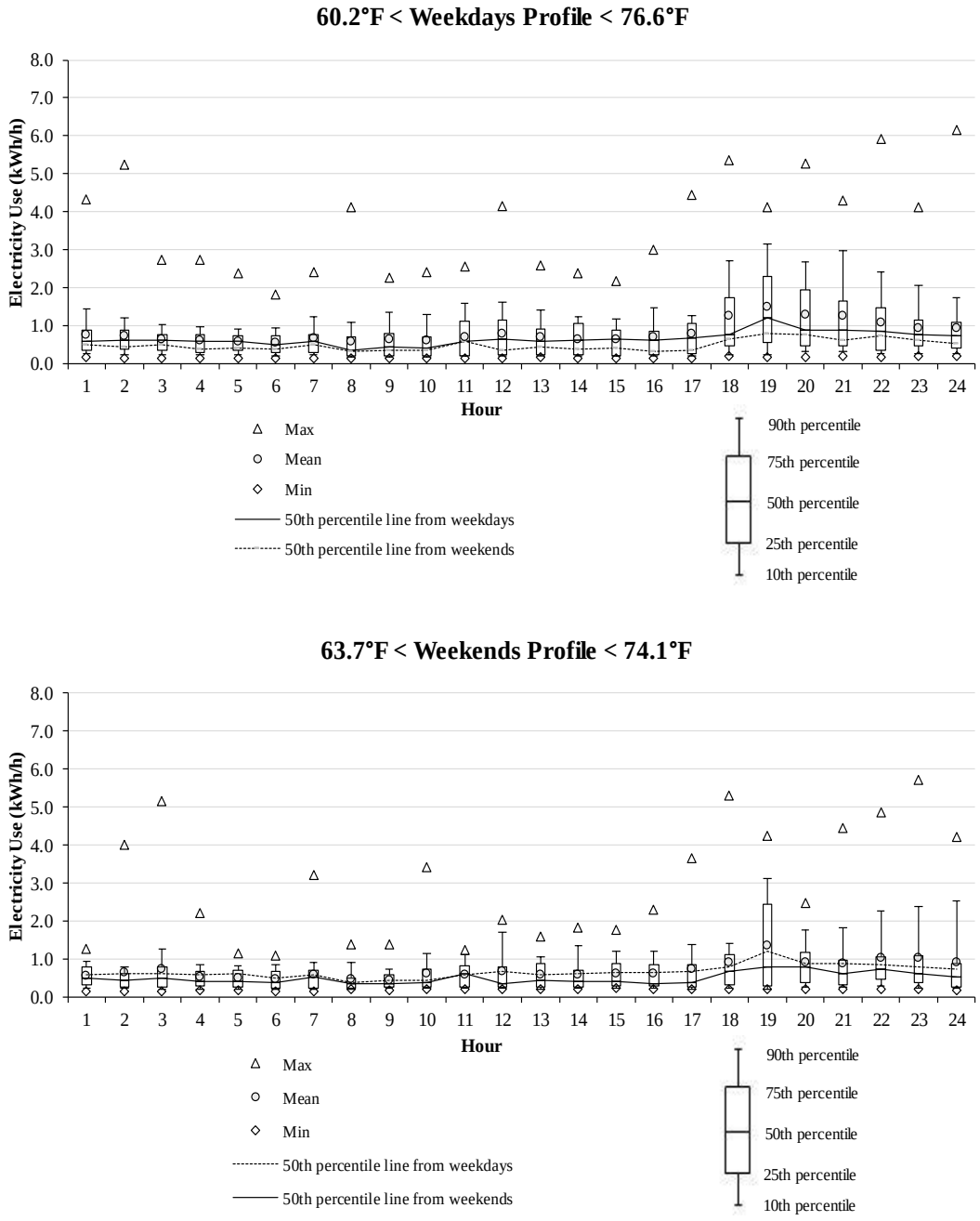

Figure 5-19. New weather day-typing plot using the quartile approach during weekdays (upper) and weekends/holidays (lower) for the weather-independent period.

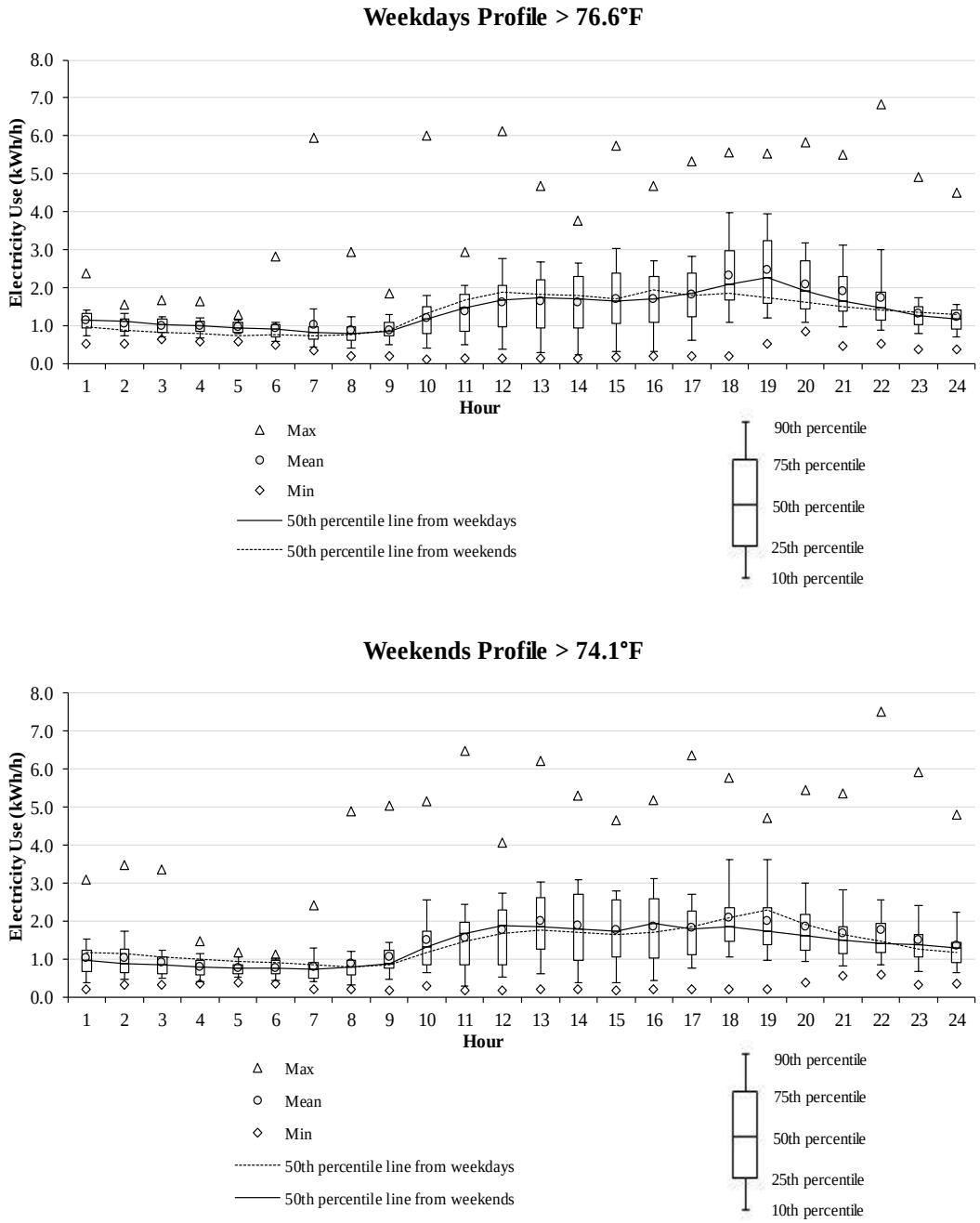

Figure 5-20. New weather day-typing plot using the quartile approach during weekdays (upper) and weekends/holidays (lower) for the cooling period.

Finally, in the next step of the Level 0 Analysis, the 50th percentile of the hourly electricity use data for the weekdays and the weekends/holidays were compared to determine the potential energy savings of HADs for a representative hour-of-the-day energy pattern for heating, weather-independent, and cooling periods. In the analysis, it was assumed that the 50th percentile of the hourly electricity use was representative of the average hour-of-day electricity use pattern.

Figure 5-21 shows both the 50th percentiles for the weekdays and the weekends/holidays for the heating period in the upper plot and the differences between the medians in the lower plot. The results showed that during most of time for the heating period, the homeowner can realize energy saving opportunities with the heating related-systems from 4:00 am through 10:00 am and from 2:00 pm through 3:00 pm if the occupant's energy use pattern during the weekdays followed the energy use pattern during the weekends/holidays (i.e., the blue-filled area). In a similar fashion, the homeowner can have energy saving opportunities at 1:00 am through 4:00 am, 10:00 am through 2:00 pm, and 4:00 pm through 12:00 am if the occupant's energy use pattern during the weekends/holidays followed the energy use pattern during the weekdays (i.e., the orange-filled area). This energy savings calculation method used the homeowner's previously-recorded, hour-of-day energy use patterns, so this method could be applied non-intrusively to hourly electricity use data based on an occupant's energy behavior patterns.

Figure 5-22 shows the results of the 50th percentile differences between the weekdays and the weekends/holidays for the weather-independent period. In this

analysis, it was assumed that the homeowner could save energy if the energy use pattern during the weekdays (i.e., 50th percentile) followed the energy use pattern during the weekends/holidays (i.e., the blue-filled area).

Figure 5-23 shows the 50th percentile differences between the weekdays and the weekends/holidays for the cooling period. This analysis assumed the homeowner could save energy from 1:00 am through 8:00 am and from 5:00 pm trough 9:00 pm if the energy use pattern during the weekdays followed the energy use pattern during the weekends/holidays (i.e., the blue-filled area). In the same way, the homeowner could save energy from 9:00 am through 4:00 pm if the energy use pattern during the weekends/holidays followed the energy use pattern during the weekdays (i.e., the orange-filled area).

The differences (blue or orange-filled areas) of the plots represented potential energy savings of a typical day based on the hour-of-day energy pattern differences between weekdays and weekends/holidays. In other words, there is a possibility that a homeowner can save energy based on the previous hour-of-day energy patterns between weekdays and weekends.

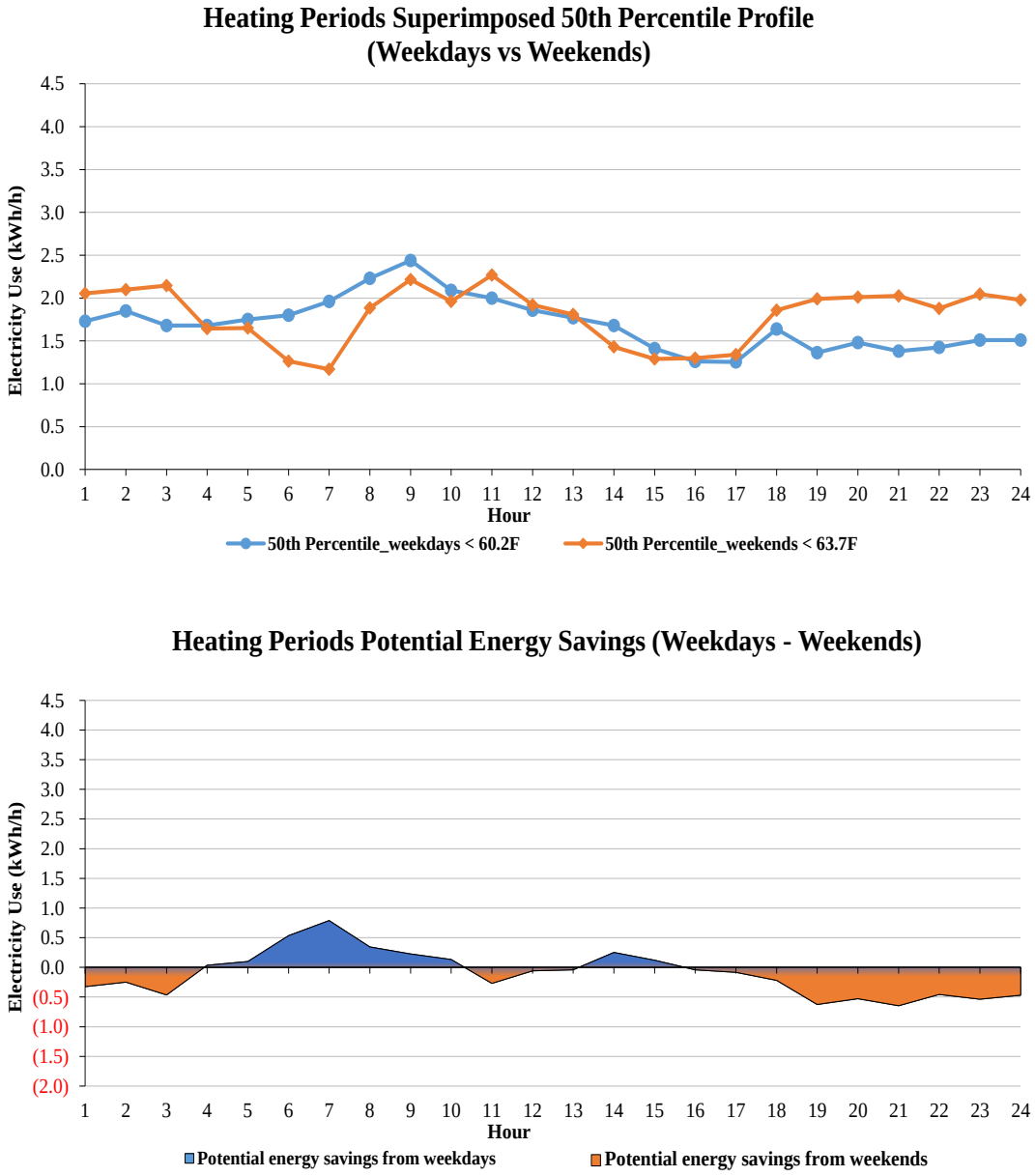

Figure 5-21. Potential electricity savings for the heating period calculated by comparing the 50th percentile between the weekdays and the weekends/holidays.

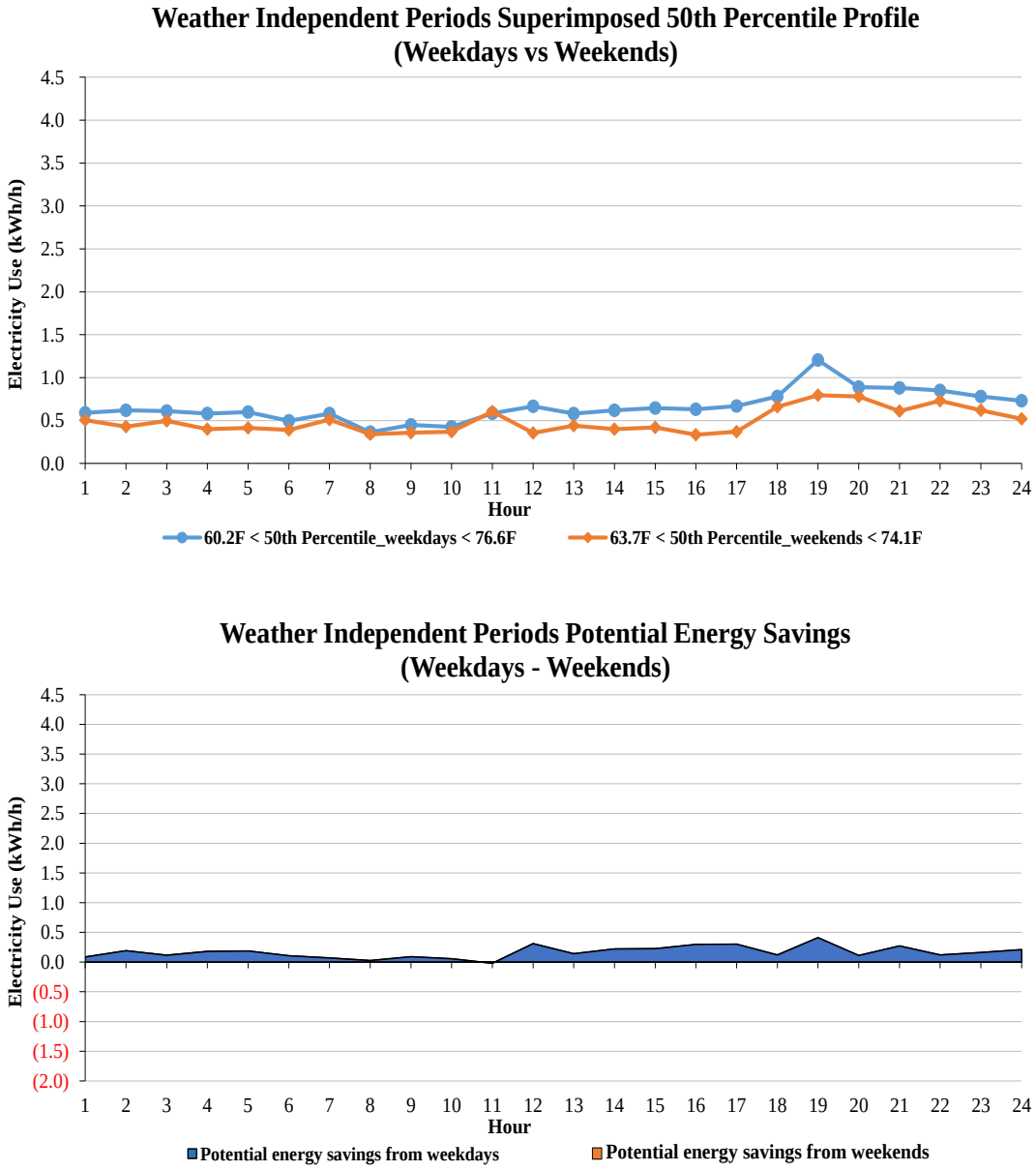

Figure 5-22. Potential electricity savings for the weather-independent period calculated by comparing the 50th percentile between the weekdays and the weekends/holidays.

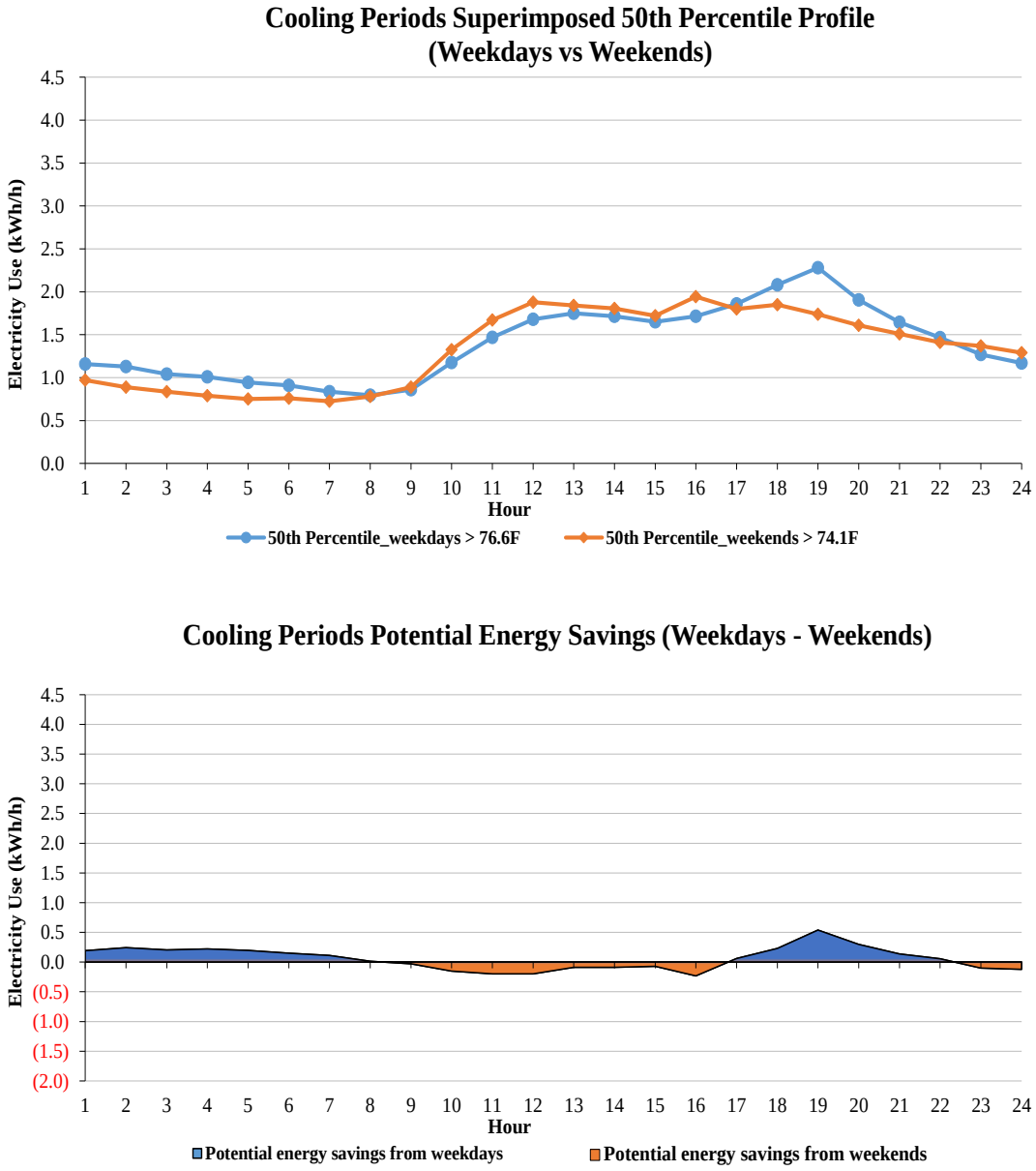

Figure 5-23. Potential electricity savings for the cooling period calculated by comparing the 50th percentile between the weekdays and the weekends/holidays.

In Figure 5-21, the potential energy savings of the representative day for the heating period is 6.9 kWh, based on this method. The potential energy savings of 2.4 kWh is from weekdays (i.e., the blue-filled area), and the potential energy savings of 4.5 kWh is from weekends (i.e., the orange-filled area). The daily total potential savings of 6.9 kWh may be from heating related systems or appliances.

These daily savings can also be quantified annually based on the days during the heating period when the outside air temperatures (OAT) were below the heating balance-point temperature (i.e., Regions I and IV). In this example, the heating balance-point temperatures are 60.2 °F and 63.7 °F for the weekdays and the weekends/holidays, respectively. Thus, the days during the heating period below these balance-point temperatures would be 58 days and 42 days, respectively. Therefore, to quantify the annual energy savings, the weekday's potential daily energy savings of 2.4 kWh is multiplied by 58 days, and the weekend/holiday's savings of 4.5 kWh is multiplied by 42 days. This results in 328.4 kWh saved with an expected cost savings of $38.0. In this study, the rate of electricity was assumed to be $0.1156/kWh, which is based on the US EIA's data for 2015 Texas (US EIA, 2016). Table 5-4 summarizes the results of the potential energy savings during the heating period, the weather-independent period, and the cooling period.

The potential energy savings from this method would be increased if two different types of days (one type when occupant(s) stayed at home with normal activities (e.g., weekdays) and the other type when occupant(s) did not stay at home or did not

Table 5-4. Potential electricity savings from Level 0 Analysis.

Balance-point temperature (°F)			
from Weekdays	from Weekends/holidays		
60.2	63.7		
Number of heating days (Region I+IV)			
from Weekdays	from Weekends/holidays	Total days	
58	42	100	
Number of weather-independent days (Region II+V)			
from Weekdays	from Weekends/holidays	Total days	
99	30	129	
Number of cooling days (Region III+V)			
from Weekdays	from Weekends/holidays	Total days	
90	46	136	
Daily potential electricity savings (kWh) for heating period			
from Weekdays	from Weekends/holidays	Total savings (kWh)	
2.4	4.5	6.9	
Daily potential electricity savings (kWh) for weather-independent period			
from Weekdays	from Weekends/holidays	Total savings (kWh)	
3.8	0.003	3.8	
Daily potential electricity savings (kWh) for cooling period			
from Weekdays	from Weekends/holidays	Total savings (kWh)	
2.5	1.2	3.7	
Annual potential electricity savings (kWh) for heating period			
from Weekdays	from Weekends/holidays	Total savings (kWh)	Total cost savings ($)
140.6	187.8	328.4	38.0
Annual potential electricity savings (kWh) for weather-independent period			
from Weekdays	from Weekends/holidays	Total savings (kWh)	Total cost savings ($)
379.9	0.1	380.0	43.9
Annual potential electricity savings (kWh) for cooling period			
from Weekdays	from Weekends/holidays	Total savings (kWh)	Total cost savings ($)
225.0	54.4	279.4	32.3
Grand total Annual potential electricity savings (kWh)			
from Weekdays	from Weekends/holidays	Grand total savings (kWh)	Grand total cost savings ($)
745.5	242.3	987.8	114.2
Grand total Annual potential electricity savings (%)			
from Weekdays	from Weekends/holidays	Grand total savings (%)	Grand total cost savings (%)
9.5	6.0	8.3	8.3

have normal activities (e.g., weekends/holidays)) were decided, rather than using the different energy patterns between typical weekdays and weekends/holidays.

In summary, in this section, a non-intrusive statistical method (i.e., Level 0 Analysis) was presented that automatically detects and quantifies potential electricity energy savings from HADs using SM electricity use data from a residence. To detect electricity energy use and occupancy patterns, the IMT was used to analyze the hourly electricity use data along with coincident hourly weather data to find an appropriate regression model and the balance-point temperatures to differentiate between the heating, weather-independent, and cooling periods. For the case-study house, as shown in Figure 4-17, using this method, the hourly SM electricity use data was categorized into the three periods for the weekdays and the weekends/holidays. In addition, the hourly electricity use data was categorized into the six regions using the previously-described quartile approach. Finally, using the six regions, the 3D energy use plots and the hour-of-the-day, day-of-the-week, stacked histogram plots were then used to further identify the energy use patterns and the occupancy patterns to better analyze the estimated potential energy savings.

To help quantify potential energy savings, an improved weather day-typing method, which includes a quartile analysis, was used to find the hour-of-day energy use patterns between the weekdays and the weekends/holidays for each period. Using the method, potential energy savings was quantified using differences in the 50^{th} percentiles of the energy use patterns between the weekdays and the weekends/holidays for each period.

5.2. Results of the Calibrated Simulation Method (Level I Analysis)

This sections summarizes the results of Level I Analysis using the calibrated simulation model. In this part of the analysis, an hourly DOE-2.1E simulation model of the case-study house was created and calibrated using the hourly electricity use, Indoor Air Temperature (IAT), and thermostat data from the case-study house along with the coincident weather data for the one week. The calibrated model was then used to quantify the detailed, annual and monthly average daily electricity savings of the HADs.

Figure 5-24 shows a rendering of the hourly simulation model of the case-study house using a visualization tool (i.e., DrawBDL (Huang, 2002)) for the input file of the DOE-2.1E program. In this figure, the yellow surfaces are roofs, red surfaces are walls, brown surfaces are doors, blue surfaces are windows, and gray surfaces are the interior walls that separate the residence from the adjacent residences. The hourly simulation model was developed using information from drawings of the case-study residence, the 2000 or 2009 IECC performance path (ICC, 2000, 2009), and the DOE-2.1E libraries (i.e., nominal values) (Winkelmann et al., 1993). Then, after an initial simulation model was created with the nominal values, the hourly simulation model was calibrated using the hourly electricity use, IATs, thermostat settings, coincident weather, and occupancy data from one week of the post-retrofit period (February 20th, 2017 to February 26th, 2017).

Next, the hourly simulation model was calibrated by changing the parameters during the seven days of the post-retrofit period shown in Table 5-5. Each run shows the parameter changes and the resultant changes to the calibration using an average of

NMBE % and an average of CV-RMSE % from the seven days for both IATs and electricity use (i.e., a two-way calibration).

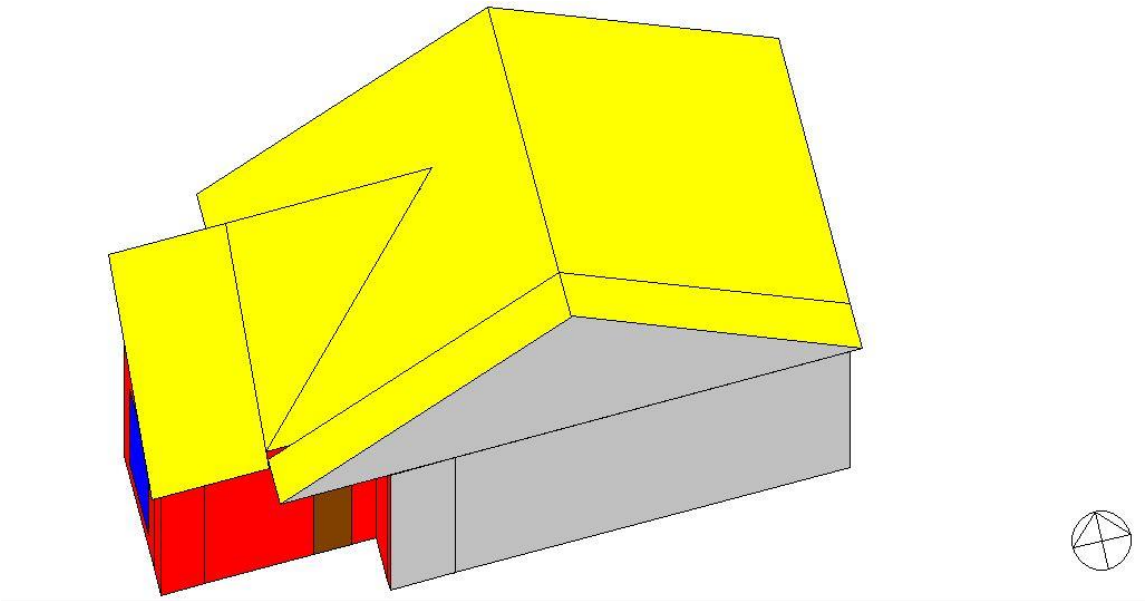

Figure 5-24. The 3D view of the hourly building simulation model for the case-study house.

Run #1 shows the nominal, base-case model results (see Figure 5-25). It should be noted that the measured, average IATs from the seven zones were used for the thermostat schedules of the simulation model to better match the simulated IATs with the measured IATs, which resulted in a high goodness-of-fit for the IATs. However, for example, on Feb 20th, 2017, the simulation did not exactly match the measured electricity use because the simulated HVAC system was running more often than the measured HVAC electricity use. As a result, in Run #1, the base-case model showed an NMBE of 0.1% and a CV-RMSE of 0.2% for the IATs and an NMBE of -92.1% and a CV-RMSE of 135.4% for the electricity use.

Table 5-5. Parameter changes for the hourly calibration for the period from February 20th, 2017 to February 26th, 2017.

Run	Parameter	IAT			Whole-building electricity use			Figure #
		MBE (°F)	NMBE (%)	CV-RMSE (%)	MBE (kWh)	NMBE (%)	CV-RMSE (%)	
1	Base-case model (nominal)	0.08	0.11	0.17	-0.56	-92.07	135.44	5-25
2 (1+2)	Changed heating and cooling setpoints based on the measured data	1.22	1.65	2.48	-0.42	-69.81	123.88	5-26
3 (1+2+3)	Changed heating and cooling system schedules based on the measured data	5.59	7.58	8.78	0.00	-1.79	95.11	5-27
4 (1+2+3+4)	Adjusted the U-effectiveness of a floor from 0.078 to 0.001	3.15	4.27	6.15	0.02	1.30	83.85	5-28
5 (1+2+3+4+5)	Adjusted Window Frame Conductance from 3.04 to 1.00	3.15	4.27	5.97	0.03	2.27	83.64	5-29
6 (1+2+3+4+5+6)	Modified Weighting Factor from 0 to 130	1.56	2.11	2.62	0.06	6.31	84.07	5-30
7 (1+2+3+4+5+6+7)	Changed the infiltration rate from 3.0 ACH50 to 0.03 ACH50 when HVAC system is on	1.48	2.01	2.56	0.14	18.28	69.76	5-31
8 (1+2+3+4+5+6+7+8)	Modified lighting, equipment, and DHW system schedules based on the Level 0 analysis and trends of the whole-building electricity	1.04	1.41	2.17	-0.02	-2.67	10.89	5-32

For Run #2, the heating and cooling setpoints were changed based on the measured setpoint data. Figure 5-26 shows the results from the heating and cooling setpoint changes for Run #2. The results show the setpoint changes made a larger difference between the measured IATs and the simulated IATs because the base-case simulation model's characteristics did not exactly match the measured indoor conditions. However, the setpoint change improved the goodness-of-fit of the simulated electricity use because it helped to correct the runtime of the heating and cooling system when IATs were below the heating setpoint or above the cooling setpoint. As a result, Run #2 showed an NMBE of 1.7% and a CV-RMSE of 2.5% for the IATs and an NMBE of -69.8% and a CV-RMSE of 123.9% for the electricity use.

For Run #3, the heating and cooling system schedules were modified further based on the measured system runtime data. Figure 5-27 shows the results of the heating and cooling system schedule change for Run #3. Unfortunately, the system schedule change worsened the difference in the measured IATs and the simulated IATs because the base-case simulation model did not have accurate characteristics for the indoor environment. However, the system schedule change significantly improved the goodness-of-fit of the electricity use because the schedule corrected the runtime of the heating and cooling system according to the actual system schedule. As a result, Run #3 showed an NMBE of 7.6% and a CV-RMSE of 8.8% for the IATs and an NMBE of -1.8% and a CV-RMSE of 95.1% for the electricity use.

Run #4 shows the results of the adjusted U-effectiveness used for the case-study house's slab-on-grade floor (see Figure 5-28). In this run, the U-effectiveness was

adjusted from 0.078, which was calculated from the underground surface heat transfer calculation method (Winkelmann, 2002), to 0.001. The adjustment improved the goodness-of-fit of both the IATs and the electricity use. Run #4 showed an NMBE of 4.3% and a CV-RMSE of 6.2% for the IATs and an NMBE of 1.3% and a CV-RMSE of 83.8% for the electricity use.

Run #5 shows the results of the adjusted effective window frame conductance from 3.04 Btu/hr-ft^2-°F to 1.00 Btu/hr-ft^2-°F (see Figure 5-29). In this run, the adjustment slightly improved the goodness-of-fit of the IATs, but it did not improve the goodness-of-fit of the simulated versus measured electricity use. This trend was also found when the effective wall R-value was adjusted. Run #5 showed an NMBE of 4.3% and a CV-RMSE of 6.0% for the IATs and an NMBE of 2.3% and a CV-RMSE of 83.6% for the electricity use.

Run #6 shows improved results by modifying DOE-2.1E's weighting factors from 0 to 130 lb/ft^2 (see Figure 5-30), where the weighting factors of "0" mean custom weighting factors and the weighting factors of 130 lb/ft^2 are normally used for pre-calculated weighting factors for heavy construction. Since the material properties of the actual floor, walls, and ceiling were not specifically known for the simulation model, the pre-calculated weighting factors gave a more reasonable fit for simulated the IATs. However, it worsened the goodness-of-fit of the simulated electricity use versus measured electricity use. Run #6 showed an NMBE of 2.1% and a CV-RMSE of 2.6% for the IATs and an NMBE of 6.3% and a CV-RMSE of 84.1% for the electricity use.

Run #7 shows improved results by changing the infiltration rate from 3 ACH50 to 0.03 ACH50 when the heating or the cooling system was on (see Figure 5-31). This adjustment assumed the infiltration rate was normally reduced when the system was turned on because the supply fan of the system pressurizes the house. The change slightly improved the goodness-of-fit of the IATs. In addition, the change improved the CV-RMSE of the electricity use. However, the change worsened the NMBE of the electricity use. Run #7 showed an NMBE of 2.0% and a CV-RMSE of 2.6% for the IATs and an NMBE of 18.3% and a CV-RMSE of 69.8% for the electricity use.

Run #8 was the final calibration obtained by modifying lighting, equipment, and DHW system schedules based on the information from the Level 0 Analysis and the trends of the hourly electricity use data (see Figure 5-32). The modification significantly increased the goodness-of-fit of both the IATs and the electricity use. Run #8 showed an NMBE of 1.4% and a CV-RMSE of 2.2% for the IATs and an NMBE of -2.7% and a CV-RMSE of 10.9% for the electricity use.

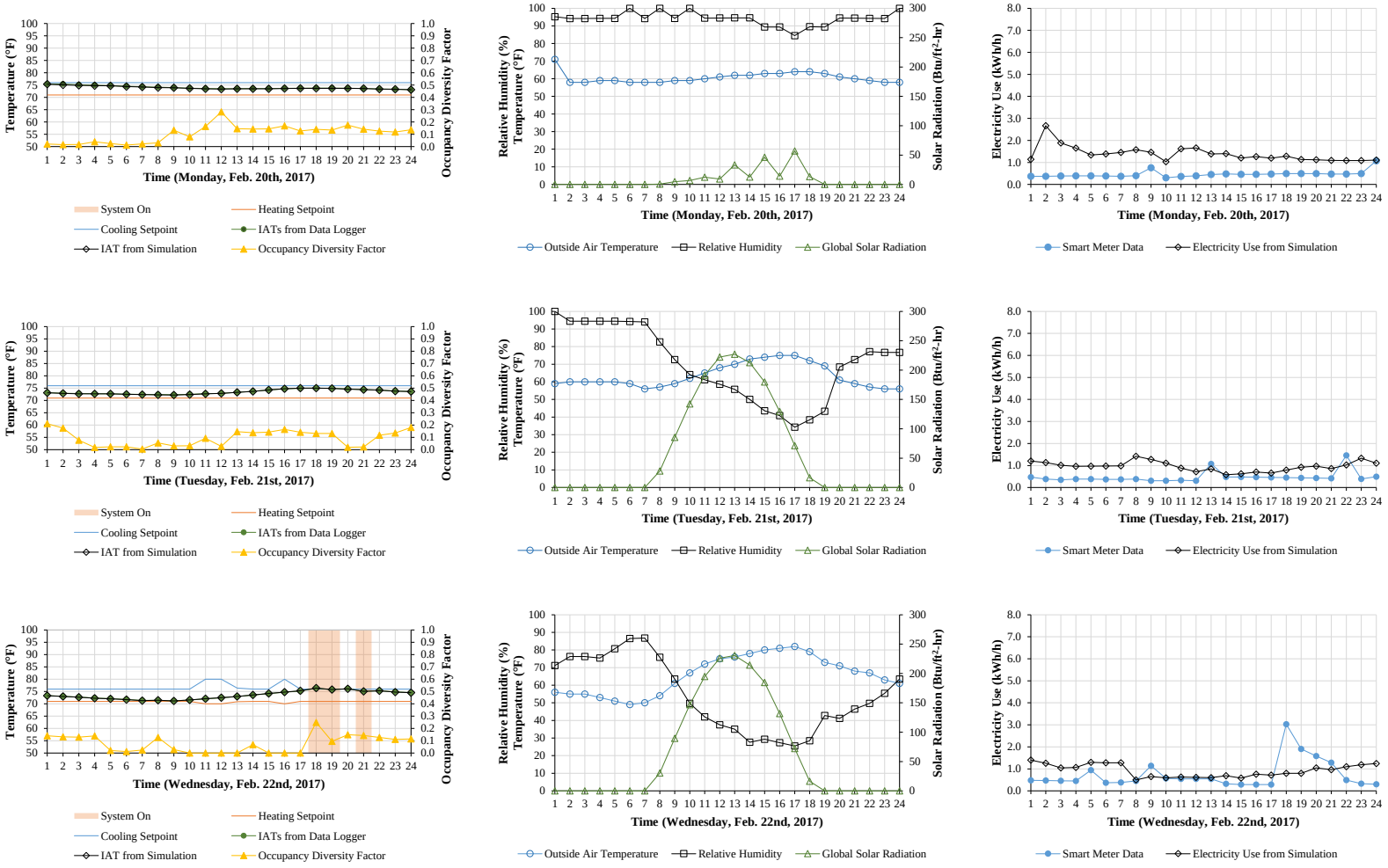

Figure 5-25. Run #1 base-case simulation model results showing IATs, coincident weather data, and electricity use from Monday to Sunday (from February 20th, 2017 to February 26th, 2017).

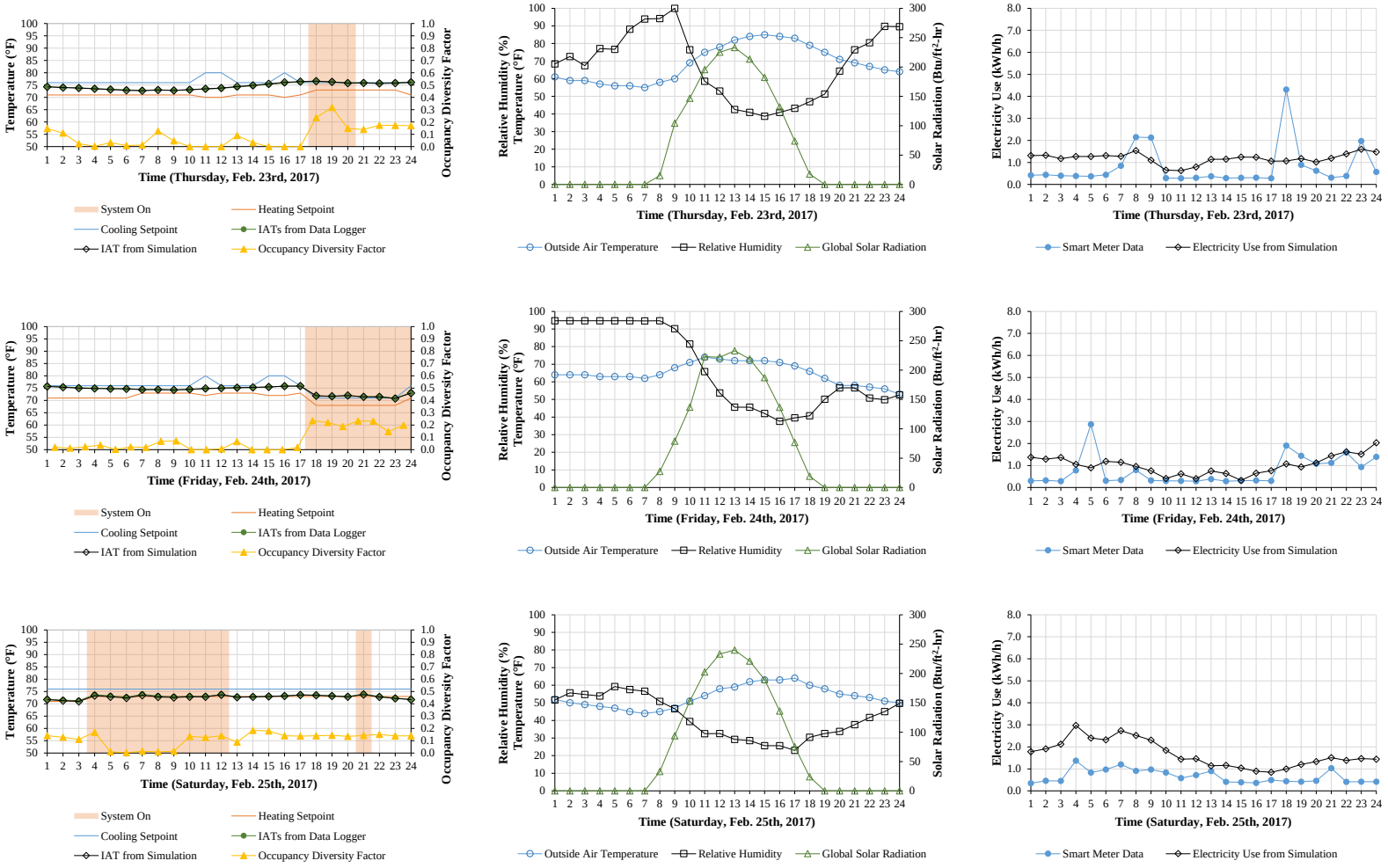

Figure 5-25. Continued.

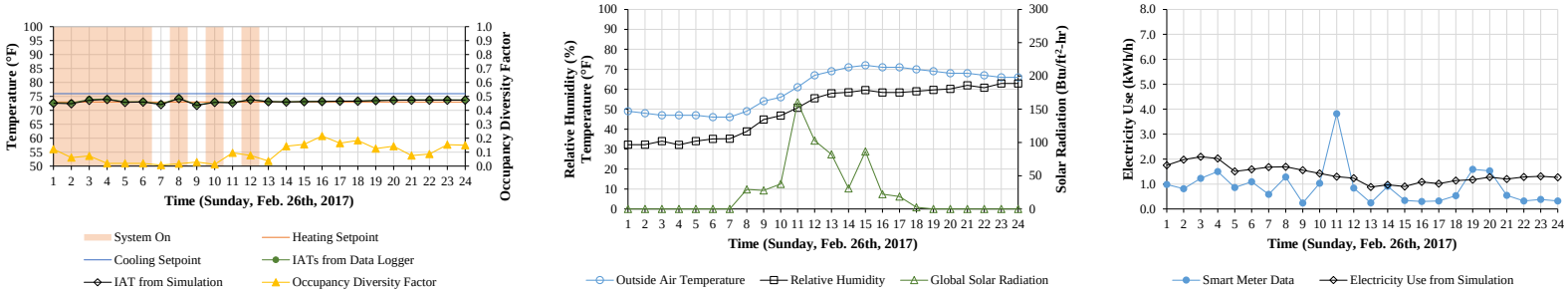

Figure 5-25. Continued.

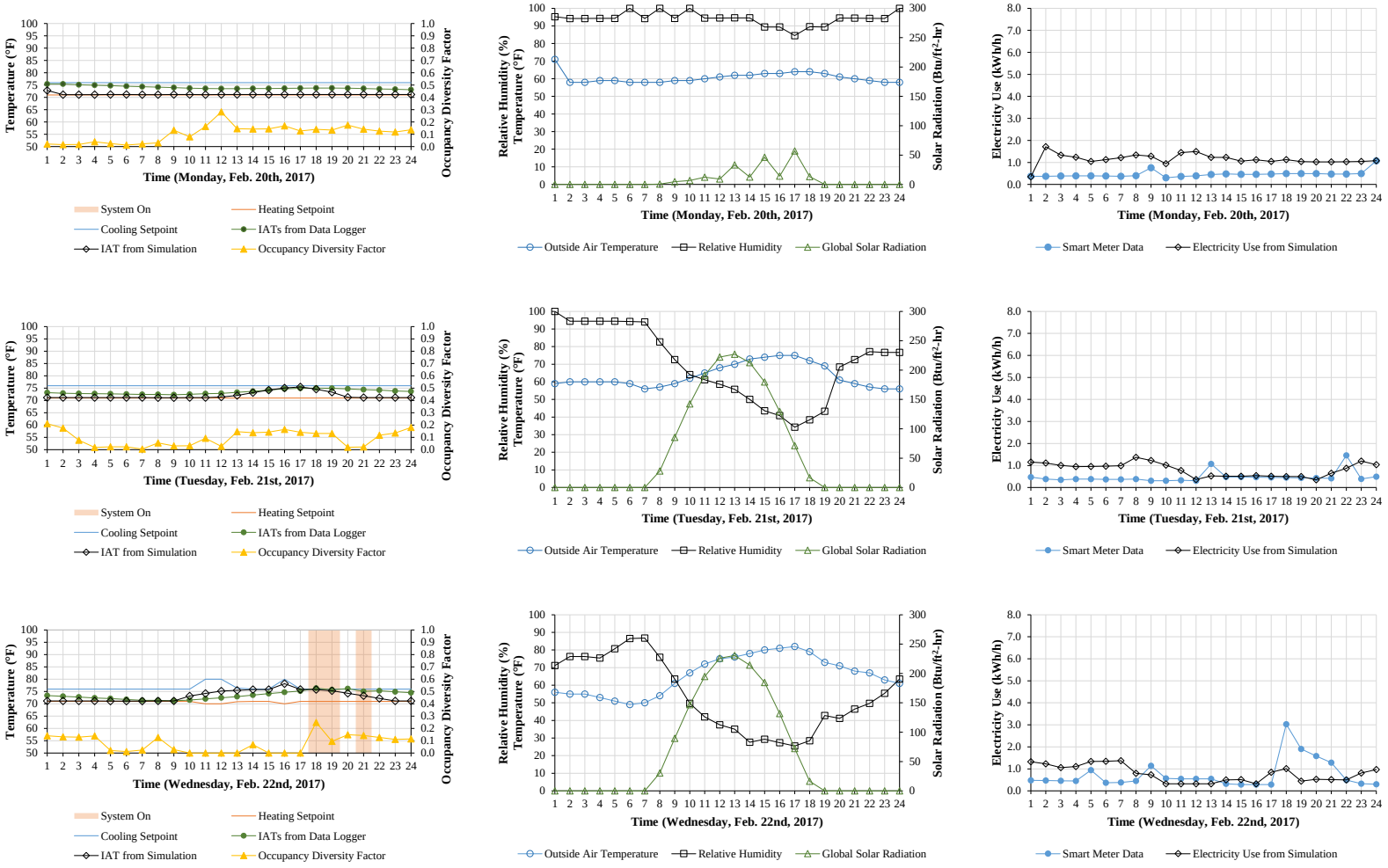

Figure 5-26. Run #2 simulation model results showing IATs, coincident weather data, and electricity use from Monday to Sunday (from February 20th, 2017 to February 26th, 2017).

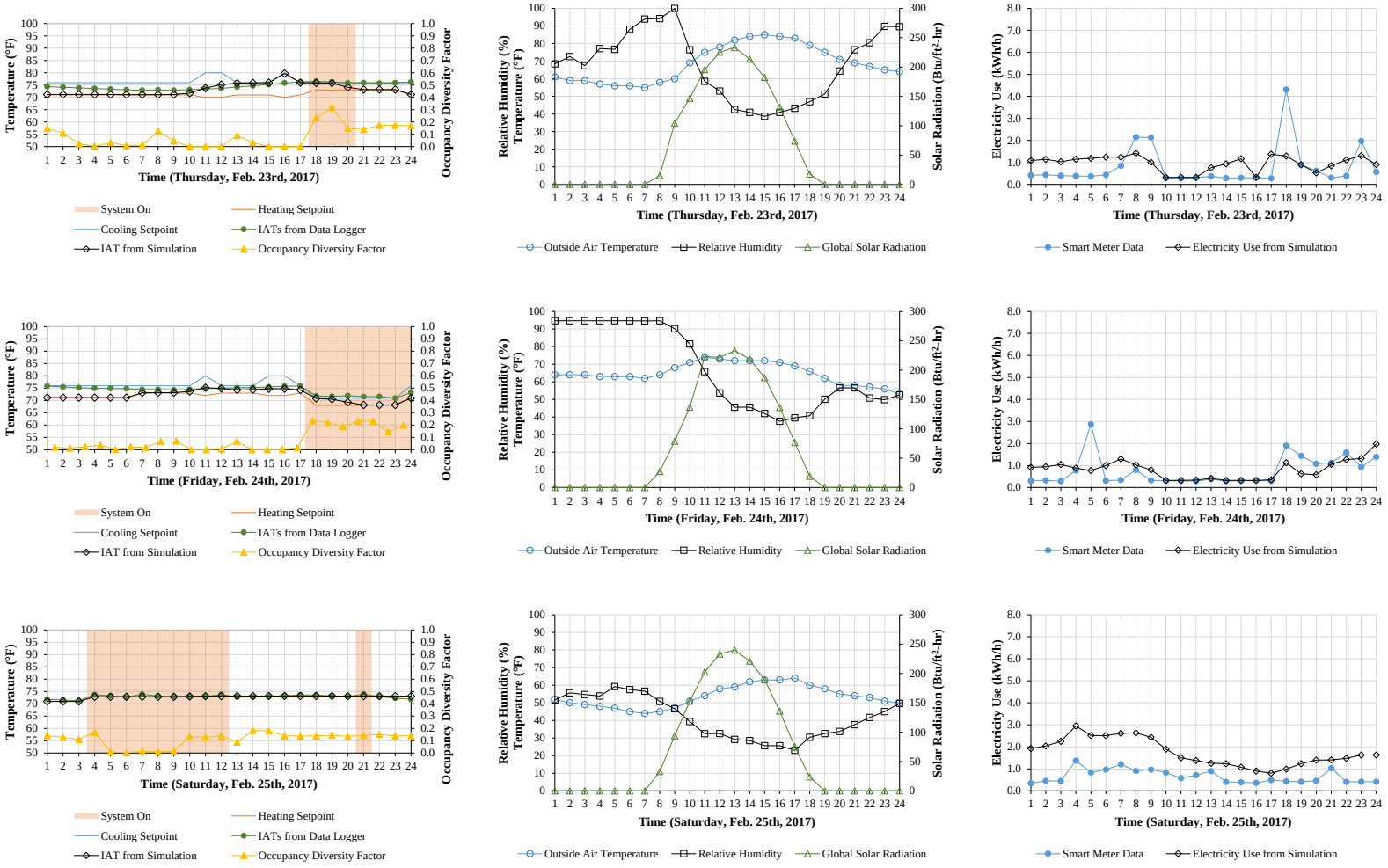

Figure 5-26. Continued.

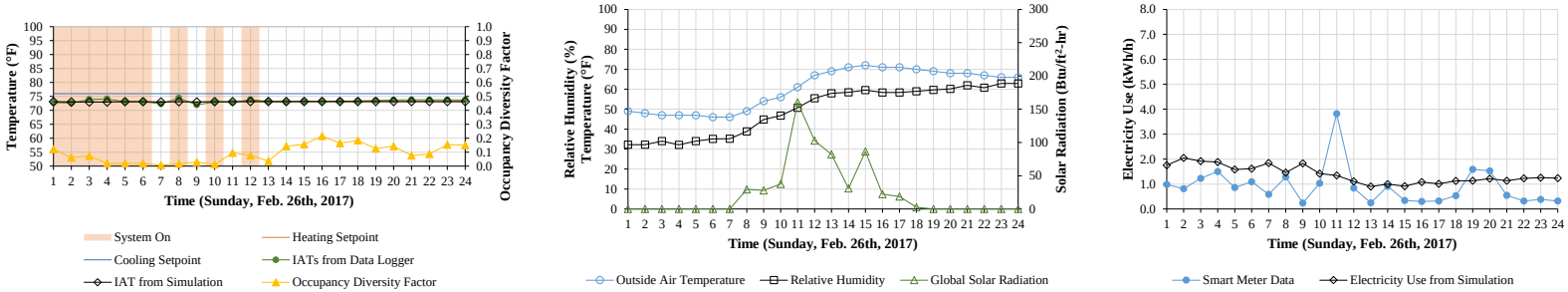

Figure 5-26. Continued.

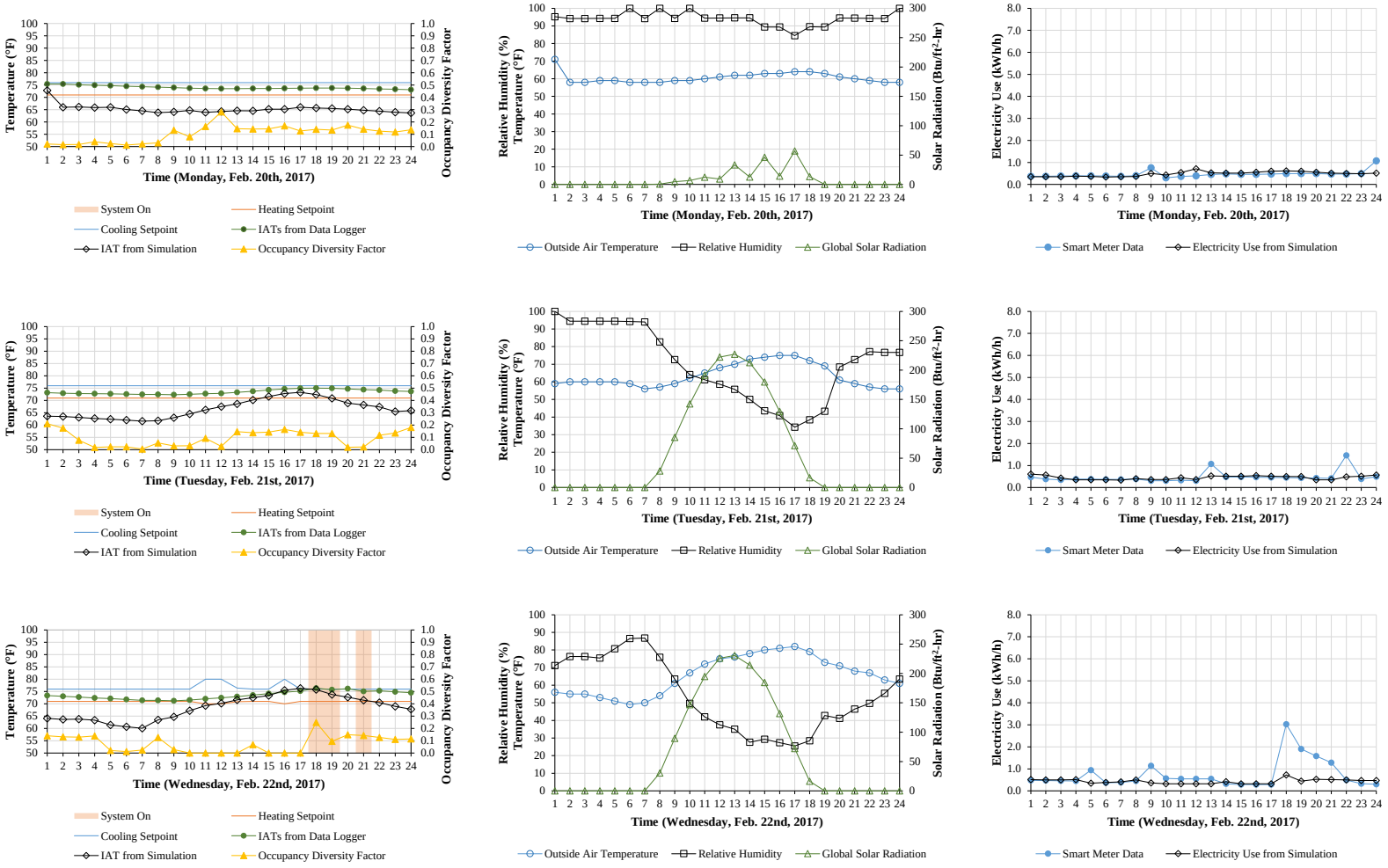

Figure 5-27. Run #3 simulation model results showing IATs, coincident weather data, and electricity use from Monday to Sunday (from February 20th, 2017 to February 26th, 2017).

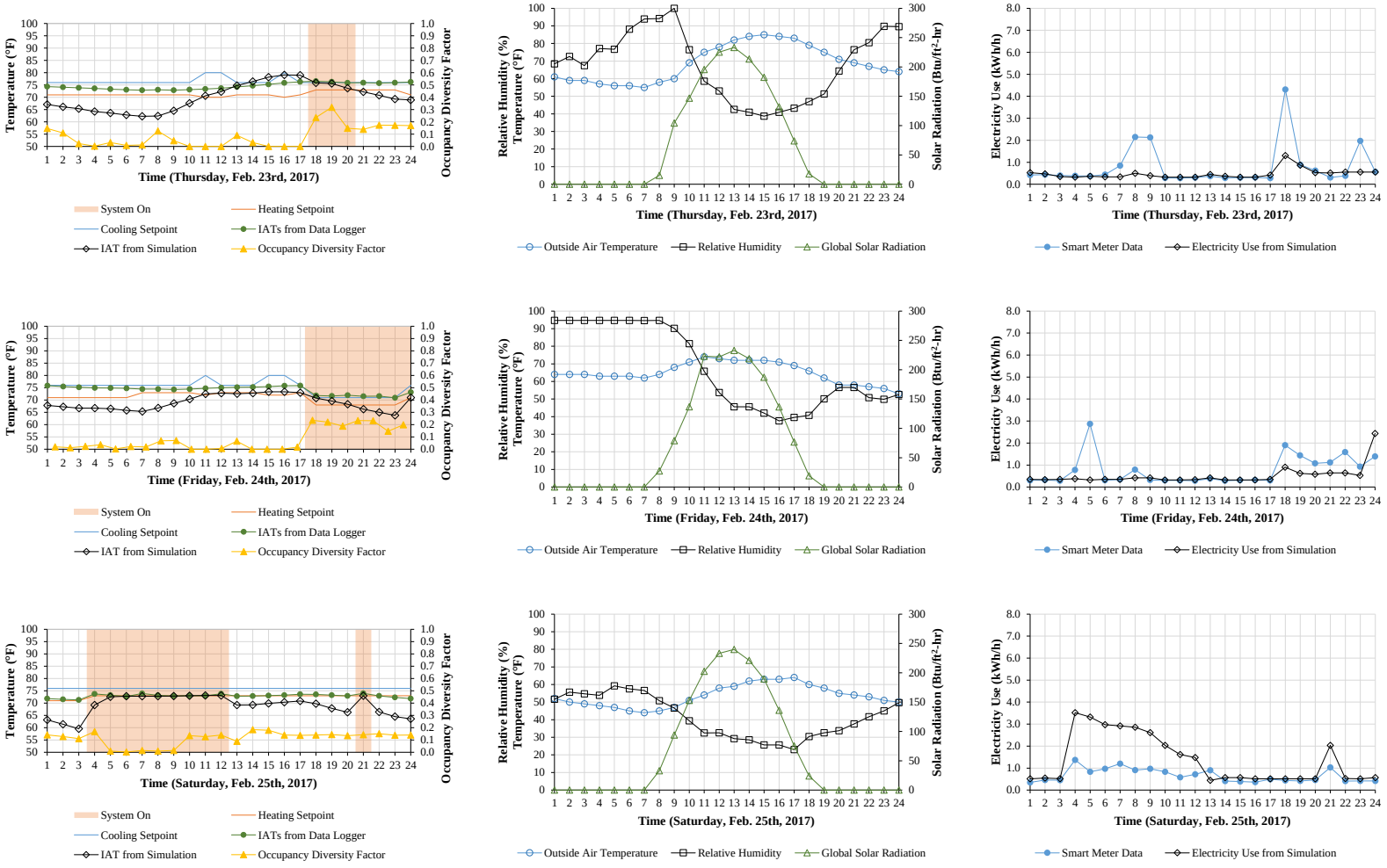

Figure 5-27. Continued.

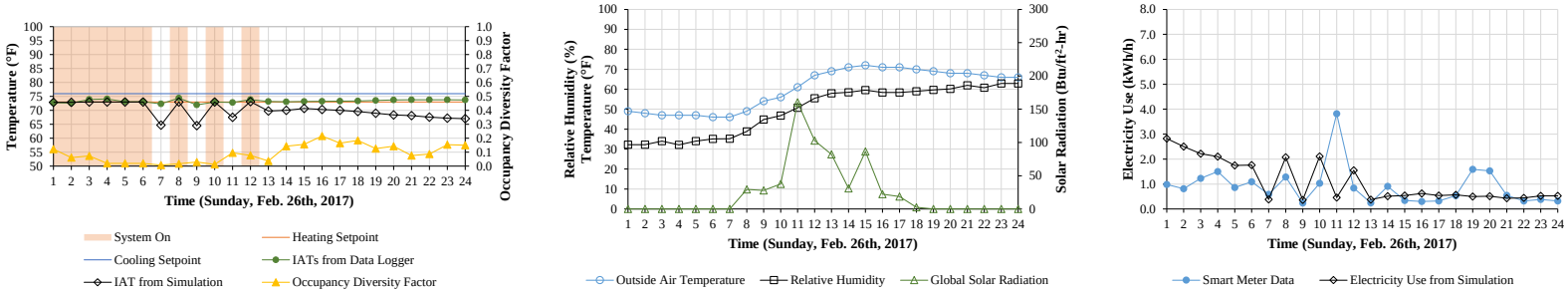

Figure 5-27. Continued.

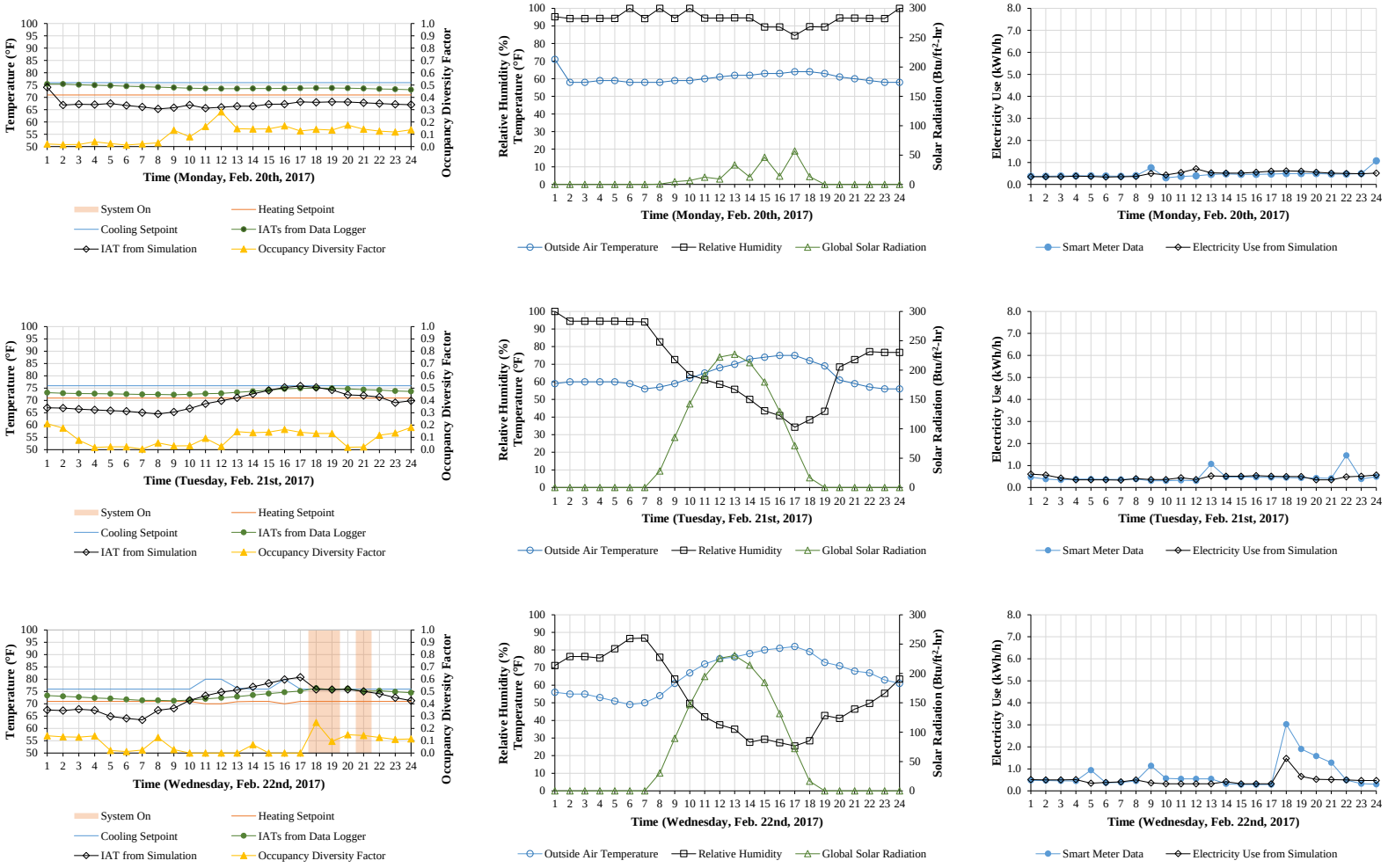

Figure 5-28. Run #4 simulation model results showing IATs, coincident weather data, and electricity use from Monday to Sunday (from February 20th, 2017 to February 26th, 2017).

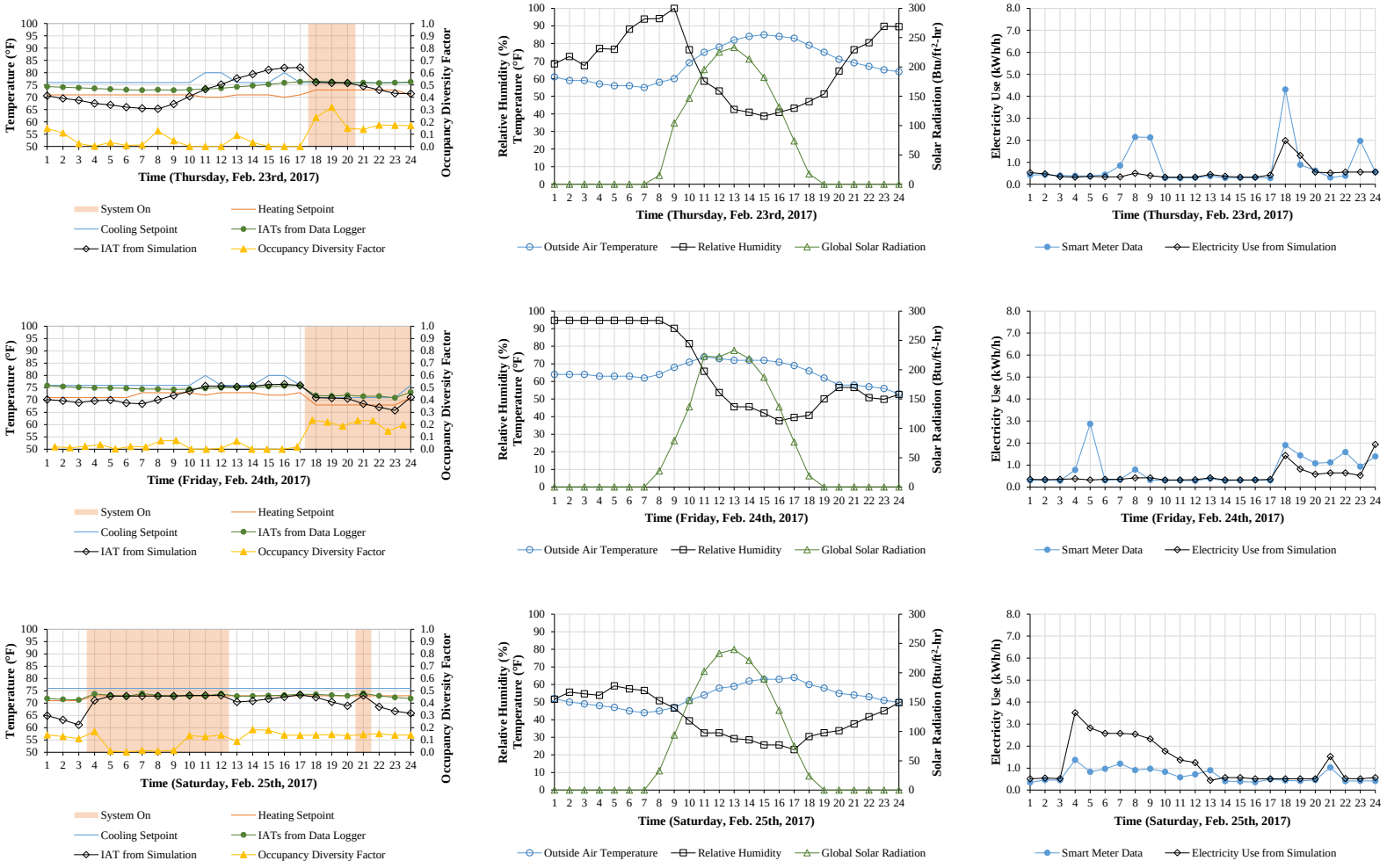

Figure 5-28. Continued.

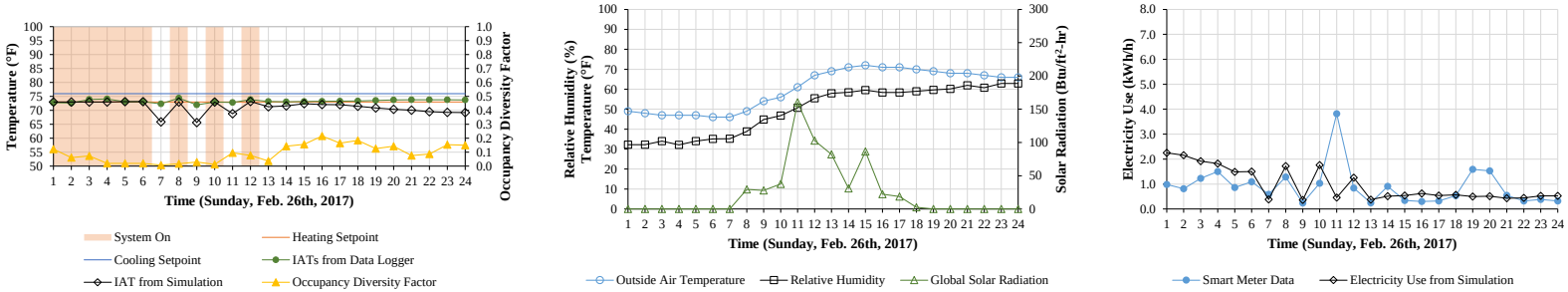

Figure 5-28. Continued.

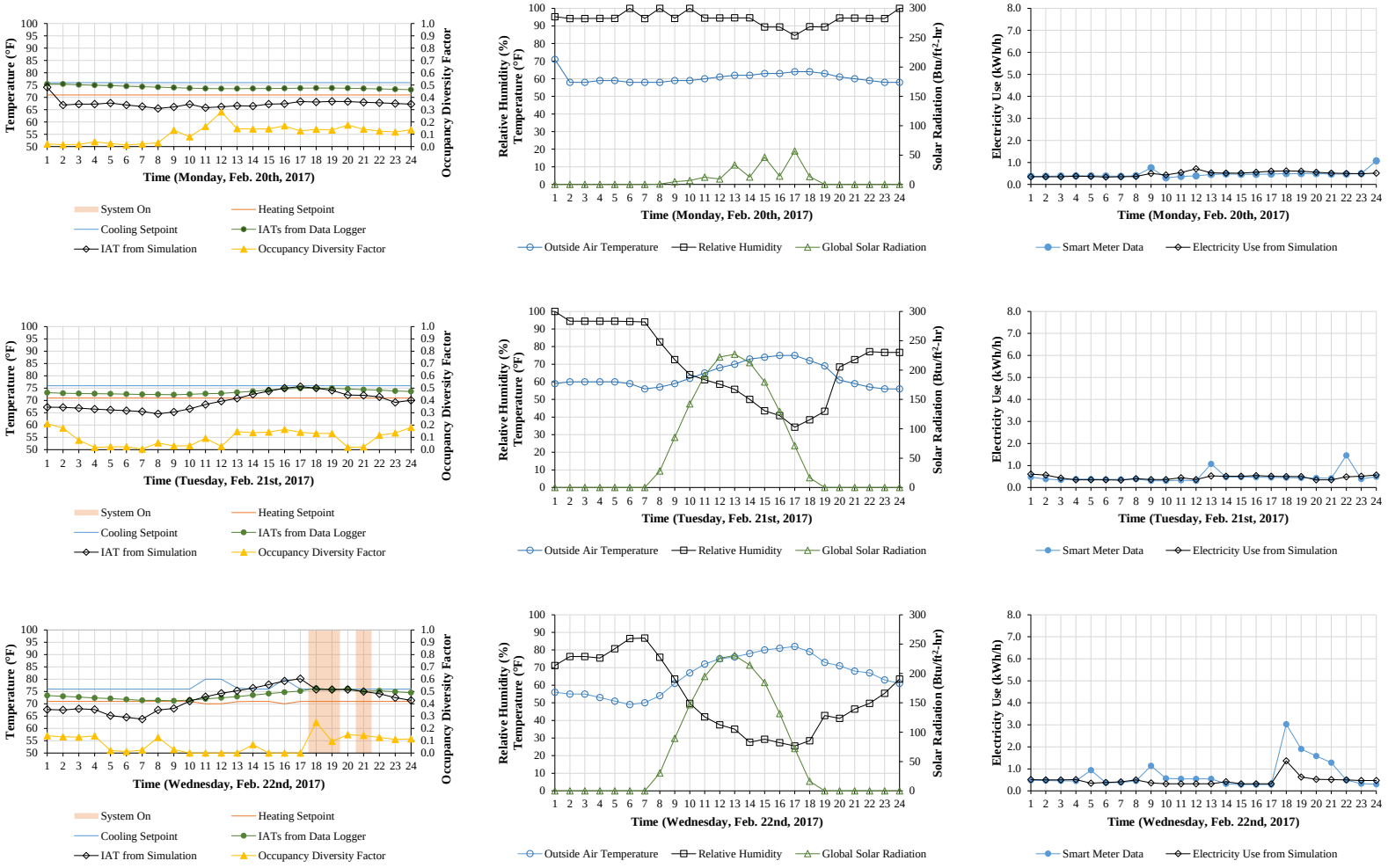

Figure 5-29. Run #5 simulation model results showing IATs, coincident weather data, and electricity use from Monday to Sunday (from February 20th, 2017 to February 26th, 2017).

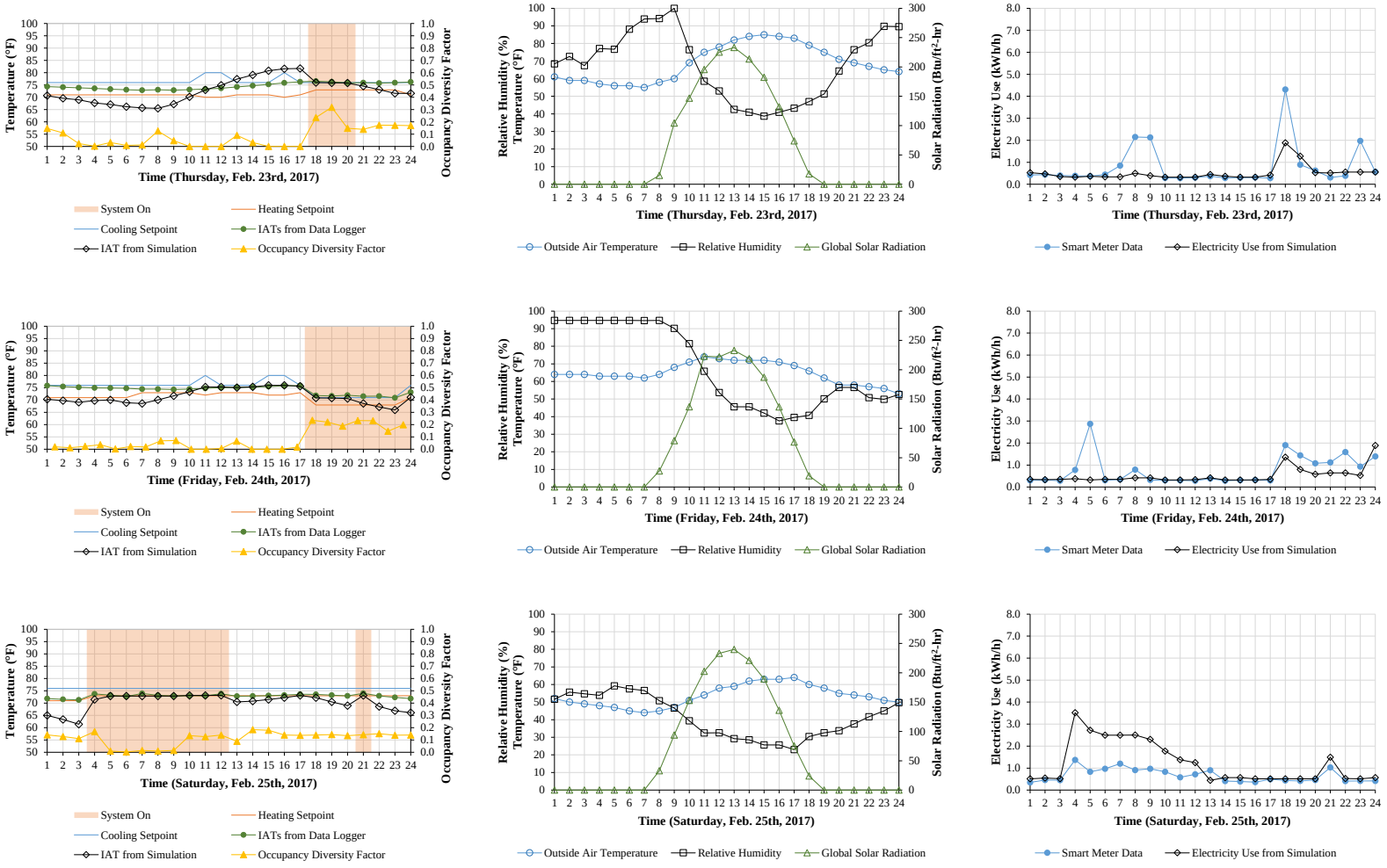

Figure 5-29. Continued.

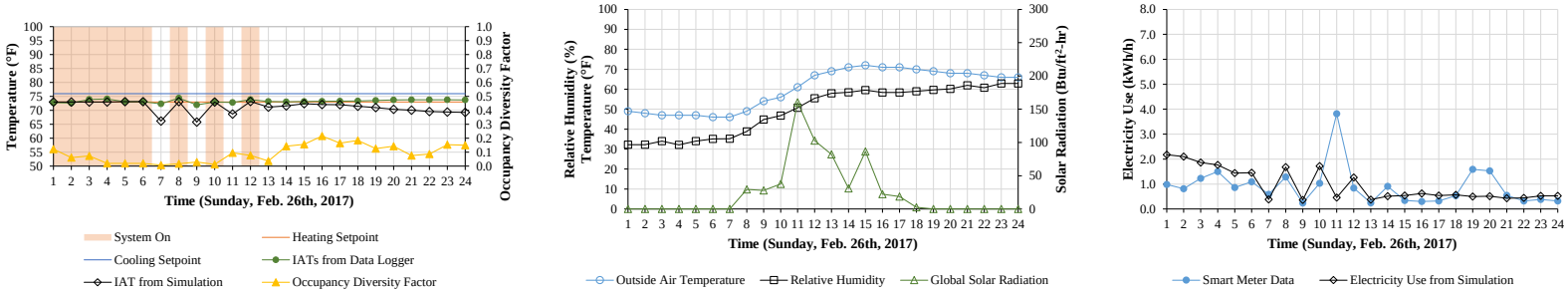

Figure 5-29. Continued.

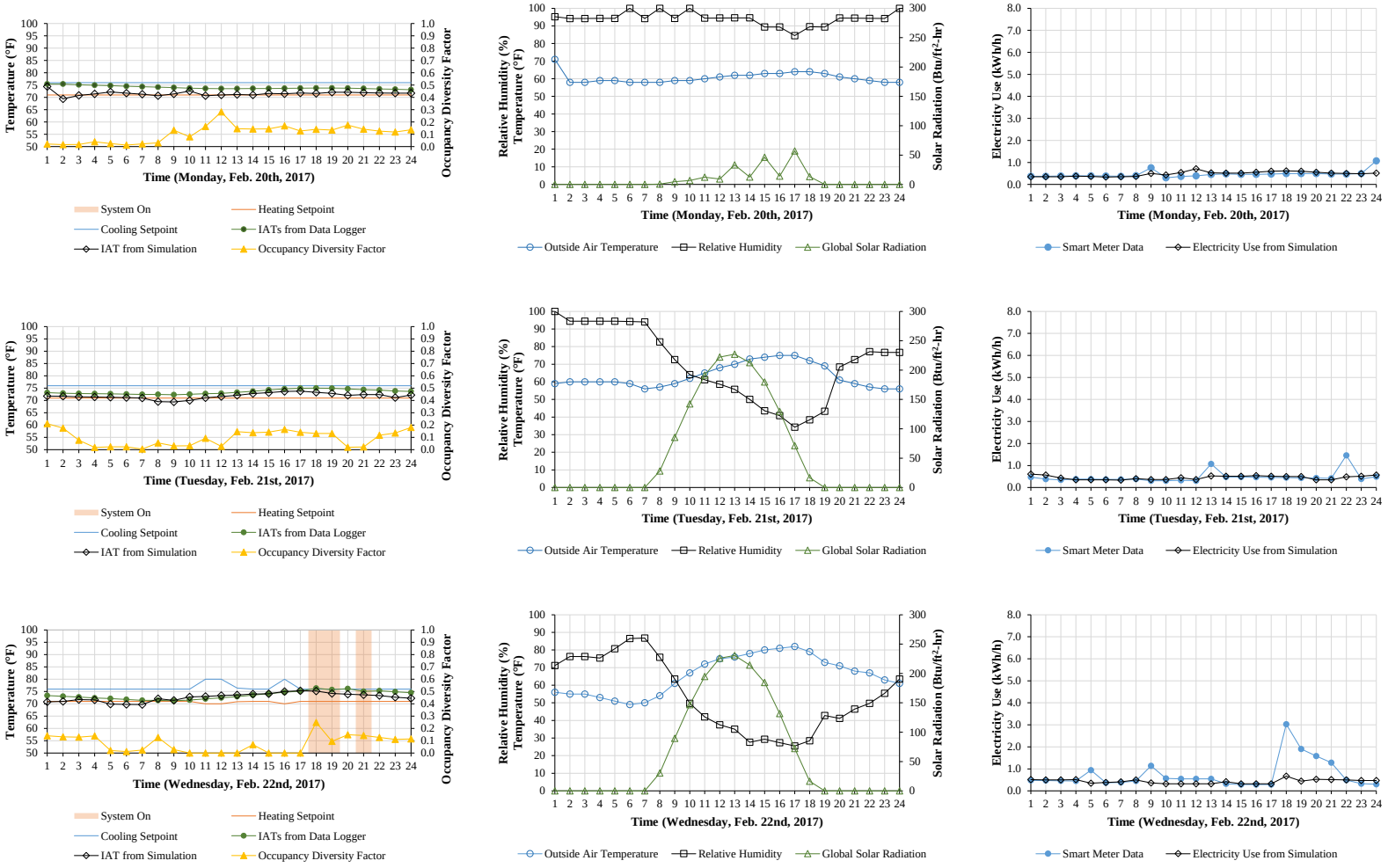

Figure 5-30. Run #6 simulation model results showing IATs, coincident weather data, and electricity use from Monday to Sunday (from February 20th, 2017 to February 26th, 2017).

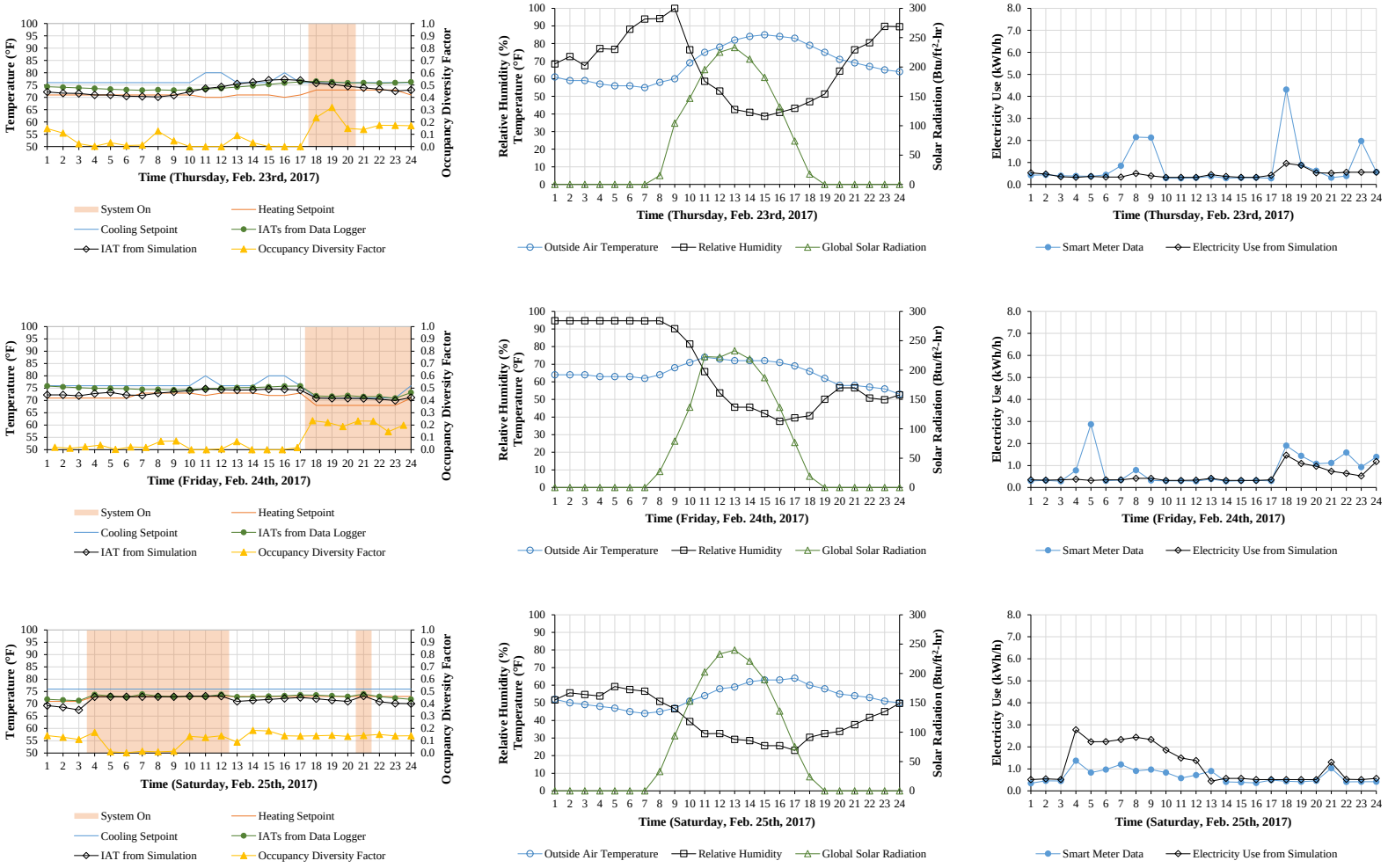

Figure 5-30. Continued.

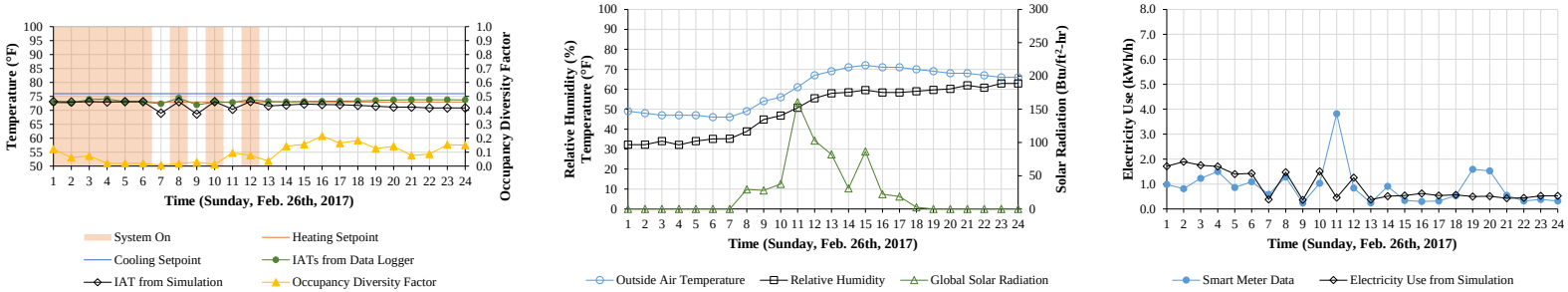

Figure 5-30. Continued.

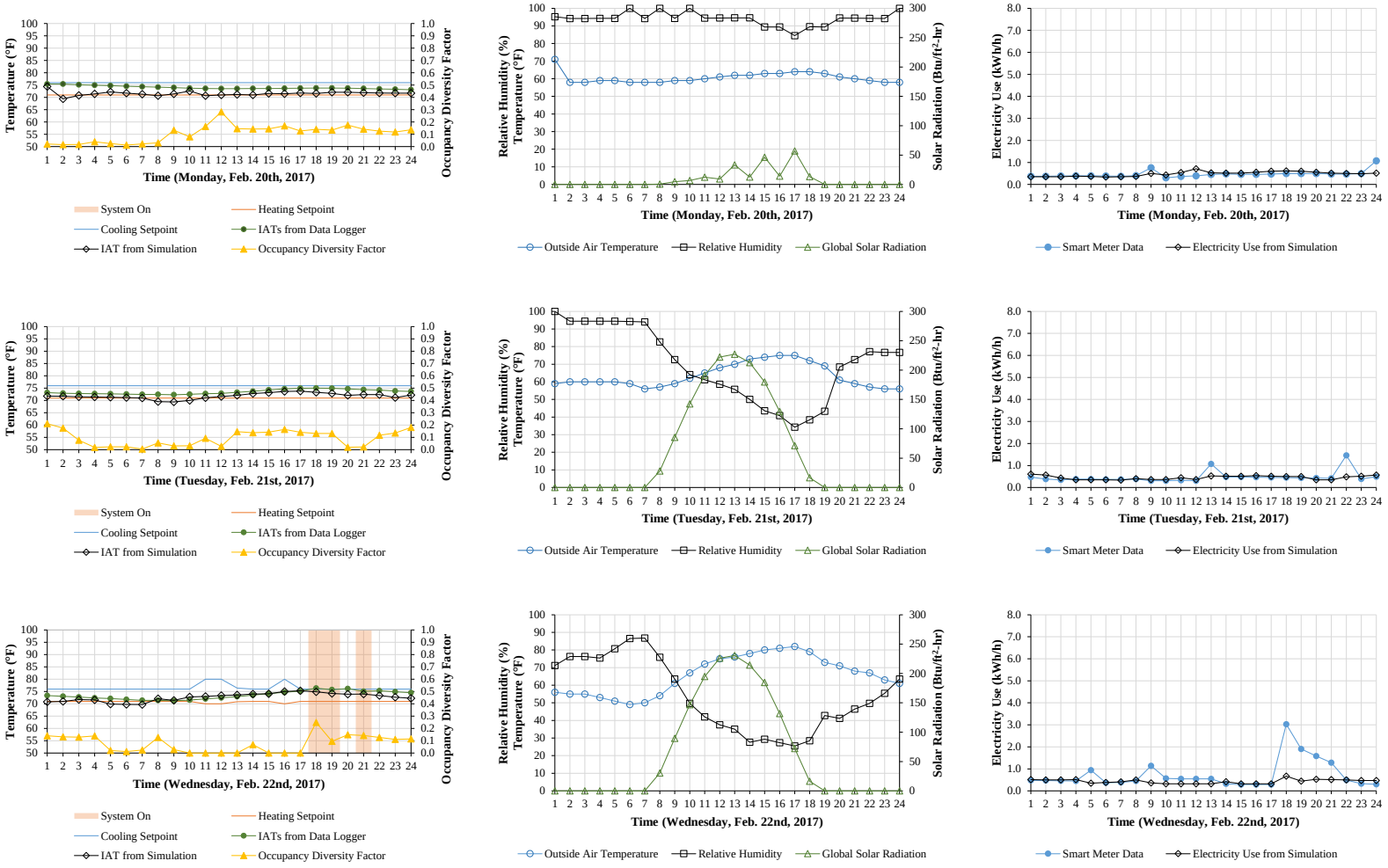

Figure 5-31. Run #7 simulation model results showing IATs, coincident weather data, and electricity use from Monday to Sunday (from February 20th, 2017 to February 26th, 2017).

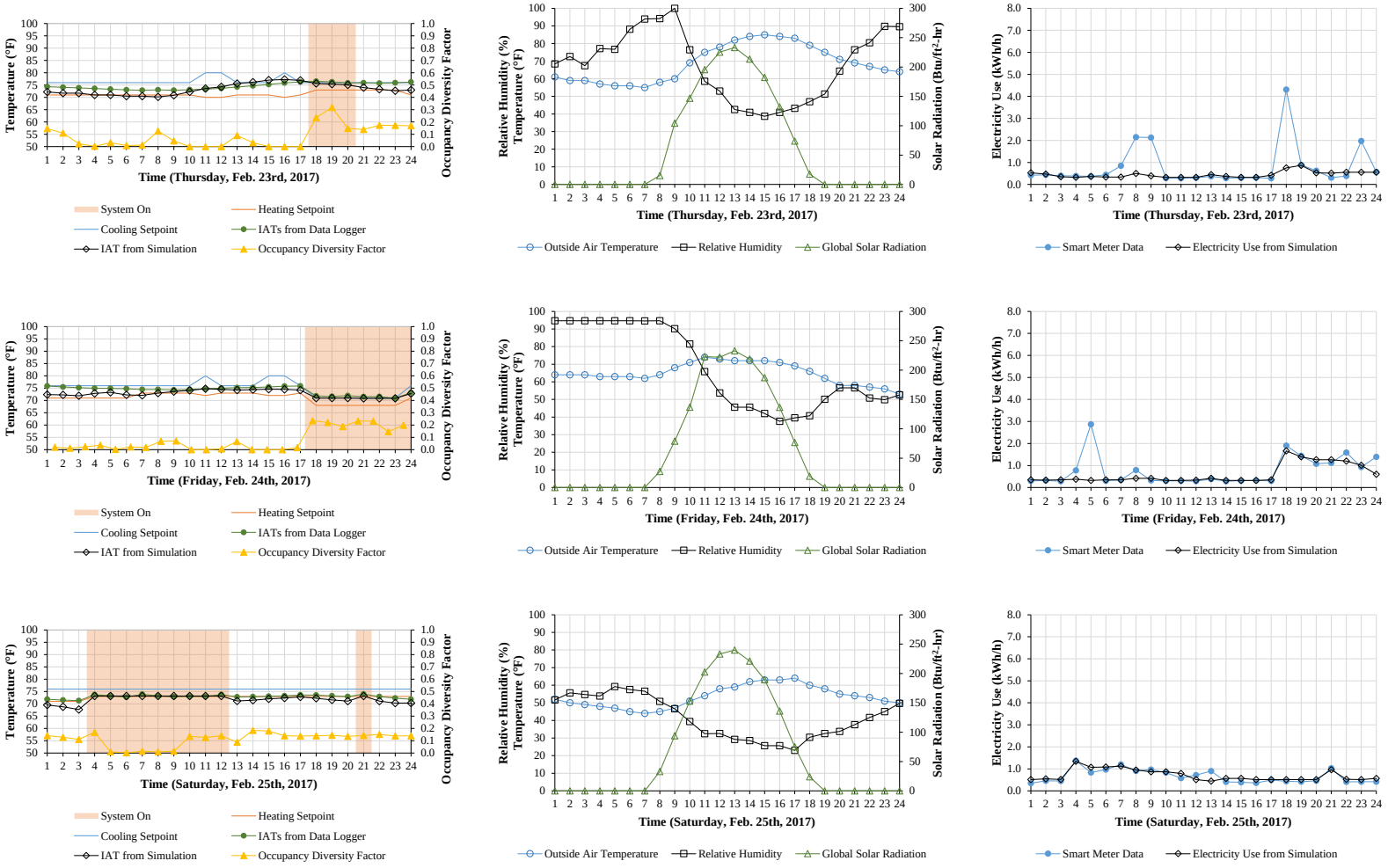

Figure 5-31. Continued.

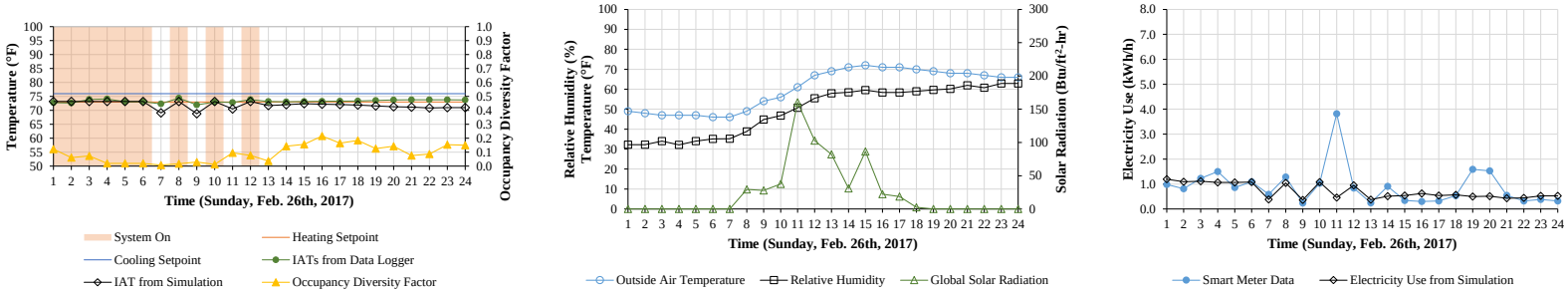

Figure 5-31. Continued.

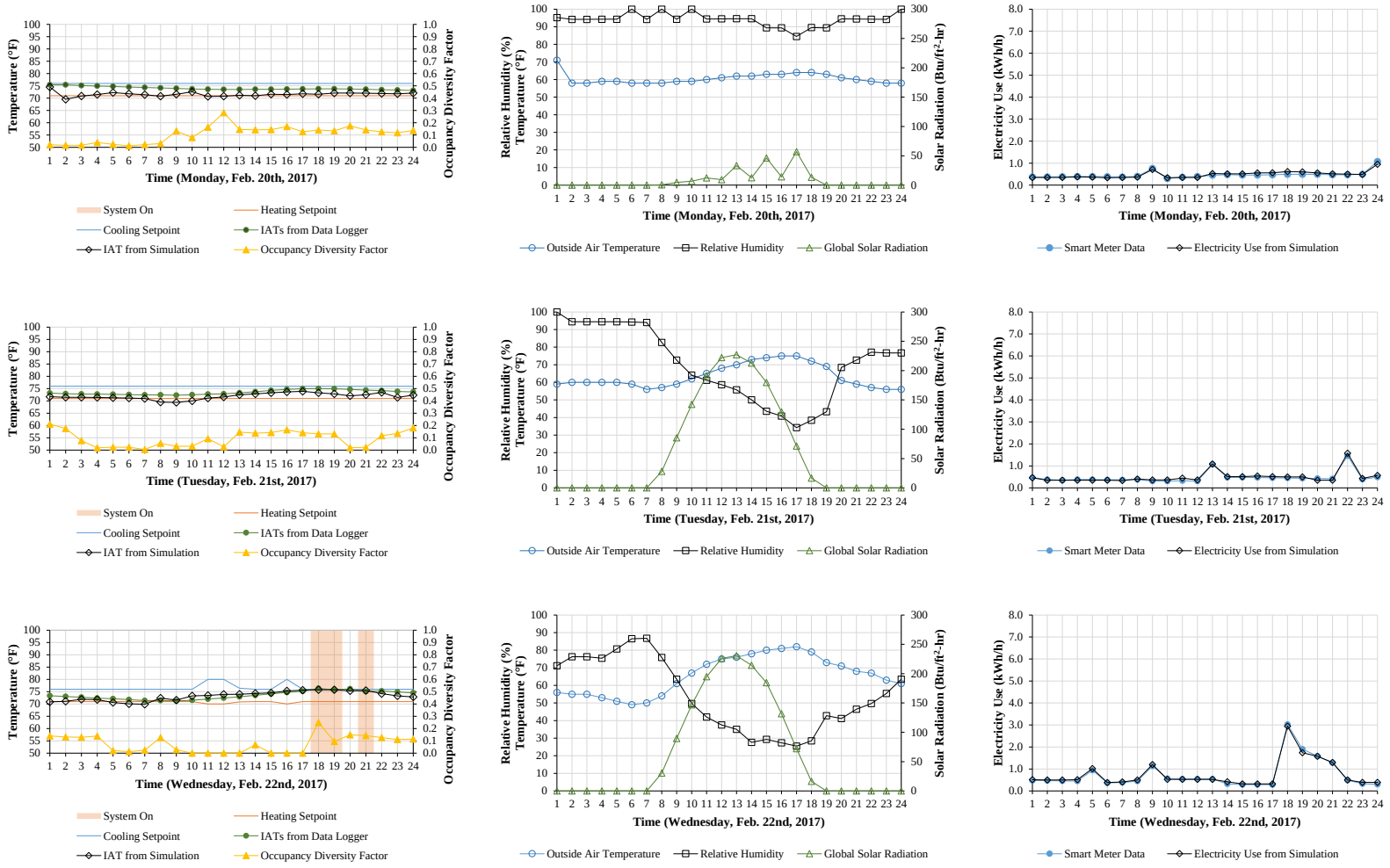

Figure 5-32. Run #8, final simulation model results showing IATs, coincident weather data, and electricity use from Monday to Sunday (from February 20th, 2017 to February 26th, 2017).

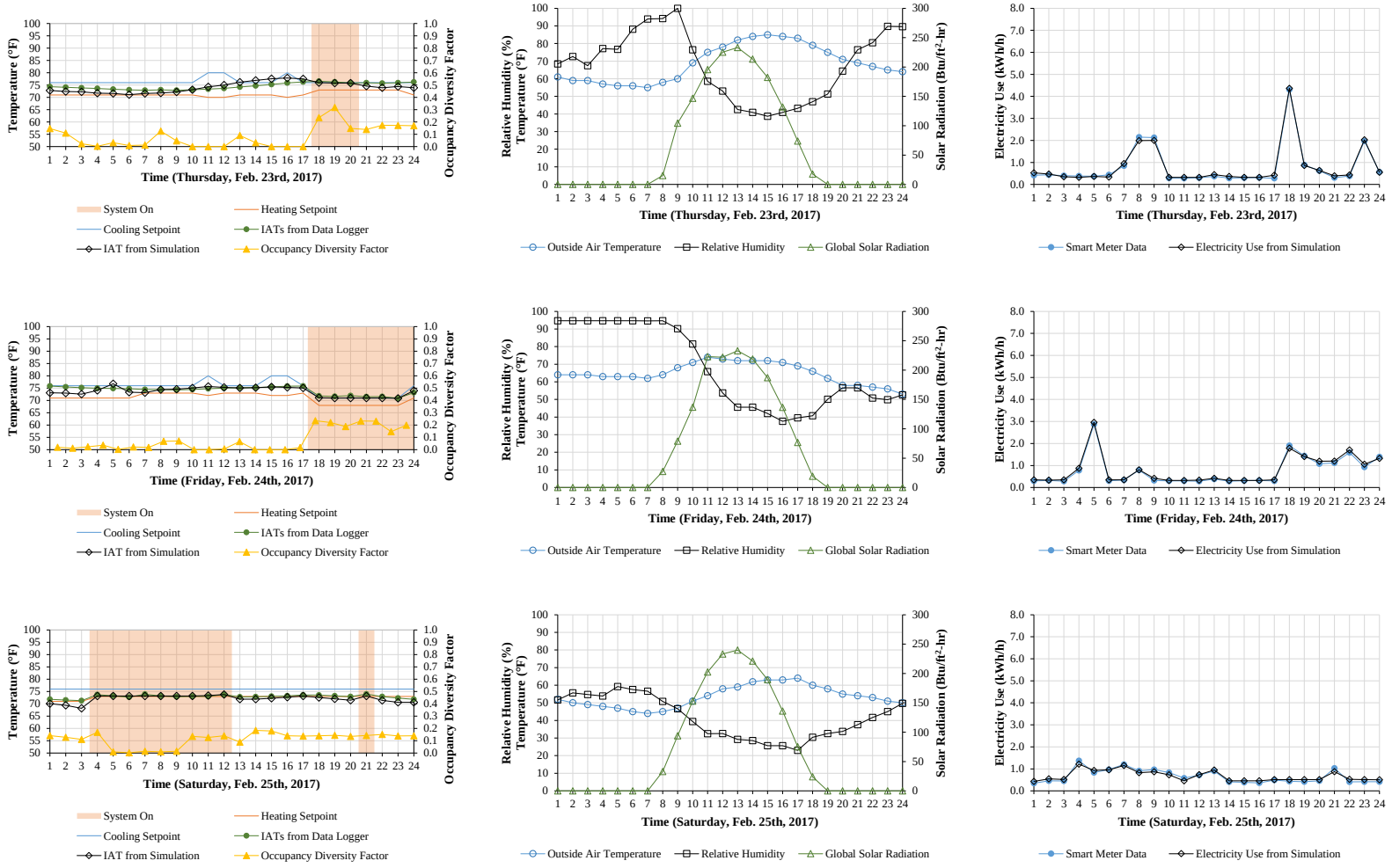

Figure 5-32. Continued.

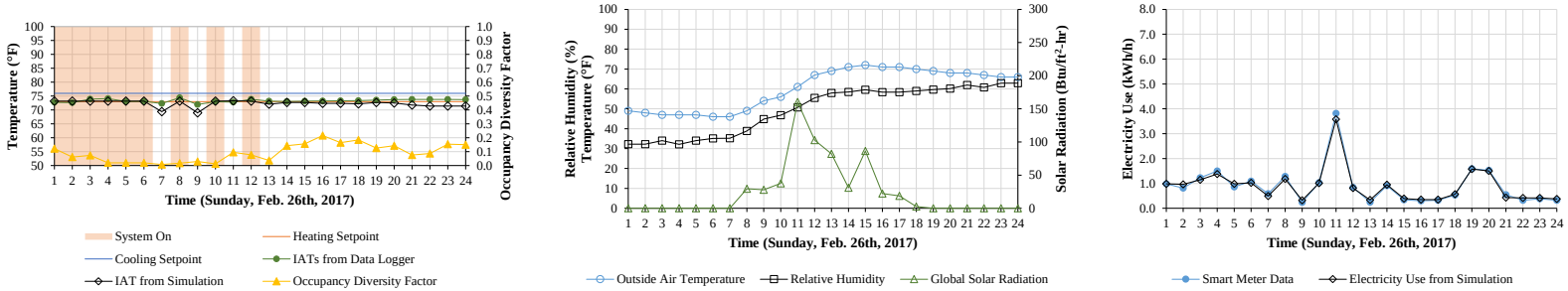

Figure 5-32. Continued.

In order to check the accuracy of the calibrated hourly model for one year from the previous calibration step, monthly average daily electricity use was compared between the measured, baseline hourly electricity use and the simulated hourly electricity use. For the annual simulation, the weather data (i.e., TRY format) of the baseline period from April 15th, 2015 to April 14th, 2016 was used with the case-study house information from Table 4-5. The initial comparison shows an NMBE of -3.0% and a CV-RMSE of 14.3% (see Figure 5-33). Using the sensitivity analysis method with the 5P model coefficients (Kim, 2014), the inputs to the hourly calibrated model were modified by lowering the heating system efficiency from HSPF 6.8 to HSPF 6.0 and changing the lighting and equipment schedules to have less electricity use from March to May and from October to November. The lower heating system efficiency gave the simulated heating electricity use a higher heating slope, and the lower lighting and equipment electricity use lowered the simulated weather-independent electricity use. The final comparison shows an NMBE of -2.4% and a CV-RMSE of 8.9% (see Figure 5-34).

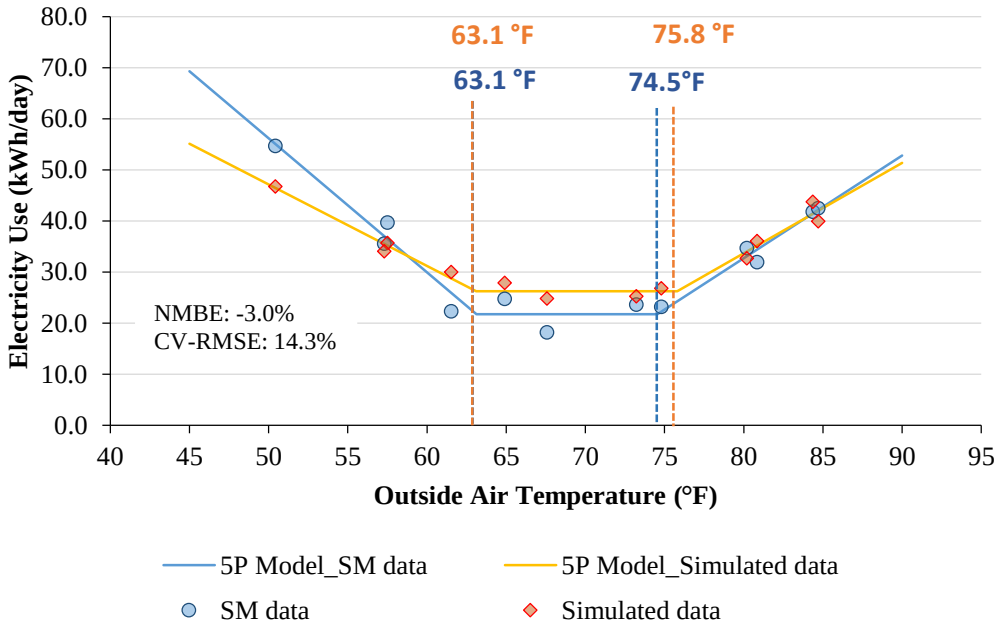

Figure 5-33. Comparison between the baseline electricity use data and the hourly, calibrated simulation model results using the monthly average daily electricity use.

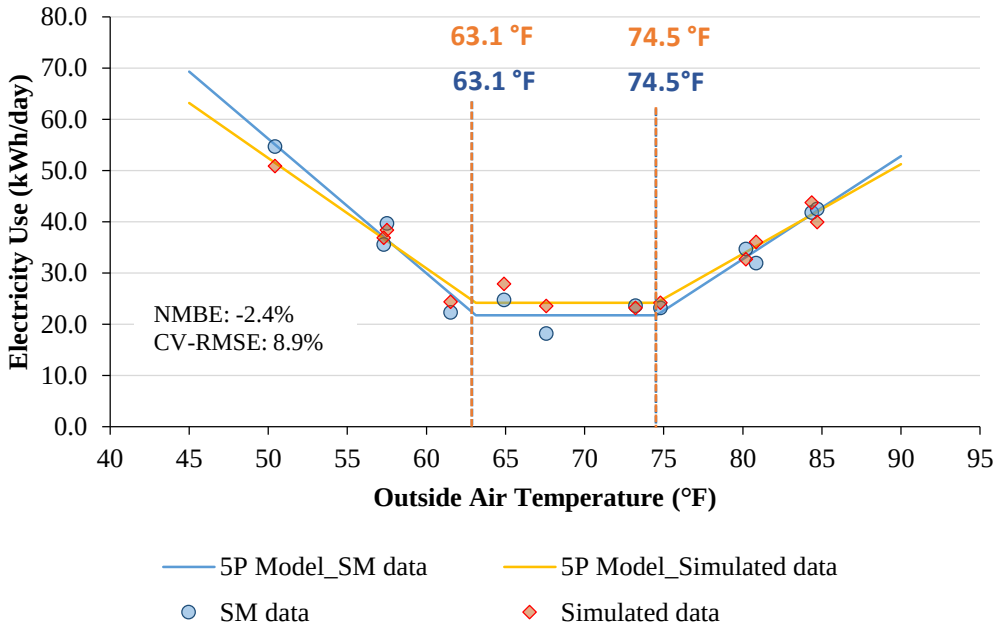

Figure 5-34. Comparison between the baseline electricity use data and the hourly, calibrated simulation model results after the simulation model was calibrated.

Finally, the calibrated simulation model was used to quantify the detailed-potential electricity savings from the use of HADs using the scenarios mentioned in Section 4.2.3.2. The heating balance-point temperature of 63.1 °F and the cooling balance-point temperature of 74.5 °F were used to represent the heating period, the weather-independent period, and the cooling period, respectively. The balance points were obtained from the monthly average daily 5P model of the baseline period (from April 15th, 2015 to April 14th, 2016).

The first scenario investigated a thermostat setback schedule for a whole day. In the analysis, the baseline thermostat setpoints of 74 °F for heating and 75 °F for cooling were used. Next, new setback schedules were simulated by decreasing the heating setpoint from 1 °F to 5 °F and increasing the cooling setpoint from 1 °F to 5 °F. The 1 °F setback schedule shows electricity savings of 7.4%, and the 5 °F setback shows electricity savings of 25.2%. The highest savings of 10.2 kWh/day occurred in May when the 5 °F setback was used. The lowest savings of 1.3 kWh/day occurred in August when the 1 °F setback was used. The monthly average daily outside temperatures for May and August were 74.8 °F and 84.7 °F, respectively. In the cooling period, the highest savings were acheived (see Figure 5-35).

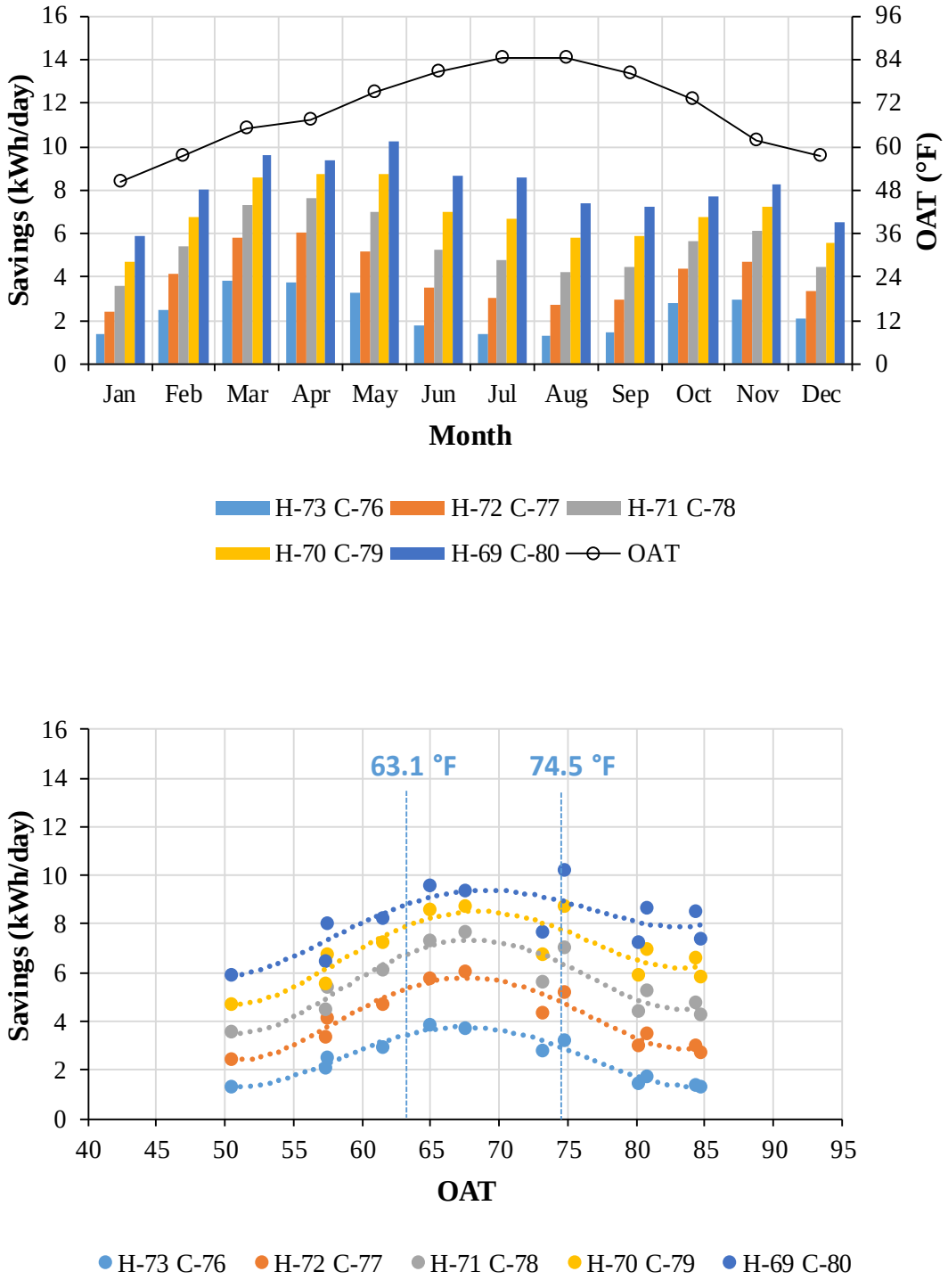

Figure 5-35. Scenario #1: Simulated savings from an all-day thermostat setback schedules.

The second scenario used the thermostat nighttime setback schedules from 11:00 pm to 6:00 am. The new nighttime setback schedules were simulated by changing the heating setpoint from 1 °F to 5 °F and changing the cooling setpoint from 1 °F to 5 °F during the same time period. The results showed the 1 °F nighttime setback schedule had electricity savings of 2.5%, and the 5 °F nighttime setback had electricity savings of 7.7%. The highest savings of 3.6 kWh/day occurred in July when the 5 °F setback was used. The lowest savings of 0.5 kWh/day occurred in January when the 1 °F setback was used. The monthly average daily outside temperatures of July and January were 84.4 °F and 50.4 °F, respectively (see Figure 5-36).

The third scenario used the thermostat setback schedules that utilized occupancy detection. This scenario used typical occupancy schedules when the occupant was not in the case-study house. In this analysis, it was assumed that setback schedules using occupancy detection (i.e., when nobody is inside the house) were operated from 10:00 am to 12:00 pm and from 3:00 pm to 5:00 pm. In this analysis, setback schedules using occupancy detection were simulated by decreasing the heating setpoint from 1 °F to 5 °F and increasing the cooling setpoint from 1 °F to 5 °F during the same time period. The 1 °F setback schedule using occupancy detection showed electricity savings of 1.3%, and the 5 °F nighttime setback showed electricity savings of 4.6%. The highest savings of 2.2 kWh/day occurred in June when 5 °F setback was used. The lowest savings of 0.02 kWh/day occurred in July when 1 °F setback was used. The monthly average daily outside temperatures of June and July were 80.9 °F and 84.3 °F, respectively (see Figure 5-37).

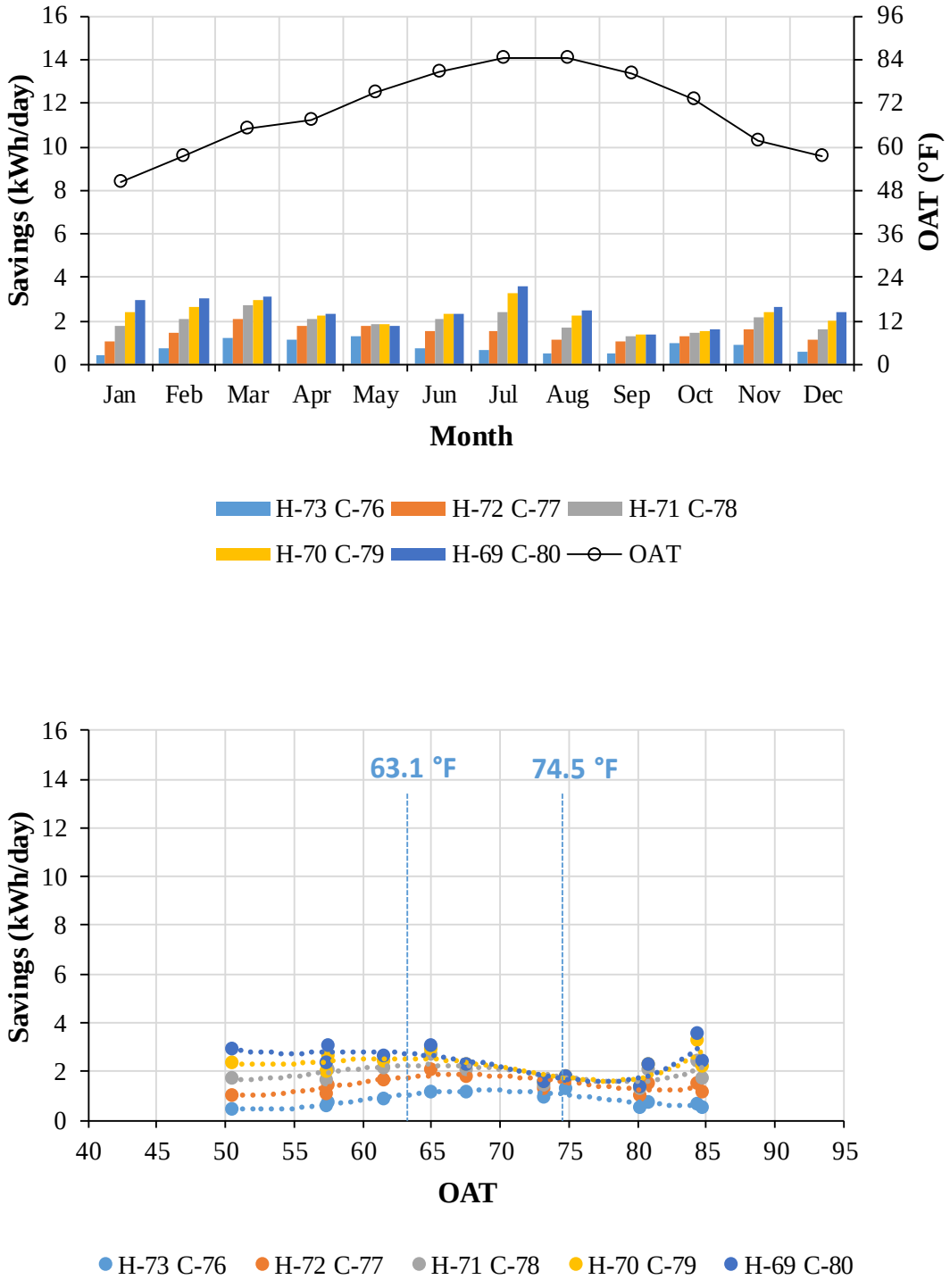

Figure 5-36. Scenario #2: Simulated savings from nighttime thermostat setback schedules from 11:00 pm to 6:00 am.

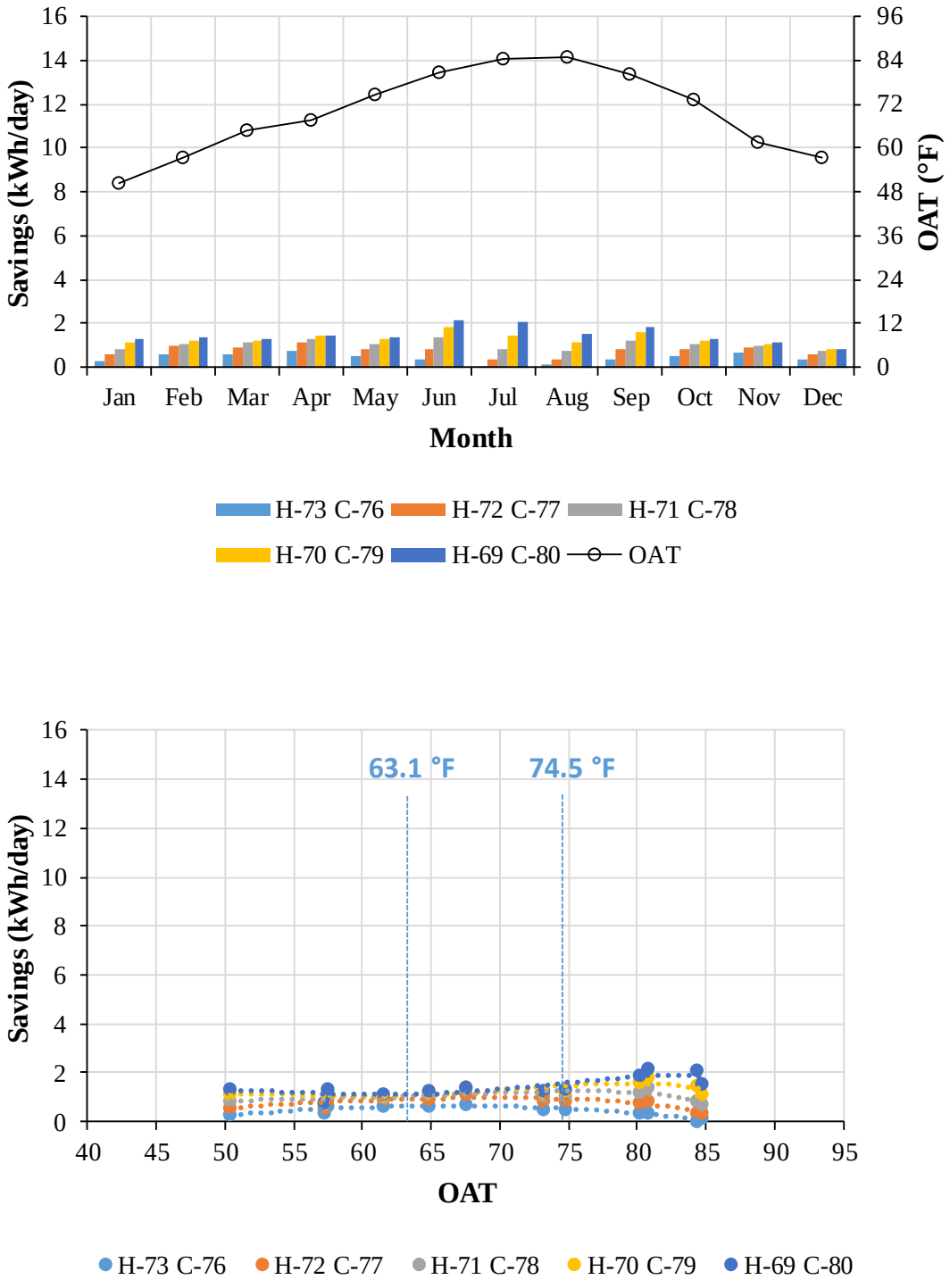

Figure 5-37. Scenario #3: Simulated savings from setback schedules using occupancy detection (i.e., when nobody is inside the house) from 10:00 am to 12:00 pm and from 3:00 pm to 5:00 pm.

The fourth scenario used individual thermostatic multi-zone control for each room in the case-study house using occupancy detection. This scenario used the setback schedules with occupancy detection data (i.e., hourly diversity factors) from one week of measurements (February 20th, 2017 to February 26th, 2017). When the occupant was not in some of the zones, individual thermostat setback schedules were applied for each zone. In order to simulate multi-zone controls, a seven zone, Package Terminal Air Conditioner (PTAC) system was chosen for the DOE-2.1E model instead of the existing single zone Residential System (RESYS), which was used for the single zone model for calibration. The monthly average daily electricity use between the models with the seven zones (PTAC) and the single zone (RESYS) showed an NMBE of -0.1% and a CV-RMSE of 5.6%, which showed good agreement. New setback schedules for each zone control that used the occupancy detection were then simulated by decreasing the heating setpoint from 1 °F to 5 °F and increasing the cooling setpoint from 1 °F to 5 °F when the occupant was not in some of the zones, based on the occupancy detection data. The 1 °F setback schedule showed electricity savings of 7.3%, and the 5 °F setback showed electricity savings of 14.4%. The highest savings of 7.9 kWh/day occurred in July when the 5 °F setback was used. The lowest savings of 0.8 kWh/day occurred in January when the 1 °F setback was used. The monthly average daily outside temperatures of July and January were 84.4 °F and 50.4 °F, respectively (see Figure 5-38).

The fifth scenario modified the lighting schedules to use occupancy detection. This scenario used the one week occupancy detection data (i.e., hourly diversity factors) when the occupant was not in some zones of the case-study house. New lighting

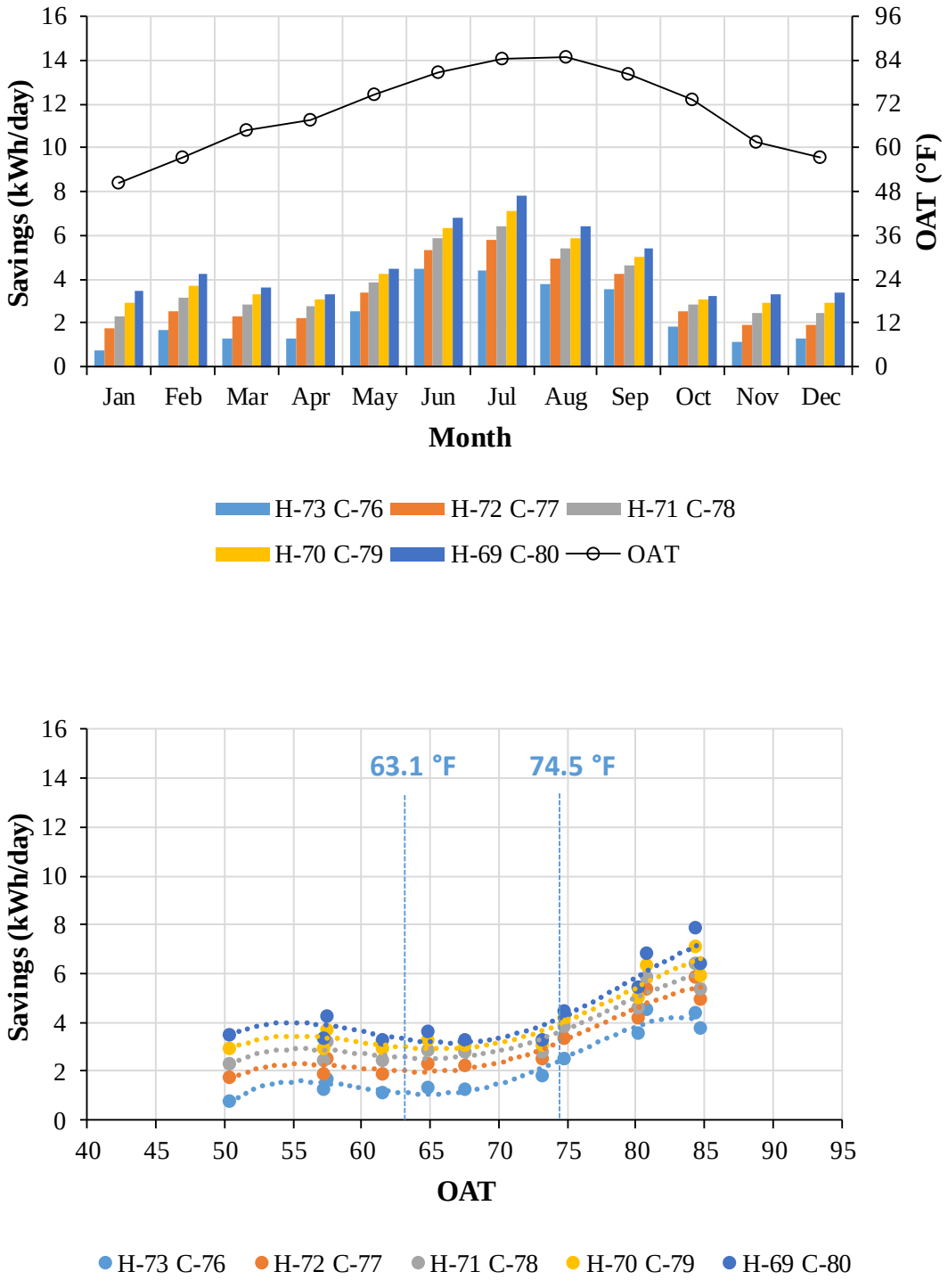

Figure 5-38. Scenario #4: Simulated savings from individual thermostatic multi-zone control using occupancy detection.

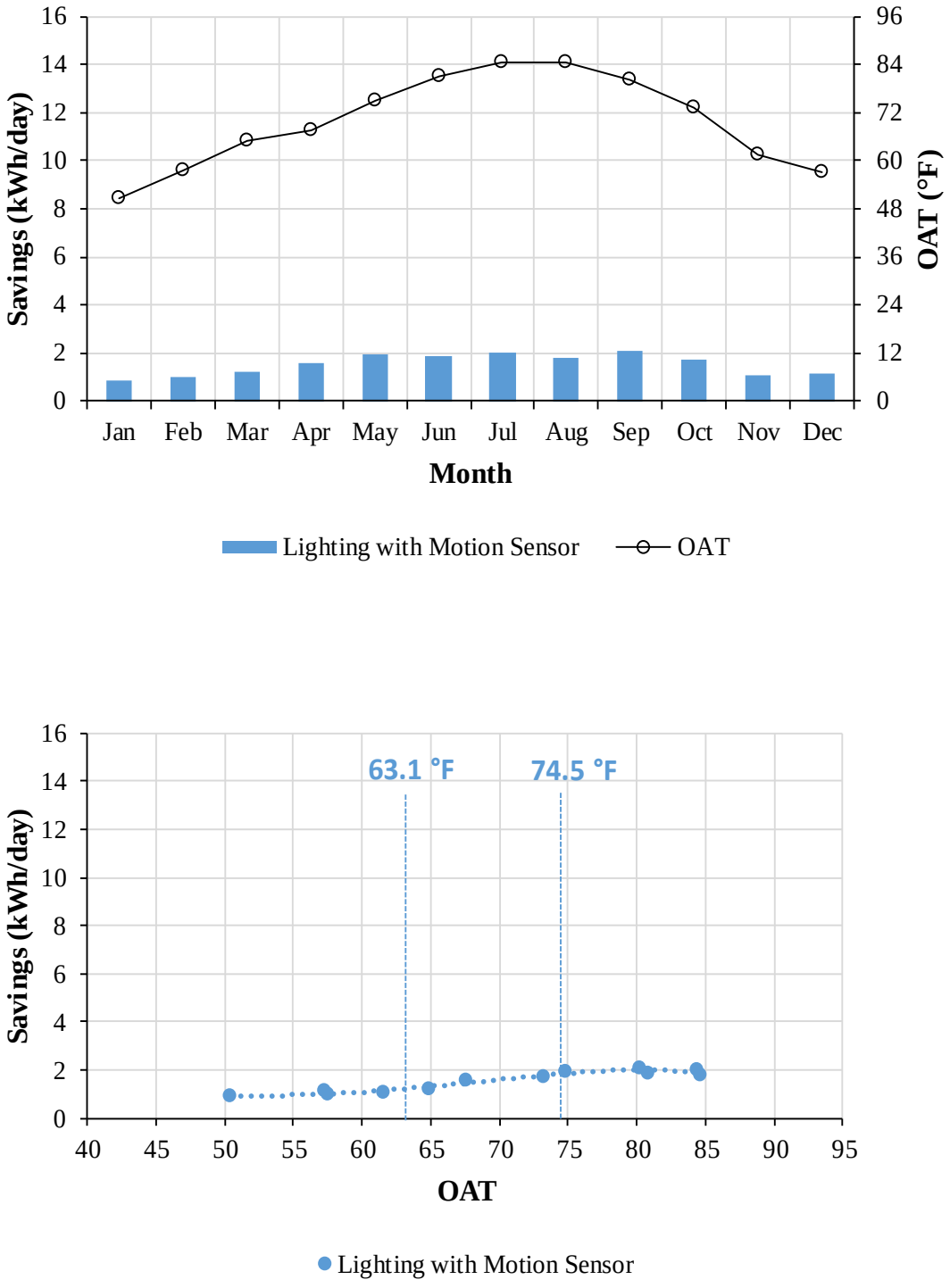

Figure 5-39. Scenario #5: Simulated savings from lighting schedule with occupancy detection.

schedules using occupancy detection were simulated for the baseline year. The lighting schedules using occupancy detection showed an annual electricity savings of 4.7%. The highest savings of 2.1 kWh/day occurred in September, and the lowest savings of 0.9 kWh/day occurred in January. The monthly average daily outside temperatures of September and January were 80.2 °F and 50.4 °F, respectively (see Figure 5-39). The higher electricity savings was achieved when the OAT was warmer. Table 5-6 summarizes the detailed-potential annual savings from the final, hourly calibrated simulation model using the scenarios. The highest electricity savings was achieved when the 5 °F setback was used for a whole day (i.e., Scenario #1). The lowest electricity savings was achieved when the 1 °F setback was used for the time periods when the occupant was not at home (Scenario #3).

Table 5-6. Summary of detailed, potential annual savings from Level I Analysis.

Component	**Scenario 1** **Savings (kWh/%) from thermostat setback schedule**	**Scenario 2** **Savings (kWh/%) from thermostat nighttime setback schedule**	**Scenario 3** **Savings (kWh/%) from thermostat setback schedule using occupancy detection**	**Scenario 4** **Savings (kWh/%) from HVAC system multi-zone control using occupancy detection**	**Scenario 5** **Savings (kWh/%) from lighting schedule using occupancy detection**
Figure #	5-35	5-36	5-37	5-38	5-39
1 ℉ setback	866.6 kWh/ 7.4%	298.1 kWh/ 2.5%	157.9 kWh/ 1.3%	853.5 kWh/ 7.3%	-
2 ℉ setback	1466.9 kWh/ 12.5%	531.1 kWh/ 4.5%	276.7 kWh/ 2.4%	1182.7 kWh/ 10.1%	-
3 ℉ setback	2004.8 kWh/ 17.1%	710.5 kWh/ 6.1%	378.1 kWh/ 3.2%	1372.3 kWh/ 11.7%	-
4 ℉ setback	2503.6 kWh/ 21.3%	829.8 kWh/ 7.1%	468.4 kWh/ 4.0%	1539.6 kWh/ 13.1%	-
5 ℉ setback	2961.7 kWh/ 25.2%	899.9 kWh/ 7.7%	534.0 kWh/ 4.6%	1693.5 kWh/ 14.4%	-
Lighting schedule with occupancy detection	-	-	-	-	553.3 kWh/ 4.7%

5.3. Results of the Application of the M&V Method (Level II Analysis)

This section summarizes the results of the application of Level II Analysis. In this analysis, the IATs during the pre-retrofit and post-retrofit periods were analyzed to check the indoor environment of the case-study house. After that, weather-normalized savings for 50 days from February 10th to March 31st (i.e., the post-retrofit period) were calculated by comparing the hourly electricity use data during the post-retrofit period with the electricity use predicted by the 5P models from the baseline period (i.e., the pre-retrofit period from April 15th, 2015 to April 14th, 2016). In addition, extended savings for one year were calculated by comparing the electricity use predicted by the 5P models for the baseline period with the electricity use predicted by the models for the post-retrofit period. In the analysis, the OATs of the baseline period were used to calculate the extended, annual savings. In addition, average, hourly occupancy diversity factors from all zones (i.e., seven zones) in the case-study house were used to categorize the occupied hours and unoccupied hours. These diversity factors were calculated from the 1-minute interval data collected from the seven occupancy data loggers at the case-study house.

5.3.1. Observations from the IATs during the Pre-Retrofit and Post-Retrofit Periods

The IATs of the case-study house were measured during a nine month period (from August 1st, 2016 to January 31st, 2017) to check the indoor environment in each zone of the case-study house for the pre-retrofit period. Figure 5-40 and Figure 5-41 show the IATs using a 5 °F binned, quartile analysis. In these figures, one plot from the

temperature data logger is shown for each of the seven zones (see Figures 4-26 and 4-27) as well as the location of the thermostat (i.e., return air path). In each plot, the statistically determined, balance-point (change-point) temperatures are shown from the 5P change-point linear regression models of the baseline period (i.e., pre-retrofit period). In addition, the heating and cooling setpoints during the baseline period are shown in the plots.

Figure 5-40 shows the IATs of each zone during the weekdays. The heating balance-point temperature of 60.2 °F and the cooling balance-point temperature of 76.6 °F were used to represent the heating period, the weather-independent period, and the cooling period, respectively. The balance points were obtained from the weekday 5P model of the baseline period (from April 15th, 2015 to April 14th, 2016). During the period, the heating setpoint of 74.0 °F and the cooling setpoint of 75.0 °F were used. It was observed that Data Logger #2 located in Zone #2 (dining room) had large variations over the OATs, especially during the heating period. This was because the dining room had large windows facing west. It was also observed that Data Loggers #4 (bathroom), #5 (1/2 bathroom), #7 (bedroom #2), and #8 (living room) had higher IATs than the heating setpoint during the heating period and the weather-independent period. This was most likely caused by the internal heat gains from the nearby hot water use and the occupant's equipment use. During the weekdays, both the maximum (81.7 °F) and the minimum (63.9 °F) IATs out of all the data loggers were recorded at Data Logger #2 (dining room), which was due to the large, west-facing windows.

Figure 5-41 shows the IATs of each zone during weekends/holidays. In a similar fashion as the weekdays, the heating balance-point temperature of 63.7 °F and the cooling balance-point temperature of 74.1 °F were used to represent the heating period, the weather-independent period, and the cooling period. The balance-point temperatures were obtained from the weekend/holiday 5P model of the baseline period (from April 15th, 2015 to April 14th, 2016). During the weekends/holidays, the maximum (82.5 °F) IAT was recorded at Data Logger #3 (kitchen) when the OAT was inside the 70-75 °F bin. The minimum (65.8 °F) was recorded at Data Logger #2 (dining room) when the OAT was inside the 20-25 °F bin.

In addition, using the 5 °F binned quartile analysis, the BWM plots of the weekends/holidays (see Figure 5-41) shows wider IQRs compare to the BWM plots of the weekdays (see Figure 5-40). Thus, it was expected that the thermostat setpoints during the weekends/holidays was more unpredictable. In other words, more frequently, the thermostat setpoints were changed, or the heating or cooling system was turned off during the weekends/holidays than similar periods during the weekdays.

It was also observed that the IATs from the seven zones (i.e., Data Loggers #2 through #8) were significantly different from the heating and cooling setpoints, except the IATs from Data Logger #1 installed near the HVAC thermostat (i.e., return air path). It should be noted that the building energy simulation programs such as DOE-2.1E, eQEUST, and EnergyPlus should consider average IATs (i.e., well mixed, average zone temperatures) from each zone, rather than constant, desired IATs for the thermostat.

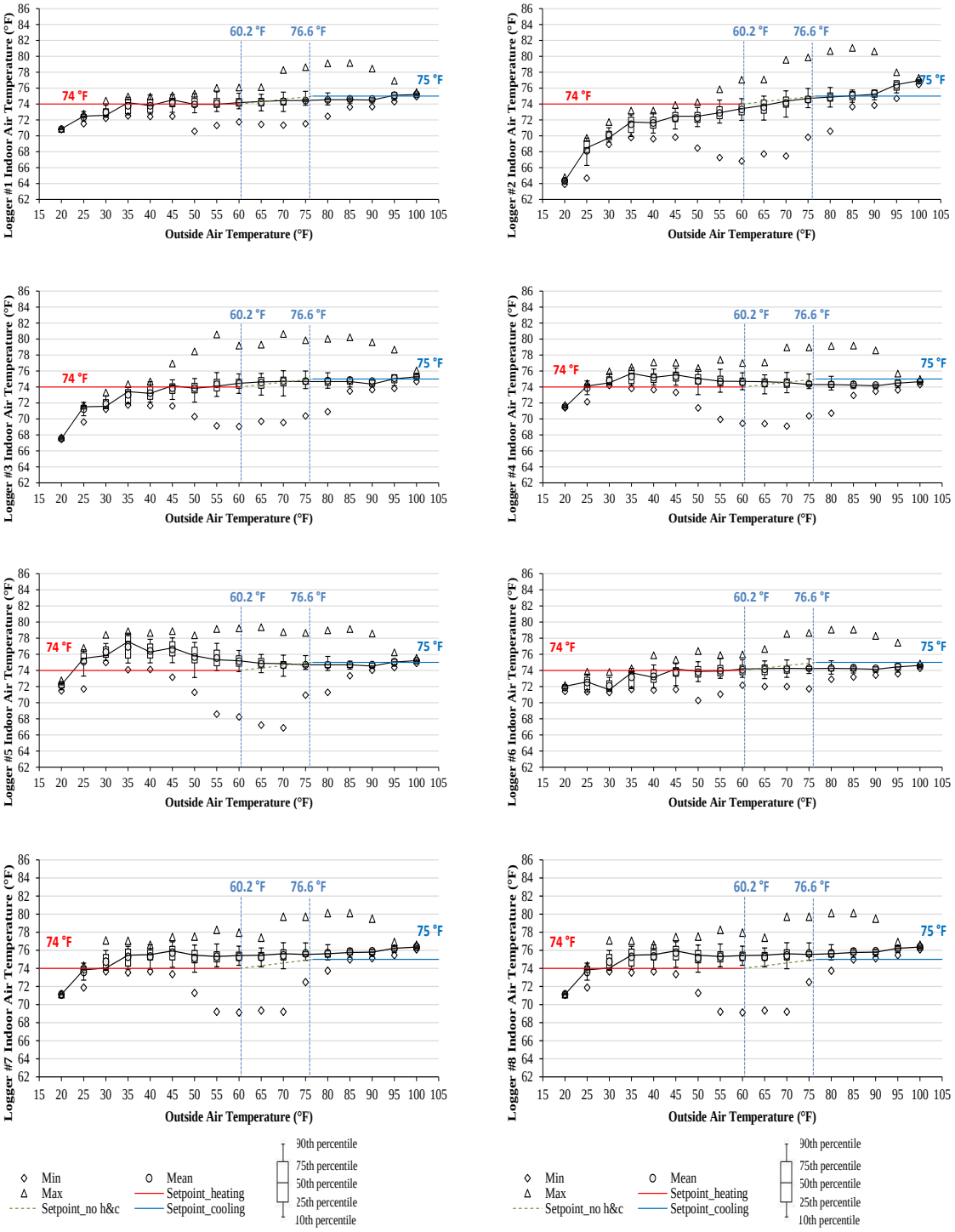

Figure 5-40. IATs versus OATs from the eight data loggers installed in the case-study residence during the pre-retrofit period for weekdays (August 1st, 2016 to January 31st, 2017).

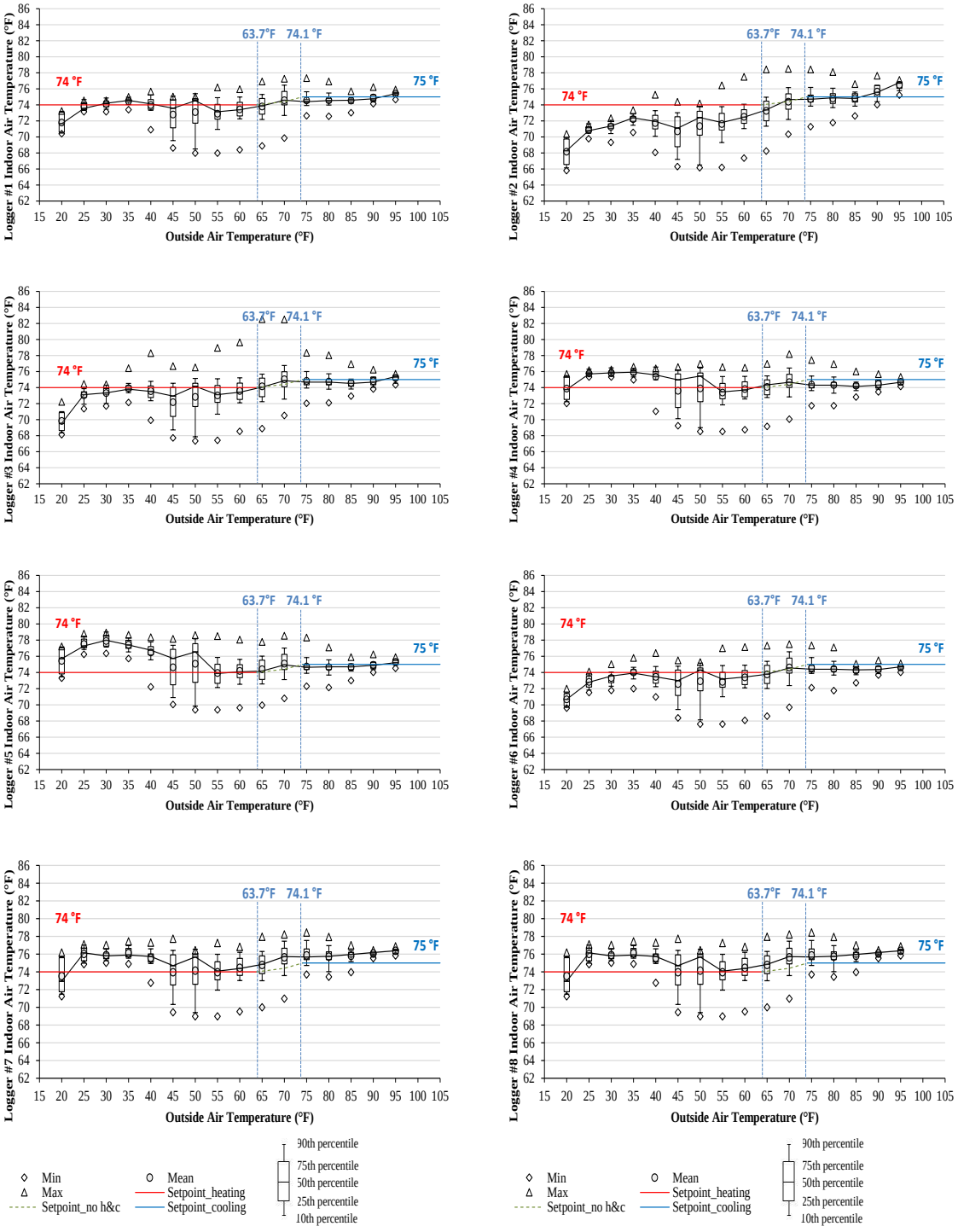

Figure 5-41. IATs versus OATs from the eight data loggers installed in the case-study residence during the pre-retrofit period for weekends/holidays (August 1st, 2016 to January 31st, 2017).

Figure 5-42 and Figure 5-43 show the measured IATs during the post-retrofit period (from February 10th, 2017 to March 31th, 2017) for weekdays and weekends/holidays, respectively. The two figures show the superimposed 50th percentile from the pre-retrofit period. The difference in the 50th percentiles between the pre-retrofit and the post-retrofit periods show that the IATs of the post-retrofit period were lower during the heating period and higher during the cooling period compared to the IATs of the pre- retrofit period. The trend implies the new thermostat schedule had lower heating setpoints and higher cooling setpoints compared to the previous thermostat schedule, which should contribute to electricity saving opportunities for heating and cooling systems.

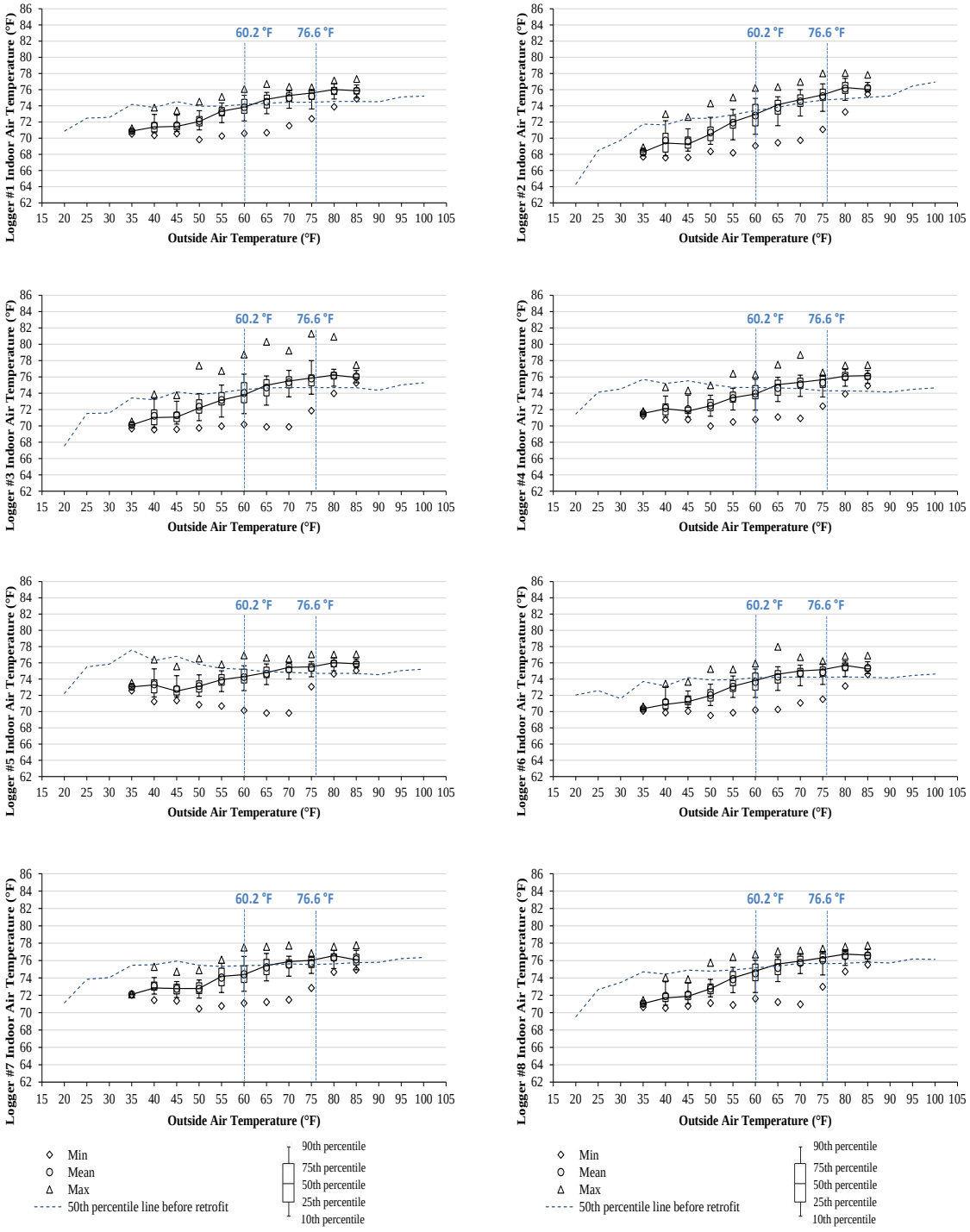

Figure 5-42. IATs against OATs from the eight data loggers during the post-retrofit period for weekdays (February 10th, 2017 to March 31th, 2017).

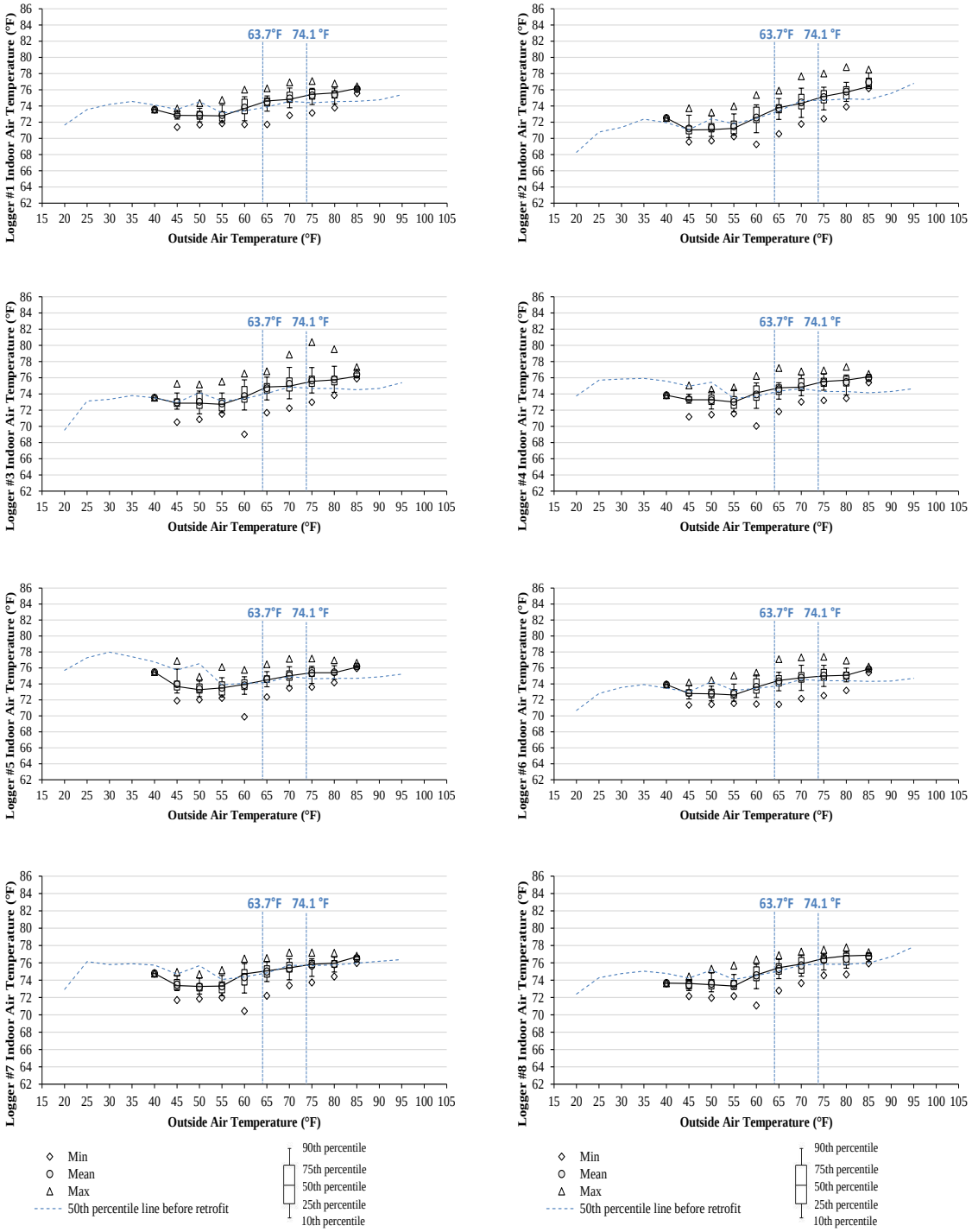

Figure 5-43. IATs against OATs from the eight data loggers during the post-retrofit period for weekends/holidays (February 10th, 2017 to March 31th, 2017).

Figure 5-44 and Figure 5-45 show the comparisons of the superimposed 50th percentiles from each data logger during the pre-retrofit[4] and the post-retrofit periods, respectively. In these plots, several observations can be made. In Figure 5-44, during the weekdays (upper plot), there was more variation compared to the heating setpoint when the OATs were lower than the 50-55 ℉ bin. The IATs from Data Logger #5 located at the 1/2 bathroom showed higher values compared the heating setpoint, and the IATs from Data Logger #2 located at the dining room showed lower values. During the weekends/holidays (lower plot), the IATs from the eight data loggers generally showed higher temperatures compared to the IATs during the weekdays. Furthermore, during the weekends/holidays, the IAT from Data Logger #8 located at the living room showed higher temperatures compared to the IATs during the weekdays, which implies higher internal heat gains from the occupant or equipment. It was also found that the IATs from the eight data loggers showed similar values when the OATs were ranged between the 65-70 ℉ bin and the 90-95 ℉ bin for both the weekdays and the weekends/holidays periods.

Compared to the IATs during the pre-retrofit period, the IATs during the post-retrofit period appeared to have less variations, which may be due to the improved IAT measurement of the new thermostat using the average IATs from the seven different zones (see Figures 4-26 and 4-27), rather than the IAT measurement from only the location of the thermostat.

[4] The IAT data in the post-retrofit period was limited in the range between 35 ℉ and 85 ℉.

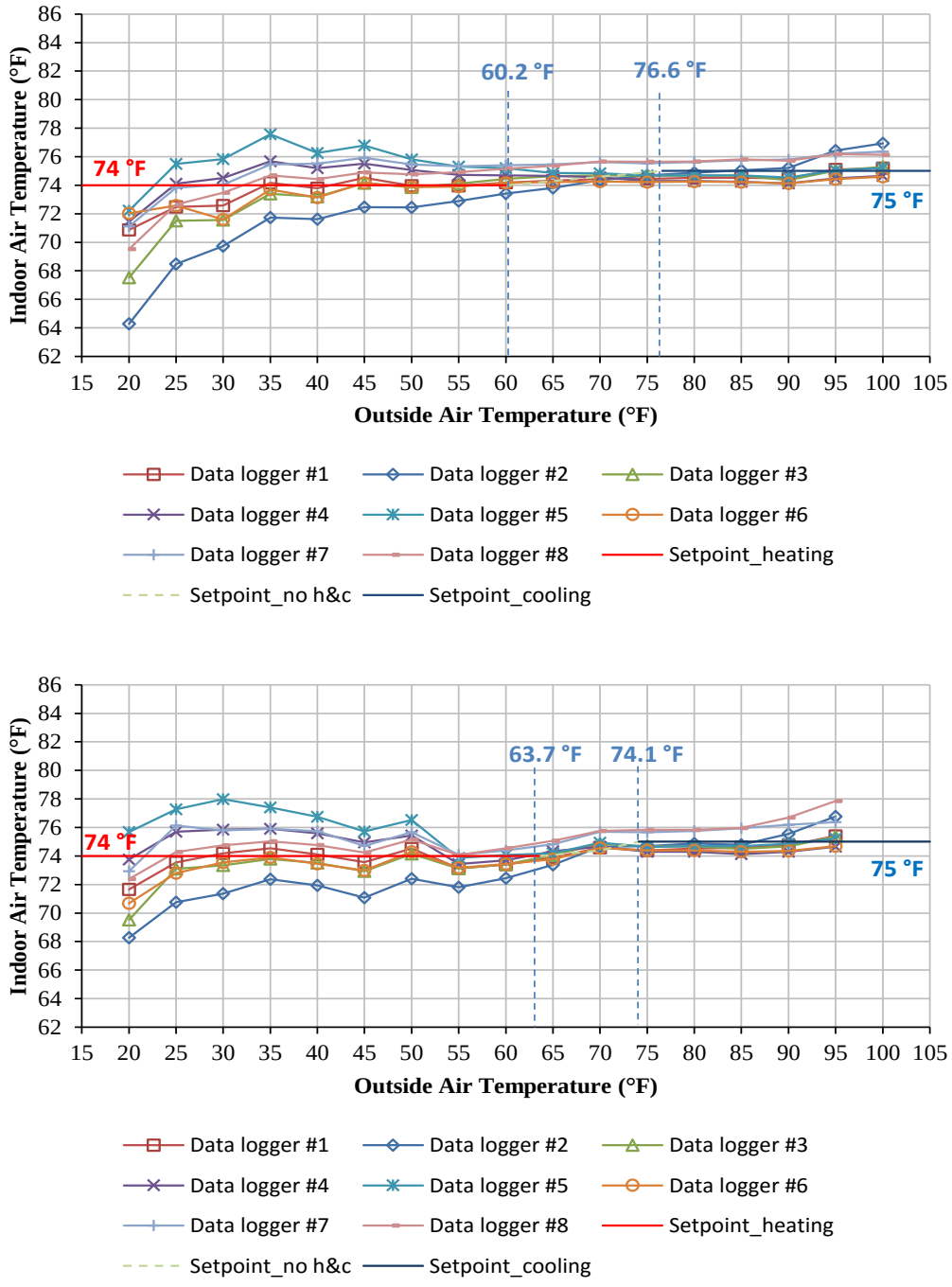

Figure 5-44. IATs versus OATs from the eight data loggers using 50th percentiles for the weekdays (upper) and the weekends/holidays (lower) during the pre-retrofit period (August 1st, 2016 to January 31st, 2017).

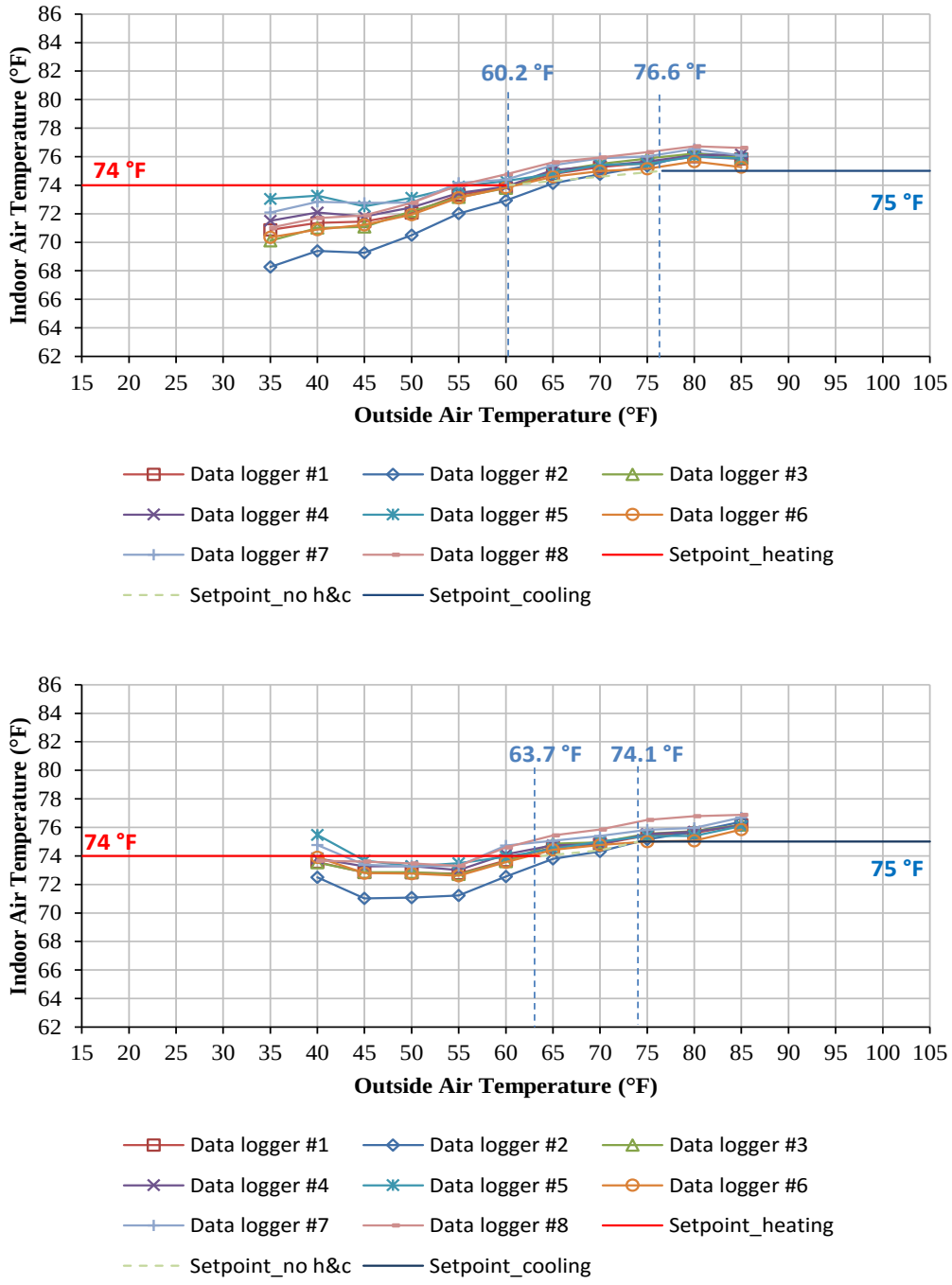

Figure 5-45. IATs versus OATs from the eight data loggers using 50th percentiles for the weekdays (upper) and the weekends/holidays (lower) during the post-retrofit period (February 10th, 2017 to March 31th, 2017).

5.3.2. Results from Weather-Normalized Electricity Savings of Level II Analysis

The 5P models and the binned quartile analysis were used to quantify and compare the electricity use between the baseline period and the post-retrofit period under weather-normalized conditions using the OATs of the post-retrofit period. Figure 5-46 and Figure 5-47 show the 5P models and the binned quartile analysis during weekdays and weekends/holidays, respectively. The analysis showed the range between the heating balance point and the cooling balance point of the post-retrofit period was larger than the range of the baseline period. A review of the data also showed the weather-independent range of data collected from the new thermostat was larger than weather-independent range collected from the previous thermostat. In addition, the binned quartile analysis (i.e., the lower plots of Figures 5-46 and 5-47) of the post-retrofit period showed that the 50^{th} percentile electricity use of the post-retrofit was lower than the superimposed 50^{th} percentile of the baseline period. This trend clearly shows the new thermostat achieved electricity savings by using the thermostat setback schedules. Furthermore, in Figures 5-46 and 5-47, it was observed that larger electricity savings occurred during the heating period and the cooling period, rather than the weather-independent period.

The actual electricity savings for 50 days from February 10^{th} to March 31^{st} (i.e., the post-retrofit period) was calculated by comparing the hourly electricity use during the post-retrofit period with electricity use predicted by the model for the baseline period. The calculated savings were 354.3 kWh (39.5%) for the weekdays and 142.1 kWh (34.5%) for the weekends/holidays. The total electricity savings was 496.4 kWh (37.9 %) with the total cost savings of $57.4.

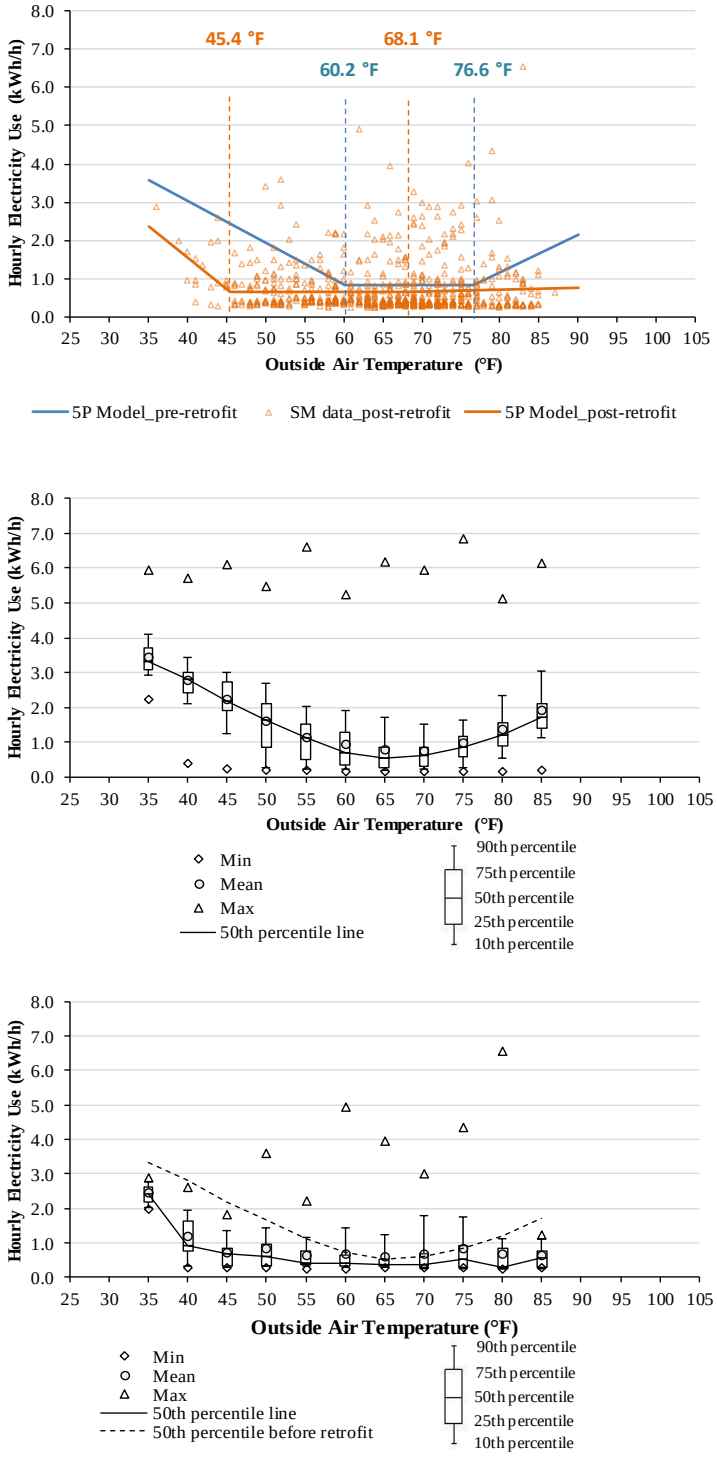

Figure 5-46. Comparison of 5P models of the SM data (upper) between baseline period and post-retrofit period for weekdays, quartile analysis for baseline period (middle) and for post-retrofit period with superimposed pre-retrofit median (lower).

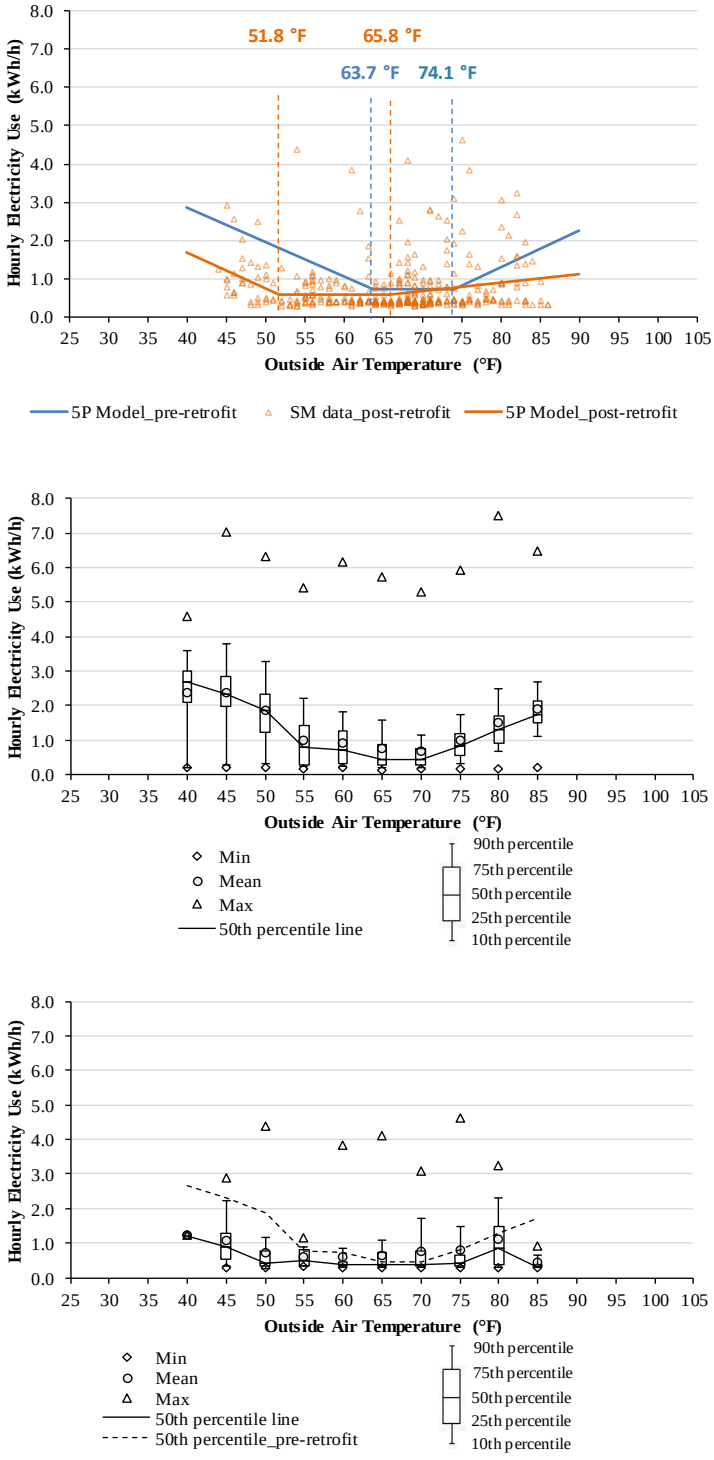

Figure 5-47. Comparison of 5P models of the SM data (upper) between baseline period and post-retrofit period for weekends/holidays, quartile analysis for baseline period (middle), and for post-retrofit period with superimposed pre-retrofit median (lower).

In addition, the quartile analysis of the post-retrofit period showed that the maximum electricity use of the post-retrofit period was lower than the maximum electricity use of the baseline period. Most likely, this could be from the lowered electricity use of the heating and cooling system by the thermostat setback schedules of the new thermostat with occupancy sensors.

Using the average, hourly occupancy diversity factors from all the zones, the hourly electricity use data of the post-retrofit data was categorized into occupied hours and unoccupied hours. Figure 5-48 and Figure 5-49 show the 5P models and the binned quartile analysis for occupied hours during weekdays and weekends/holidays, respectively. As previously mentioned, the separation of the heating balance point and the cooling balance point of the post-retrofit period was larger than the range of the baseline period, which is an indicator of reduced heating and cooling electricity use. In addition, the binned quartile analysis of the post-retrofit period shows that the median electricity use of the post-retrofit was lower than the superimposed median electricity use of the baseline period. This trend indicates the new thermostat achieved electricity savings for the occupied hours. It was also observed that larger electricity savings occurred during the heating period and the cooling period, when they were compared to the electricity savings during the weather-independent period.

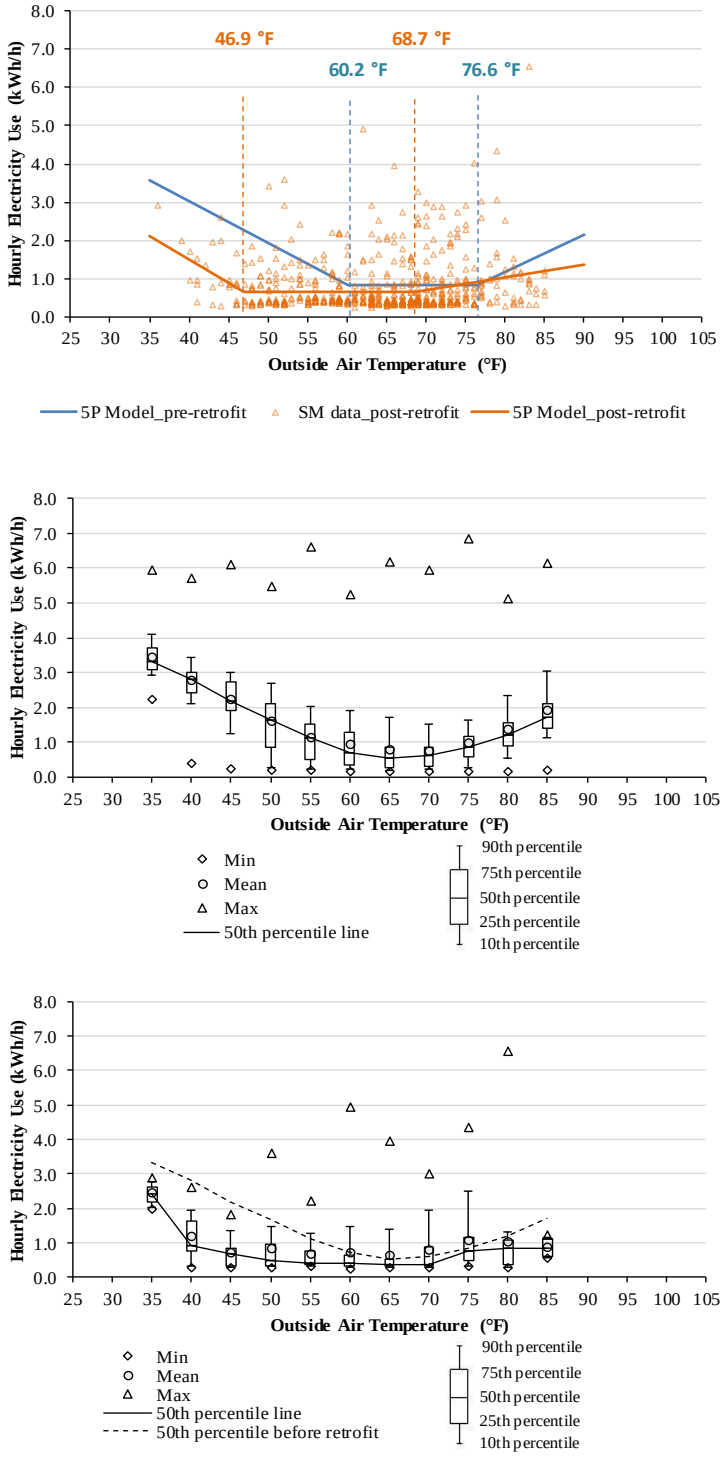

Figure 5-48. Comparison of 5P models (upper) between baseline period and post-retrofit period for occupied hours during weekdays, quartile analysis for baseline period (middle) and for post-retrofit period with superimposed pre-retrofit median (lower).

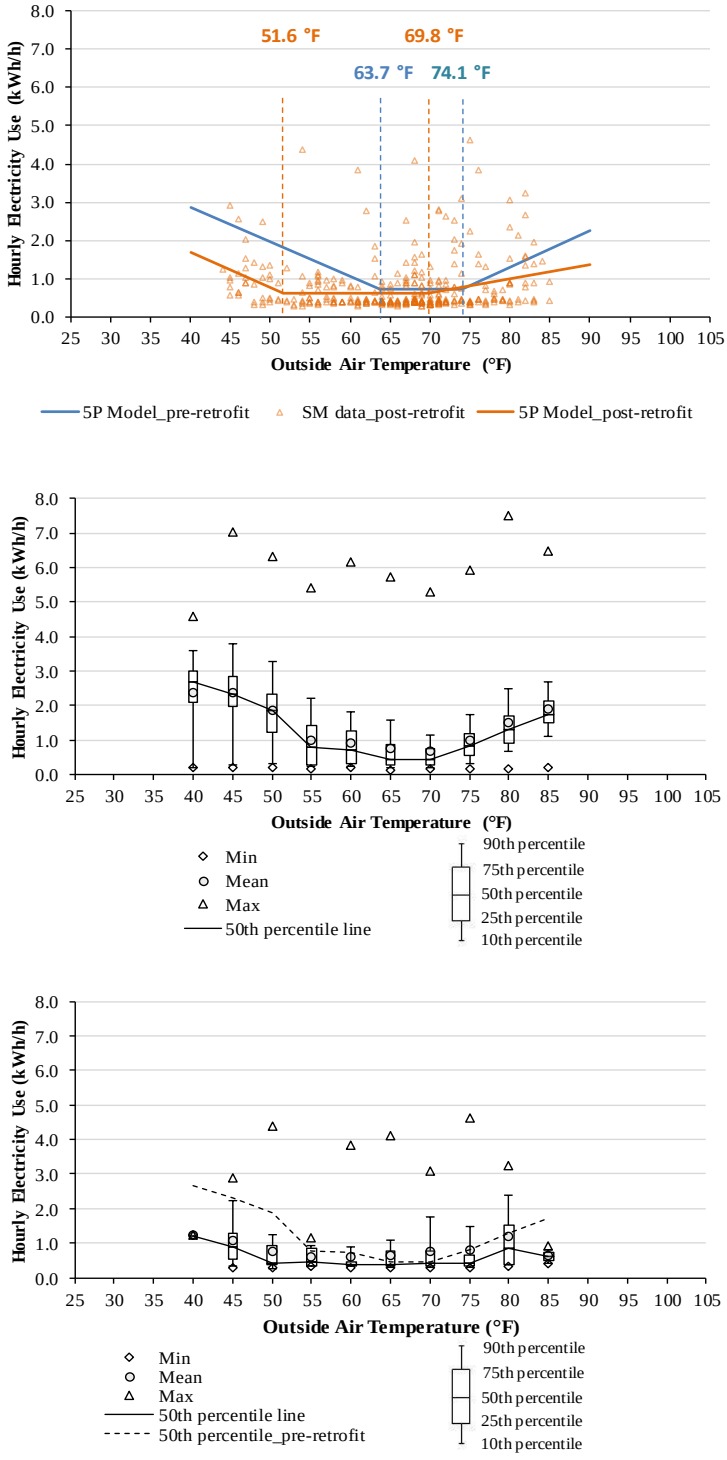

Figure 5-49. Comparison of 5P models (upper) between baseline period and post-retrofit period for occupied hours during weekends, quartile analysis for baseline period (middle) and for post-retrofit period with superimposed pre-retrofit median (lower).

The calculated savings of the post-retrofit period (50 days) for the occupied hours was 250.2 kWh (27.9%) for the weekdays and 121.5 kWh (29.5%) for the weekends/holidays. The total electricity savings was 371.7 kWh (28.4 %) and the total cost savings was $43.0 (see Table 5-7). The binned quartile analysis of the post-retrofit period also shows that the maximum electricity use of the post-retrofit period was lower than the maximum electricity use of the baseline period.

Figure 5-50 and Figure 5-51 show the 5P models and the binned quartile analysis for unoccupied hours during weekdays and weekends/holidays, respectively. Using the 5P models, the calculated savings of the post-retrofit period (50 days) for the unoccupied hours was 104.0 kWh (11.6 %) for the weekdays and 20.6 kWh (5.0 %) for the weekends/holidays. The total electricity savings was 124.7 kWh (9.5 %) and the total cost savings was $14.4 (see Table 5-7). The binned quartile analysis of the post-retrofit period also shows that the maximum electricity use of the post-retrofit period was much lower than the maximum electricity use of the baseline period. Finally, it was observed that large electricity savings occurred during all the heating period, the weather-independent period, and the cooling period, especially during the weekdays (see upper and lower plots in Figure 5-50).

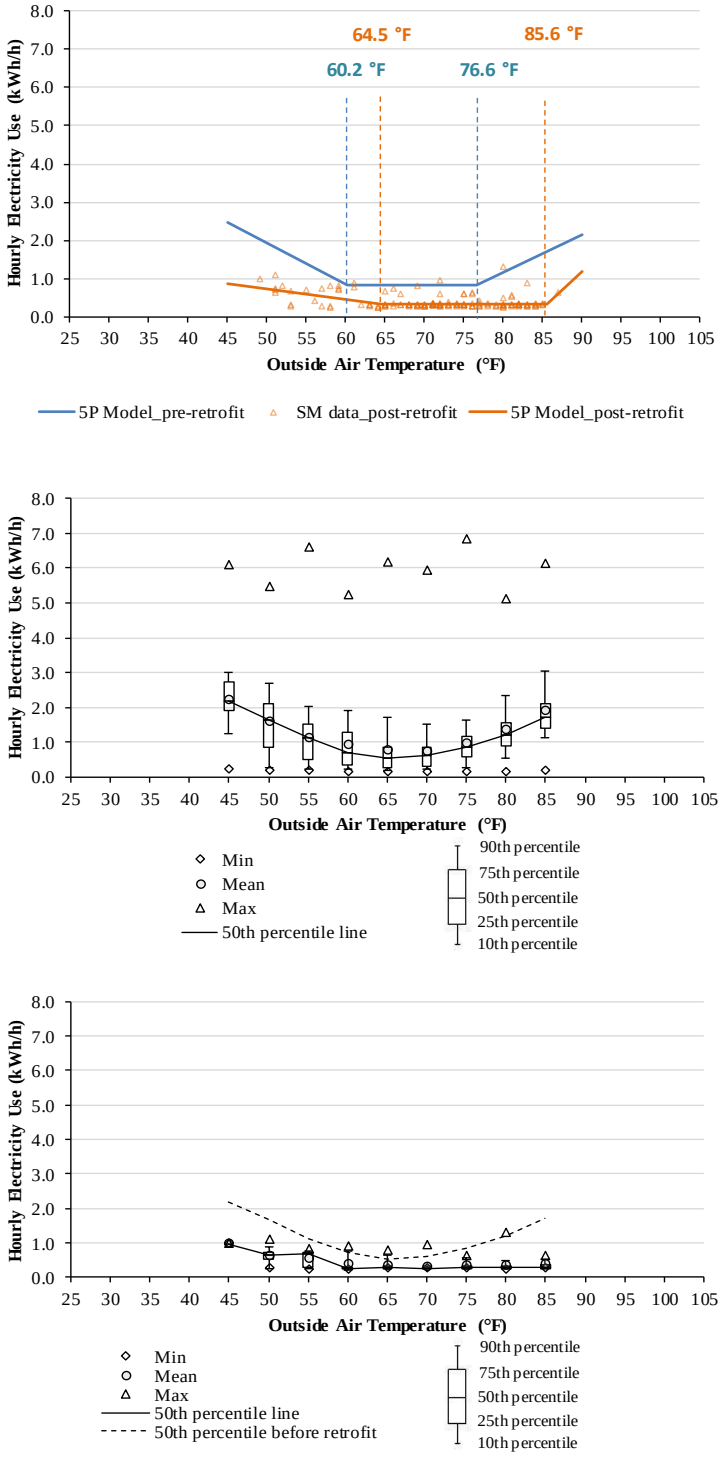

Figure 5-50. Comparison of 5P models (upper) between baseline period and post-retrofit period for unoccupied hours during weekdays, quartile analysis for baseline period (middle) and for post-retrofit period with superimposed pre-retrofit median (lower).

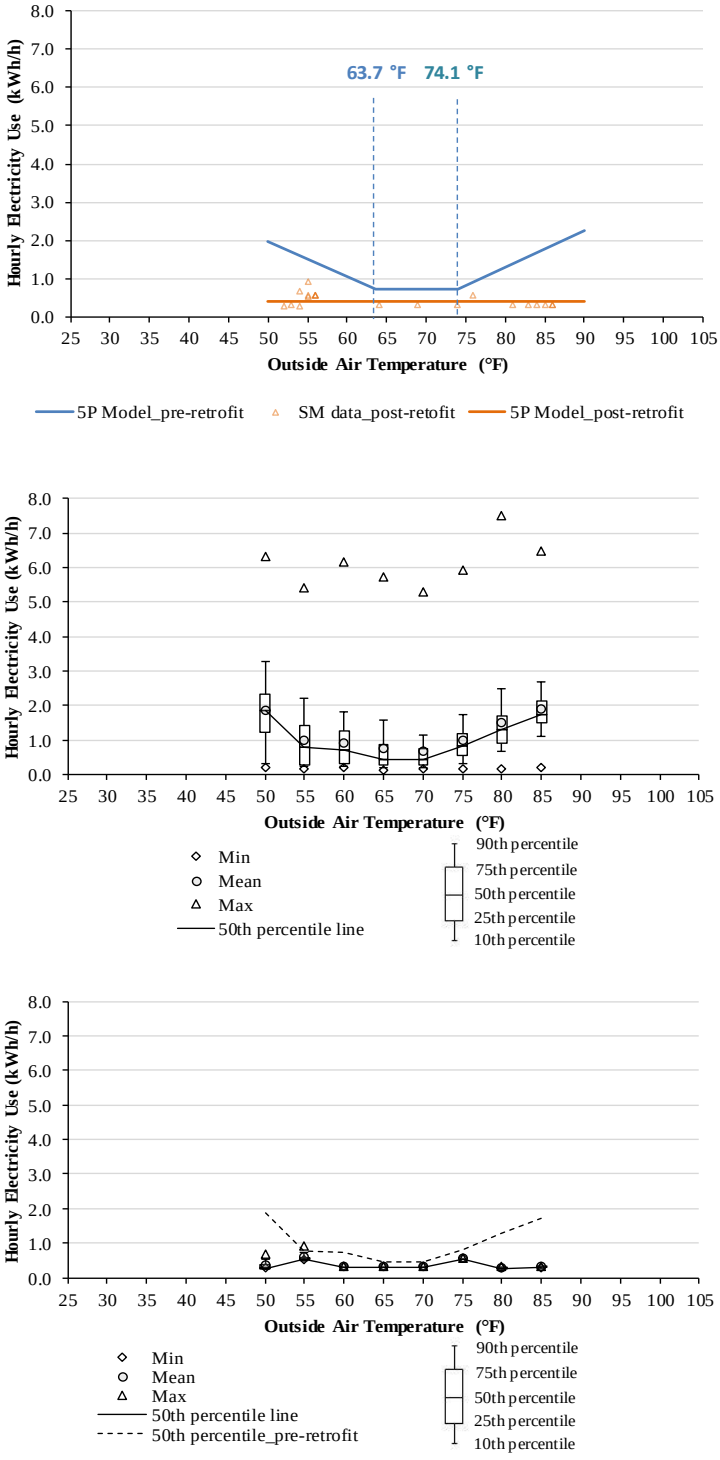

Figure 5-51. Comparison of IMT models (upper) between baseline period and post-retrofit period for unoccupied hours during weekends, quartile analysis for baseline period (middle) & for post-retrofit period with superimposed pre-retrofit median (lower).

The annual electricity savings was then calculated by comparing the 5P model for the post-retrofit period with the 5P model for the baseline period using the weather normalization method. In this analysis, the 1P model was used for the unoccupied hours of the post-retrofit period because the 5P model was no longer appropriate (i.e., application of the 5P model to the dataset yielded invalid results). The OATs of the baseline period were used to calculate the extended annual actual savings. The annual savings was also categorized into the occupied hours and the unoccupied hours. The annual savings was 3,610.0 kWh (45.9%) for the weekdays and 1,598.4 kWh (39.3%) for the weekends/holidays. The total electricity savings was 5,208.4 kWh (43.6 %) and the total cost savings was $620.1. The electricity savings of 4,456.3 kWh (37.3 %) and the cost savings $515.2 were achieved from the occupied hours, whereas the electricity savings of 1,007.9 kWh (8.4 %) and the cost savings $116.5 were achieved from the unoccupied hours. When the cost of the new thermostat ($249) with the seven motion sensors ($237), including the installation fee ($100), was considered, the simple payback period was 1.0 year (see Table 5-8).

Table 5-7. Actual electricity savings (50 days) summary from the programmable thermostat with occupancy detection (Level II Analysis).

	Actual savings (50 days)		**Actual savings (50 days) from occupied hours**		**Actual savings (50 days) from unoccupied hours**	
	weekdays	**weekends/holidays**	**weekdays**	**weekends/holidays**	**weekdays**	**weekends/holidays**
Electricity use (kWh) savings	354.3	142.1	250.2	121.5	104.0	20.6
Electricity % savings	39.5	34.5	27.9	29.5	11.6	5.0
Cost ($) savings	41.0	16.4	28.9	14.0	12.0	2.4
Total electricity use (kWh) savings	496.4		371.7		124.7	
Total electricity % savings	37.9		28.4		9.5	
Total cost ($) savings	57.4		43.0		14.4	

Table 5-8. Annual electricity savings summary from the programmable thermostat with occupancy detection (Level II Analysis).

	Annual statistical savings		**Annual statistical weighted savings from occupied hours**		**Annual statistical weighted savings from unoccupied hours**	
	weekdays	**weekends/holidays**	**weekdays**	**weekdays**	**weekends/holidays**	**weekdays**
Electricity use (kWh) savings	3610.0	1598.4	2941.1	1515.2	854.1	153.8
Electricity % savings	45.9	39.3	37.4	37.3	10.9	3.8
Cost ($) savings	417.3	184.8	340.0	175.2	98.7	17.8
Total electricity use (kWh) savings	5208.4		4456.3		1007.9	
Total electricity % savings	43.6		37.3		8.4	
Total cost ($) savings	602.1		515.2		116.5	
Simple payback (year)	1.0					

In addition, the Level II Analysis results were partially verified with actual utility billing data. Table 5-9 shows an available utility period and the coincident electricity consumption and savings from the utility data by comparing to the estimated electricity consumption and savings from the 5P change-point linear regression models. The comparison shows the measured savings and the estimated savings have a small difference of only 24.3 kWh (1.0%).

Table 5-9. Comparison of measured and estimated (Level II Analysis) electricity savings.

Period	Measured (kWh)	Estimated (kWh)	Period	Measured (kWh)	Estimated (kWh)	Measured savings (kWh/%)	Estimated savings (kWh/%)
2/10/2016-3/31/2016	1390.1	1364.9	2/10/2017-3/31/2017	812.9	812.0	577.2/41.5	552.9/40.5
Difference (Measured – Estimated)		25.2			0.9		24.3/1.0

5.3.3. Thermal Comfort Check for Electricity Savings from Level II Analysis

The thermal comfort was examined using the average IATs from the seven zones during the occupied and the unoccupied hours of the post-retrofit period, as well as the Relative Humidity (RH) from the location of the wireless, programmable thermostat during the same period. Figure 5-52 shows the trend of the average IATs between the occupied (upper) and the unoccupied hours (lower) using a 5 °F binned quartile analysis. During the weekdays of the post-retrofit period, the average IATs from the unoccupied hours were mostly lower than the occupied hours for the heating and the weather-independent periods based on the balance-point temperatures of the baseline period. This showed the thermostat setback schedule for the heating setpoint was mostly used for the

unoccupied hours during the weekdays. During the weekends/holidays, the average IATs from the unoccupied hours were mostly higher than the occupied hours. This showed the thermostat setback schedule for the cooling setpoint was mostly used for the unoccupied hours during the weekends/holidays.

Figure 5-53 shows the indoor environmental conditions in the case-study house during the post-retrofit period superimposed on the psychrometric chart (i.e., the humidity ratio versus the average IAT graph). Based on ASHRAE Standard 55-2013 (ASHRAE, 2013b), it was found that the occupant's thermal comfort was mostly met for both the occupied and the unoccupied hours because the indoor environmental conditions were inside the middle range of the winter and summer comfort zones. It was also found that it normally took from 5 minutes to 15 minutes to reach desired heating or cooling setpoint from the unoccupied hours to the occupied hours.

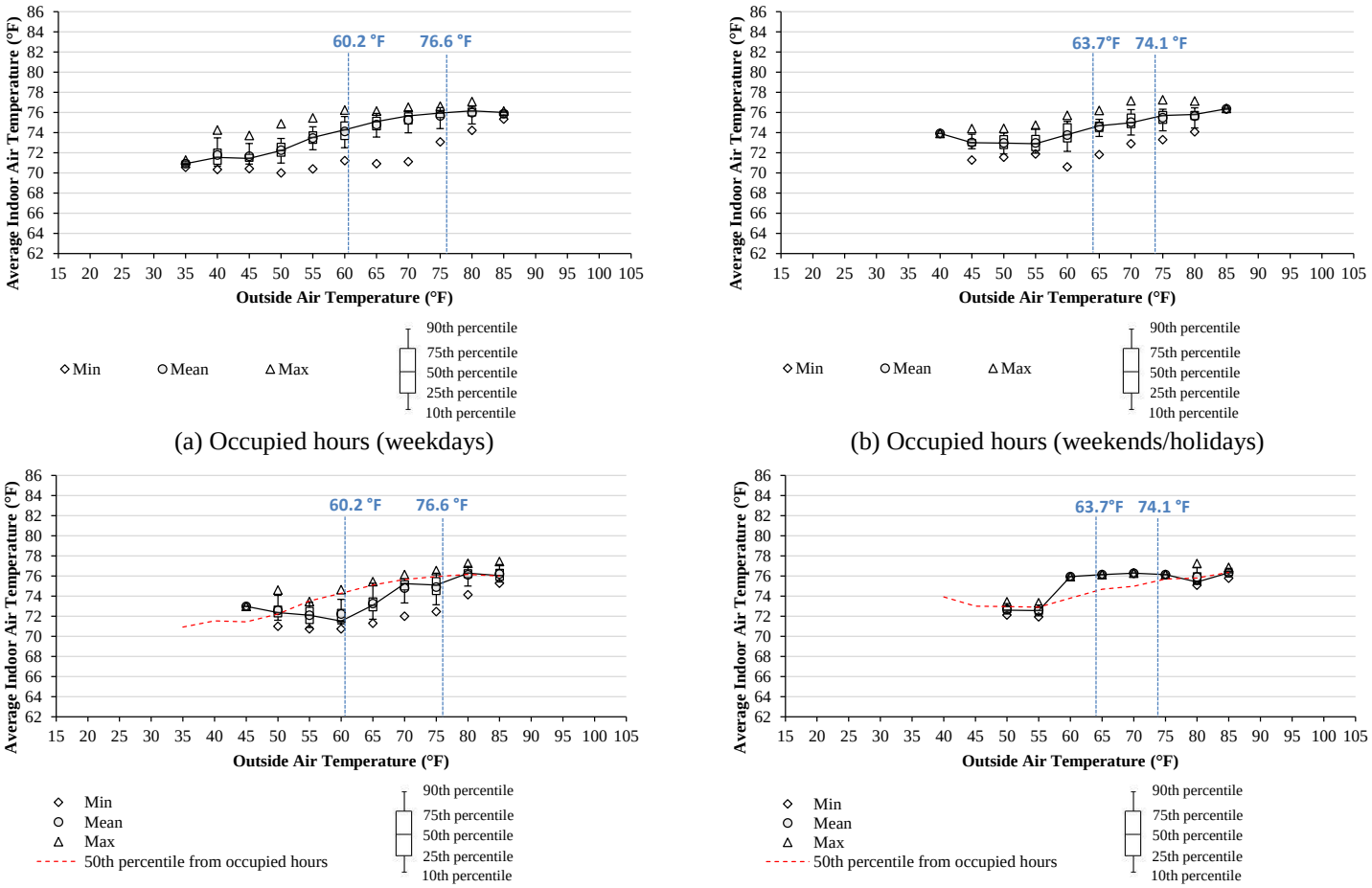

(a) Occupied hours (weekdays)

(b) Occupied hours (weekends/holidays)

(c) Unoccupied hours (weekdays)

(d) Unoccupied hours (weekends/holidays)

Figure 5-52. Average IATs from occupied hours (upper) and average IATs from unoccupied hours (lower) with superimposed, average IATs of the 50th percentile from occupied hours for weekdays (left) and weekends/holidays (right) during the post-retrofit period.

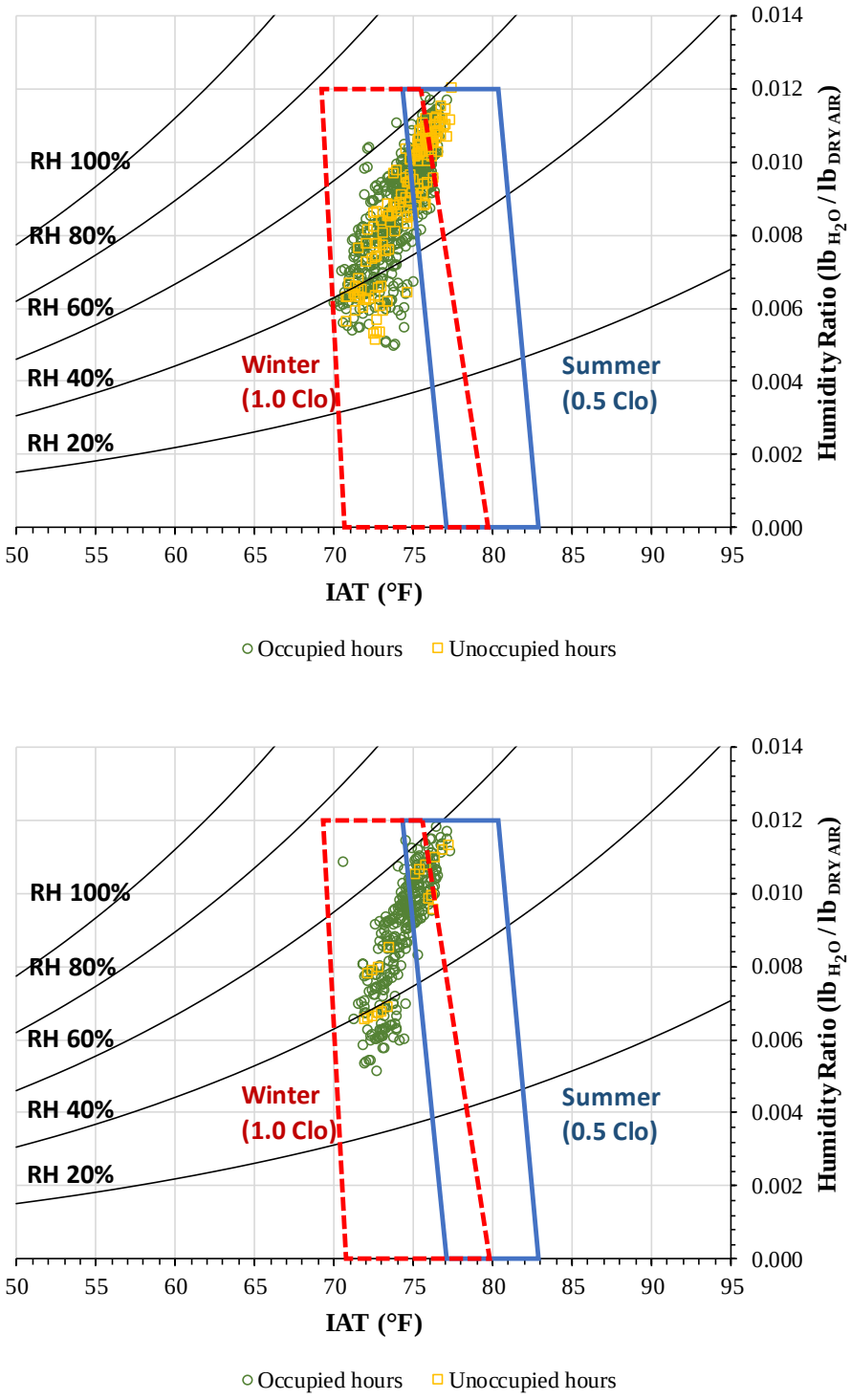

Figure 5-53. Average IAT/humidity ratio in the winter and summer comfort zones during weekdays (upper) and weekends/holidays (lower).

However, the results suggest that it is important to determine if detailed thermal comfort is maintained with the new occupancy-based thermostat in the acceptable ranges when the programmable thermostat setback (i.e., occupied hours) and the occupancy detection setback (i.e., unoccupied hours) are used to achieve electricity savings.

5.3.4. Findings from Level I Analysis and Level II Analysis

Possible reasons for the differences between the results from the calibrated simulation method (Level I Analysis) and the M&V method (Level II Analysis) were reviewed. Figure 5-54 shows the hourly electricity use data recorded by the SM and the 5-minute interval thermostat data (i.e., heating and cooling setpoint and system run time) recorded by the wireless programmable thermostat (i.e., HAD), as well as the simulated and measured, average IATs and the measured OATs during the time from 4:05 pm to 12:00 am on Wednesday, February 22nd, 2017 of the post-retrofit period. The figure shows that the cooling system was turned on at 5:55 pm and 6:45 pm during the 5 minutes and at 8:25 pm during the 10 minutes, respectively, because the IATs were higher than the cooling setpoints. In addition, the heating or cooling system was not turned on from 4:05 pm to 5:00 pm, 7:05 pm to 8:00 pm, and 9:05 pm to 12:00 am because the IATs were within the heating and cooling setpoints, including the throttling ranges. The heating and cooling setpoints started to change at 4:55 pm because the occupant was detected at the time.

It should be noted that the simulated IATs were the hourly interval and the measured IATs were the 5-minute interval. In addition, there were differences the

simulated IATs and the measured IATs. These differences could cause the different results between Level I Analysis and Level II Analysis because hourly building energy simulation program (e.g., DOE-2.1E) cannot accurately calculate the 5-minunte interval IATs by considering actual indoor conditions of the case-study house. In addition, the actual heating or cooling system was turned on during the sub-hourly time as shown in the figure, whereas the simulation was only on or off for the whole hour. Clearly, from the appearance of the data, if sub-hourly electricity use data is available, a more accurate analysis can be conducted to find the uncertainty between Level I Analysis and Level II Analysis. Future work will be conducted to further analyze this issue.

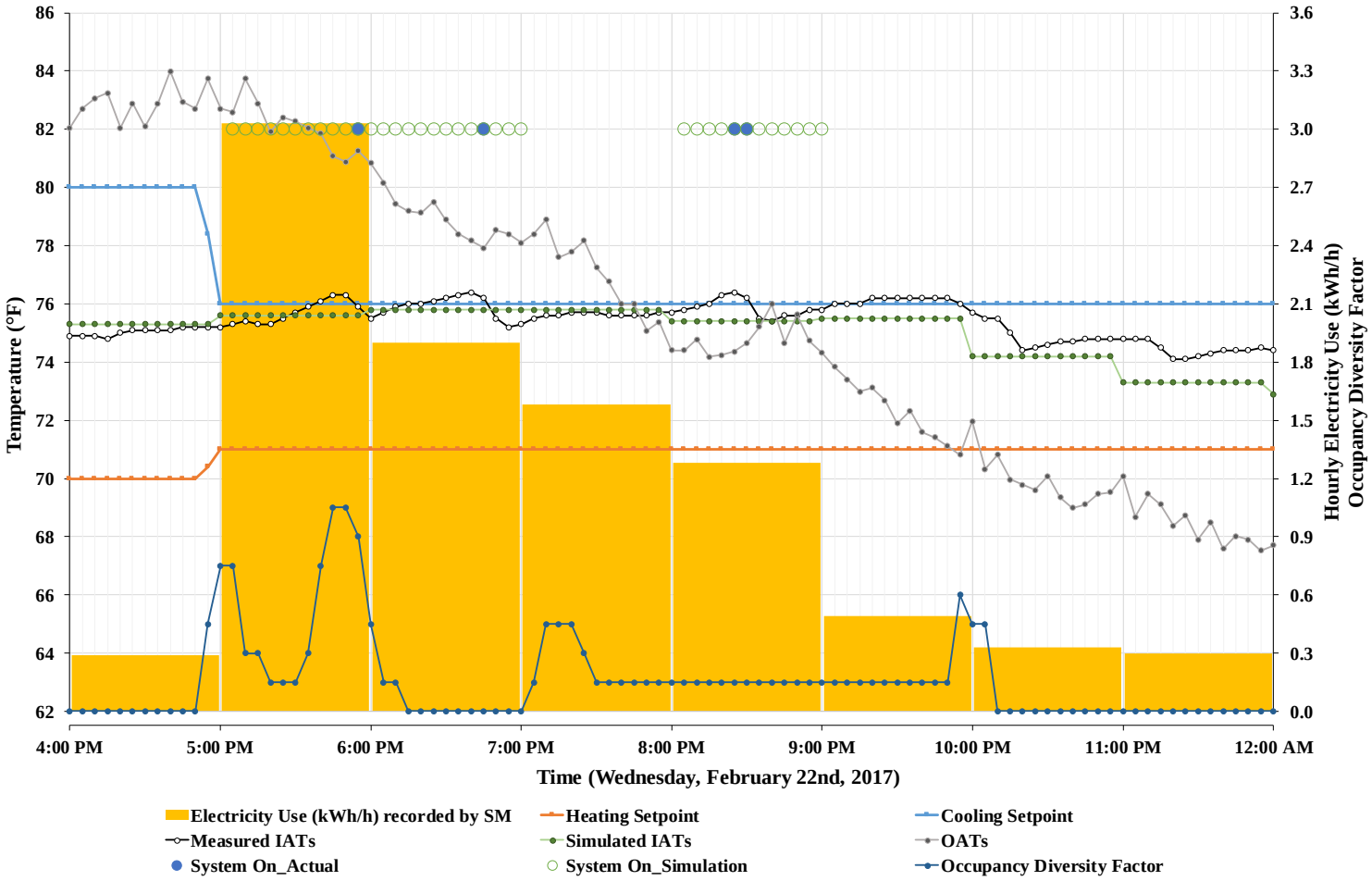

Figure 5-54. Hourly SM electricity use, hourly simulated IATs, sub-hourly heating and cooling setpoints, IATs, OATs, system run time, and occupancy detection data during the cooling hours of the post-retrofit period.

5.4. Summary of Results

The results of the analysis from the three methods are summarized in this chapter. The three methods include: Level 0 Analysis of estimated, potential electricity savings from HADs using SM data only; Level I Analysis of detailed, potential electricity savings achieved by simulation scenarios using a two-way calibrated simulation model; and Level II Analysis of actual electricity savings measured from the case-study house.

Level 0 Analysis showed an event detection process and an energy quantification process. In this analysis, the balance-point temperatures from the IMT, quartile analysis by temperature bin, 3D energy use plots, and the hour-of-the-day, the day-of-the-week, stacked histogram plots were provided for a detection process that showed the frequency of events above the 90^{th} and below the 10^{th} percentile during the weekdays and the weekends/holidays in the six different regions. They were used to identify the energy use patterns and the occupancy patterns that could be used for estimated potential energy savings. Overall, the most frequent occurrence above the 90^{th} percentile took place during the cooling period. Therefore, there could be opportunities for reducing energy savings by reducing high energy use during these periods. Similarly, the most frequent occurrence of events below the 10^{th} percentile also occurred during the cooling period, which may be hours when the occupant was inactive (e.g., in sleep) or outside the house.

Next, using the balance-point temperatures from the IMT and a weather day-typing method, an energy quantification process was presented that calculated the annual estimated, potential electricity savings of 987.8 kWh (8.3 %) by analyzing the hourly

electricity use data (i.e., whole-building energy use) patterns between weekdays and weekends/holidays for one year (i.e., the baseline period). Using this method, the estimated savings from the heating period, the weather-independent period, and cooling period was 328.4 kWh (2.8 %), 380.0 kWh (3.2 %), and 279.4 kWh (2.3 %), respectively.

Level I Analysis showed detailed, potential electricity savings using a two-way calibrated simulation model (i.e., the model was calibrated to the IATs and the SM electricity use data) of the case-study residence with five scenarios: 1) a whole-day thermostat setback schedule, 2) a nighttime thermostat setback schedule, 3) a thermostat setback schedule using occupancy detection, 4) thermostat zone control using occupancy detection, and 5) a lighting schedule using occupancy detection. The thermostatically controlled HAD (i.e., wireless programmable thermostat) and the non-thermostatically controlled HAD (i.e., lighting equipment using occupancy detection) were analyzed using a two-way calibrated simulation model. The results showed the detailed, potential electricity savings from the HADs in specific usage scenarios. The largest annual electricity savings of 2,961.7 kWh (25.2 %) was achieved from the 5 °F setback schedule for a whole day.

Level II Analysis calculated the annual electricity savings measured from the HAD installed in the case-study house using the weather normalization method. The measured electricity savings for 50 days from February 10th to March 31st (i.e., the post-retrofit period) was calculated by comparing the hourly electricity use data during the post-retrofit period with the electricity use predicted by the models for the baseline

period. The total electricity savings for the 50 days was 496.4 kWh (37.9 %) and the total cost savings was $57.4. Using the average, hourly occupancy diversity factors from all the zones, the hourly electricity use of the post-retrofit data was categorized into the occupied hours and the unoccupied hours. The total electricity savings from the occupied hours was 371.7 kWh and the total cost savings was $43.0. The total electricity savings from the unoccupied hours was 124.7 kWh and the total cost savings was $14.4.

Weather-normalized, annual electricity savings were calculated using the change-point linear models for the post-retrofit period and 5P models for the baseline period. The OATs of the baseline period were used to calculate the annual savings. The annual electricity savings was 5,208.4 kWh (43.6 %) with the total cost savings of $620.1. When the cost of the new thermostat ($249) with the seven motion sensors ($237), including the installation fee ($100), was considered, the simple payback was 1.0 year. Thermal comfort during the post-retrofit period was also examined, and the analysis showed no significant degradation of thermal comfort from the electricity savings.

CHAPTER VI

CONCLUSIONS AND FUTURE WORK

This section provides the conclusions of this study, which include: 1) a non-intrusive estimation method of the potential electricity savings from HADs using hourly electricity use recorded by a SM, 2) an analysis of the detailed, potential electricity savings of the case-study residence achieved by five simulation scenarios, and 3) actual electricity savings from the use of the HAD measured from the case-study house. This section also provides recommendations to help quantify and better predict electricity savings using interval electricity use data recorded by SMs from residences equipped with HADs. Finally, this section describes future work relevant to this study.

6.1. Conclusions

Three new methods have been developed to help quantify the electricity savings from the use of HADs, including an energy event detection process and a potential energy saving quantification process (i.e., Level 0 Analysis), a detailed-potential electricity saving method from simulations using a two-way calibrated simulation model (i.e., Level I Analysis), and a method to calculate measured electricity savings (i.e., Level II Analysis) from the use of HADs in a case-study residence. In this study, the methods focus on electricity savings in residences, but these can be extended to analyze other energy sources (e.g., natural gas) and other types of buildings (e.g., commercial buildings).

When hourly electricity use data recorded by SMs are available only, Level 0 Analysis can be useful to estimate the energy savings from the use of HADs at a large group of buildings before HADs are installed. First, homeowners and utilities can use Level 0 Analysis to detect the signature and patterns of energy consumption using its historical data, which can help them better understand their energy use patterns and enhance their energy saving opportunities. Second, Level 0 Analysis can also provide an approach to quantify the potential energy savings. If homeowners know their energy usage patterns well (i.e., different behavior patterns) between two different types of days (e.g., weekdays and weekends/holidays), Level 0 Analysis can calculate potential energy savings from the use of HADs before HADs are installed. The assumption is that the energy use of HADs normally depends on two different energy behavior patterns. Utilities can also use Level 0 Analysis to find potential candidates that can benefit from the installation of HADs using the two different behavior patterns.

If the detailed information of a building is available, Level I Analysis can be useful to quantify detailed-potential energy savings from the use of HADs. Level I Analysis uses a two-way calibration method for a whole-building energy simulation program that includes specific equations to calculate building energy loads and energy use. The two-way calibration provides an approach to match both simulated energy use and IATs with measured data, so the reliability of the calibration method can be enhanced by reflecting the inside performance of buildings. After the calibration process, a whole-building simulation program can simulate several scenarios for the multitude and specific use of HADs.

If HADs are installed in buildings, Level II Analysis will be useful to quantify actual energy savings from the use of HADs. Level II Analysis uses a weather normalization method for occupied and unoccupied hours to accurately quantify the actual energy savings using before and after HAD retrofit energy use and OAT data. To create a reliable baseline energy use before HAD retrofit, one year's energy use is recommended. The longer the energy use data after HAD retrofit, the more accurate the results can be. If one year's before and after HAD retrofit energy use data are available, Level 0 Analysis can also be used to analyze the signature and patterns from the use of HADs.

However, the different results from the three analysis methods should be further analyzed. The results showed that the maximum annual electricity savings calculated from Level 0 Analysis, Level I Analysis, and Level II Analysis were 987.8 kWh (8.3%), 2,961.7 kWh (25.2%), and 5,208.4 kWh (43.6%), respectively. The reason for the reduced savings from Level 0 Analysis versus Level I Analysis and Level II Analysis appears to be due to the difference in electricity patterns before the retrofit (i.e., Level 0 Analysis) between two different day types (e.g., weekdays and weekends/holidays), which does not account for all potential savings from the use of HADs (e.g., all devices' post-retrofit efficiency and operation). Another observation that may explain the differences of savings from Level I Analysis versus Level II Analysis was that the runtime of the simulated HVAC system was controlled by the hourly system schedule in the DOE-2.1E simulation program (i.e., Level I Analysis). However, the actual runtime of the HVAC system was controlled by the sub-hourly schedule (e.g., 10 minutes per

hour) in the new thermostat operation (i.e., Level II Analysis). Therefore, the runtime differences between the simulated system and the actual system can cause a significant uncertainty when quantifying electricity savings from the use of HADs with a calibrated simulation model. Finally, to better quantify and predict electricity savings for residences equipped with HADs using electricity consumption recorded by SMs, the following recommendations are provided:

- The difference in the electricity usage patterns (i.e., different behavior patterns) between two different types of days (e.g., weekdays and weekends/holidays) is important when calculating potential electricity savings from the use of HADs using electricity use data only (SM data) (i.e., Level 0 Analysis). Level 0 Analysis will be useful to find potential candidates that can benefit from the installation of HADs using two different electricity behavior patterns. However, in Level 0 Analysis, the potential electricity savings do not accurately account for the savings from efficient system operation (e.g., a thermostat setback schedule). Therefore, more detailed methods (e.g., Level I Analysis and Level II Analysis) are needed to better quantify electricity savings from HADs.
- A programmable thermostat setback schedule or an automatic thermostat setback schedule with occupancy detection is recommended to achieve significant electricity savings. Level I Analysis and Level II Analysis showed the electricity savings up to 43.6 % could be obtained in the case-study residence.

- Lighting equipment controlled by occupancy detection is recommended to achieve lighting electricity savings, although these savings could be smaller than the savings from the improved HVAC system operation. Level I Analysis showed the electricity savings of 4.7 % were possible from HAD-controlled lighting.
- Sub-hourly electricity use data (SM data) (e.g., 1-minute or 5-minute interval data) would be very useful to help identify additional electricity saving opportunities because the improved thermostat information from the HADs would include sub-hourly data (see Level II Analysis).
- Occupancy detection data for each room is very important to non-intrusively categorize the potential electricity savings from occupied hours and unoccupied hours. Level II Analysis showed the electricity savings of 37.3 % and 8.4 % from the occupied hours and the unoccupied hours, respectively. To enhance accuracy, the 1-minute interval occupancy data should be used because the 5-minute interval loggers could not accurately detect the occupant when one moved to different rooms in the 5-minute interval.
- IAT and thermostat data are important factors to help disaggregate heating, cooling, and appliance electricity consumption and to improve detailed electricity saving opportunities (see Level II Analysis).
- A thermostat setback schedule or an automatic thermostat setback schedule with occupancy detection for the HVAC system can reduce electrical demand as well as electricity consumption (see Level II Analysis). However, electric demand savings may not be guaranteed because homeowner(s) can inadvertently use large amounts of electricity during peak demand times for other appliances.

6.2. Future Work

During this study, the following future work is highly recommended:

- Expand Level 0 Analysis using a longer period from post-retrofit data. By comparing the before/after retrofit electricity consumption, electricity savings will be quantified, and electricity use patterns (i.e., signature analysis) will be analyzed for the before/after retrofit periods.
- Verify the occupancy pattern detection method of Level 0 Analysis using the measured occupancy detection data after the post-retrofit.
- Further study of Level II Analysis using a longer post-retrofit data period. It is expected that the 5P models for the post-retrofit period will have higher cooling balance-point temperatures if more SM data is collected for the cooling period (e.g., over 80 °F of the OATs) due to higher cooling setpoints.
- Further study of the thermal comfort in each zone from the smart thermostat by measuring RH in each zone. Operative temperatures calculated from mean radiant temperatures and dry-bulb temperatures should also be considered to examine the thermal comfort.

- Further study the reasons for the different results between Level I Analysis and Level II analysis. Level I Analysis using sub-hourly electricity use and OAT data will be useful to more accurately calibrate simulation models. Normally, OAT data from the national institute is hourly, so sub-hourly data loggers for OAT will be needed to measure it outside a building. Sub-hourly OAT data will help better analyze the whole-building electricity consumption for Level I Analysis (i.e., simulation) as well as Level 0 Analysis and Level II Analysis (i.e., statistical methods) because sub-hourly OAT data can be used to observe the signatures of the electricity use patterns from occupancy and building systems.
- Further analyze the electricity savings from the new thermostat during unoccupied hours because it was found that two-hour time shift occurred for setback schedules during unoccupied hours.
- Further analyze IAT impact and the relationship with occupancy detection data for electricity saving opportunities using electricity consumption and OAT interval data. This study showed that IAT data could improve electricity saving estimation from thermostat operation and occupancy behavior.

- Further analyze thermostat control with occupancy sensors to improve occupancy comfort as well as electricity savings by better controlling zone temperatures. This study showed the simulated annual electricity savings using individual zone control, but did not show measured annual electricity savings and occupancy comfort for individual zones.
- Further develop new calibration methods for the two-way calibrations using IATs and electricity use data (SM data). Sensitivity analysis will be useful to better calibrate simulation models using the two-way method.
- Expand the new Level 0, I, and II Analysis using sub-hourly SM data. This study showed that more saving opportunities and more accurate savings could be found if sub-hourly electricity use data (e.g., 1-minute, 5-minute, or 15-minute interval data) is provided.
- Develop a method to better calibrate occupancy detection data loggers because this study showed inaccurate occupancy detection when the occupant of the case-study residence was sleeping. Even though the occupant was in bed, the occupancy logger did not fully detect the occupant at all times. Additional sensors, such as a CO_2 sensor, would be needed.
- Develop a method to better identify detailed, electric demand saving opportunities using electricity use data recorded by a SM. This study did not focus on electric demand savings because the electricity use and capacity of each appliance were not measured.

- Expand this study to other case-study residences. Especially, Level 0 Analysis would be very useful to analyze potential electricity savings from hundreds of houses (i.e., data mining) when only electricity use (SM data) and coincident weather data are available.
- Expand this study to other climate zones. Different weather conditions will affect the amount of electricity savings during heating, weather-independent, and cooling periods due to different heat loss and heat gain through floors, walls, windows, and ceilings as well as different electricity use patterns.
- Expand this study to commercial buildings. It is expected that the new methods developed in this study are not limited to residential buildings. Different occupancy schedules of residential and commercial buildings will make different electricity savings for the time-of-use patterns of Level 0 Analysis and the actual electricity use and savings of Level II Analysis. In addition, the IAT observations of Level I Analysis before/after retrofit in the zones of residences would show different patterns from the IAT in commercial buildings. As 15-min whole-building electricity use data becomes more available for commercial buildings rather than residences, new analysis methods for M&V, FDD, and commissioning will be needed to better analyze the signatures of sub-hourly electricity use from occupants and building systems.

- Further analyze how the statistical plots for individual zones developed in this study can be used to better evaluate how well an HVAC system is providing comfort levels (or not) for each zone in a residence.
- Integrate the newly developed methods with the energy and demand saving opportunities of Distributed Generation (DG) (e.g., renewable energy), Electric Vehicle (EV), and Energy Storage (ES) of the Smart Grid (SG).

REFERENCES

Abushakra, B., Reddy, A., and Singh, V. (2012). *ASHRAE research project report (1404-RP): Measurement, modeling, analysis and reporting protocols for short-term M&V of whole building energy performance.* Atlanta, GA: ASHRAE.

Abushakra, B., Sreshthaputra, A., Haberl, J. S., and Claridge, D. E. (2001). *ASHRAE research project report (1093-RP): Compilation of diversity factors and schedules for energy and cooling load calculations* (Report Number ESL-TR-01/04-01). College Station, TX: Texas A&M University.

Accenture. (2011). *Revealing the values of the new energy consumer - Accenture end-consumer observatory on electricity management 2011.* Dublin, Ireland: Accenture.

Akbari, H. (1995). Validation of an algorithm to disaggregate whole-building hourly electrical load into end uses. *Energy, 20,* 1291–1301.

Akbari, H, Heinemeier, K., Flora, D., and LeConiac, P. (1988). Analysis of commercial whole-building 15-minute-interval electric load data. *ASHRAE Transactions, 94*(2), 855-871.

Alford, R. (2015). *U.S. likelihood of purchasing HEMS doubles; ownership remains flat.* Retrieved from http://etsinsights.com/news/u-s-likelihood-of-purchasing-hems-doubles-ownership-remains-flat/#sthash.DH0McR8H.dpuf

Ali, M. T., Mokhtar, M. M., and Chiesa, M., and Armstrong, P. R. (2011). A cooling change-point model of community-aggregate electrical load. *Energy and Buildings, 43*(1), 28-37.

Armstrong, P. R., Leeb, S. B., and Norford, L. K. (2006). Control with building mass – part I: Thermal response model. *ASHRAE Transactions, 112*(1), 449-461.

American Society of Heating, Refrigerating and Air-Conditioning Engineers (ASHRAE). (1962). *ASHRAE Guide and Data Book – Applications.* Chapter 12 - Estimating Fuel Consumption or Energy for Space Heating. Atlanta, GA: ASHRAE.

ASHRAE. (1976). *ASHRAE Handbook – Systems.* Chapter 43 - Energy Estimating Methods. Atlanta, GA: ASHRAE.

ASHRAE. (1981). *ASHRAE Handbook – Fundamentals.* Chapter 28 - Energy Estimating Methods. Atlanta, GA: ASHRAE.

ASHRAE. (1985). *ASHRAE Handbook – Fundamentals.* Chapter 28 - Energy Estimating Methods. Atlanta, GA: ASHRAE.

ASHRAE. (2013a). *ASHRAE Handbook – Fundamentals.* Chapter 19 - Energy Estimating and Modeling Methods. Atlanta, GA: ASHRAE.

ASHRAE. (2013b). *ASHRAE Standard 55-2013 - Thermal Environmental Conditions for Human Occupancy*. Atlanta, GA: ASHRAE.

ASHRAE. (2014). *ASHRAE Guideline 14-2014 - Measurement of energy, demand, and water savings.* Atlanta, GA: ASHRAE.

ASTM. (2014). *ASTM E77-14 Standard Test Method for Inspection and Verification of Thermometers.* West Conshohocken, PA: ASTM International.

Arduino. (2015). *What is Arduino?* Retrieved from http://www.arduino.cc/

Bacot, P., Neveu, A., and Sicard, J. (1984). Analyse modale des phenomenes thermiques en regime variable dans le batiment (Modal analysis of thermal phenomena in variable in the building). *Revue Generale de Thermique (General Heat Magazine), 267,* 189.

Baltazar, J. (2006). *Development of an automated methodology for calibration of simplified air-side HVAC system models and estimation of potential savings from retrofit/commissioning measures*. (Doctoral Dissertation). College Station, TX: Texas A&M University.

Baltazar, J., Mao, C., and Haberl, J. (2014). Verification of energy savings from the implementation of the residential building codes in Texas. *ASHRAE Transactions.*

Biggest Energy Saver (BES). (2013). *Meet the 2011 CenterPoint energy service area Biggest energy Saver winners.* Retrieved from http://www.biggestenergysaver.com/winners/2011/

Blanc, S. (1999). *Improving the cost effectiveness of building diagnostics, measurement and commissioning using new techniques for measurement, verification and analysis* (Report Number P600-00-024). San Francisco, CA: Pacific Gas and Electric Company.

Bojanczyk, K. (2013a). *Redefining home energy management systems.* Retrieved from www.greentechmedia.com/articles/read/home-energy-management-systems-redefined

Bojanczyk, K. (2013b). *Home energy management systems: Vendors, technologies and opportunities 2013-2017.* Retrieved from www.greentechmedia.com/research/report/home-energy-management-systems-2013-2017

Bouhou, N. (2014). Observed performance of demand-side residential electricity technologies. *Presentation at the meeting of Pecan Street, Inc., Austin, TX.*

Bou-Saada, T. (1994). *An improved procedure for developing a calibrated hourly simulation model of an electrically heated and cooled commercial building*. (Master's Thesis). College Station, TX: Texas A&M University.

Bou-Saada, T., and Haberl, J. S. (1995a). A weather-day typing procedure for disaggregating hourly end-use loads in an electrically heated and cooled building from whole-building hourly data. *Proceedings of the 30th Intersociety Energy Conversion Engineering Conference, July 31-August 4, Orlando, Florida,* 349-356.

Bou-Saada, T., and Haberl, J. S. (1995b). An improved procedure for developing calibrated hourly simulation models. *Proceedings of Building Simulation '95. International Building Performance Simulation Association, August 14-16, Madison, WI.*

Bronson, D. J., Hinchey, S. B. Haberl, J. S. and O'Neal, D. L. (1992). A procedure for calibrating the DOE-2 simulation program to non-weather-dependent measured loads. *ASHRAE Transactions, 98*(1), 636-652.

Buchberg, H. (1958). Cooling load from thermal network solutions. *ASHVE Transactions, 64*, 111-128.

Buhl, F. (1999). *DOE-2 Weather Processor.* Berkeley, CA: Lawrence Berkeley National Laboratory.

California Public Utilities Commission (CPUC). (2010). *The benefits of smart meters.* Retrieved from http://www.cpuc.ca.gov/PUC/energy/Demand+Response/benefits.htm

Carroll, W. L., and Hitchcock, R. J. (1993). Tuning simulated building descriptions to match actual utility data: methods and implementation. *ASHRAE Transactions, 99*, 928–934.

Carvallo, A., and Cooper, J. (2011). *The advanced smart grid - Edge power driving sustainability.* Norwood, MA: Artech House.

CenterPoint Energy. (2017). *Smart meters.* Retrieved from http://www.centerpointenergy.com/en-us/business/services/electric-utility/electric-technology/smart-meters?sa=ho

Christensen, C. (1984). *Digital and color energy maps for graphic display of hourly data* (Report Number SERI/TP-253-2461). Golden, CO: Solar Energy Research Institute.

Coakley, D., Raftery, P., and Keane, M. (2014). A review of methods to match building energy simulation models to measured data. *Renewable and Sustainable Energy Reviews, 37*, 123–141.

Cole, W. J., Powell, K. M., Hale, E. T., and Edgar, T. F. (2014). Reduced-order residential home modeling for model predictive control. *Energy and Building, 74*, 69-77.

Crawley, D. B., Lawrie, L. K., Winkelmann, F. C., and Pedersen, C. O. (2001). EnergyPlus: New capabilities in a whole-building energy simulation program**.** *Proceedings of Building Simulation 2001, Rio de Janeiro, Brazil, August,* 51-58.

Curtiss, P. S., Haberl, J. S., Huang, J., Jump, D., Kreider, J. F., Rabl, A., Reddy, T. A., and Sherman, M. (2001). HVAC design calculations. *In J. F. Kreider (Ed.), Handbook of Heating, Ventilation, and Air Conditioning* (pp. 6-1-6-155). New York, NY: CRC Press.

Darby, S. (2010). Smart metering: what potential for householder engagement? *Building Research & Information, 38*(5), 442-457.

Dhar, A. (1995). *Development of Fourier series and artificial neural network approaches to model hourly energy use in commercial buildings.* (Doctoral Dissertation). College Station, TX: Texas A&M University.

Dhar, A., Reddy, T. A., and Claridge, D. E. (1998). Modeling hourly energy use in commercial buildings with Fourier series functional forms. *Journal of Solar Energy Engineering, 120,* 217-223.

Dhar, A., Reddy, T. A., and Claridge, D. E. (1999a). A Fourier series model to predict hourly heating and cooling energy use in commercial buildings with outdoor temperature as the only weather variable. *Journal of Solar Energy Engineering, 121*(1), 47-53.

Dhar, A., Reddy, T. A., and Claridge, D. E. (1999b). Generalization of the Fourier series approach to model hourly energy use in commercial buildings. *Journal of Solar Energy Engineering, 121, 54-62.*

Diamond, S. C., and Hunn, B. D. (1981). Comparison of DOE-2 computer program simulations to metered data for seven commercial buildings. *ASHRAE Transactions 87*(1): 1222- 1231.

Ehrhardt-Martinez, K., Donnelly, K. A., and Laitner, J. A. (2010). *Advanced metering initiatives and residential feedback programs : A meta-review for household electricity-saving opportunities* (Report Number E105). Washington, D.C.: American Council for an Energy-Efficient Economy.

Eisenhower, B., O'Neill, Z., Narayanan, S., Fonoberov V. A., and Mezić, I. (2012). A methodology for meta-model based optimization in building energy models. *Energy and Buildings, 47,* 292–301.

Electric Power Research Institute (EPRI). (2008). *The green grid: energy savings and carbon emissions reductions enabled by a smart grid* (Report Number 1016905). Palo Alto, CA: EPRI.

Electric Power Research Institute (EPRI). (2014). *EPRI Smart Grid Demonstration Initiative – Final update.* Palo Alto, CA: EPRI.

Faruqui, A., Sergici, S., and Sharif, A. (2010). The impact of informational feedback on energy consumption-A survey of the experimental evidence. *Energy, 35*(4), 1598–1608.

Faruqui, A., Mitarotonda, D., Wood, L., Cooper, A., and Schwartz, J. (2011). *The costs and benefits of smart meters for residential customers.* Washington, DC: The Edison Foundation Institute for Electric Innovation.

Fels, M. F. (1986). PRISM: An introduction. *Energy and Buildings, 9,* 5-18.

Fitts, A. S. (2014). *How the internet of things revved up my apartment – and sort of creeped me out.* Retrieved from http://www.popularmechanics.com/technology/gadgets/how-to/a10527/i-automated-my-apartment-and-it-kind-of-creeped-me-out-16708938/

Fischer, C. (2008). Feedback on household electricity consumption: a tool for saving energy? *Energy Efficiency 1*:79-104.

Frizell, S. (2014). At your service meet the startup trying to create – and control – the internet of your home. Time Magazine. July 14, 2014.

Gardner, G. T., and Stern, P. C. (2008). The short list: The most effective actions U.S. households can take to curb climate change. *Environment: Science and Policy for Sustainable Development, 50*(5), 12–25.

Google. (n.d.). Retrieved October 6, 2016, from the Google map: https://www.google.com/maps

Haberl, J. S. (1986). *An expert system for the analysis of building energy consumption* (Doctoral Dissertation). College Station, TX: Texas A&M University.

Haberl, J. S., Bronson, D. Hinchey, S. and O'Neal, D. (1993a). Graphical tools to help calibrate the DOE-2 simulation program to non-weather dependent measured loads. *ASHRAE Journal, 35*(1), 27-32.

Haberl, J. S., Bronson, D. O'Neal, D. (1993b). Impact of using measured weather data versus TMY weather data in a DOE-2 simulation. *ASHRAE Transactions, 101*(2).

Haberl, J. S., Kissock, K. Belur, R. and Sparks, R. (1993c). Improving the paradigm for displaying complex building energy consumption data. *Proceedings of the ASMESED International Solar Energy Conference,* 475-485.

Haberl, J. S., Sparks, R. and Culp, C. (1996). Exploring new techniques for displaying complex building energy consumption data. *Energy and Buildings*, *24,* 27-38.

Haberl, J. S., and Abbas, M. (1998a). Development of graphical Indices for viewing building energy data: Part I. *ASME Journal of Solar Energy Engineering, 120,* 156-161.

Haberl, J. S., and Abbas, M. (1998b). Development of graphical indices for viewing building energy data: Part II. *ASME Journal of Solar Energy Engineering, 120,* 162-167.

Haberl, J. S., and Bou-Saada, T. E. (1998). Procedures for calibrating hourly simulation models to measured building energy and environmental data. *ASME Journal of Solar Energy Engineering, 120*(3), 193-204.

Haberl, J. S., and Culp, C. C. (2013). Measurement and verification of energy savings. In S. Doty and W. C. Turner (Eds.), *Energy Management Handbook* (pp. 685-748). Lilburn, GA: The Fairmont Press, Inc.

Haves, P., Salsbury, T., Claridge, D. E., and Liu, M. (2001). Use of whole building simulation in on-line performance assessment: Modeling and implementation issues. *7th IBPSA Conference, Rio de Janeiro, Brazil, Aug. 13-15,* 335-342.

Hitchcock, R. J., Carroll, W.L., and Birdsall, B. E. (1991). *RESEM: retrofit energy savings estimation model reference manual.* Berkeley, CA: Lawrence Berkeley Laboratory (LBL, now LBNL).

Home Network. (n.d.). Retrieved May 26, 2015, from the Wikipedia: http://en.wikipedia.org/wiki/Home_network

Honeywell. (2015). *Lyric.* Retrieved from http://lyric.honeywell.com/

Hong, T., D'Oca, S., and Langevin, J. (2017). *Understanding and integrating occupant behavior in the building life cycle* (White Paper, draft in-progress). Atlanta, GA: ASHRAE Multidisciplinary Task Group on Occupant Behavior in Buildings.

Hsieh, E. S. (1988). *Calibrated computer models of commercial buildings and their role in building design and operation.* (Master's Thesis). Princeton, NJ: Princeton University.

Huang, J. (2002). DrawBDL 3.0. *Building Energy Simulation User News, 23*(6), 13.

Hunn, B. D., Banks, J. A., and Reddy, S. N. (1992). Energy analysis of the Texas capitol restoration. *Proceedings of the 8th Symposium on Improving Building Systems in Hot and Humid Climates, May 13-14, Dallas, TX,* 165-173.

International Code Council (ICC). (2000). *2000 International Energy Conservation Code*. Washington, DC: ICC, inc.

International Code Council (ICC). (2009). *2009 International Energy Conservation Code*. Washington, DC: ICC, inc.

INSTEON. (2014). *About INSTEON.* Retrieved from http://www.insteon.com/about-home.html

Jasper. (2015). *Meet the Titans of IoT.* Retrieved from http://www.titansofiot.com/internetofthings/meet-the-titans-of-iot

Johnson, B.J., Starke, M.R., Abdelaziz, O.A., Jackson, R.K., and Tolbert, L.M. (2014). A MATLAB based occupant driven dynamic model for predicting residential power demand. *IEEE PES T&D Conference and Exposition, Chicago, IL, Apr. 14-17,* 1-5.

Katipamula, S., and Brambley, M.R. (2005). Methods for Fault Detection, Diagnostics, and Prognostics for Building Systems – A review, Part I. *Science and Technology for the Built Environment, 11*(1), 3-25.

Katipamula, S., and Claridge, D.E. (1993). Use of simplified systems model to measure retrofit energy savings. *ASME Journal of Solar Energy Engineering, 115*(2), 57-68.

Katipamula, S., Reddy, T. A., and Claridge, D. E. (1998). Multivariate regression modeling. *Journal of Solar Energy Engineering, 120*(3), 177-184.

Kaplan, M. B., McFerran, J., Jansen, J. and Pratt, R. (1990a). Reconciliation of a DOE2.1 C model with monitored end-use data for a small office building. *ASHRAE Transactions, 96*(1), 981-993.

Kaplan, M. B., Jones, B., and Jansen, J. (1990b). DOE-2.1C model calibration with monitored end-use data. *Proceedings from the ACEEE 1990 Summer Study on Energy Efficiency in Buildings, Vol. 10,* 10.115-10.125.

Kim, H. (2012). *Methodology for rating a building's overall performance based on the ASHRAE/CIBSE/USGBC performance measurement protocols for commercial building.* (Doctoral Dissertation). College Station, TX: Texas A&M University.

Kim, K. H. (2014). *Development of an improved methodology for analyzing existing single-family residential energy use.* (Doctoral Dissertation). College Station, TX: Texas A&M University.

Kim, K. H., and Baltazar, J. (2010). *Procedure for packing weather files for DOE-2.1e* (Report Number ESL-TR-10-09-03). College Station, TX: Texas A&M University.

King, C. (2010). *HAN smart meter interface: What can we expect?* Retrieved from www.emeter.com/smart-grid-watch/2010/han-smart-meter-interface-what-can-we-expect/

Kintner-Meyer M, Schneider, K. and Pratt, R. (2007). Impact assessment of plug-in hybrid vehicles on electric utilities and regional U.S. power grids. Part 1: Technical analysis. *Journal of EUEC, 1*, Paper No. 04.

Kissock, K. (2015). Principles of energy efficient HVAC for manufacturing facilities. *ASHRAE Annual Conference Seminar 41, Atlanta, GA.*

Kissock, K., Reddy., T. A., and Claridge, D. E. (1998). Ambient temperature regression analysis for estimating retrofit savings in commercial buildings. *Journal of Solar Energy Engineering, 120*(3), 168-176.

Kissock, K., Haberl, J. S., and Claridge, D. E. (2001). *Inverse modeling toolkit: User's guide* (ASHRAE Final Report for RP-1050). Atlanta, GA: ASHRAE.

Kissock, K., Haberl, J. S., and Claridge, D. E. (2003). Inverse modeling toolkit: Numerical algorithms (RP-1050). *ASHRAE Transactions, 109*, 425-434.

Klein, S. A., Beckman, W. A., and Duffle, J. A. (1976). TRNSYS - A transient simulation program. *ASHRAE Transactions 82*(1), 623-633.

Knebel, D. E. (1983). *Simplified energy analysis using the modified bin method.* Atlanta, GA: ASHRAE.

Kreider, J. F., and Haberl, J. S. (1994). Predicting hourly building energy use: the great energy predictor shootout—overview and discussion of results. *ASHRAE Transactions, 100*(2), 1104–1118.

Kreider, J. F., and Wang, X. A. (1991). Artificial neural networks demonstration for automated generation of energy use predictors for commercial buildings. *ASHRAE Transactions, 97*(1), 775-779.

Kroposki, B, Margolis, R., Kuswa, G., Torres, J. Bower, W., Key, T., and Ton, D. (2008). *Renewable systems interconnection: Executive summary* (Report Number NREL/TP-581-42292). Golden, CO: National Renewable Energy Laboratory.

Lawrence Berkeley National Laboratory (LBNL) and James J. Hirsch & Associates (JJH). (1998). *Overview of DOE-2.2.* Retrieved from http://www.doe2.com/download/Docs/22_Oview.pdf

Liu, M., and Claridge, D. E. (1998). Use of calibrated HVAC system models to optimize system operation. *ASME Journal of Solar Energy Engineering, 120,* 131-138.

Liu, M., Claridge, D. E., Bensouda, N., Heinemeier, K., Lee, S. U., and Wei, G. (2003). *High performance commercial building systems: manual of procedures for calibrating simulations of building systems* (Report Number HPCBS#E5P23T2b). Sacramento, CA: California Energy Commission.

Liu, M., Song, L., Wei, G., and Claridge, D. E. (2004). Simplified building an air handling unit model calibration and applications. *ASME Journal of Solar Energy Engineering, 126,* 601-609.

Long, N. (2006). *Real-time weather data access guide* (Report Number NREL/BR-550-34303). Golden, CO: National Renewable Energy Laboratory.

Lunneberg, T. A. (1999). Improving simulation accuracy through the use of short-term electrical end-use monitoring. *IBPSA Conference, Kyoto, Japan,* 13-15.

MacKay, D. (1994). Bayesian nonlinear modeling for the prediction competition. *ASHRAE Transactions, 100,* 1053–1062.

Manke, J. M., Hittle, D. C., and Hancock, C. E. (1996). Calibrating building energy analysis models using short-term test data. *Proceedings of the ASME International Solar Energy Conference, March 31-April 3, San Antonio, TX,* 369-378.

Mathieu, J. L., Price, P. N., Kiliccote, S., and Piette, M. A. (2011). Quantifying changes in building electricity use, with application to demand response. *IEEE Transactions on Smart Grid, 2,* 507-518.

Miller, C. C. (2014). *For Google, a toehold into goods for a home.* Retrieved from http://www.nytimes.com/2014/01/14/technology/google-to-buy-nest-labs-for-3-2-billion.html

Mitalas, G. P., and Stephenson, D. G. (1967). Room thermal response factors. *ASHRAE Transactions, 73, Pt.1,* 1-10.

Mohsenian-Rad, A. H., Wong, V. W. S., Jatskevich, J., Schober, R., and Leon-Garcia, A. (2010). Autonomous demand-side management based on game-theoretic energy consumption scheduling for the future smart grid. *IEEE Transactions on Smart Grid, 1*(3), 320–331.

Moorhead, P. (2013). *The problem with home automation's Internet of Things (IoT).* Retrieved from www.forbes.com/sites/patrickmoorhead/2013/09/26/the-problem-with-home-automations-iot/

National Oceanic and Atmospheric Administration (NOAA). (2016). *Quality controlled local climatological data.* Retrieved from http://www.ncdc.noaa.gov/qclcd/QCLCD?prior=N

Nest. (2015). *Nest thermostat.* Retrieved from https://nest.com/thermostat/meet-nest-thermostat/

Neto, A. H., and Fiorelli, F. A. S. (2008). Comparison between detailed model simulation and artificial neural network for forecasting building energy consumption. *Energy and Buildings*, *40*, 2169–2176.

Norford, L. K., Socolow, R. H., Hsieh, E. S., and Spadaro, G. V. (1994). Two-to-one discrepancy between measured and predicted performance of a 'low-energy' office building: insights from reconciliation based on the DOE-2 model. *Energy and Buildings*, *21*, 121-131.

Oh, S. (2013). *Origins of analysis methods in energy simulation programs used for high performance commercial buildings*. (Master's Thesis). College Station, TX: Texas A&M University.

Oh, S., and Haberl, J. (2016). Origins of analysis methods used to design high-performance commercial buildings: Whole-building energy simulation. *Science and Technology for the Built Environment*, *22*(1), 118-137.

Oh, S., Haberl, J., and Baltazar, J. (2014). *A review of real-time Fault Detection & Diagnostics (FDD), real-time commissioning, real-time M&V, and Building Automation System (BAS)/Energy Management & Control System (EMCS)* (Report Number ESL-ITR-14-07-02). College Station, TX: Energy Systems Laboratory.

Ott, R. L., and Longnecker, M. (2010). *An introduction to statistical methods and data analysis* (6th ed.). Belmont, CA: Brooks/Cole, Cengage Learning.

Opower. (2015). *Energy efficiency – Unleash the full potential of your energy efficiency investment.* Retrieved from http://www.opower.com/solutions/energy-efficiency/residential

Paschkis, V. (1942). Periodic heat flow in building walls determined by electrical analogy method. ASHVE Transactions 48, 75-90.

Paulus, M. (2012). *Measurement, modeling, analysis and reporting protocols for short-term monitoring and verification of whole building energy performance.* (Master's Thesis). Milwaukee, WI: Milwaukee School of Engineering.

Pedersen, C. O., Fisher, D. E., and Liesen, R. J. (1997). Development of a heat balance procedure for calculating cooling loads. *ASHRAE Transactions, 103,* 459-468.

Pedrini, A., Westphal, F. S., and Lamberts, R. (2002). A methodology for building modeling and calibration in warm climates. *Building and Environment, 37,* 903-912.

Pratt, R. G., Balducci, P., Gerkensmeyer, C., Katipamula, S., Kintner-Meyer, M. C. W., Sanquist, T. F., Schneider, K. P., and Secrets, T. J. (2010). *The smart grid: an estimation of the energy and CO_2 benefits* (Report Number PNNL-19112). Richland, WA: Pacific Northwest National Laboratory (PNNL).

Price, P., Granderson, J., Sohn, M., Addy, N., and Jump, D. (2013). *Commercial building energy baseline modeling software: Performance metrics and method testing with open source models and implications for proprietary software testing* (Report Number ET12PGE5312). San Francisco, CA: Pacific Gas and Electric Company.

Rabl, A. (1988). Parameter estimation in buildings: Methods for dynamic analysis of measured energy use. *Journal of Solar Energy Engineering, 110,* 52–66.

Ramchurn, S., Vytelingum, P., Rogers, A., and Jennings, N. (2011). Agent-based control for decentralised demand side management in the smart grid. *Proceedings of the 10th International Conference on Autonomous Agents and Multiagent Systems-Volume 1*, 5–12.

Raspberry Pi. (2015). *What is a Raspberry Pi?* Retrieved from https://www.raspberrypi.org/help/what-is-a-raspberry-pi/

Reddy, T. A. (1989). Application of dynamic building inverse models to three occupied residences monitorcd non-intrusively. *Proceedings of the Thermal Performance of Exterior Envelopes of Buildings IV,* ASHRAE/DOE/BTECC/CIBSE.

Reddy, T. A. (2006). Literature review on calibration of building energy simulation programs: Uses, problems, procedures, uncertainty, and tools. *ASHRAE Transactions, 112*(1), 226-240.

Reddy, T. A., Saman, N. F., Claridge, D. E., Haberl, J. S., Turner, W. D., and Chalifoux, A. T. (1997). Baselining methodology for facility-level monthly energy use - Part 1: theoretical aspects. *ASHRAE Transactions, 103*(2), 336–347.

Reddy, T. A., Deng, S., and Claridge, D. E. (1999). Development of an inverse method to estimate overall building and ventilation parameters of large commercial buildings. *Journal of Solar Energy Engineering, 121,* 40–46.

Reddy, T. A., Maor, I., and Panjapornpon, C. (2007a). Calibrating detailed building energy simulation programs with measured data – Part I: general methodology (RP-1051). *HVAC&R Research, 13,* 221–241.

Reddy, T. A., Maor, I., and Panjapornpon, C. (2007b). Calibrating detailed building energy simulation programs with measured data – Part II: application to three case study office buildings (RP-1051). *HVAC&R Research, 13,* 243–265.

Ruch, D., and Claridge, D. (1991). A four-parameter change-point model for predicting energy consumption in commercial buildings. *Proceedings of the ASME International Solar Energy Conference*, 433-440.

San Diego Gas & Electric (SDGE). (2015a). *Radio frequency concerns.* Retrieved from http://www.sdge.com/residential/about-smart-meters/radio-frequency-concerns

San Diego Gas & Electric (SDGE). (2015b). *Home and business area network devices.* Retrieved from http://www.sdge.com/residential/about-smart-meters/radio-frequency-concerns

Seem, J. E., and Hancock, C. E. (1985). A method for characterizing the thermal performance of a solar storage wall from measured data. *Proceedings of ASHRAE/DOE/BTECC (Thermal Performance of the Exterior Envelopes of Buildings III (ASHRAE SP-49:351-363)), Clearwater Beach, FL,* 1304-1315.

Sever, F., Kissock, K., Brown, D., and Mulqueen, S. (2011). Estimating industrial building energy savings using inverse simulation. *Proceedings of the ASHRAE Winter Conference, Las Vegas, NV*.

Shonder, J. A., Hughes, P. J. and Thornton, J.W. (1998). Using calibrated engineering models to predict energy savings in large-scale geothermal heat pump projects. *ASHRAE Transactions, 104*(1), 944-954.

Sigma Designs, Inc. (2014). *About Z-Wave.* Retrieved from http://www.z-wave.com/what_is_z-wave

Smart Grid Consumer Collaborative (SGCC). (2011). *Radio frequencies and smart meters.* Retrieved from https://www.bge.com/smartenergy/smartgrid/smartmeters/Documents/SGCC-RF-Fact-Sheet1.pdf

Smart Meter Texas (SMT). (2014). *About smart meter Texas.* Retrieved from https://www.smartmetertexas.com/CAP/public/home/home_faq.html

Soebarto, V. I. (1997). Calibration of hourly energy simulations using hourly monitored data and monthly utility records for two case study buildings. *IBPSA Conference Proceedings, Prague, Czech Republic, September 13-15.*

Sonderegger, R. C. (1978). *Dynamic models of house heating based on equivalent thermal parameters.* (Doctoral dissertation). Princeton, NJ: Princeton University.

Sonderegger, R. C. (1998). A baseline model for utility bill analysis using both weather and non-weather related variables. *ASHRAE Transactions, 104*(2):859-870.

Stephenson, D. G., and Mitalas, G. P. (1967). Cooling load calculations by thermal response factor method. *ASHRAE Transactions, 73*(1), 1-7.

Subbarao, K. (1988). *PSTAR-Primary and secondary terms analysis and renormalization: A unified approach to building energy simulations and short-term monitoring.* (Report Number SERI/TR-253-3175). Golden, CO: Solar Energy Research Institute (now, National Renewable Energy Laboratory).

Sun, J., and Reddy, T. A. (2006). Calibration of building energy simulation programs using the analytic optimization approach (RP-1051). *HVAC&R Research, 12,* 177–196.

Thamilseran, S., and Haberl, J. S. (1994). A bin method for calculating energy conservation retrofit savings in commercial buildings. *Proceedings of the 9th Symposium on Improving Building Systems in Hot and Humid Climates, Arlington, TX, May 19-20*.

Thumann, A., and Younger, W. (2008). *Handbook of energy audits.* (7th ed.). Lilburn, GA: Fairmont Press.

Tishman Research Corporation (TRC). (1984). *DOE-2: Comparison with measured data: design and operational energy studies in a new high-rise office building-Vol. 5.* Washington, DC: U.S. Department of Energy (US DOE).

Todd, D., Caufield, M., Helms, B., Starke, M., Kirby, B., and Kueck, J. (2009). *Providing reliability services through demand response: A preliminary evaluation of the demand response capabilities of Alcoa Inc* (Report Number ORNL/TM-2008/233). Oak Ridge, Tennessee: Oak Ridge National Laboratory.

Tyler, H., Stefano, S., Alberto, P., Dustin, M., and Kyle, S. (2013). *CBE thermal comfort tool - Center for the Built Environment, University of California Berkeley.* Retrieved from http://cbe.berkeley.edu/comforttool/

U.S. Department of Energy (US DOE). (2012). *Demand reductions from the application of advanced metering infrastructure, pricing programs, and customer-based systems – initial results.* Washington, DC: U.S. DOE Electricity Delivery & Energy Reliability.

U.S. Department of Energy (US DOE). (2015). *The smart grid: An introduction.* Retrieved from http://energy.gov/sites/prod/files/oeprod/DocumentsandMedia/DOE_SG_Book_Single_Pages.pdf

U.S. Energy Information Administration (US EIA). (2013a). *How many smart meters are installed in the United States, and who has them?.* Retrieved from http://www.eia.gov/tools/faqs/faq.cfm?id=108&t=3

U.S. Energy Information Administration (US EIA). (2013b). *Heating and cooling no longer majority of U.S. home energy use.* Retrieved from http://www.eia.gov/todayinenergy/detail.cfm?id=10271&src=‹ Consumption Residential Energy Consumption Survey (RECS)-b1

U.S. Energy Information Administration (US EIA). (2015). *An assessment of interval data and their potential application to residential electricity end-use modeling.* Washington, DC: U.S. DOE.

U.S. Energy Information Administration (US EIA). (2016). *Electricity - Form EIA-861M (formerly EIA-826) detailed data – Sales and revenue.* Retrieved from https://www.eia.gov/electricity/data/eia861m/index.html

Walsh, B. (2014). Model citizens: A community in Austin tracks every watt of energy it uses – So the rest of us can live smarter. Time Magazine. July 14, 2014.

Wei, G., Liu, M., and Claridge, D. E. (1998). Signatures of heating and cooling energy consumption for typical AHUs. *Proceedings of the 11th Symposium on Improving Building Systems in Hot and Humid Climates, Fort Worth, TX,* 387-402.

Wesoff, E. (2011). *Microsoft follows Google to home energy graveyard.* Retrieved from http://www.greentechmedia.com/articles/read/microsoft-follows-google-to-the-home-energy-monitor-graveyard

Wetter, M., Zuo, W., and Nouidui, T. S. (2011). Modeling of heat transfer in rooms in the Modelica "buildings" library. *12th IBPSA Conference, Sydney, Nov. 14-16,* 1096-1103.

Wi-Fi Alliance. (2014). *Who we are.* Retrieved from http://www.wi-fi.org/who-we-are

Winkelmann, F. C., Birdsall, B. E., Buhl, W. F., Ellington, K. L., Erdem, A. E., Hirsch, J. J., and Gates, S. (1993). *DOE-2 supplement version 2.1E* (Report Number LBL-34947). Berkeley, CA: Lawrence Berkeley Laboratory (LBL, now LBNL).

Winkelmann, F. C. (2002). Underground surfaces: How to get a better underground surface heat transfer calculation in DOE-2.1E. *Building Energy Simulation User News, 23*(6), 19-26.

X10.com. (2013). *X10 Basics.* Retrieved from http://www.x10.com/x10-basics.html

Yoon, J., Lee, E. J., and Claridge, D. E. (2003). Calibration procedure for energy performance simulation of a commercial building. *Journal of Solar Energy Engineering, 125,* 251-257.

ZigBee Alliance. (2014). *Understanding ZigBee.* Retrieved from http://www.zigbee.org/About/UnderstandingZigBee.aspx

APPENDIX A

APPROVAL FROM THE INSTITUTIONAL REVIEW BOARD (IRB)

Figure A-1 shows the IRB approval for this study.

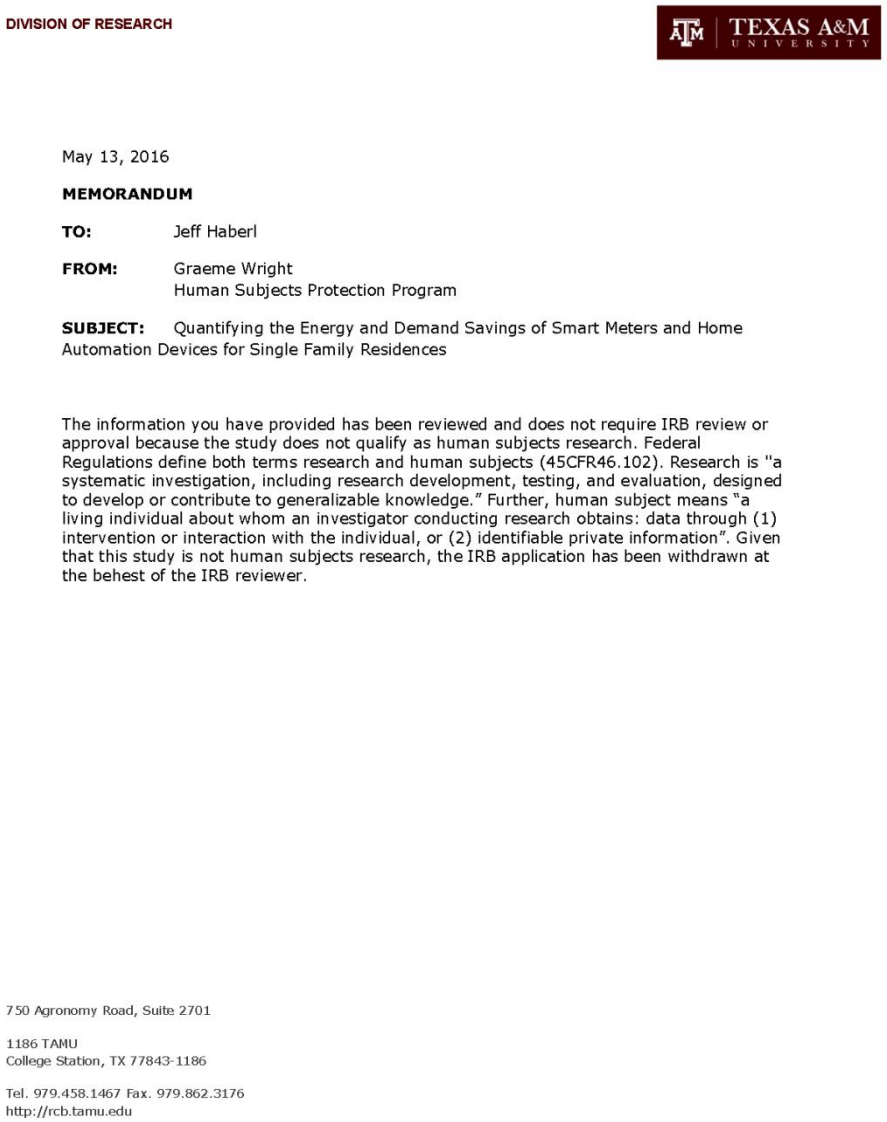

DIVISION OF RESEARCH

TEXAS A&M UNIVERSITY

May 13, 2016

MEMORANDUM

TO: Jeff Haberl

FROM: Graeme Wright
Human Subjects Protection Program

SUBJECT: Quantifying the Energy and Demand Savings of Smart Meters and Home Automation Devices for Single Family Residences

The information you have provided has been reviewed and does not require IRB review or approval because the study does not qualify as human subjects research. Federal Regulations define both terms research and human subjects (45CFR46.102). Research is "a systematic investigation, including research development, testing, and evaluation, designed to develop or contribute to generalizable knowledge." Further, human subject means "a living individual about whom an investigator conducting research obtains: data through (1) intervention or interaction with the individual, or (2) identifiable private information". Given that this study is not human subjects research, the IRB application has been withdrawn at the behest of the IRB reviewer.

750 Agronomy Road, Suite 2701

1186 TAMU
College Station, TX 77843-1186

Tel. 979.458.1467 Fax. 979.862.3176
http://rcb.tamu.edu

Figure A-1. IRB approval letter for this study.

APPENDIX B

COMPARISON BETWEEN SMART METER AND MONTHLY UTILITY BILLING DATA

Table B-1 and Figure B-1 show the differences between hourly, summed monthly electricity use data from the SM and monthly billing data. It was observed that the data from the monthly utility bill was slightly different from the SM data. One of the possible reasons could be the different times when the electricity use data are recorded.

Table B-1. Comparison between SM and actual monthly utility billing data.

	Billing period		**Days in billing period**	**Hourly sum monthly electricity use (kWh) from SM**	**Monthly Electricity Use (kWh) from utility**	**Difference**
	Start date	**End date**				
April	4/15/2015	5/13/2015	29	620.37	653.00	32.63
May	5/14/2015	6/15/2015	33	898.06	774.00	-124.06
June	6/16/2015	7/15/2015	30	1015.19	950.00	-65.19
July	7/16/2015	8/13/2015	29	1315.00	1460.00	145.00
August	8/14/2015	9/14/2015	32	1277.68	1241.00	-36.68
September	9/15/2015	10/14/2015	30	841.49	892.00	50.51
October	10/15/2015	11/12/2015	29	595.76	621.00	25.24
November	11/13/2015	12/16/2015	34	1014.06	896.00	-118.06
December	12/17/2015	1/13/2016	28	1269.18	1255.00	-14.18
January	1/14/2016	2/11/2016	29	1530.87	1589.00	58.13
February	2/12/2016	3/15/2016	33	880.37	878.00	-2.37
March	3/16/2016	4/13/2016	29	670.07	731.00	60.93
Total or Average			365	11,928.10	11,940.00	11.90

Figure B-1. Comparison between electricity use data (SM data) and actual monthly utility billing data.

APPENDIX C

TPE AND INP FORMATS USED FOR THE DOE-2.1E MODEL

Figure C-1 shows an example of the TPE format. This format includes the hourly information of one year's dry-bulb temperature (°F), wet-bulb temperature (°F), dew-point temperature (°F), wind speed (knot), wind direction (degree), global solar radiation (Btu/hr-ft2), direct normal solar radiation (Btu/hr-ft2), and station pressure (inHg).

```
039040480440390200142999099999999999999999999999999999900000000      2015010100
039040480430370200133001099999999999999999999999999999900000000      2015010101
039040480430360100103002099999999999999999999999999999900000000      2015010102
039040470420360100133002099999999999999999999999999999900000000      2015010103
039040460420360200123003099999999999999999999999999999900000000      2015010104
039040450410370100103006099999999999999999999999999999900000000      2015010105
039040450410370100093007099999999999999999999999999999900000000      2015010106
039040440410360100133009099999999999999999999999999999900050000      2015010107
039040440410363600133012099999999999999999999999999999900160000      2015010108
```

Figure C-1. Example of the .TPE format.

Figure C-2 shows an example of the INP format. This format includes the general weather information of a selected location.

```
PACK
T_CLL 2015
TRY    03904  -999     6 30.6  96.4 30-BITSOLAR      4 20.  0.025

-999.
LIST
PACKED  -999  -999     1    12
END
```

Figure C-2. Example of the .INP format.

APPENDIX D

CALIBRATION METHOD FOR TEMPERATURE DATA LOGGERS

This Appendix D shows the method to calibrate the eight temperature data loggers. This appendix also describes the results of the calibration for the eight temperature data loggers. After the calibration, the eight temperature data loggers were installed in the case-study house to measure Indoor Air Temperatures (IATs) in each zone, which was described in Section 4.3.

The ASTM Standard E77-14 was used to calibrate the temperature data loggers (ASTM, 2014). In this study, Fluke 52 II Thermometer (with Type-K thermocouple bead probe) and Vaisala HMI41 Meter (with HMP42 probe) were used instead of ASTM certified liquid-in-glass thermometers. Figure D-1 shows the procedure of the calibration. To begin with, Fluke 52 II Thermometer and Vaisala HMI41 Meter were calibrated using the ice point temperature environment with distilled water as shown in Figure D-2. 1.1 °F offset was used for the thermometer. Then, the eight temperature data loggers were calibrated using three different environments in a temperature chamber, as shown in Figure D-3. Using the average temperatures from the Fluke 52 II Thermometer and the Vaisala HMI41 Meter, the temperature of the three different environments were measured (see Figure D-4). Finally, the measured temperatures were compared with the temperatures of the eight temperature data loggers, respectively. Table D-1 shows the scales and the offsets from the comparisons. Figures D-5 and D-6 show the residual plots of pre-calibration and post-calibration using the scales and the offsets.

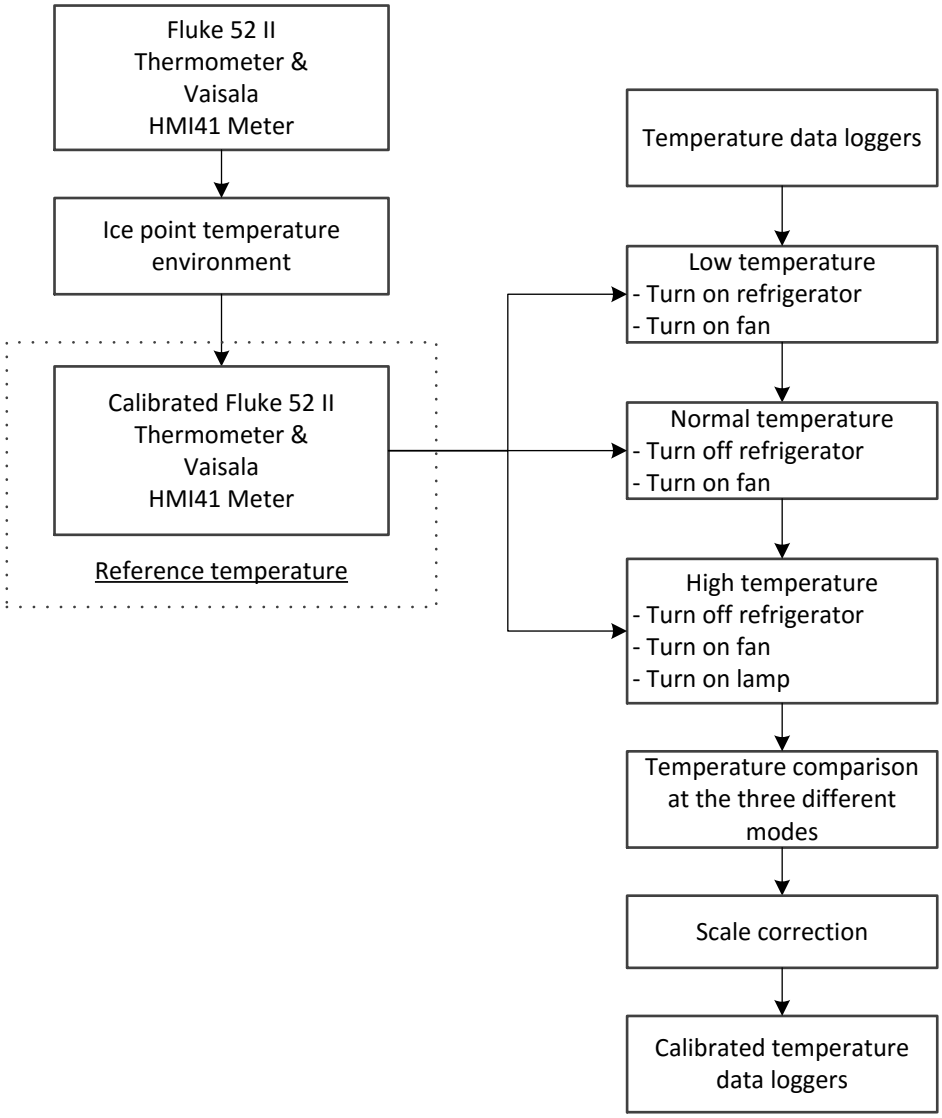

Figure D-1. Procedure of the temperature data logger calibration.

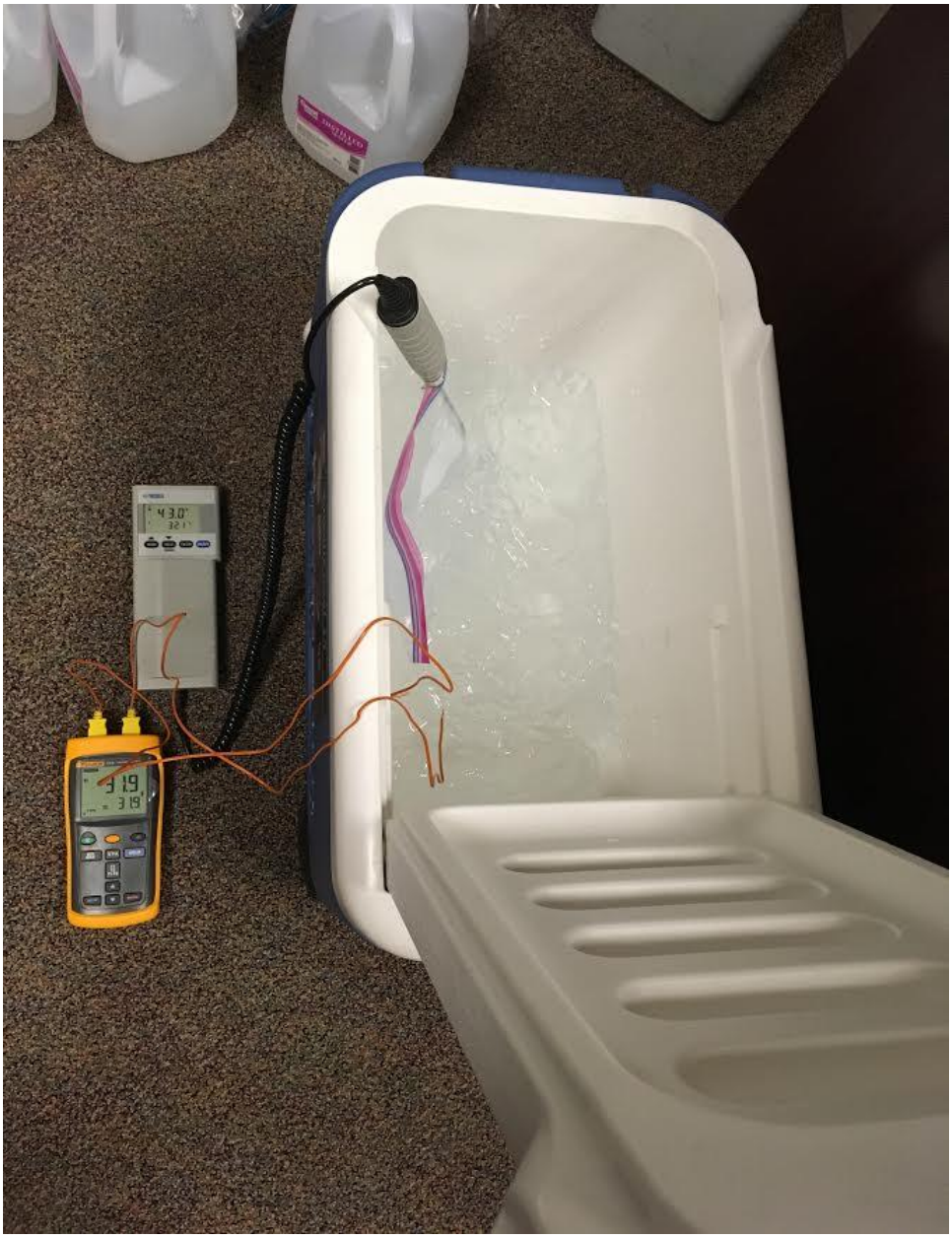

Figure D-2. Ice point temperature environment (Author's photo).

Figure D-3. Temperature calibration chamber (Author's photo).

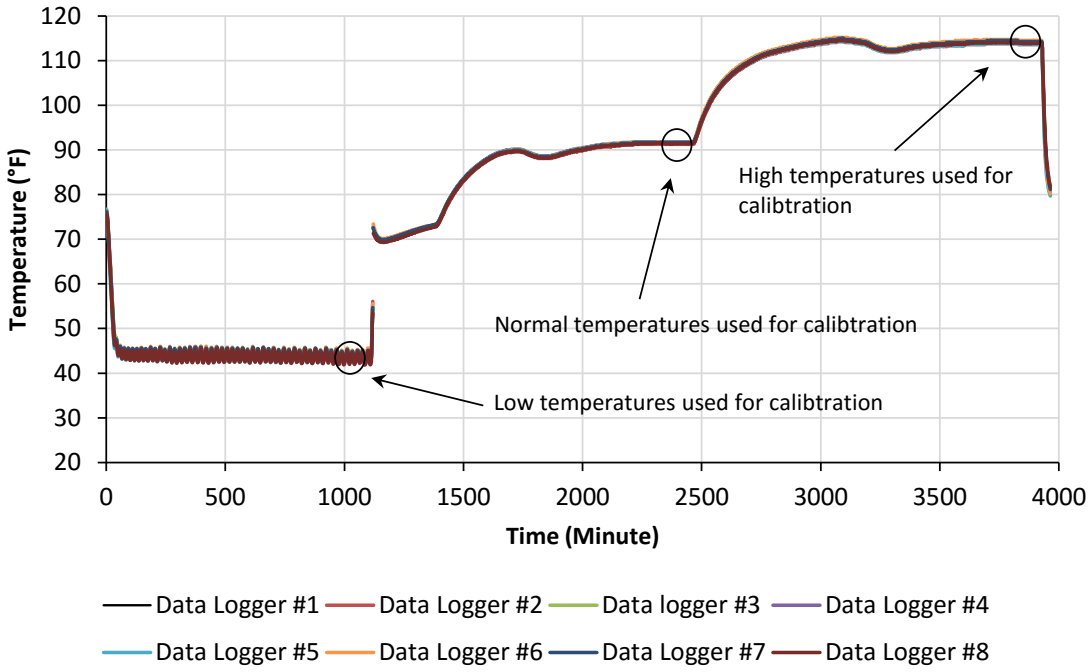

Figure D-4. Temperatures of three different environments.

Table D-1. Scales and offsets.

Data logger #	Scale	Offset
1	0.0004	0.3279
2	0.0048	-0.1888
3	0.0063	0.1597
4	0.0108	-0.3198
5	0.0068	-0.2495
6	0.0100	-0.0413
7	0.0122	-0.4007
8	0.0146	-1.0102

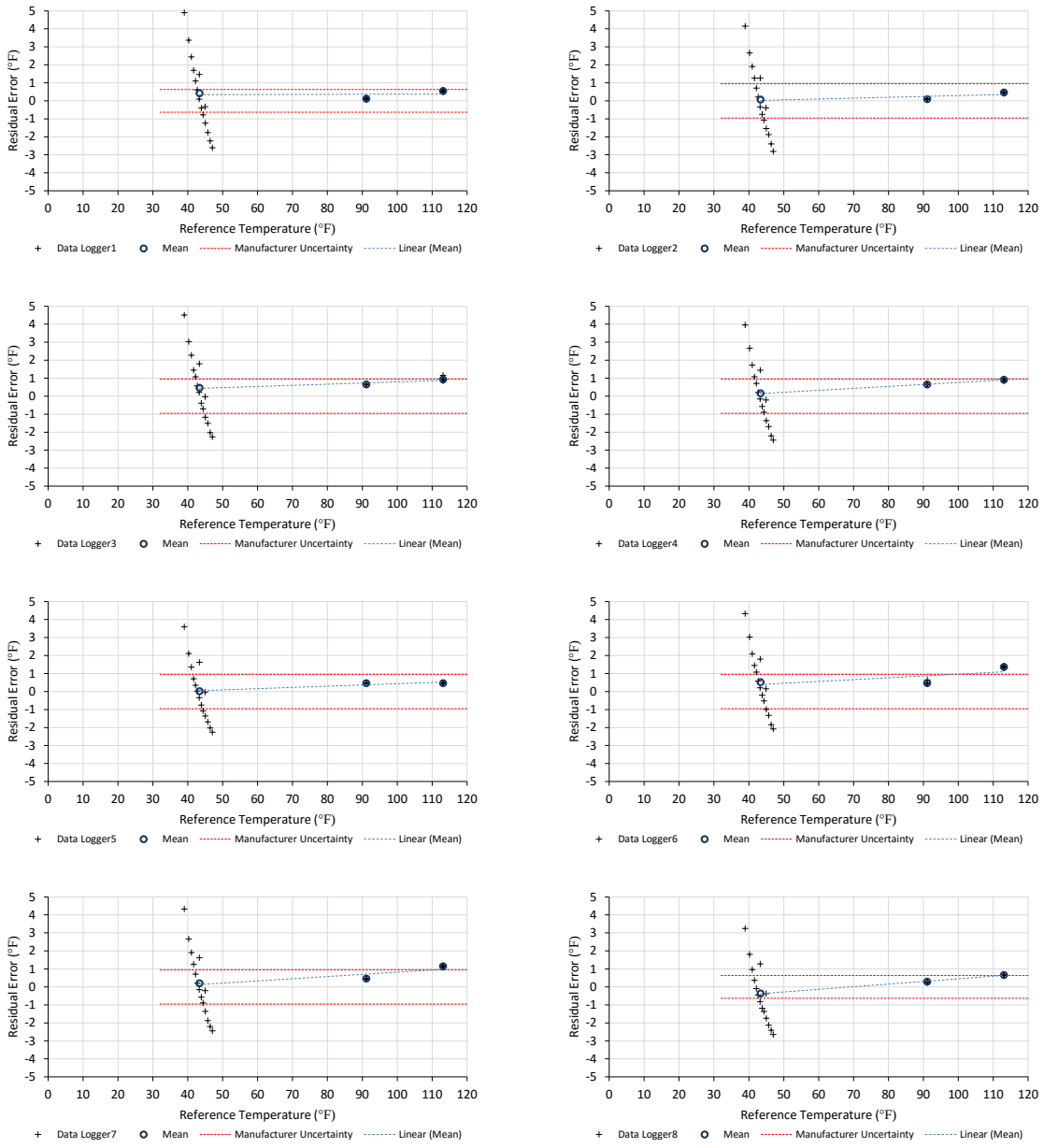

Figure D-5. Residual plots of pre-calibration.

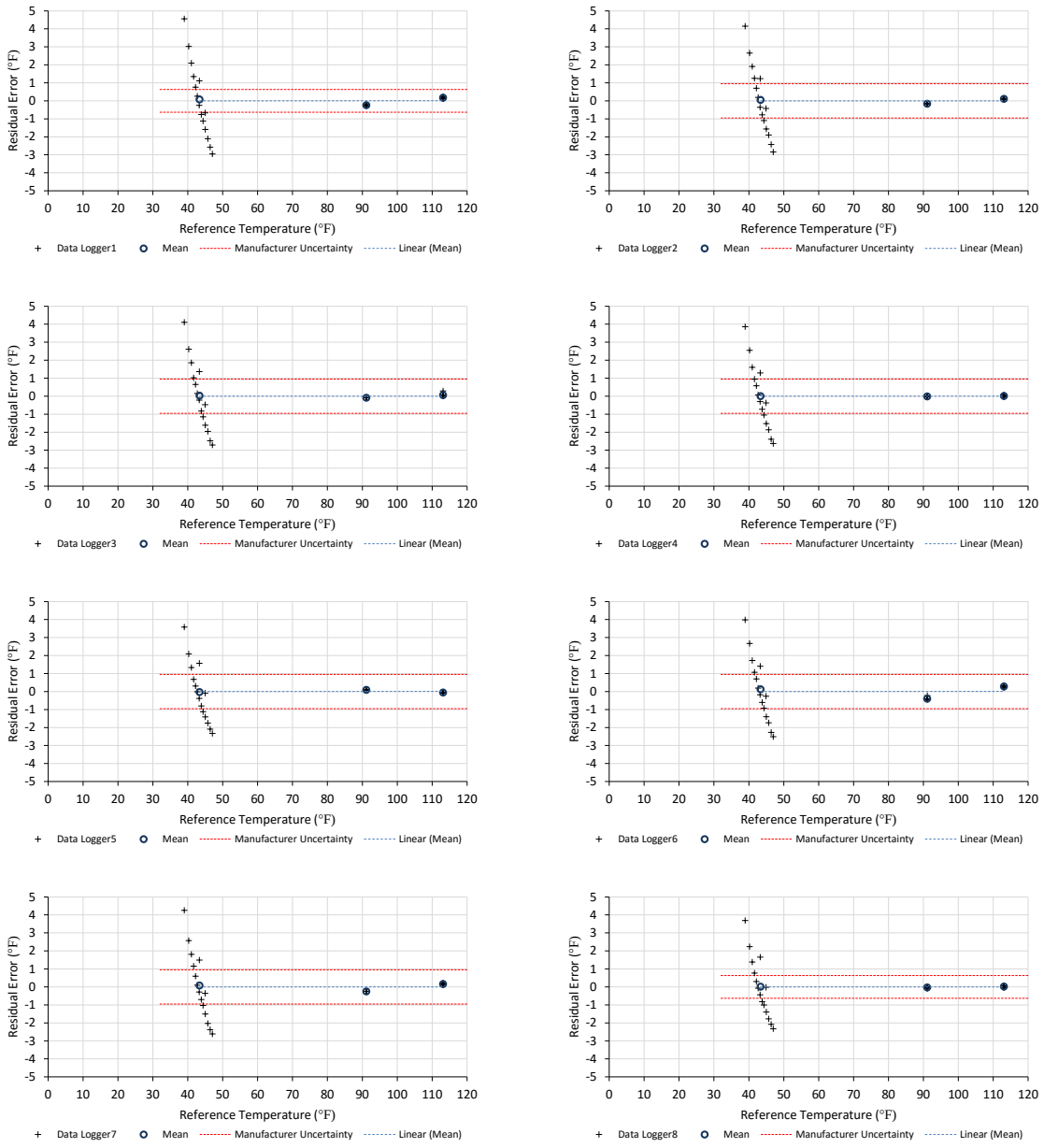

Figure D-6. Residual plots of post-calibration.

APPENDIX E

DATA LOGGERS USED FOR THE CASE-STUDY HOUSE

Table E-1 shows the specifications of the data loggers installed in the case-study house.

Table E-1. Specifications of the sensors installed in the case-study house.

Product	**Model #**	**Accuracy**	**Measurement Range**	**Cost**	**Picture**
ONSET HOBO Temperature/ Relative Humidity Data Logger	U12-013	Temp: ± 0.63°F from 32° to 122°F RH: ±2.5% from 10% to 90% RH (typical), to a maximum of ±3.5%	Temp: -4° to 158°F RH: 5% to 95%	$140	
HOBO Occupancy/Light (12m Range) Data Logger	UX90-006	Detection Range UX90-005x: maximum 5 m (15.4 ft); UX90-006x: maximum 12 m (39.4 ft) Detection Performance UX90-006: 102° (±51°) Horizontal; 92° (±46°) Vertical	Occupancy sensor range: 20° to 60°C (-4° to 140°F); 15 to 85% RH (non-condensing)	$205	

APPENDIX F

HADS INSTALLED FOR THE CASE-STUDY HOUSE

Table F-1 shows the specifications of the HADs installed in the case-study house.

Table F-1. Specifications of the HADs installed in the case-study house.

Product	**Quantity**	**Component Cost**	**Total Cost**	**Power Use**	**Notes**	**Picture**
Programmable Thermostat (Ecobee3) with one motion/ temperature sensor	1	$249	$249	3.5 VA (2.8 W when Power Factor is 0.8)	It controls home's heating and cooling operation. It can be connected (range: 45 ft) with several motion/ temperature sensor(s) up to 32.	
Motion/ temperature Sensors (Ecobee3)	6	$39.5	$237	Lithium Cell 3V	It detects movement in a certain area of home (up to 15 ft; 120° horizontal; 30° vertical) and measures indoor temperature (32 F° to 130 F°).	

APPENDIX G

THERMOSTAT INSTALLED FOR THE CASE-STUDY HOUSE

Figure G-1 shows the previous thermostat and wiring (upper figure) and the new thermostat and wiring (lower figure) installed in the case-study house.

Figure G-1. Previous thermostat and wiring (upper) and new thermostat and wiring (lower) installed in the case-study house.